

Vol. 12 No. 1 April 2025



Jurnal Farmasi dan Ilmu Kefarmasian Indonesia

E-ISSN: 2580-8303

P-ISSN: 2406-9388



PUBLISHED BY:
FACULTY OF PHARMACY UNIVERSITAS AIRLANGGA in collaboration with
INDONESIAN PHARMACISTS ASSOCIATION (IAI) OF EAST JAVA



Accredited SINTA 2
No: B/1796/E5.2/KI.02.00/2020

Jurnal Farmasi dan Ilmu Kefarmasian Indonesia

Chief Editor:

Elida Zairina, S.Si, MPH., Ph.D., FISQua., Apt.

Editorial Boards:

Prof. Dewi Melani Hariyadi, S.Si, M.Phil., PhD., Apt.

Prof. Dr. Wiwied Ekasari, M.Si., Apt.

Prof. Dr. Alfi Khatib

Prof. Dr. Long Chiau Ming

Prof. Dr. Susi Ari Kristina, M.Kes., Apt.

Dr.rer.nat Maria Lucia Ardhani D. L., S.Si., M.Pharm, Apt.

Suciati, S.Si., M.Phil, PhD., Apt.

Dr. Yunita Nita, S.Si., M.Pharm., Apt.

Chrismawan Ardianto, S.Farm., M.Sc., Ph.D., Apt.

Tutik Sri Wahyuni, S.Si., M.Si., Ph.D., Apt.

Helmy Yusuf, S.Si., MSc., Ph.D., Apt.

Dr. Ariyanti Suhita Dewi, S.Si., M.Sc.

Dr. Adliah Mhd. Ali

Asst. Prof. Dr. Nungruthai Suphrom

Assist. Prof. Dr.rer.nat. Nuttakorn Baisaeng

Didik Setiawan, Ph.D., Apt.

Debra Dorotea, Ph.D.

Deby Fapyane, Ph.D.

Tina Tran, PharmD

Administrative Editor:

Susmiandri, S.Kom.

Peer Reviewers

Prof. Dr.rer.nat. apt Raden Rara Endang Lukitaningsih, M.Si.

Prof. Dr. apt. Budi Suprapti, M.Si.

Prof. Dr. apt. Ika Puspita Sari, S.Si., M.Si.

Prof. apt. Rr. Retno Widyowati, S.Si., M.Pharm, Ph.D.

Prof. Dr. apt. Juni Ekowati, M.Si.

Prof. Dr. apt. Tristiana Erawati, M.Si.

Prof. Dr. apt. Sukardiman, MS.

Prof. Dra. Apt. Esti Hendradi, M.Si., PhD.

Dr. apt. Ni Luh Dewi Aryani, M.Si.

Dr. apt. Fahrauk Faramayuda, M.Sc.

Dr. apt. Burhan Ma'arif, M.Farm.

Dr. apt. Dewi Susanti Atmaja, S.Farm., M.Farm-Klin.

Dr. apt. Aguslina Kirtishanti, S.Si, M.Kes.

Dr. apt. Neny Purwitasari, S.Farm., M.Sc.

Dr.rer.nat. apt. Nanang Fakhruddin

Dr. apt. Adeltrudis Adelsa Danimayostu, M.Farm.Klin.

Dra. apt. Tri Murti Andayani, Sp.FRS., Ph.D.

apt. Andang Miatmoko, M.Pharm.Sci., Ph.D.

apt. Pinus Jumaryatno, S.Si., M.Phil., Ph.D.

apt. Anna Wahyuni Widayanti, MPH., Ph.D.

apt.. Lili Fitriani, S.Si, M.Pharm.SC.

apt. Aditya Trias Pradana, M.Si.

apt. Lia Laila, M.Sc

Jurnal Farmasi dan Ilmu Kefarmasian Indonesia (Pharmacy and Pharmaceutical Sciences Journal) P-ISSN: 2406-9388; E-ISSN: 2580-8303 is an official journal published by the Faculty of Pharmacy, Universitas Airlangga in collaboration with Indonesian Pharmacists Association (IAI) of East Java which the articles can be accessed and downloaded online by the public (open-access journal).

This journal is a peer-reviewed journal published three times a year on topics of excellence of research outcomes in the fields of pharmacy service and practise, community medicine, pharmaceutical technology, and health science disciplines that are closely related. This journal only accepts English-language submission. The following are the research areas that this journal focuses on

1. Clinical Pharmacy
2. Community Pharmacy
3. Pharmaceutics
4. Pharmaceutical Chemistry
5. Pharmacognosy
6. Phytochemistry

This journal receives a manuscript from the research results, systematic reviews and meta analyses that are closely related to the health sector, particularly the pharmaceutical field. Selected manuscripts for publication in this journal will be sent to two reviewers, experts in their field, who are not affiliated with the same institution as the author(s). Reviewers are chosen based on the consideration of the editorial team. Manuscripts accepted for publication are edited copies checked for the grammar, punctuation, print style, and format. The entire process of submitting manuscripts to make a final decision for publishing is conducted online.

Faculty of Pharmacy, Universitas Airlangga
Jl. Dr. Ir. H. Soekarno, Mulyorejo, Surabaya,
East Java – 60115, Indonesia
Phone. (6231) 5933150, Fax. (6231) 5932594
<http://e-journal.unair.ac.id/index.php/JFIKI>
jfiki@ff.unair.ac.id

Table of Content

No	Title	Page
1.	Optimization Using D-Optimal Design of Nanostructured Lipid Carrier (NLC) with Variation of Surfactants and Co-surfactant	1-14
	Wafa'ul Athiyyah, Widji Soeratri, Noorma Rosita, Siti Hartini Hamdan	
2.	Design and Optimization of Nanostructured Lipid Carriers for Quercetin in Skin Lightening Applications	15-25
	Ressa Marisa, Widji Soeratri, Tristiana Erawati Munandar	
3.	<i>Curcuma caesia</i>. Roxb as a Potential Inhibitor of STAT3 and EGFR: a Molecular Docking Approach in Diabetic Nephropathy	26-36
	Muhammad Farid, Shalahuddin Almaduri, Sujono Riyadi	
4.	Potassium Profile in Heart Failure Patients Before and After Hospitalization at Prof. Dr. I.G.N.G. Ngoerah Hospital	37-49
	Kadek Indra Aryani, Ni Putu Ika Swastiartha, Ni Komang Ayu Krisma Suriatha Putri, Ni Kadek Mas Ari Pratiwi, Made Suta Wahyudi, Rini Noviyani	
5.	Antiinflammatory Activity of Bangle Rhizome (<i>Zingiber purpureum</i> Roxb) Ethanol Extract on Rat Carrageenan Induced and Erythema Method	50-58
	Mia Ariasti, Muhammad Eka Putra Ramandha, Sri Winarni Sofya	
6.	Assessment of Geriatrics Patients with Cardiovascular Disease Prescriptions for Appropriateness of Medications by Using Beers Criteria in Muhammadiyah Lamongan Hospital	59-66
	Dyah Puspita Sari, Irma Susanti, Anisa Zulfa Fatihah	
7.	Antihypertensive Activity of Black Garlic Extract in Rats and Its Phytochemical Analysis using GC-MS	68-76
	Daru Estiningsih, Moch. Saiful Bachri, Laela Hayu Nurani, Muhammad Ma'ruf, Sapto Yuliani, Vivi Sofia, Dian Prasasti	

8. **Formulation and Physical Evaluation of Kratom (*Mitragyna speciosa* Korth.) Leaf Extract Emulgel as an Analgesic in Mice (*Mus musculus*)** 77-84
Iqmal Zulhakim, Kathina Deswiasqa, Jane Arantika

 9. ***In Vitro* Evaluation of Antidiabetic and Anti-Inflammatory Activities of Five Selected *Syzygium* Leaves Ethanolic Extract as Alpha-Glucosidase Inhibitors and Anti-denaturation of Bovine Serum Albumin (BSA)** 85-94
Meiliza Ekayanti, Feri Setiadi, Siti Aminah, Alam Almaaz Afandi

 10. ***In Silico* Study of Green Tea (*Camellia sinensis*) Compound as Potential Anxiolytic Drug Material Targeting Estrogen Alpha Receptor** 95-105
Harfiah Nur Aini, Susanti Susanti, Richa Mardianingrum

 11. **Influence of Hesperetin Concentration in Poloxamer P84 and TPGS Mixed Micelles on Physical Characteristics and Cytotoxicity in T47D Cell Line** 106-115
Nanda Intan Aulia, Muh. Agus Syamsur Rijal, Helmy Yusuf

 12. **Formulation, Characterization, and In Vitro Evaluation of Sunscreen Cream Containing Kenikir (*Cosmos caudatus* Kunth.) Extract and Chicken Bone Collagen Hydrolysate** 117-127
Annisa Zukhruf, Ika Qurrotul Afifah

 13. **Formulation of Lip Balm Extract of Temu Mangga Rhizome (*Curcuma mangga* Val) as Moisturizer** 128-144
Rina Andriani, Mus Ifaya, Rismayanti Fauziah, Dian Rahmaniar Trisnaputri, Wa Ode Ida Fitriah, Qur'ani
-



Optimization Using D-Optimal Design of Nanostructured Lipid Carrier (NLC) with Variation of Surfactants and Co-surfactant

Wafa'ul Athiyyah¹, Widji Soeratri^{2,3}, Noorma Rosita^{2,3*}, Siti Hartini Hamdan⁴

¹Master Program of Pharmaceutical Sciences, Faculty of Pharmacy, Universitas Airlangga, Surabaya, Indonesia

²Department of Pharmaceutical Science, Faculty of Pharmacy, Universitas Airlangga, Surabaya, Indonesia

³Skin and Cosmetic Technology Centre of Excellent, Universitas Airlangga, Surabaya, Indonesia

⁴Technical Foundation Section, Universiti Kuala Lumpur Institute of Chemical & Bioengineering Technology (MICET), Melaka, Malaysia

*Corresponding author: noorma-r@ff.unair.ac.id

Orcid ID: 0009-0006-5802-7742

Submitted: 29 August 2024

Revised: 13 January 2025

Accepted : 22 January 2025

Abstract

Background: Nanostructured lipid carriers (NLC) are topical delivery systems designed to address the challenges associated with active ingredients, such as poor solubility and limited skin penetration. NLCs incorporate surfactants, such as sorbitan monooleate and lauryl glucoside, to stabilize the system, while the addition of soy lecithin as a co-surfactant further enhances NLC stability. A D-optimal design was employed to optimize the NLC components, ensuring that the formulation achieved the desired characteristics. **Objective:** To determine the optimal NLC formulation. **Method:** Optimization was conducted using the D-optimal design method. The NLCs were prepared using the high-shear homogenization method with an Ultra-Turrax device. Characterization included measuring the particle size, polydispersity index (PDI), pH, and creaming index. **Results:** All formulations resulted in homogeneous emulsions with a white color, slight aroma of castor oil, smooth texture, and thick consistency. The particle sizes ranged from 200 to 500 nm, although the polydispersity index was not significantly influenced by surfactants or co-surfactants. All the formulations maintained an appropriate pH range for skin compatibility and product stability. The %creaming index demonstrated that the co-surfactant effectively reduced creaming in the NLCs. **Conclusion:** The optimal formulation consisted of 0.284% sorbitan monooleate, 3.429% lauryl glucoside, and 0.287% soy lecithin.

Keywords: d-optimal design, lauryl glucoside, nanostructured lipid carrier, sorbitan monooleate, soy lecithin

How to cite this article:

Athiyyah, W., Soeratri, W., Rosita, N. & Hamdan, S. H. (2025). Optimization Using D-Optimal Design of Nanostructured Lipid Carrier (NLC) with Variation of Surfactants and Co-surfactant. *Jurnal Farmasi dan Ilmu Kefarmasian Indonesia*, 12(1), 1-14. <http://doi.org/10.20473/jfiki.v12i12025.1-14>

INTRODUCTION

Nanostructured Lipid Carriers (NLC) are lipid-based delivery systems consisting of a mixture of solid and liquid lipids in an oil-in-water (O/W) system with particle sizes ranging from 50-1000 nm (Mohammadi et al., 2019). NLCs are typically used to improve physicochemical stability, such as difficulty in dissolving and penetrating the skin (Apostolou et al., 2021). The NLC system contains a combination of solid and liquid lipids of various types and concentrations that affect the HLB. It must be stabilized with surfactants and co-surfactants so that it can be stable in aqueous solvents. Emulsion stability is achieved if the required-HLB (rHLB) and HLB of surfactants/co-surfactants are close to or almost the same (Wang et al., 2023).

In a previous study by De Barros et al. (2022), NLC Quercetin was prepared using only one type of surfactant, sorbitan monooleate (HLB=4.3), and liquid lipids of five types of oils and solid lipids of myristic acid. In the characteristic test, various particle sizes were obtained (160–505 nm), while the results of the stability test showed that there was a fluctuation in PDI from 0.5 to 0.6. This is certainly an interesting finding because the HLB of the surfactant used had a range of values far from the rHLB of the lipid used.

The lipids used in this study were castor oil (HLB=14), glyceryl monostearate (HLB=5.8) and cetaryl alcohol (HLB=15.5). In the present study, the required HLB was 14.21. The combination of sorbitan monooleate (HLB=4.3) and lauryl glucoside (HLB=16) as surfactants and soy lecithin as a co-surfactant (HLB=7) can obtain a HLB that is close to the HLB required for lipids to stabilize the NLC.

Surfactants are used to reduce the surface tension between lipids and water, prevent particle aggregation, and maintain small particle sizes (Sar et al., 2019). Non-ionic surfactants such as sorbitan monooleate and lauryl glucoside are often used because they are considered safer and have lower skin irritation effects (Lechuga et al., 2023). Surfactants can affect NLC characteristics because they reduce the surface tension. When surfactants reach the critical micelle concentration (CMC), the cohesive forces between particles decrease, encapsulating the particles in micelles and forming smaller particles (Moulik et al., 2024). To obtain the appropriate HLB, sorbitan monooleate can be combined with a lauryl glucoside surfactant to produce a more stable emulsion.

Lauryl glucoside is a bio-based surfactant derived from natural sources with good solubility in water (HLB=16). It belongs to the Alkyl Polyglucoside (APG)

group and can be used to replace ethoxylated nonionic surfactants such as polysorbate (Tween) because it has a similar HLB (HLB=13-16) (Pavoni et al., 2020). Alkyl polyglucoside surfactants are better than polysorbate surfactants owing to their natural biodegradability, resistance to oxidation at room temperature, and low dermatological irritation (Wieczorek and Kwasniewska, 2020). APG surfactant also provides skin softness and hydration due to its glucose content, is gentle on the skin (Das et al., 2024), and may enhance skin penetration due to the interaction of the alkyl tail of the surfactant with lipids in the stratum corneum. The use of lauryl glucoside in leave-on cosmetic products is generally at concentrations of 0.03-8%, but it is often used below 5% to prevent excess foam.

Jafar et al. (2022) reported that the use of 2% (w/v) lauryl glucoside produces NLC with vitamin E with small particle size (280 nm), low polydispersity index (0.44), zeta potential of -28 mV, and entrapment efficiency of 95%. However, based on patch tests conducted on 24,097 people in North America, 470 people showed allergies to APG surfactants, only 35 of whom showed allergies to lauryl glucoside (Warshaw et al., 2022). In the guinea pig sensitization test, APG solution resulted in an irritation (Bhoirul et al., 2019). Moreover, several cosmetic products containing a combination of sorbitan monooleate and lauryl glucoside are available in the market, indicating that these two surfactants are compatible when combined in a product (INCI decoder, 2024).

Sorbitan monooleate and lauryl glucoside, as non-ionic surfactants, offer formulation advantages for cosmetic and pharmaceutical products. Both are stable under various conditions, such as acidic and mildly basic electrolytes, and do not react with ionic substances, especially lauryl glucoside, which is stable across pH 4-5.5 (Seweryn et al., 2019). The combination of sorbitan monooleate and lauryl glucoside allows the preparation of various emulsion systems, both oil-in-water (O/W) and water-in-oil (W/O). Sorbitan monooleate (sorbitan ester) is produced by dehydration of sorbitol. The HLB value of this surfactant decreases with increasing esterification, providing a higher solubility in lipophilic substances (Hong et al., 2018). However, sorbitan monooleate, which has a low HLB, is mostly used to prepare water-in-oil (W/O) emulsions.

Another component of NLC is the co-surfactant, which stabilizes the surfactant performance at low concentrations, making the resulting emulsion more thermodynamically stable. An example of a co-surfactant is soy lecithin. Soy lecithin has an HLB of 7-

9, which has HLB value between the HLB of sorbitan monooleate (HLB=4.3) and lauryl glucoside (HLB=16). In leave-on products, soy lecithin is usually used at low concentration (1-2%), which can stabilize 10% of the surfactant. It is commonly used at ratios of 1:1, 1:3, and 1:5. In this study, only up to 0.8% surfactant was used, assuming that the surfactant was used in the range of 3.5-4% (ratio 1:5). Thus, a combination of sorbitan monooleate and lauryl glucoside surfactants, along with the co-surfactant soy lecithin, is expected to produce NLC with optimal characteristics for nanolipid-based topical applications.

This study aims to optimize NLC formulations using castor oil, glyceryl monostearate, and cetearyl alcohol as lipid matrix with a combination of sorbitan monooleate, lauryl glucoside, and soy lecithin to achieve a stable and effective topical delivery system. A D-Optimal Design was applied to determine the optimal formula of mixture ingredients consisting of three factors (sorbitan monooleate, lauryl glucoside, and soy lecithin) and four responses (particle size, polydispersity index, pH, and creaming index). Particle size is an important characteristic parameter because it can affect the stability of NLC. Smaller particles reduce the effects of gravity and prevent sedimentation and creaming. While PDI also affects stability, a low PDI (<0.5) has a narrow particle size distribution, indicating good size uniformity, which can ensure homogeneity in the NLC systems. pH is also considered as NLC preparations are used for topical delivery; a pH closer to the skin's physiological range (4.5–5.5) ensures reduced irritation and improves skin compatibility.

MATERIALS AND METHODS

Materials and instruments

Materials used in this research are Castor Oil (Thai Castor Oil Industries Co.Ltd., Thailand), Cetearyl Alcohol (Lexemul®, Inolex, USA), Glyceryl Monostearate (CIMS, Surabaya, Indonesia), Lauryl Glucoside (Plantacare®1200UP, BASF, China), Sorbitan Monooleate (Elotant™, LG Healthcare, South Korea), Soy Lecithin Granule (Hongwan Biotechnology, China), Citric Acid Monohydrate pro analysis (Merck, Germany), Natrium Citric Dihydrate pro analysis (Merck, Germany), NaOH pellets pro analysis (Merck, Germany), Aquadest (CIMS, Surabaya, Indonesia). Instruments used in this research are Digital Ultra-Turrax IKA®T25 (Germany), Thermo Scientific Cimarec+ (USA), Analytical Balance OHAUS® (USA), Delsa™Nano C Particle Analyzer

Beckman Coulter® (USA), pH meter SI Analytics Lab 865 (Germany), Ruler.

Methods

Application of D-optimal design for NLC optimization

In this study, blank NLC containing various surfactants and cosurfactants were optimized. Different NLC formulations were prepared using a high-shear homogenization method. Owing to the mixed nature of the components under investigation, a mixed statistical design was deemed appropriate. D-Optimal was chosen as the mixture design because it does not require 1 in the total mixture (Annisa et al., 2022). In fact, if the total components are set to 1, then one of the components will be set to 1, so that in a 100% mixture containing only that ingredient, it will affect the HLB value of the system. Therefore, we prepared a system of 4% surfactant (w/w) and co-surfactant.

The three components of the surfactant and co-surfactant mixture investigated were sorbitan monooleate, lauryl glucoside, and soy lecithin. Upper and lower limits were applied to the components of the mixture to ensure that each mixture contained all three components. The same range was specified for each component of the mixture, as listed in Table 1. The responses resulting from the optimization process are listed in Table 2.

The D-optimal mixed design minimizes the variance associated with the approximate regression coefficient for the model described and is used to select the design points (Montgomery, 2013). This model was built using Design Expert software (Version 13.0.5.0, Windows 64-bit, Stat-Ease Inc., Minneapolis, 2021). A total of 15 experiments were performed (12 different design points and three replications). Design Expert is used to analyze the generated data by describing the appropriate regression model for each response, explaining how it is affected by mixed components. The significance level was set at 0.0005. The results of 15 trials (F1–F15) are presented in Table 2. The preparation and characterization of the different trials were performed accordingly.

An ANOVA test was conducted to determine the suitability of the model and the strength of the correlation between factors and responses. The model was considered suitable if it had a 'Not Significant' lack of fit (P-value >0.0005). The correlation between the factors and responses was considered strong if the correlation coefficient (R-square) was close to 1. A positive correlation coefficient indicated a positive correlation between the factors and the resulting

response. Table 5, 6, 7, and 8 present the ANOVA results.

Contour plots and 3D surfaces are essential in the Design of Experiments (DoE) for visualizing and analyzing the interactions between different factors and their effects on responses. Color variations depicted response values, with lighter shades (yellow or red) indicating higher response values and darker shades (blue or green) indicating lower response values. The contour lines represent areas with equal response values. Tightly packed contour lines indicate rapid changes in response to changes in factors, while widely spaced contour lines indicate slower changes in response.

The steps for working using D-Optimal Design are as follows:

1. The upper and lower limits of the independent variables and factors were determined for sorbitan monooleate, lauryl glucoside, and soy lecithin.
2. The responses to the test were recorded. In this study, the parameters were particle size, PDI, pH, and creaming index.
3. Fifteen optimization formulas were prepared according to their applications.
4. The obtained data were analyzed.
5. Four solutions were generated using the optimization formula. Observations were then performed again (wet-lab observations) to compare the predicted and observed data.

Table 1. Factors (mixture components) and responses to their targets

Factors and responses			HLB Values	Range of HLB values from mixed surfactants/co-surfactant	Actual values (% w/w)		Real values (Proportions)	
Variable/Mixture components					Lower bond	Upper bond	Lower bond	Upper bond
Sorbitan monooleate			4.3	13.41 – 14.74	0	0.5	0	0.125
Lauryl glucoside			16		3	3.5	0.75	0.875
Soy lecithin			7-9		0	0.8	0	0.2
Responses	Model	Goals	Constraints					
Particle Size	Special Quartic	Minimize	Below 300 nm					
Polydispersity Index (PDI)	Special Quartic	In range	0.2 up to 0.4					
pH	Linear	In range	4.5 up to 4.8					
Creaming Index	Cubic, with transform Base ¹⁰ Log, k=0.0093	Minimize	Below 10%					

Table 2. Observed response of NLC prepared according to D-optimal design

Trial formula code	Run	Mixture Components			HLB Values	Y ₁ = Particle Size (nm)	Y ₂ = Polydispersity Index	Y ₃ = pH	Y ₄ = Creaming Index (%)
		X ₁ = Sorbitan monooleate (SMO)	X ₂ = Lauryl glucoside (LG)	X ₃ = Soy lecithin (SL)					
F1	1	0.5	3.5	0	14.54	538.8	0.447	4.86	9.3
F2	2	0.1	3.23539	0.664607	14.2	295.5	0.374	4.67	0
F3	3	0.5	3.24975	0.250253	13.97	322.8	0.363	4.7	0
F4	4	0	3.41163	0.588371	14.67	362.4	0.374	4.64	0
F5	6	0	3.41163	0.588371	14.67	290.7	0.395	4.65	0
F6	7	0.164554	3.36776	0.467686	14.47	352.3	0.42	4.72	0
F7	8	0.37944	3.44052	0.180043	14.48	234.3	0.388	4.76	0
F8	9	0.332123	3.30842	0.359453	14.22	271.1	0.421	4.51	0
F9	10	0.2	3.5	0.3	14.74	205.9	0.441	4.6	2.32
F10	11	0.130975	3.06902	0.8	13.82	355.6	0.476	4.5	0
F11	14	0.317798	3	0.682202	13.53	477.4	0.375	4.55	9.3
F12	15	0.5	3.5	0	14.54	512.4	0.455	4.82	9.3
F13	13	0.130975	3.06902	0.8	13.82	356.8	0.429	4.6	0
F14	12	0.5	3	0.5	13.41	488.2	0.435	4.52	2.32
F15	5	0.270637	3.19759	0.531775	14.01	364.7	0.46	4.53	2.32

The total amount of surfactant and co-surfactant components were 4% (w/w)

Table 3. NLC optimization formula

Formula	Materials						
	Oil Phase (% w/w)				Water Phase (% w/w)		
	Castor Oil	Glyceryl Monostearate	Cetearyl Alcohol	Sorbitan Monooleate	Lauryl Glucoside	Soy Lecithin	Citrate Buffer pH 4.5±0.3
F1	6	1	3	0.5	3.5	0	86
F2	6	1	3	0.1	3.23	0.67	86
F3	6	1	3	0.3	3.25	0.25	86
F4	6	1	3	0	3.41	0.59	86
F5	6	1	3	0	3.41	0.59	86
F6	6	1	3	0.16	3.37	0.47	86
F7	6	1	3	0.38	3.44	0.18	86
F8	6	1	3	0.33	3.31	0.36	86
F9	6	1	3	0.2	3.5	0.3	86
F10	6	1	3	0.13	3.07	0.8	86
F11	6	1	3	0.32	3	0.68	86
F12	6	1	3	0.5	3.5	0	86
F13	6	1	3	0.13	3.07	0.8	86
F14	6	1	3	0.5	3	0.5	86
F15	6	1	3	0.27	3.2	0.53	86

Preparation of NLC

The NLC were prepared using a high-shear homogenization method with Ultra-Turrax with modifications (Azzahrah et al. 2022). Solid lipids (cetearyl alcohol and glyceryl monostearate) were melted at 60°C. Once the solid lipid melted, castor oil was added. The lipid phase was stirred at a low speed (200-300 rpm) using a magnetic stirrer.

Lauryl glucoside was heated until it melted (at 40°C) while the lipid phase was homogenized. Soy lecithin was dissolved in citrate buffer and homogenized using an Ultra-Turrax at 15,000 rpm for 2 min. At a temperature of 55-60°C, the melted lauryl glucoside was dissolved in the lipid phase until it was well-homogenized. Subsequently, the water and lipid phases were homogenized at 5,000 rpm using an Ultra-Turrax for two cycles of 5 min each. After homogenization, the emulsion was stirred at 16,000 rpm for 2 min. The NLC were then cooled to room temperature (25°C) while continuously stirring with a magnetic stirrer at 500 rpm.

All prepared NLCs were divided into two bottles. One set was stored at room temperature (22-25°C) for 24 h for further characterization tests (particle size, PDI, and pH), whereas the other set was stored at room temperature (22-25°C) for 14 days to assess the stability of the NLCs by observing the creaming index.

Characterization of NLC

Particle size (PS) and polydispersity index (PDI) testing

The PS and PDI of the NLC were determined as reported by Mayangsari et al. (2021) by weighing 50 mg of NLC and diluting it with 50 ml of water (1:1). The

mixture was stirred at a moderate speed (400-500 rpm) for 10 min. Then, 2 ml of the dilution was mixed with 8 ml of water and stirred again at a low speed (100-200 rpm). The mixture was then placed into a cuvette and filled to ¾ of its volume with distilled water. The analysis was performed using dynamic light scattering (DLS) with a DelsaNano instrument.

pH testing

The pH was measured by weighing 1 g of the NLC preparation and diluting it with 10 mL of CO₂-free water in a glass beaker, followed by stirring until it was evenly mixed. The pH of the solution was measured at 25 °C using a pH meter (Suzliana et al., 2020).

Creaming index testing

The creaming index was measured based on the methods described by Tan et al. (2020) and Wangpradit et al. (2022), with modifications. The NLC formulation was stored at room temperature (22-25°C) for 14 d. Changes in the organoleptic properties of the formulation were visually observed, including phase separation (Rohmah et al., 2019). Phase separation was naturally observed between the serum (transparent appearance) and the total emulsion height using a ruler. The height of the emulsions prepared in this study was 4.3 cm. The %creaming index was calculated using the following formula (Haji et al., 2023; Wangpradit et al., 2022):

$$\% \text{Creaming Index (\%CI)} = \frac{H_c}{H_e} \times 100\%$$

H_c = Height of cream layer (cm)

H_e = Height of emulsion prepared (cm)

RESULTS AND DISCUSSION

All the prepared samples appeared as white, homogeneous emulsions. All the formulas had an opaque white color, a slight characteristic odor of castor oil, a smooth texture, and a thick consistency.

Particle size testing

Measuring the particle size is essential for determining the dimensions of the particles and ensuring that they meet the desired size range. Typically, the diameter of Nanostructured Lipid Carriers (NLC) ranges from 10 to 1000 nm, with a preferred size of 50–300 nm for targeted drug delivery. For topical applications, such as hair and skin, NLCs are generally the most effective when their maximum particle size is approximately 300–500 nm (Amasya et al., 2019; Ghasemiyeh et al., 2019; Shinde et al., 2019). Although the human pore diameter ranges from 40–80 μm to 0.05–0.2 mm, achieving an NLC particle size of approximately 300 nm is crucial for optimal product stability and effectiveness.

Based on the experimental results, four formulations had particle sizes above 300 nm, six had particle sizes of approximately 300 nm, and five had particle sizes below 300 nm. It was also found that increasing the concentration of soy lecithin resulted in larger particle sizes. However, the stability of the emulsion improved, as evidenced by the decrease in the creaming index (no creaming was observed). The amphiphilic nature of lecithin, which possesses both hydrophobic and hydrophilic regions, makes it an ideal surfactant for stabilizing oil/water emulsions. By modifying the interfacial properties, lecithin helps

create a stable oil/water interface, which is crucial for maintaining emulsion stability (Tabaniag et al., 2023).

Higher concentrations of lecithin also resulted in larger particle size. This can be attributed to the formation of complex systems that grow larger owing to the dynamic exchange of lecithin molecules between particles. As this exchange occurred, larger aggregates were formed, which increased the overall particle size. The increased size occurs because lecithin molecules move from one aggregate to another, causing structural modifications in the aggregates, leading to their growth. When the lecithin concentration was high, more of these dynamic exchanges occurred, leading to the growth of larger vesicles. This exchange can lead to phase separation and structural modifications, contributing to an increase in particle size (Tabaniag et al., 2023).

Moderate amounts of lecithin helped stabilize the emulsion because excessive concentrations decreased stability. This is because excess lecithin molecules form a denser layer at the droplet interface, intensifying the attractive forces between droplets and leading to coalescence. Furthermore, aggregated molecules can act as nuclei for new droplet growth, destabilizing the emulsion (Tabaniag et al., 2023).

The analysis of variance (ANOVA) in Table 5 shows that the model is a linear mixture with a P-value of 0.0011; thus, there are significant differences in the particle size of each formula, and the Lack of Fit is “Not Significant” meaning that the model can be used for further research. An R^2 value of 0.9819 indicated a very strong relationship between the surfactant/co-surfactant and particle size.



Figure 1. The 15 NLC optimization formulas

Table 5. Analysis of variance (ANOVA) for particle size

Source	Sum of Squares	df	Mean Square	F-value	p-value	
Model	1.337E+05	8	16712.34	18.44	0.0011	significant
⁽¹⁾ Linear Mixture	29615.96	2	14807.98	16.34	0.0037	
Residual	5436.51	6	906.09			
Lack of Fit	4552.67	3	1517.56	5.15	0.1057	not significant
R²	0.9819					

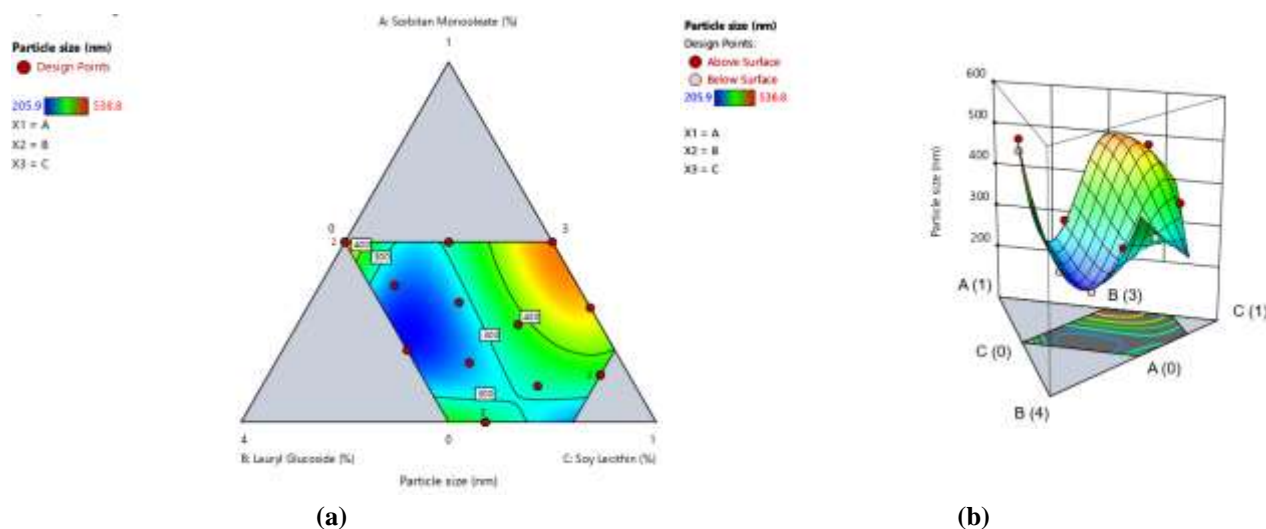


Figure 2. Contour plot (a), 3D surface diagram (b) of NLCs particles size

As shown in Figures 2 (a) and (b), the color gradient represents different particle sizes. The blue areas (205.9 nm) indicate smaller particles, whereas the red areas (538.8 nm) represent larger particles. The 3D plot shows how the particle size changed across the different factor levels. Widely spaced contour lines suggest a gradual change in particle size, indicating that small changes in factor levels do not significantly affect particle size.

Polydispersity index (PDI) testing

The polydispersity index (PDI) describes the homogeneity of a dispersion and ranges from 0 to 1 (Garcia et al., 2019; Hoseini et al., 2023). A PDI value close to 0 indicates a homogeneously dispersed formulation with monodisperse particles. The particle size and PDI were influenced by the surfactants. Theoretically, a polydisperse system is formed when the surfactant concentration is 100–1000 times greater than the minimum concentration required to form micelles. This is because excess surfactant leads to the elongation and formation of molecular links, thereby increasing the mobility of the tail groups. This destabilizes the aggregates, resulting in larger micelles with varying sizes. Consequently, this results in a high PDI,

indicating a broad particle size distribution (Nazarova et al., 2022).

Various acceptable limits have been reported, allowing the particle size distributions to be classified as narrow, relatively broad, or broad. A PDI of 0.2 is often considered indicative of a narrow distribution, and a value of 0.5 is generally regarded as the upper limit for a relatively broad distribution (Garcia et al., 2019). Based on the experimental results, all formulations had PDI values of < 0.5. However, in this study, the upper limit of the PDI was set at 0.4. Six formulations had a PDI below 0.4, and nine formulations had a PDI above 0.4. However, variations in PDI were not significantly correlated with changes in surfactant and co-surfactant concentrations.

The analysis of variance (ANOVA) in Table 6 shows that the model is a linear mixture with a P-value of 0.4216; thus, there are no differences in the polydispersity index of each formula, and the Lack of Fit is “Not Significant” meaning that the model can be used for further research. An R^2 value of 0.6165 indicated a strong relationship between the surfactant/co-surfactant and the polydispersity index.

Table 6. Analysis of variance (ANOVA) for polydispersity index

Source	Sum of Squares	Df	Mean Square	F-value	p-value	
Model	0.0113	8	0.0014	1.21	0.4216	not significant
⁽¹⁾ Linear Mixture	0.0002	2	0.0001	0.0812	0.9230	
Residual	0.0070	6	0.0012			
Lack of Fit	0.0038	3	0.0013	1.16	0.4519	not significant
R²	0.6165					

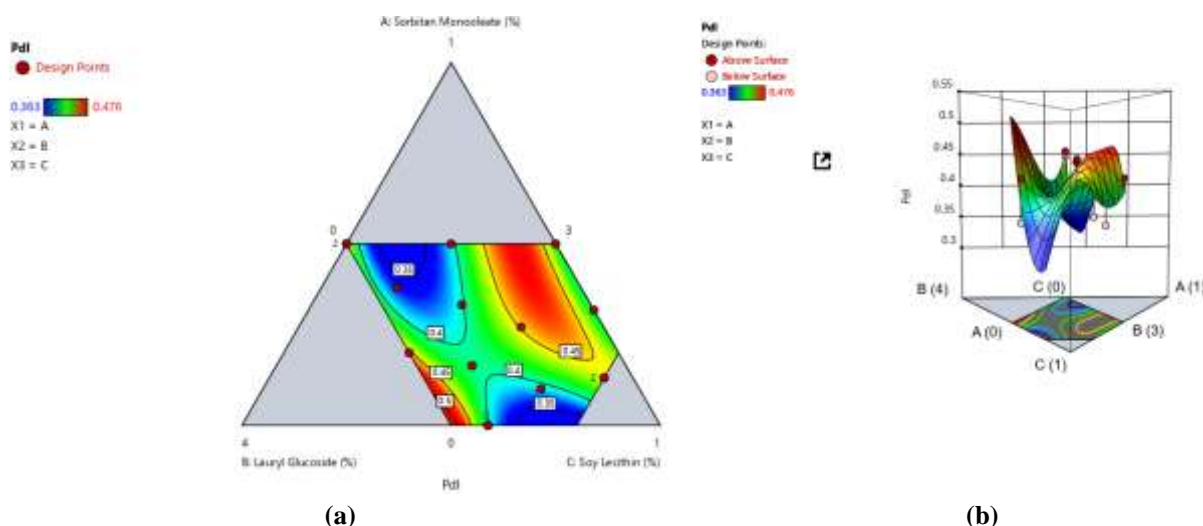


Figure 3. Contour plot (a), 3D surface diagram (b) of NLCs polydispersity index

According to Figure 3 (a) and (b), the blue areas (0.363) indicate a lower PDI, which indicates a more uniform particle size distribution. The red areas (0.476) indicate a higher PDI, indicating a broader particle-size distribution. Widely spaced contour lines suggest a gradual change in the polydispersity index, indicating that small changes in factor levels do not drastically affect the polydispersity index.

pH testing

The pH of the Nanostructured Lipid Carrier (NLC) system is crucial for ensuring its safety and compatibility with the body, particularly in the skin and mucous membrane areas. Based on the experiment, all formulations had a pH range of 4.5–4.8, which is within the safe limits for skin and formula stability. An increase in pH was observed with an increase in lauryl glucoside concentration. This was evident in F1 and F12, which exhibited higher pH levels, although they remained within the physiological pH range of the skin.

Ethoxylated surfactants, such as sorbitan monooleate, contain carboxyl groups ($-\text{COOH}$) with acidic properties; thus, increasing their concentration results in a lower pH. In contrast, alkyl glycoside surfactants, such as lauryl glucoside, contain sugars and fatty alcohols and tend to have a higher pH than ethoxylated surfactants because of their hydroxyl groups ($-\text{OH}$). The pH of dilute lauryl glucoside is typically neutral to slightly acidic or basic; however, it does not significantly alter the overall pH of the formulation. Therefore, the use of a buffer solution is recommended to maintain a stable pH level in topical products without compromising their stability.

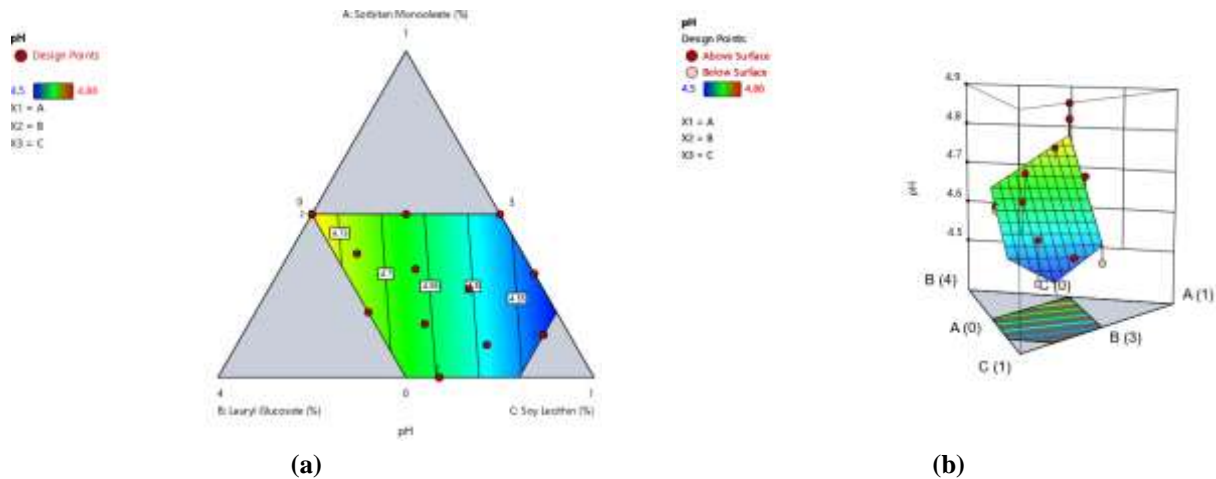
The ideal pH range for NLC systems intended for skin use is 4.5–5.5. Recent studies have shown that the normal pH of the skin surface is moderately acidic, typically ranging from 4.1–5.8, with an average value of 4.9. This acidic environment is vital for maintaining the physical, chemical, and microbiological barrier functions of the skin. Therefore, topical formulations designed to preserve and support the physiological pH of the skin at more acidic levels may provide significant benefits.

Topical formulations with low pH and sufficient buffer capacity are specifically designed to align with the skin's natural acidic environment, typically ranging from pH to 4.5–5.5. A low pH helps maintain the optimal acidic state of the skin, which is essential for preserving its barrier function and preventing microbial growth. An adequate buffer capacity ensures that the pH remains stable, even when exposed to external factors that can alter it. By combining a low pH with a robust buffer capacity, these products effectively support and stabilize the natural pH of the skin, enhance barrier integrity, promote hydration, and reduce the risk of irritation (Mehlich et al., 2021).

The analysis of variance (ANOVA) in Table 7 shows that the model is a linear mixture with a P-value of 0.0046; therefore, there are significant differences in the pH of each formula, and the Lack of Fit is “Not Significant” meaning that the model can be used for further research. The R^2 value of 0.5924 indicates a strong relationship between the surfactant/co-surfactant and the pH.

Table 7. Analysis of variance (ANOVA) for pH

Source	Sum of Squares	df	Mean Square	F-value	p-value	
Model	0.1069	2	0.0534	8.72	0.0046	significant
⁽¹⁾ Linear Mixture	0.1069	2	0.0534	8.72	0.0046	
Residual	0.0736	12	0.0061			
Lack of Fit	0.0677	9	0.0075	3.86	0.1470	not significant
R²	0.5924					

**Figure 4.** Contour plot (a), 3D surface diagram (b) of NLCs pH

As shown in Figures 4 (a) and (b), the blue areas (pH 4.5) indicate a lower pH, whereas the red areas (pH 4.86) represent a higher pH. The lack of curvature and tightly

packed lines suggest that pH is relatively stable across a range of factor combinations and shows minimal sensitivity to changes in these factors.

Creaming index testing

The creaming index was assessed by monitoring the extent of creaming in emulsions. A more stable emulsion exhibits less visible phase separation, whereas an unstable emulsion exhibits more pronounced separation (Nollet et al., 2019). Creaming occurs when oil droplets rise to the surface of an emulsion because they are less dense than the water. Creaming stability refers to an emulsion's ability to resist this separation; however, the cream layer can be easily redispersed into the emulsion by shaking it (Loi et al., 2019). The creaming indices of the emulsions were determined by visual observations. An ideal emulsion has a creaming index of 0%. However, the maximum creaming index tolerated by an emulsion is 20% (Wangpradit et al. 2022).

For some formulations, an increase in the creaming index was observed as the HLB decreased. The higher the HLB, the greater the emulsion stability, as a highly hydrophilic surfactant content forms a thick layer at the interface. An increase in the interfacial film thickness indicates the presence of van der Waals forces, which

form steric hindrance and prevent particle coalescence. However, the ability to reduce interfacial tension is considered more important than the HLB value alone (Yan et al., 2023).

Emulsion stability is evaluated by observing the extent of creaming, a phenomenon in which droplets of the dispersed phase rise to the top or settle at the bottom owing to gravitational forces, depending on their density relative to the continuous phase. A stable emulsion maintains a uniform distribution of droplets with minimal macroscopic phase separation, meaning that the droplets remain well dispersed without forming distinct layers over time. Conversely, the unstable emulsion exhibited significant creaming, where the droplets coalesced and separated from the continuous phase, resulting in visible layers. Thus, less creaming indicates a more stable emulsion, whereas more creaming indicates greater instability and a higher propensity for phase separation.

Based on the experimental results, the addition of a co-surfactant in optimal amounts prevented creaming, indicating better stability of the Nanostructured Lipid Carriers (NLC) compared to formulations without a co-surfactant. A co-surfactant is used to lower the interfacial tension and improve drug solubility in NLCs more effectively than surfactants alone (Javed et al., 2022). The use of co-surfactants with shorter chain lengths reduced the rigidity of the system and enhanced its flexibility. This decrease in particle size results from

the increased fluidity of the interfacial film, which promotes better intermicellar exchange, leading to smaller particle sizes (Waghule et al., 2019).

Soy lecithin has carbon chain lengths ranging from medium to long. To enhance the flexibility of the interfacial film, soy lecithin can be combined with other co-surfactants of short to medium chain lengths, such as poloxamer 188, which can further reduce particle size (Azzahrah et al., 2022).

The analysis of variance (ANOVA) in Table 8 showed that the model was a linear mixture with a P-value <0.0001; thus, there were significant differences in the creaming index of each formula, and the Lack of Fit was not calculated because the degree of freedom (df) was too small. The creaming index was identified as a number that was too small; therefore, it was not included as a response in subsequent research.

As shown in Figures 5 (a) and (b), the blue areas (0%) indicate no creaming, whereas the red areas (9.3%) indicate a higher degree of creaming or phase separation. Tightly packed contour lines suggest a steep change, indicating that the creaming index is highly sensitive to changes in the formulation factors. Thus, a minor modification in the concentration of surfactants, co-surfactants, or other components can significantly affect the stability of the NLC system.

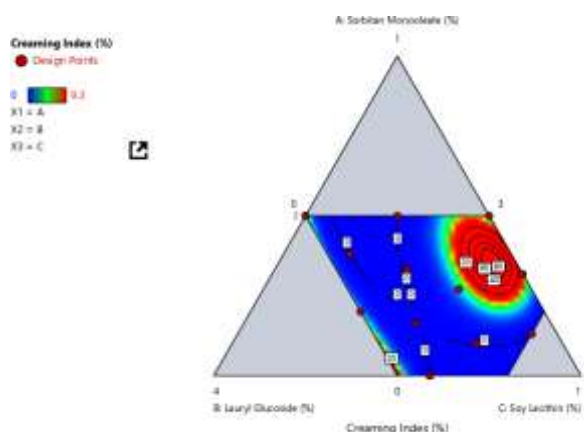
Verification of the models

A design of experiments (DoE) model was used to ensure that the solutions or formulas derived from the experiments were effective and accurate under real conditions compared to the predicted values (Vinayaka et al., 2021). The verification process involved several steps: the formulas obtained from the experiments were applied in the actual process or system to observe whether the expected results were achieved; the experiments were repeated under the same conditions used in the model to confirm that the obtained results were consistent and reproducible; and the results were compared with the predicted values from the model to verify that the difference between the predicted and actual values was minimal. This verification was crucial to ensure that the DoE model was reliable, provided real observed benefits, and enabled a more effective process optimization.

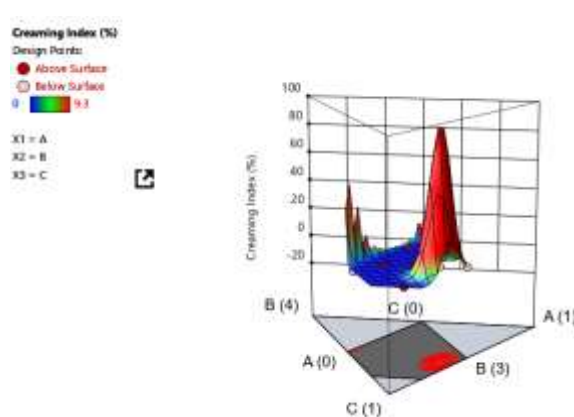
Based on the application used, the design recommended formula 1 as the optimum formula, with a desirability value of 0.976. For Equations 3 and 4, the particle sizes were not in accordance with their creaming index. Stokes' law states that the smaller the particle size, the lower the flocculation rate, which makes coalescence difficult. However, the creaming index from the observation results was still within the acceptance limit of 10%, so that the resulting emulsion was still physically stable.

Table 8. Analysis of variance (ANOVA) for creaming index

Source	Sum of Squares	df	Mean Square	F-value	p-value
Model	26.76	9	2.97	716.47	< 0.0001
⁽¹⁾ Linear Mixture	8.16	2	4.08	982.61	< 0.0001
Residual	0.0207	5	0.0041		
Lack of Fit	0.0207	2	0.0104		
R²	0.9992				



(a)



(b)

Figure 5. Contour plot (a), 3D surface diagram (b) of NLCs creaming index



Figure 6. NLCs have been prepared

Table 9. Solutions of optimal formula

No.	SMO (%)	LG (%)	SL (%)	HLB	Particle size (nm)		PDI		pH		Creaming Index (%)		Desirability
					Prediction	Observed	Prediction	Observed	Prediction	Observed	Prediction	Observed	
1	0.284	3.429	0.287	14.52	210.433	220.4±11.28	0.388	0.382±0.004	4.708	4.69±0.017	0.000	0	0.976
2	0.000	3.200	0.800	14.20	253.060	258.3±9.2	0.320	0.365±0.0012	4.554	4.51±0.025	0.000	0	0.706
3	0.125	3.352	0.523	14.46	279.817	288.1±10.33	0.400	0.374±0.002	4.644	4.67±0.031	0.000	2.3	0.463
4	0.500	3.327	0.173	14.15	282.561	277.8±10.7	0.342	0.454±0.0025	4.705	4.68±0.022	0.000	2.3	0.430

CONCLUSION

The optimal formula contained 0.284% sorbitan monooleate, 3.429% lauryl glucoside, and 0.287% soy lecithin, which showed close alignment between the observed and predicted data. This formulation achieved the desired characteristics for Nanostructured Lipid Carriers (NLC), as evidenced by their homogeneous consistency, suitable particle size, pH range, and polydispersity index. The physical stability of NLC, as indicated by the creaming index, showed that this combination of surfactant and co-surfactant effectively improved the stability of NLC and produced an optimal formula for further development.

ACKNOWLEDGMENT

We thank our supervisors for their guidance and support throughout this study. We also thank the Department of Pharmaceutical Sciences, Faculty of Pharmacy, Universitas Airlangga for providing the necessary resources and facilities.

AUTHOR CONTRIBUTIONS

Conceptualization, W.A., W.S., N.R.; Methodology, W.A., W.S., N.R.; Software, W.A.; Validation, W.A., W.S., N.R.; Formal Analysis, W.A.; Investigation, W.A., W.S., N.R.; Resources, W.A., W.S., N.R.; Data Curation, W.A., W.S., N.R.; Writing - Original Draft, W.A., W.S., N.R.; Writing - Review & Editing, W.A., W.S., N.R.; Visualization, W.A.; Supervision, W.S., N.R.; Project Administration, W.S., N.R.; Funding Acquisition, W.A.

CONFLICT OF INTEREST

The authors declare that they have no conflicts of interest.

REFERENCES

- Amasya, G., Aksu, B., Badilli, U., Onay-Besikci, A. & Tarimci, N., (2019). Qbd Guided Early Pharmaceutical Development Study: Production of Lipid Nanoparticles by High Pressure Homogenization for Skin Cancer Treatment. *International Journal of Pharmaceutics*; 563; 110-121. doi: 10.1016/j.ijpharm.2019.03.056.
- Annisa, R., Mutiah, R., Yuwono, M. & Hendradi, E. (2022). The Development Formulation of *Eleutherine palmifolia* Extract-Loaded Self-Nanoemulsifying Drug Delivery System (SNEDDS) using D-Optimal Mixture Design Approach. *International Journal of Applied Pharmaceutics*; 15; 1-8. doi: 10.22159/ijap.2023v15i5.47645.
- Apostolou, M., Assi, S., Fatokun, A.A. & Khan, I., (2021). The Effects of Solid and Liquid Lipids on the Physicochemical Properties of Nanostructured Lipid Carriers. *Journal of Pharmaceutical Sciences*; 110; 2859-2872. doi: 10.1016/j.xphs.2021.04.012.
- Azzahrah, R., Rosita, N., Purwanto, D.A. & Soeratri, W. (2022). The Effect of Decyl Glucoside on Stability and Irritability of Nanostructured Lipid Carriers-Green Tea Extract as Topical Preparations. *Pharmacy & Pharmaceutical Sciences Journal/Jurnal Farmasi Dan Ilmu Kefarmasian Indonesia*; 9; 220-228. doi: 10.20473/jfiki.v9i32022.220-228.
- Bhojyul, B., Solman, L., Kirk, S., Orton, D. & Wilkinson, M. (2019). Patch Testing with Alkyl Glucosides: Concomitant Reactions are Common but not Ubiquitous. *Contact Dermatitis*; 80(5); 286-290. doi: 10.1111/cod.13186.
- Das, R., Mallik, N., Adhikari, A. & Bhattarai, A. (2024). A Comprehensive Review on the Creation, Description, and Utilization of Surfactants Containing Multiple Hydroxyl Groups. *International Journal of Polymer Science*; 2024; 1-31. doi: 10.1155/2024/6120535.
- Garcia, N.O., Fernandes, C.P. & da Conceição, E.C. (2019). Is it Possible to Obtain Nanodispersions with Jaboticaba Peel's Extract Using Low Energy Methods and Absence of Any High Cost Equipment? *Food Chemistry*; 276; 475-484. doi: 10.1016/j.foodchem.2018.10.037.
- Ghasemiyeh, P., Azadi, A., Daneshamouz, S., Heidari, R., Azarpira, N. & Mohammadi-Samani, S. (2019). Cyproterone Acetate-Loaded Nanostructured Lipid Carriers: Effect of Particle Size on Skin Penetration and Follicular Targeting. *Pharmaceutical Development and Technology*; 24; 812-823. doi: 10.1080/10837450.2019.1596133.
- Haji, M., Hosseinzadeh, M., Jahangiri, Y., Farajzadeh, Z., Sufiani, A.M., Olyaei, Y.A., Namarvar, B.B., Ghaffari, T. & Olyaei, N.A. (2023). Ghee Based Nanostructured Lipid Carriers (Nlcs) with Improved Wound-Healing Effects: Ghee Based Nanostructured Lipid Carriers (Nlcs). *Iranian Journal of Pharmaceutical*

- Sciences*; 19; 293-303. doi: 10.22037/ijps.v19i4.42194.
- Hoseini, B., Jaafari, M.R., Golabpour, A., Momtazi-Borojeni, A.A., Karimi, M. & Eslami, S. (2023). Application of Ensemble Machine Learning Approach to Assess the Factors Affecting Size and Polydispersity Index of Liposomal Nanoparticles. *Scientific Reports*; 13; 1-11. doi: 10.1038/s41598-023-43689-4.
- Jafar, G., Salsabilla, S. & Santoso, R. (2022). Development and Characterization of Compritol Ato® Base in Nanostructured Lipid Carriers Formulation with the Probe Sonication Method. *International Journal of Applied Pharmaceutics*; 14; 64-66. doi: 10.22159/ijap.2022.v14s4.PP04.
- Javed, S., Mangla, B., Almoshari, Y., Sultan, M.H. & Ahsan, W. (2022). Nanostructured Lipid Carrier System: A Compendium of Their Formulation Development Approaches, Optimization Strategies by Quality by Design, and Recent Applications in Drug Delivery. *Nanotechnology Reviews*; 11; 1744-1777. doi: 10.1515/ntrev-2022-0109.
- Lechuga, M., Avila-Sierra, A., Lobato-Guarnido, I., García-López, A.I., Ríos, F. & Fernández-Serrano, M. (2023). Mitigating the Skin Irritation Potential of Mixtures of Anionic and Non-Ionic Surfactants by Incorporating Low-Toxicity Silica Nanoparticles. *Journal of Molecular Liquids*; 383; 1-10. doi: 10.1016/j.molliq.2023.122021.
- Loi, C.C., Eyres, G.T. & Birch, E.J. (2019). Effect of Mono-and Diglycerides on Physical Properties and Stability of a Protein-Stabilised Oil-In-Water Emulsion. *Journal of Food Engineering*; 240; 56-64. doi: 10.1016/j.jfoodeng.2018.07.016.
- Mayangsari, F.D., Erawati, T., Soeratri, W. & Rosita, N. (2021). Karakteristik dan Stabilitas Fisik NLC-Koenzim Q10 dalam Sleeping Mask dengan Minyak Nilam. *Jurnal Farmasi Dan Ilmu Kefarmasian Indonesia*; 8; 178-186. doi: 10.20473/jfiki.v8i22021.178-186.
- Mohammadi, M., Assadpour, E. & Jafari, S.M. (2019). Encapsulation of Food Ingredients by Nanostructured Lipid Carriers (NLCs). in Jafari, S.M. (Ed.). *Lipid-based Nanostructures for Food Encapsulation Purposes*. Academic Press; 2; 217-270. doi: 10.1016/B978-0-12-815673-5.00007-6.
- Moulik, S.P., Rakshit, A.K. & Naskar, B. (2024). Physical Chemical Properties of Surfactants in Solution and Their Applications: A Comprehensive Account. *Journal of Surfactants and Detergents*; 27; 895-925. doi: 10.1002/jsde.12757.
- Nazarova, A., Yakimova, L., Filimonova, D. & Stoikov, I. (2022). Surfactant Effect on the Physicochemical Characteristics of Solid Lipid Nanoparticles Based on Pillar [5] Arenes. *International Journal of Molecular Sciences*; 23; 1-14. doi: 10.3390/ijms23020779.
- Nollet, M., Boulghobra, H., Calligaro, E. & Rodier, J.D. (2019). An Efficient Method to Determine The Hydrophile - Lipophile Balance of Surfactants Using the Phase Inversion Temperature Deviation of Cie/N - Octane/Water Emulsions. *International Journal of Cosmetic Science*; 41; 99-108. doi: 10.1111/ics.12516.
- Pavoni, L., Perinelli, D.R., Ciacciarelli, A., Quassinti, L., Bramucci, M., Miano, A., Casettari, L., Cespi, M., Bonacucina, G. & Palmieri, G.F. (2020). Properties and Stability of Nanoemulsions: How Relevant is the Type of Surfactant?. *Journal of Drug Delivery Science and Technology*; 58; 1-9. doi: 10.1016/j.jddst.2020.101772.
- Rohmah, M., Raharjo, S., Hidayat, C. & Martien, R. (2019). Formulasi dan Stabilitas Nanostructured Lipid Carrier dari Campuran Fraksi Stearin dan Olein Minyak Kelapa Sawit. *Jurnal Aplikasi Teknologi Pangan*; 8; 23-30. doi: 10.17728/jatp.3722.
- Seweryn, A., Klimaszewska, E. and Ogorzałek, M., 2019. Improvement in the Safety of Use of Hand Dishwashing Liquids Through the Addition of Sulfonic Derivatives of Alkyl Polyglucosides. *Journal of Surfactants and Detergents*; 22; 743-750. doi: 10.1002/jsde.12299.
- Sar, P., Ghosh, A., Scarso, A. & Saha, B. (2019). Surfactant for Better Tomorrow: Applied Aspect of Surfactant Aggregates from Laboratory to Industry. *Research on Chemical Intermediates*; 45; 6021-6041. doi: 10.1007/s11164-019-04017-6.
- Shinde, U.A., Parmar, S.J. & Easwaran, S. (2019). Metronidazole-Loaded Nanostructured Lipid Carriers to Improve Skin Deposition and

- Retention in the Treatment Of Rosacea. *Drug Development and Industrial Pharmacy*; 45; 1039-1051. doi: 10.1080/03639045.2019.1569026.
- Suzliana, R.M., Erawati, T., Prakoeswa, C.R.S., Rantam, F.A. and Soeratri, W. (2020). Pengaruh Asam Hialuronat-Space Peptide terhadap Karakteristik, Stabilitas Fisik Gel Amniotic Membran-Stemcell Metabolite Product. *Jurnal Farmasi dan Ilmu Kefarmasian Indonesia*; 7; 66-73. doi: 10.20473/jfiki.v7i22020.66-73.
- Tabaniag, J.S.U., Abad, M.Q.D., Morcelos, C.J.R., Geraldino, G.V.B., Alvarado, J.L.M. & Lopez, E.C.R. (2023). Stabilization of Oil/Water Emulsions Using Soybean Lecithin as a Biobased Surfactant for Enhanced Oil Recovery. *Journal of Engineering and Applied Science*; 70; 1-26. doi: 10.1186/s44147-023-00322-5.
- Tan, C.C., Karim, A.A., Uthumporn, U. & Ghazali, F.C. (2020). Effect of Thermal Treatment on the Physicochemical Properties of Emulsion Stabilized by Gelatin From Black Tilapia (*Oreochromis Mossambicus*) Skin. *Food Biophysics*; 15; 423-432. doi: 10.1007/s11483-020-09638-8.
- Vinayaka, A.S., Mahanty, B., Rene, E.R. & Behera, S.K. (2021). Biodiesel Production by Transesterification of a Mixture of Pongamia and Neem Oils. *Biofuels*; 12; 187-195. doi: 10.1080/17597269.2018.1464874.
- Waghule, T., Rapalli, V.K., Singhvi, G., Manchanda, P., Hans, N., Dubey, S.K., Hasnain, M.S. & Nayak, A.K. (2019). Voriconazole Loaded Nanostructured Lipid Carriers Based Topical Delivery System: Qbd Based Designing, Characterization, in-Vitro and ex-Vivo Evaluation. *Journal of Drug Delivery Science and Technology*; 52; 303-315. doi: 10.1016/j.jddst.2019.04.026.
- Wang, Q., Zhang, H., Han, Y., Cui, Y. & Han, X. (2023). Study on the Relationships Between the Oil HLB Value and Emulsion Stabilization. *RSC Advances*; 13; 24692-24698. doi: 10.1039/D3RA04592G.
- Wangpradit, N., Macha, S., Phooteh, N., Yusohyo, N., Waedoloh, A. & Manee, S. (2022). Determination of Required Hydrophilic-Lipophilic Balance of Amesiodendron Chinense (Merr.) Hu Oil and Development of Stable Cream Formulation. *OCL*; 29; 1-8. doi: 10.1051/ocl/2022011
- Warshaw, E.M., Xiong, M., Atwater, A.R., DeKoven, J.G., Pratt, M.D., Maibach, H.I., Taylor, J.S., Belsito, D.V., Silverberg, J.I., Reeder, M.J. & Zug, K.A. (2022). Patch Testing with Glucosides: The North American Contact Dermatitis Group Experience, 2009-2018. *Journal of the American Academy of Dermatology*; 87; 1033-1041. doi: 10.1016/j.jaad.2022.04.058.
- Wieczorek, D. & Kwasniewska, D. (2020). Novel Trends in Technology of Surfactants. In: Chemical Technologies and Processes 223-250. Berlin: Walter de Gruyter GmbH.
- Yan, G., Wang, S., Li, Y., He, L., Li, Y. & Zhang, L. (2023). Effect of Emulsifier HLB on Aerated Emulsions: Stability, Interfacial Behavior, and Aeration Properties. *Journal of Food Engineering*; 351; 1-8. doi: 10.1016/j.jfoodeng.2023.111505.



Design and Optimization of Nanostructured Lipid Carriers for Quercetin in Skin Lightening Applications

Ressa Marisa¹, Widji Soeratri^{2,3*}, Tristiana Erawati Munandar^{2,3}

¹Master Program of Pharmaceutical Sciences, Faculty of Pharmacy, Universitas Airlangga, Surabaya, Indonesia

²Department of Pharmaceutical Sciences, Faculty of Pharmacy, Universitas Airlangga, Surabaya, Indonesia

³Skin and Cosmetic Technology Centre of Excellent, Universitas Airlangga, Surabaya, Indonesia

*Corresponding author: widji.soeratri@yahoo.com

Orcid ID: 0000-0002-7382-6597

Submitted: 30 September 2024

Revised: 14 January 2025

Accepted : 6 February 2025

Abstract

Background: Quercetin, a potential skin-lightening agent, reduces intracellular and fungal tyrosinase activity. However, its poor water solubility and limited skin permeability hinder its application. Nanostructured lipid carriers (NLCs), composed of biocompatible and biodegradable lipids, enhance drug stability and skin penetration. Lipid type, surfactant concentration, and formulation parameters influence NLC stability. **Objective:** This study aimed to optimize NLC formulations for quercetin delivery by evaluating organoleptic properties, particle size, polydispersity index (PDI), and pH. **Method:** NLCs was prepared using 10% total lipids (4% solid and 6% liquid lipids) and surfactant mixtures at varying concentrations via High Shear Homogenization. Initial formulations using myristic acid and castor oil were unstable, undergoing phase separation within five days. **Results:** Substituting the solid lipid with a 1:3 combination of beeswax and cocoa butter produced a stable formulation during storage. The lipid and surfactant composition significantly influenced particle size and PDI. While pH remained stable, statistical analysis revealed significant changes in particle size and PDI across formulations. **Conclusion:** Optimized NLC formulations for quercetin delivery demonstrated improved stability and potential for effective skin-lightening applications. Further research is warranted to evaluate in vivo efficacy and scalability.

Keywords: quercetin, NLC, formula optimization, cosmetic delivery system, skin lightening

How to cite this article:

Marisa, R., Soeratri, W. & Munandar, T. E. (2025). Design and Optimization of Nanostructured Lipid Carriers for Quercetin in Skin Lightening Applications. *Jurnal Farmasi dan Ilmu Kefarmasian Indonesia*, 12(1), 15-25. <http://doi.org/10.20473/jfiki.v12i12025.15-25>.

INTRODUCTION

Melanin levels, which determine skin color, vary due to genetic factors and environmental influences like sun exposure. While melanin protects against skin damage, its excessive accumulation can lead to hyperpigmentation, causing aesthetic concerns. Conditions like melasma, freckles, and age spots often result from prolonged UV exposure, which increases reactive oxygen species (ROS) and triggers inflammatory responses (Choi & Shin, 2016).

Quercetin, a naturally occurring flavonoid in fruits and vegetables, has demonstrated potent anti-tyrosinase and antioxidant properties, making it a promising candidate for skin-lightening applications. Compared to conventional agents like kojic acid and arbutin, quercetin exhibits superior anti-tyrosinase activity ($IC_{50} 1.59 \pm 0.38 \mu\text{g/mL}$ vs. $98.14 \pm 1.45 \mu\text{g/mL}$ for arbutin) but suffers from poor water solubility and limited skin penetration (Hatahet et al., 2016; Lu et al., 2019). These limitations necessitate advanced delivery systems to improve its stability, bioavailability, and efficacy.

Nanostructured Lipid Carriers (NLCs) offer a promising solution, leveraging biocompatible and biodegradable lipids to enhance drug stability and penetration through the skin. The stability of NLCs depends on formulation parameters such as lipid type, surfactant concentration, and particle size distribution. Smaller, uniformly distributed particles (<0.5 PDI) are associated with enhanced stability and reduced aggregation (de Barros et al., 2022). However, physical instability, including creaming, phase separation, or sedimentation, remains a challenge. Factors such as viscosity, lipid crystallization, and storage conditions significantly impact NLC performance and require careful optimization (Sakellari et al., 2021).

Myristic acid, as a solid lipid, has a fairly high melting point and excellent crystal properties, so it can provide stability to the NLC system. However, the use of myristic acid also has limitations related to the retention and release capabilities of active ingredients. Research shows that myristic acid can reduce the process of molecular diffusion but is not always optimal in increasing the encapsulation efficiency of bioactive compounds. This can cause physical instability if not balanced with appropriate liquid lipids (Husnawiyah et al., 2023).

Beeswax and oleum cacao present an intriguing substitute for solid lipids in NLC formulations. This combination not only provides better stability but also

improves the emollient properties of the final product. Beeswax has the ability to form a beneficial film on the skin surface, while oleum cacao is known for its moisturizing properties. This combination can improve the retention of active ingredients and reduce the risk of creaming or phase separation during storage (Khasanah & Rochman, 2022). The physical stability of NLC using a beeswax-oleum cacao combination tends to be superior compared to the use of myristic acid. Research shows that this solid lipid replacement can reduce particle size and improve particle distribution in the system. Smaller particle size contributes to increased stability because it reduces the potential for aggregation. In addition, beeswax can help stabilize the interface between solid and liquid lipids, thereby preventing recrystallization (Husnawiyah et al., 2023).

This study aims to optimize NLC formulations for quercetin delivery by evaluating key parameters, including organoleptic properties, particle size, polydispersity index (PDI), and pH. The findings will contribute to the development of stable and effective delivery systems for skin-lightening applications.

MATERIALS AND METHODS

Material

Quercetin (Sigma-Aldrich, Germany), Beeswax (Sigma-Aldrich, China), Cocoa Butter (PT Darjeeling Sembrani Aroma, Indonesia), Myristic Acid (Sisco Research Laboratories PVT. LTD, India), Castor Oil (Sigma-Aldrich, China), Tween 80 (Sigma-Aldrich, Germany), Span 80 (Sigma-Aldrich, Germany), Propylene Glycol (Supelco, Germany), Phenoxyethanol (Raja Kimia, Indonesia), Potassium Dihydrogen Phosphate (Merck, Germany), and Potassium Hydroxide (Merck, Germany).

Method

Procedure for making NLC

NLC Quercetin was produced by amalgamating the aqueous and lipid phases utilizing a high-speed stirrer. This study employed the Ultra Turrax IKA®T25 Digital High Shear Homogenizer. The oil phase was created by melting myristic acid or beeswax-cocoa butter, castor oil, and Span 80, at approximately 70°C using a hotplate stirrer. The aqueous phase consisted of Tween 80, propylene glycol, phenoxyethanol, and phosphate buffer at pH 5. After mixing the two ingredients in a single beaker until they completely blended, the mixture was heated to 70°C. After the oil phase was ready, the water phase was added slowly. The mixture was stirred for 10 minutes using an Ultra Turrax IKA® T25 Digital High Shear Homogeniser at a speed of 5000 rpm.

Table 1. Optimization of NLC formula composition (% w/w)

Composition	Function	F1	F2	F3	F4	F5	F6
Myristic Acid	Solid lipids	4	4	6	6	-	-
Beeswax	Solid lipids	-	-	-	-	1	1
Oleum Cacao	Solid lipids	-	-	-	-	3	3
Castor Oil	Liquid lipids	6	6	4	4	6	6
Span 80	Surfactants	2.02	2.02	2.47	2.47	5.05	6.73
Tween 80	Surfactants	9.98	9.98	9.53	9.53	9.95	13.27
Propylene glycol	Co-Surfactants	3.5	10	3.5	10	5.0	5.0
Phenoxyethanol	Preservatives	0.5	0.5	0.5	0.5	0.5	0.5
Phosphate buffer pH 5 ad	Aqueous phase	100	100	100	100	100	100

The velocity was then increased to 16,000 rpm and stirred for 2 minutes. Stirring was continued with a hotplate stirrer at a speed of 500 rpm until the hotplate stirrer reached approximately 25°C (Mayangsari et al., 2021).

Physical characteristics testing procedure

Organoleptic

Organoleptic evaluation employs the five senses to evaluate color, aroma, texture, and potential phase separation (Mayangsari et al., 2021).

Particle size and polydispersity index (IP)

The preliminary stage entails the dilution of the formulation. Weigh 50 mg of the sample using an analytical balance and subsequently add distilled water to reach a final volume of 50.0 mL. A magnetic stirrer mixes the solution at 500 revolutions per minute for 10 minutes. Subsequently, take 2.0 mL of the solution and include 8 mL of distilled water. Stir the mixture again for 10 minutes at a velocity of 100 revolutions per minute. The next step involves using the DelsaTM nano submicron particle size analyzer to evaluate the particle size and polydispersity index (Mayangsari et al., 2021).

pH.

Calibrate the pH meter using a standard solution of pH 7.0 before assessing the sample's pH value and then clean and dry the electrode. The subsequent stage involves diluting the sample with distilled water at a ratio of 1:9. The pH is measured via the SI Analytics pH Meter Lab 855 (Mayangsari et al., 2021).

Real time test

This investigation involved a real-time physical stability assessment of preparations stored in an air-conditioned room at a temperature of 20°C ± 1°C, with a relative humidity of 65% and shielded from sunlight. The examination was administered over a duration of three months (90 days). The stability test evaluated organoleptic properties, particle size, polydispersity index (PDI), and pH value. The assessment was performed on days 0, 30, 60, and 90 (Mayangsari et al., 2021).

Statistical analysis

The data use the one-way analysis of variance (ANOVA) method to statistically evaluate physical characteristic parameters. This strategy is employed when the data are homogeneous and regularly distributed. Alternatively, you can employ non-parametric statistical tests, specifically the Kruskal-Wallis test with a post hoc test.

RESULTS AND DISCUSSION

Organoleptic

Table 2 illustrates that organoleptic assessments of the formulations (F1-F4) indicated that NLC had a white hue, possessed a distinct odor, and presented a semi-solid consistency with a soft texture. Creaming, oil phase separation, and sedimentation of high-density components are all examples of physical instability in emulsion-based carrier systems. Table 2 illustrates the phase separation occurring during storage, with a distinct layer at the bottom signifying system instability on the fifth day. Creaming in NLC systems refers to the phenomenon where lipid particles in suspension ascend and create a creamy layer above the dispersion system. Inadequate surfactant levels necessary for sustaining the NLC system during the storage duration may result in phase separation (Suyuti et al., 2023). The lipid-to-surfactant ratio significantly impacts the stability of the system, highlighting the crucial role of surfactants in stabilizing the NLC system. Surfactants can rapidly decrease surface tension, inhibit particle aggregation, and prevent recrystallization. Additional research has indicated that the concentration and type of surfactants can influence the stability of the NLC system. The surfactant-to-oil ratio and the specific type of oil can influence the stability of the colloidal dispersion system.

This can establish macroscopic carrier systems at lipid to surfactant ratios above 1:2, but the process for NLC formation also influences this. Elevated surfactant concentrations facilitate the formulation of lipid-based carrier systems. Low-density lipids can influence



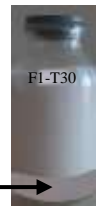
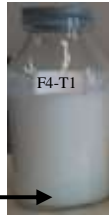


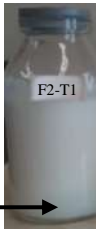
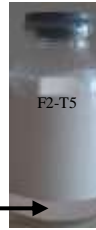
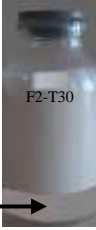



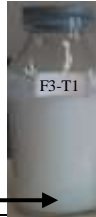

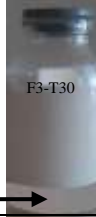



system stability, leading to creaming, flocculation, and coalescence (Rohmah et al., 2019).

The calculated HLB ratio for formulas (F1-F2) was 13.20; (F3-F4) was 12.8; and formulas (F5-F6) were 11.40. The difference in HLB values was mainly due to the difference in the composition of solid lipids of myristic acid (HLB = 12) used. In F1-F4, the ratio of the amount of solid lipids: liquid lipids (4:6) in formulas (F1-F2) and (6:4) in formulas (F3-F4). While in formulas (F5-F6), researchers replaced the type of solid lipids used with beeswax (HLB = 12) and cocoa butter (HLB = 6) with a ratio of the amount of solid lipids: liquid lipids (4:6). The HLB value affects the interfacial tension between oil and water. The right HLB value reduces the interfacial tension, thereby increasing the stability of the emulsion. Conversely, an inappropriate HLB value increases the interfacial tension, thereby accelerating coalescence and the formation of cream droplets (Smejkal et al., 2024). Solid lipids such as cacao butter or myristic acid have different crystal forms, which affect the physical properties and stability of NLCs. More stable crystal forms (such as beta cacao butter) ensure that the particles are stable and prevent coalescence or agglomeration. Oleum cacao has polymorphic forms that result in high entrapment but are less stable on storage. While beeswax base has a more regular crystal lattice than oleum cacao, the combination of oleum cacao and beeswax produces smaller particles

than when the two lipids are used separately. Oleum cacao and beeswax are used in a ratio of 75:25 because it produces a low crystallinity index, as opposed to the combinations of 25:75 and 50:50. This will increase the stability of NLCs (Munandar Erawati et al., 2023). Fluctuations in cosurfactant concentration and composition can markedly influence the stability of NLC. Research indicates that fluctuations in cosurfactant concentration and composition significantly influence the stability of NLC by diminishing the surface tension between the oil and water phases, hence decreasing the likelihood of particle aggregation and recrystallization. Elevated quantities of cosurfactants can enhance stability by preserving the surface equilibrium of the emulsifying particles (Rahmi et al., 2013).

Table 2 illustrates that the organoleptic assessment of formulas (F5-F6) revealed that the NLC was white, had a distinct odor, exhibited a semi-solid consistency, had a soft texture, and demonstrated no phase separation after storage. The crystallinity index denotes the regularity and density of the crystalline structure within the material. Solid lipids with a high crystallinity index in NLC exhibit a more uniform and stable crystalline architecture, enhancing the physical stability of the particles. The denser crystalline structure inhibits lipid diffusion and migration, hence enhancing system stability (Dragicevic & Maibach, 2016).

Table 2. Results of NLC-0 observations during storage (F1-F6)

Day	1	5	30	Day	1	5	30
F1				F4			
							
							
F2				F5			
F3				F6			

Solid lipids, such as cacao butter and myristic acid, have different crystalline structures that affect how they behave physically and how stable they are as nanostructured lipid carriers (NLCs). More stable crystalline structures (such as the beta polymorph of cocoa butter) guarantee particle stability and inhibit coalescence or agglomeration. Oleum cacao exhibits a polymorphic structure that facilitates substantial trapping yet demonstrates reduced stability during storage. The beeswax basis possesses a more uniform crystal lattice compared to oleum cacao; nonetheless, the amalgamation of oleum cacao and beeswax results in smaller particles than when the two lipids are utilized independently. Oleum cacao and beeswax are utilized in a 75:25 ratio, as this configuration yields a low crystallinity index, unlike the 25:75 and 50:50 combinations. This will enhance the entrapment efficiency (Munandar Erawati et al., 2023). Myristic acid is a saturated fatty acid including 14 carbon atoms. Its crystal structure is comparatively uncomplicated in relation to cacao butter or beeswax. Myristic acid crystals exhibit a more regular and denser structure compared to beeswax; however, they may be less intricate than cacao butter. In comparison to beeswax, myristic acid often exhibits a greater crystallinity index; however, it may be lower than that of cacao butter, mostly due to differences in crystal morphology and the intricate lipid composition of cacao butter (Müller & Careglio, 2018).

Lipids with a high crystallinity index tend to make particles in NLCs that are more stable and uniform. On the other hand, a more ordered crystalline structure can

reduce the range of particle sizes and improve the stability of particle sizes in formulations. Systems exhibiting a high crystallinity index typically possess narrower and more uniform particle size distributions. Having lipids with a solid crystalline structure makes NLCs more stable by lowering the chance of them creaming or settling. Moreover, a solid crystalline structure diminishes the probability of particle size alterations during storage and aids in safeguarding the active ingredient from degradation. The chemical stability of the active substance encapsulated in the lipid matrix can be enhanced by an increased crystallinity index (Da Silva & Martini, 2024).

Characterization of particle size and polydispersity index (IP)

The particle measurement results show that decreasing the amount of cosurfactant in formulations (F1–F2) and (F3–F4) makes the particle sizes smaller. Nevertheless, augmenting the quantity of solid lipids (F1–F4) can enhance the dimensions of NLC particles (Table 3). The particle size of the overall formula (F1–F6) ranges from 153.9 to 259.5 nm, which complies with the NLC particle size specifications of 10–1000 nm (Suyuti et al., 2023). The statistical analysis using GraphPad Prism 10 (F1–F6) in the NLC system (Figure 1) showed that particle sizes very different between the formulas. The only formulas that didn't show any significant differences (F1 and F2), (F1 and F4), (F2 and F4), and (F5 and F6). The results indicated that F5–F6 yielded the lowest particle size compared to other formulations utilizing various forms of solid lipids (F1–F4).

Table 3. Characterization results of particle size and PDI of NLC-0

Formula	Replication	Particle size (nm)	Mean \pm SD	PDI	Mean \pm SD	pH	Mean \pm SD
F1	R1	229.7	232.0 \pm 2.4	0.308	0.312 \pm 0.004	5.181	5.180 \pm 0.001
	R2	231.8		0.315		5.180	
	R3	234.4		0.314		5.179	
F2	R1	229.7	229.4 \pm 0.3	0.233	0.230 \pm 0.003	5.173	5.170 \pm 0.003
	R2	229.1		0.229		5.170	
	R3	229.5		0.227		5.167	
F3	R1	258.9	258.7 \pm 0.9	0.383	0.386 \pm 0.008	5.170	5.169 \pm 0.001
	R2	259.5		0.395		5.168	
	R3	257.7		0.379		5.169	
F4	R1	239.7	240.8 \pm 1.1	0.378	0.361 \pm 0.019	5.178	5.177 \pm 0.002
	R2	241.8		0.340		5.179	
	R3	240.8		0.365		5.175	
F5	R1	177.6	170.3 \pm 7.6	0.300	0.326 \pm 0.032	5.320	5.347 \pm 0.055
	R2	162.5		0.317		5.410	
	R3	170.7		0.362		5.310	
F6	R1	153.9	169.1 \pm 17.8	0.014	0.074 \pm 0.100	5.410	5.387 \pm 0.021
	R2	164.7		0.189		5.381	
	R3	188.7		0.018		5.370	

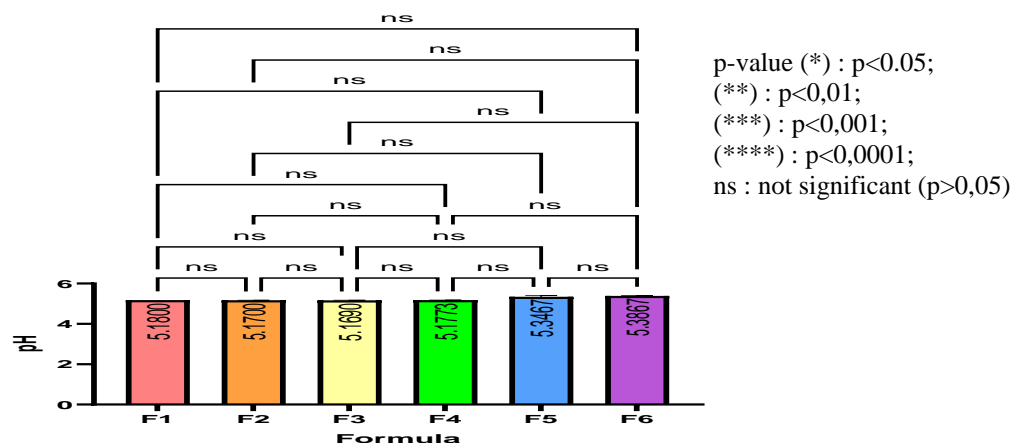


Figure 3. pH F1-F6 (data are the average of 3 replications \pm SD)

Surfactants reduce the surface tension between the lipid and water phases, facilitating the production of smaller particles during homogenization. The ideal quantity of surfactant can yield particles of reduced dimensions and a more homogeneous size distribution. Surfactants function to stabilize the produced particles by creating a protective coating surrounding the lipid particles. Insufficient surfactant can lead to particle aggregation, resulting in increased particle sizes and a broader particle size dispersion. Excessive surfactant concentration may lead to micelle formation, which can disrupt lipid particle formation and produce a broader particle size distribution (Fitriani et al., 2024).

Characterization of pH

The NLC formula was carried out by evaluating the pH of formulations F1-F6 (Table 4). The pH of the NLC formulation varied between 5.17 and 5.41. This is attributable to the presence of a phosphate buffer at pH 5 as the carrier solution, which corresponds to the utilized pH buffer, namely pH 5 ± 0.5 . The purpose of applying a pH buffer is to preserve the pH stability of the active ingredient. Furthermore, pH testing is essential to avert skin irritation and dryness. An excessively acidic pH may induce irritation and stinging, whilst a too alkaline pH can lead to itching and dryness; hence, the formulation must be sustained within a skin pH range of 4.0-7.0 (Dyah et al., 2023). The GraphPad Prism 10 statistical analysis results (F1-F6) in the NLC system (Figure 3) showed that the pH values did not change significantly between the formulas. The results indicate that F5-F6 yield the

highest pH values compared to other formulations utilizing various solid lipids (F1-F4).

Real time test

The results of the real-time physical stability test for preparations F1-F4 show that the creaming/phase separation on day 1 prevented stability testing. The stability test findings for the NLC preparation F5-F6 indicated that it could only sustain stability for 30 days.

Stability results of particle size and polydispersity index (IP)

The particle measurement data show that as the amount of surfactant in formulas F5 and F6 increased over time (t1-t30), the particle size grew (Figure 4) and the PDI value went down (Figure 5). Nonetheless, the comprehensive formula (F5-F6) continues to satisfy the criteria for NLC particle size ranging from 10 to 1000 nm and a PDI of 0 to 1 (Suyuti et al., 2023). The GraphPad Prism 10 (F5-F6) statistical analysis results in the NLC system showed that there no significant differences in particle size (Figure 4) or PDI (Figure 5) between the different formulas. The results indicate that F6 is the formulation yielding the least particle size and PDI among the two formulations. Nonetheless, the F6 formula comprises a total surfactant concentration of 20%, surpassing that of F5, which is 15%. Surfactants are crucial in stabilizing the NLC system by diminishing surface tension and inhibiting particle agglomeration. Research indicates that elevating surfactant content can enhance the stability of the NLC formulation; however, excessive surfactant may adversely affect the skin (Juanita & Aryani, 2023).

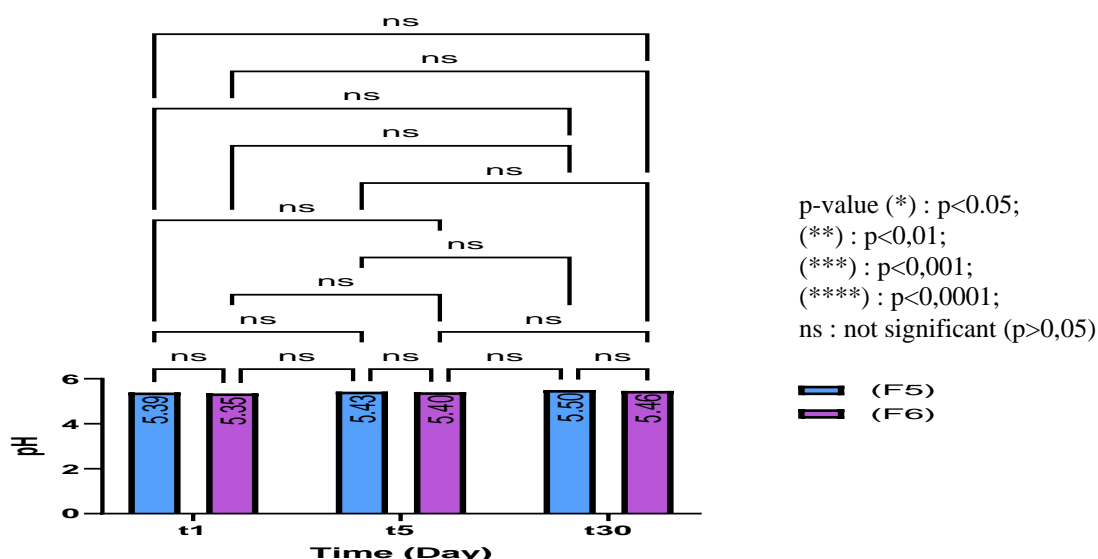


Figure 6. Graph of pH value changes F5-F6 (data are the average of three replications \pm SD)

Stability results of pH

Characteristic testing was performed on pH evaluation to understand the stability of the system during storage. The results of the pH tests show that as the amount of surfactant in formulations F5 and F6 rises over time (t1–t30), the pH value falls (table 5). The pH value of the NLC formulation varies between 5.35 and 5.50. This results from the utilization of a pH 5 phosphate buffer as the carrier solution, which corresponds to the employed pH buffer, specifically pH 5 ± 0.5 . Nonetheless, the complete formula (F5-F6) remains compliant with the stipulated skin pH range of 4.0–7.0 (Dyah et al., 2023). The GraphPad Prism 10 statistical analysis results (F5–F6) in the NLC system showed that the pH values did not change significantly across the different formulas (Figure 6). The results indicated that F5 yielded the greatest pH value compared to the other formula. The incorporation of surfactants in NLC formulations frequently results in a reduction of pH levels. Surfactants can change how lipids interact in the stratum corneum, which could affect how stable the formulation's pH is. Anionic surfactants, such as sodium lauryl sulfate (SLS), can reduce pH and enhance skin permeability, but, at elevated doses, they may induce irritation (Mukhlisah & Ningrum, 2019). The pH value significantly influences the stability of topical preparations. Formulations with unstable pH may induce physical alterations, such as precipitation or color changes, potentially leading to skin discomfort (Helmidanora et al., 2023).

CONCLUSION

The optimization of the NLC delivery system for quercetin was successfully achieved using the high shear homogenization method. The optimal NLC-0 formulation consists of 4% solid lipids (a 3:1 ratio of oleum cacao to beeswax), 6% castor oil as a liquid lipid, Tween 80 and Span 80 as surfactants with propylene glycol as a cosurfactant in a 4:1 ratio, 0.5% phenoxyethanol as a preservative, and distilled water. The resulting NLC-0 demonstrated a particle size range of 169.1–298.7 nm, a polydispersity index (PDI) between 0.074 and 0.476, and a pH range of 5.17–5.39, aligning with the skin's natural pH (4.0–7.0). Stability tests indicated that the formulation remained stable for 30 days under storage, supporting its potential as a robust carrier for quercetin delivery. These findings pave the way for the further development of NLC-based quercetin formulations in pharmaceutical and cosmetic applications.

ACKNOWLEDGMENT

The authors would like to thank the Research and Community Service Institute of the Perjuangan University Tasikmalaya for the support of the facilities for conducting this research.

AUTHOR CONTRIBUTIONS

Conceptualization, R.M.; Methodology, R.M., W.S., T.E.; Software, R.M.; Validation, R.M., W.S., T.E.; Formal Analysis, R.M., W.S., T.E.; Investigation, R.M., W.S., T.E.; Resources, R.M.; Data Curation; R.M., W.S., T.E.; Writing - Original Draft, R.M., W.S., T.E.; Writing - Review & Editing, R.M., W.S., T.E.;

Visualization, R.M., W.S., T.E.; Supervision, R.M., W.S., T.E.; Project Administration, R.M., W.S., T.E.; Funding Acquisition, R.M.

CONFLICT OF INTEREST

The authors declared no conflict of interest.

REFERENCES

- Choi, M. H. & Shin, H. J. (2016). Anti-Melanogenesis effect of Quercetin. *Cosmetics*; 3; 1–16. doi: 10.3390/cosmetics3020018
- Da Silva, T. L. T. & Martini, S. (2024). Recent Advances in Lipid Crystallization in the Food Industry. *Annual Review of Food Science and Technology*; 15; 355–379. doi: 10.1146/annurev-food-072023-034403
- Dragicevic, N. & Maibach, H. I. (2016). Percutaneous Penetration Enhancers Chemical Methods in Penetration Enhancement: Nanocarriers. Berlin: Springer Nature.
- Dyah, R., Widji, S. & Noorma, R. (2023). Characterization and Penetration Profile of Resveratrol-loaded Nanostructured Lipid Carrier (NLC) for Topical Anti-aging. *Key Engineering Materials*; 942; 65–70. doi: 10.4028/p-558sg4.
- Fitriani, E. W., Avanti, C., Rosana, Y. & Surini, S. (2024). Nanostructured Lipid Carriers: A Prospective Dermal Drug Delivery System for Natural Active Ingredients. *Pharmacia*; 71; 1–15. doi: 10.3897/pharmacia.71.e115849.
- Han, F., Li, S., Yin, R., Liu, H. & Xu, L. (2008). Effect of Surfactants on The Formation and Characterization of a New Type of colloidal Drug Delivery System: Nanostructured Lipid Carriers. *Colloids and Surfaces A: Physicochemical and Engineering Aspects*; 315; 210–216. doi: 10.1016/j.colsurfa.2007.08.005.
- Hatahet, T., Morille, M., Hommoss, A., Devoisselle, J. M., Müller, R. H. & Bégu, S. (2016). Quercetin Topical Application, From Conventional Dosage Forms to Nanodosage Forms. *European Journal of Pharmaceutics and Biopharmaceutics*; 108; 41–53. doi: 10.1016/j.ejpb.2016.08.011.
- Helmidanora, R., Jubaidah, S. & Fauziah A. A., I. (2023). Formulasi Film Forming Spray Dari Kloramfenikol Untuk Luka. *Jurnal Ilmiah Ibnu Sina (JIIS): Ilmu Farmasi Dan Kesehatan*; 8; 327–337. doi: 10.36387/jiis.v8i2.1517.
- Husnawiyah, N., Nugroho, W. & Widyaningrum, I. (2023). Pengaruh Jenis Lipid Padat Terhadap Sifat Fisika Dan Kimia Pada Sistem Penghantar Obat Nanostructured Lipid Carriers (NLC). *Bio Komplementer Medicine*; 10; 1–7.
- Juanita, G. & Aryani, N. L. D. (2023). Scale Up Nanostructured Lipid Carrier (NLC) Koenzim Q10 Menggunakan Matriks Lipid Asam Stearat-Isopropil Palmitat. *Jurnal Ners*; 7; 908–916. doi: 10.31004/jn.v7i2.16287.
- Khasanah, U. & Rochman, M. F. (2022). Stabilitas Nanostructured Lipid Carrier Coenzyme Q10 Dengan Variasi Waktu Pengadukan. *Jurnal Ilmu Farmasi Dan Farmasi Klinik*; 18; 55. doi: 10.31942/jiffk.v18i2.5958.
- Lu, B., Huang, Y., Chen, Z., Ye, J., Xu, H., Chen, W. & Long, X. (2019). Niosomal Nanocarriers for Enhanced Skin Delivery of Quercetin With Functions of Anti-Tyrosinase and Antioxidant. *Molecules*; 24; 1–17. doi: 10.3390/molecules24122322.
- Mayangsari, F. D., Erawati, T., Soeratri, W. & Rosita, N. (2021). Karakteristik dan Stabilitas Fisik NLC-Koenzim Q10 dalam Sleeping Mask dengan Minyak Nilam. *Jurnal Farmasi Dan Ilmu Kefarmasian Indonesia*; 8; 178. doi: 10.20473/jfiki.v8i22021.178-186.
- Mukhlisah, N. R. I. & Ningrum, D. M. (2019). Uji Sifat Fisik dan Iritasi Ekstrak Etanol Buah Rukem (*Flacourtia rukam*) dalam Sediaan Sunscreen Basis Gel. *Pharmaceutical and Traditional Medicine*; 3; 56–61.
- Müller, M. & Careglio, E. (2018). Influence of Free Fatty Acids as Additives on the Crystallization Kinetics of Cocoa Butter. *Journal of Food Research*; 7; 86. doi: 10.5539/jfr.v7n5p86.
- Munandar Erawati, T., Rosita, N. & Rachmania, I. (2023). The Activity of Candlenut Oil in The Nanostructured Lipid Carrier System on Hair Growth in Rats. *Journal of Public Health in Africa*; 14; 118–122. doi: 10.4081/jphia.2023.2519.
- Rahmi, D., Yunilawati, R. & Ratnawati, E. (2013). Peningkatan Stabilitas Emulsi Krim Nanopartikel Untuk Mempertahankan Kelembaban Kulit. *Jurnal Kimia Dan Kemasan*; 35; 30. doi: 10.24817/jkk.v35i1.1870.
- Rohmah, M., Raharjo, S., Hidayat, C. & Martien, R. (2019). Formulasi dan Stabilitas Nanostructured Lipid Carrier dari Campuran

Fraksi Stearin dan Olein Minyak Kelapa Sawit.
Jurnal Aplikasi Teknologi Pangan; 8; 23–30.
doi: 10.17728/jatp.3722.

Sakellari, G. I., Zafeiri, I., Batchelor, H. & Spyropoulos, F. (2021). Formulation Design, Production and Characterisation of Solid Lipid Nanoparticles (SLN) and Nanostructured Lipid Carriers (NLC) For The Encapsulation of A Model Hydrophobic Active. *Food Hydrocolloids for*

Health; 1; 1-18. doi:
10.1016/j.fhfh.2021.100024.

Smejkal, G., Gross, V., & Lazarev, A. (2024). Theoretical and Experimental Determinations of the Hydrophilic–Lipophilic Balance (HLB) of Representative Oils and Lecithins. *Colloids and Interfaces*; 8; 1-13. doi:
10.3390/colloids8020021



***Curcuma caesia*. Roxb as a Potential Inhibitor of STAT3 and EGFR: a Molecular Docking Approach in Diabetic Nephropathy**

Muhammad Farid^{1*}, Shalahuddin Almaduri², Sujono Riyadi³

¹Department of Medicine, Faculty of Medicine, Universitas Ahmad Dahlan, Yogyakarta, Indonesia

²Department of Pharmacy, Faculty of Health, Universitas Jenderal Ahmad Yani, Yogyakarta, Indonesia

³Department of Nursing and Science, Faculty of Health, Universitas Jenderal Ahmad Yani, Yogyakarta, Indonesia

*Corresponding author: muhammad2100034023@webmail.uad.ac.id

Orcid ID: 0009-0002-5301-0854

Submitted: 9 October 2024

Revised: 12 February 2025

Accepted : 24 February 2025

Abstract

Background: Diabetes mellitus (DM) is a chronic disorder marked by persistent hyperglycemia, leading to various complications, including diabetic nephropathy (DN). The STAT3-EGFR signaling axis plays a crucial role in the development and progression of diabetic nephropathy, with EGFR activation leading to STAT3 phosphorylation. *Curcuma caesia* Roxb, rich in curcuminoids, shows promise in managing DN due to its anti-inflammatory and antioxidant properties. This study aims to predict the inhibitory potential of *Curcuma caesia* compounds on STAT3 and EGFR in DN using molecular docking techniques. **Methods:** This study utilized molecular docking to evaluate the inhibitory potential of *Curcuma caesia* compounds on STAT3 and EGFR. Protein structures were obtained from the RCSB database and prepared using Biovia Discovery Studio. Redocking validated the method via RMSD analysis, while docking simulations assessed binding energy (ΔG). ADMET predictions analyzed physicochemical properties and toxicity, ensuring the compounds' suitability as drug candidates. **Results:** Redocking process validated the method, with RMSD values indicating accuracy. Curcumin (-9.71) and ar-Curcumene (-5.02) showed the lowest binding energy for both proteins, suggesting strong interactions. Visualization revealed significant amino acid interactions, particularly involving hydrogen bonds. Additionally, pharmacokinetic and toxicity analyses indicated that most compounds are suitable drug candidates, exhibiting good absorption, distribution, and safety profiles, thus supporting *Curcuma caesia*'s therapeutic promise in diabetic nephropathy management. **Conclusion:** *Curcuma caesia* demonstrates significant potential as a therapeutic agent for diabetic nephropathy, with favorable molecular interactions, strong binding affinity to STAT3 and EGFR, and promising pharmacokinetic and safety profiles.

Keywords: *Curcuma caesia*, nephropathy diabetic, molecular docking.

How to cite this article:

Farid, M., Almaduri, S. & Riyadi, S. (2025). *Curcuma caesia*. Roxb as a Potential Inhibitor of STAT3 and EGFR: a Molecular Docking Approach in Diabetic Nephropathy. *Jurnal Farmasi dan Ilmu Kefarmasian Indonesia*, 12(1), 26-36. <http://doi.org/10.20473/jfiki.v11i32025.26-36>

INTRODUCTION

Diabetes mellitus (DM) is a non-communicable disease characterized by persistent hyperglycemia. This chronic metabolic disorder arises from impaired insulin secretion, insulin resistance, or a combination of both, which are the primary factors contributing to the disease (Goyal et al., 2023). Persistent hyperglycemia in uncontrolled DM patients can lead to both acute and chronic complications. Common acute complications include hyperosmolar hyperglycemic state and diabetic ketoacidosis (Akalu & Birhan, 2020). Chronic complications frequently observed include diabetic neuropathy and nephropathy. Diabetic nephropathy affects approximately 40% of DM patients, causing alterations in renal hemodynamics and structural damage due to increased plasma flow and hydrostatic pressure in the glomerular capillaries (Badal & Danesh, 2014). The progression of diabetic nephropathy is driven by hemodynamic and metabolic factors within the kidney. Treatment aims to slow or halt the progression of renal damage (Badal & Danesh, 2014).

Therapeutic strategies for diabetic nephropathy focus on glycemic and blood pressure control, along with inhibition of the renin-angiotensin-aldosterone system (RAAS) and the Signal Transducer and Activator of Transcription 3 (STAT3) pathway. STAT3 plays a crucial role in the secretion of inflammatory mediators, contributing to glomerular sclerosis and tubulointerstitial fibrosis in the kidney, ultimately resulting in diabetic nephropathy (Elendu et al., 2023; Yu et al., 2023). Previous in vitro studies demonstrated that the JAK-STAT pathway is pivotal in the development of diabetic nephropathy. Recent advances in diabetic nephropathy treatment target TGF- β and NF- κ B pathways and incorporate stem cell- and gene-based therapies (Zheng et al., 2019). Selective inhibition of STAT3 over 16 weeks has shown promising results in slowing the progression of advanced renal damage (Elendu et al., 2023; Varghese & Jialal, 2023). Inflammatory mediator activity induces gene transcription involved in pro- and anti-inflammatory responses, including the JAK-STAT pathway, which is activated by tyrosine kinases such as TGF- β , EGFR, and FGF (Yu et al., 2023). EGFR activation plays a significant role in the pathogenesis of diabetic nephropathy by modulating key cellular processes such as fibrosis and inflammation in renal tissues (Wang & Zhang, 2024). Through the activation of downstream signaling pathways, including TGF- β , EGFR contributes to the progression of kidney damage,

making it a critical target for therapeutic intervention in diabetic kidney disease.

Turmeric is a plant known for its various species, one of which is black turmeric (*Curcuma caesia* Roxb.), renowned for its significant health benefits. Black turmeric is widely used as a natural herbal medicine to treat various diseases. The therapeutic potentials of *Curcuma caesia* include its effects as an antidiabetic, asthma treatment, analgesic, antimicrobial, anticancer, and thrombolytic agent (Ibrahim et al., 2023; Paudel et al., 2024). Research conducted by Udayani et al. (2024) demonstrated the ability of *Curcuma caesia* to reduce glucose levels in the body through in vivo studies. Additi

onally, *Curcuma caesia* can inhibit the enzymes amylase and glucosidase, which are involved in glucose metabolism and the formation of glycogen as an energy reserve (Majumder et al., 2017). Furthermore, the use of *Curcuma caesia* in the treatment of diabetic nephropathy has shown promising results, as evidenced by eGFR evaluations in in vivo studies by Aini et al. (2024). This is due to its ability to reduce oxidative stress, which mediates inflammation in the renal tubules (Grover et al., 2019). One of the active compounds in *Curcuma caesia*, curcumin, possesses anti-inflammatory and nephroprotective properties, inhibiting TLR and downregulating cadherin, thereby preventing epithelial-to-mesenchymal transition that could lead to kidney damage (Sun et al., 2014; Zhang et al., 2015).

Molecular docking studies have become a growing trend in drug development. These studies predict the binding interactions between target molecules and active compounds, enabling researchers to understand molecular-level interactions and the underlying biochemical processes. This study aims to predict the potential inhibitory activity of STAT3 and EGFR from *Curcuma caesia* and Roxb in diabetic nephropathy through a molecular docking approach.

MATERIALS AND METHODS

Validation method

STAT3 and EGFR protein structure were obtained via <https://www.rcsb.org/> with PDB ID: 6NJS and 3POZ. Protein preparation uses the Biovia discovery Studio 2021 application to clean proteins from water molecules and other cofactors and separate proteins and natural ligands. The method validation process uses the redocking method using the help of the AutoDock program. The redocking process was carried out to find the root mean square deviation (RMSD) value as a

method validation parameter. The RMSD value that can be considered valid is below 2.0 Å, which shows that there is no significant change in the ligand after the docking process (Ramírez & Caballero, 2018).

The redocking process uses the Autodock application with genetics algorithm parameters which are a combination of several other parameters (Shivanika et al., 2022). The determination of the grid box in this process is the central of the ligand enabling to find the grid point number and grid point coordinates (X,Y,Z). This research uses a specific docking method, so that in the redocking process the grid box findings are very important to obtain the grid point number and grid point coordinates (Kilambi & Gray, 2017).

Docking simulation

The entire chemical structure of the active compound *Curcuma caesia* was obtained via <https://pubchem.ncbi.nlm.nih.gov/>. Canonical SMILES storage was used to perform ADMET predictions. The compounds obtained were then optimized in structure and minimize the energy using the Avogadro and Chemdraw 3D 2019 applications. This process provides a better compound structure with lower energy (Syahputra et al., 2022). The docking simulation process uses the same method as the redocking process, with changes to the grid point number and grid point coordinates (X,Y,Z) which adjust to the results of the redocking (Lestarinigrum et al., 2024).

An analysis of the docking simulation results is found in the lowest binding energy (ΔG) value. The ΔG results of the test ligand will be compared with the natural ligand or between the docking results of the test compound and the control drug (captopril). Captopril is used in this study as a control due to its well-established role as an angiotensin-converting enzyme inhibitor, its ability to block neovascularization and modulate cellular processes in diabetic conditions makes it a relevant comparator in evaluating potential inhibitors of STAT3 and EGFR (Abdallah et al., 2015). The best ligand results were then visualized by the interaction site, binding pocket and amino acid interactions using the Biovia discovery Studio 2021 application. Analysis of the dominant amino acid interactions in each protein was carried out to find the molecular process of the

compound on the target protein. All the molecular modeling and analyses in this study were performed using free and open-source software, including AutoDock and Avogadro, while ChemDraw and Discovery Biovia were used under academic licenses.

ADMET Predictions

Prediction of the physicochemical and bioavailability of each test compound was using Canonical SMILES as a format for analysis with the help of tools (<http://www.swissadme.ch/>). Lipinski parameters are used as general parameters for oral treatment candidates in the form of molecular weight, hydrogen bond donors and acceptors, and Log-P (Abdul-Hammed et al., 2022). The pharmacokinetics of each compound were evaluated using <https://biosig.lab.uq.edu.au/pkcsim/> by entering Canonical SMILES. The parameters used are absorption (GI absorption), distribution (BBB permeability), metabolism (CYP1A2), and excretion (total clearance and renal oct2 substrate) (Abdullah et al., 2021; Ononamadu & Ibrahim, 2021; Ramadhan et al., 2024). The parameters used to predict toxicity are AMES toxicity, hepatotoxicity, and LD50.

RESULTS AND DISCUSSION

Method validation

The method was validated using a redocking process for each natural ligand to the protein using the AutoDock program. The finding of the RMSD value in the STAT3 redocking process, namely 1.50, indicates good results or the method used is valid. The finding of the RMSD value in the EGFR redocking process is 1.18, indicating good results or that the method used is valid. The results of the structural deviation due to the docking process are shown in Figure 1 which shows that there is no significant difference in the ligands before (in blue) and after the docking process (in yellow). Yellow ligands are ligands resulting from the docking process, while gray ligands are natural ligands originating from proteins. Findings The area and coordinates of the STAT3 and EGFR grid boxes are shown in Table 1, the results of which will be a specific docking reference for each target.

Table 1. Grid box analysis

Native Ligand	Number Grid Points			Coordinate Grid Points			Grid Point Spacing
	X	Y	Z	X	Y	Z	
6NJS	40	56	40	13,498	54,117	0.100	0.375 Å
3POZ	40	40	40	18,746	31,832	11,626	0.375 Å

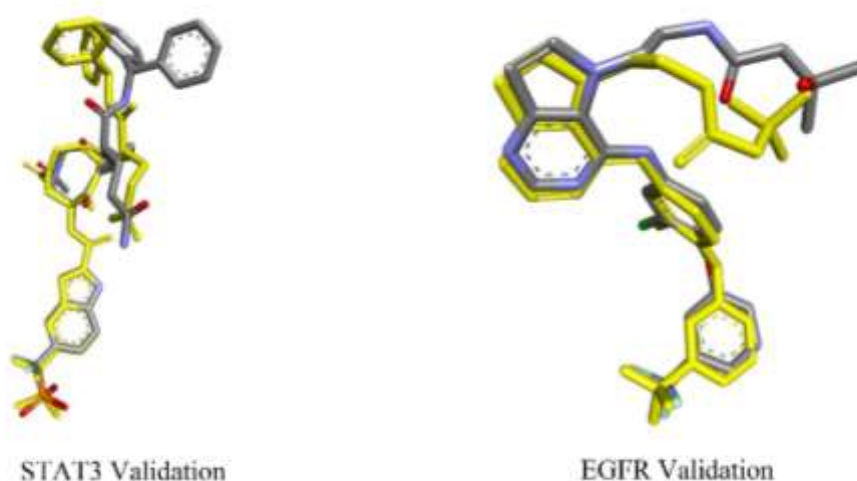


Figure 1. Ligand redocking

Docking simulation

The compounds that have been obtained are then optimized in structure and minimize the energy using the Avogadro and Chemdraw 3D 2019 applications. This process provides a better compound structure with lower energy (Syahputra et al., 2022). Each test compound is optimized and minimized energy with the aim of providing the best structural form with minimal energy. The main parameter of the docking process is the binding affinity (ΔG) between the test ligand and the protein. The lower the ΔG value indicates a good interaction, the docking results are shown in Table 2. Docking test results on *Curcuma caesia* compounds against STAT3 found that the natural ligand had the lowest ΔG , namely -10.57. ar-Curcumene has the lowest ΔG value, namely -5.04, followed by Curcumin with a ΔG value -4.87 and bornyl acetate has a ΔG value of -4.54. Captopril as a control drug in this study had a ΔG value of -4.02, where there were five *Curcuma caesia* compounds that had lower ΔG values. These results show the great potential of *Curcuma caesia* as an alternative treatment through inhibiting STAT3 activity in diabetic nephropathy.

Docking test results on *Curcuma caesia* compounds against EGFR found that the natural ligand had the lowest ΔG , namely -11.24. Captopril as a control drug in this study had a ΔG value of -5.70, where almost all *Curcuma caesia* compounds had a lower ΔG value. Curcumin has the lowest ΔG value, namely -9.71, this compound has the lowest ΔG compared to other compounds. Cineole has a ΔG value -7.25, followed by curcumen with a value of ΔG -7.24. The compound with the highest ΔG docking result is bornyl acetate, namely -4.48. These results show the great potential of *Curcuma caesia* as an alternative treatment through inhibiting EGFR activity in diabetic nephropathy. Despite having lower binding affinities toward EGFR and STAT3 compared to the native ligands, the *Curcuma caesia* compounds still show substantial potential as alternative therapeutic agents. Their competitive binding suggests that, even with lower affinity, these compounds may effectively inhibit the target proteins due to their ability to block critical pathways in diabetic nephropathy, providing a viable therapeutic alternative

Table 2. Docking simulation

Compound	STAT3	EGFR
	Energy affinity (ΔG) (kcal/mol)	Inhibition constant (Ki)(μM)
Native ligands	-10.57	17.75
Camphor	-4.28	269.70
Curcumin	-4.87	727.00
Ocimen	-4.19	845.18
Cineole	-4.12	957.13
Element	-3.86	1.48
Borneol	-3.62	2.22
Bornyl acetate	-4.54	466.69
ar-Curcumene	-5.04	203.60
Captopril	-4.02	1.13

Figure 2 is a visualization of protein crystals, binding pockets, and amino acid interactions resulting from docking in STAT3. The bond interactions formed between the native ligand and protein show that there are nine hydrogen bonds marked in green in the form of THR657, SER636, GLU638, GLU638, GLN644, SER 611, SER 613, and GLU612. There are seven non-hydrogen bonds formed, namely LYS658, ILE659, ARG609, ARG609, PRO639, PRO639, and VAL 637. Figure 3 show ar-Curcumene has one hydrogen bond, namely GLU638, and three non-hydrogen bonds, namely TYR640, VAL637, and TRP 623. Docking results in captopril shows that there are five hydrogen

bonds in the form of ARG609, SER611, SER611, SER613, and SER613 and one non-hydrogen bond PRO639. The dominant amino acid hydrogen bond interaction in this case is GLU638, where in the three test ligands analyzed there is this amino acid group even though in captopril this group does not have a specific bond. The interaction that occurs with GLU638 will bind to oxygen during peptide ligand conformation. These findings support the interaction of STAT3 and *Curcuma caesia* which could be the basis for treatment targeting STAT3 through inhibiting the action of this protein by mediating cell apoptosis resistance and cell growth (Shao et al., 2004).

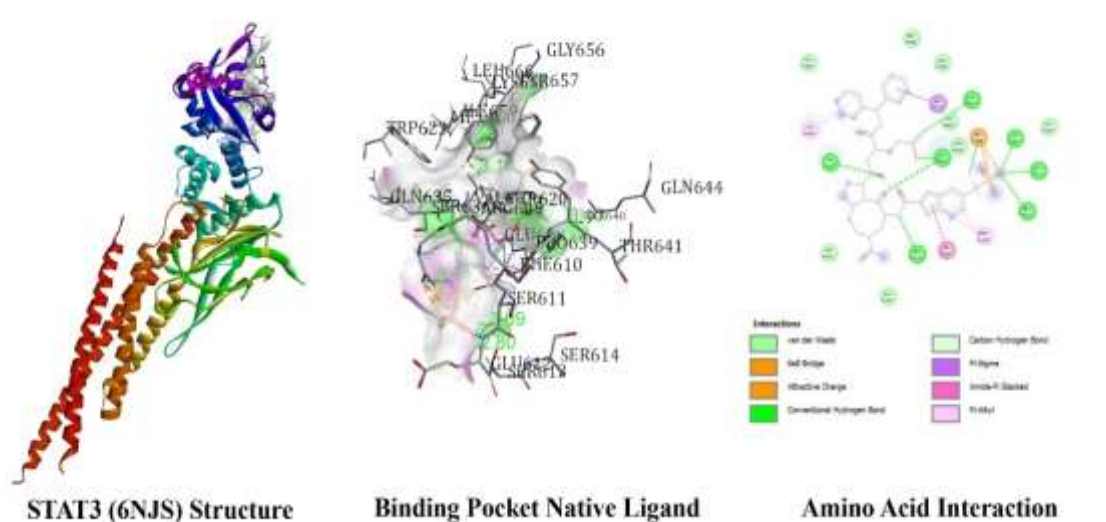


Figure 2. STAT structure and docking analysis of a native ligand

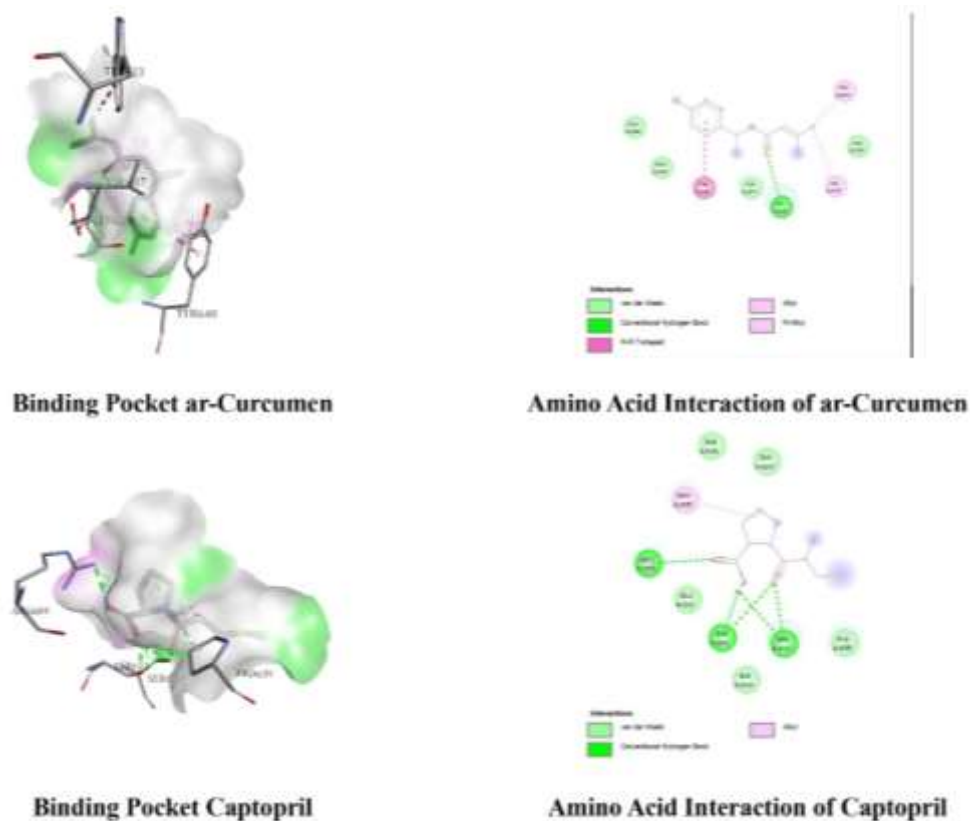


Figure 3. Visualization of the best pose docking results and amino acid interactions of ar-Curcumen and captopril

Visualization of protein crystals, binding pockets, and amino acid interactions resulting from docking of test ligands against EGFR is shown in Figure 5. It was found that there were dense amino acid bond interactions in the native ligand, there were four hydrogen bonds and 20 non-hydrogen bonds. The hydrogen bonds formed in the native ligand are LYS745, THR845, THR845, **THR790**, and GLN791. Meanwhile, the non-hydrogen bonds formed in the native ligand are LUE788, VAL726, LYS745, LYS745, **MET766**, PHE856, PHE856, ARG776, ARG776, CYS775, CYS775, CYS775, ILE853, MET793, MET793, ALA743, ALA743, LEU844, L EU844, and LEU 718. Figure 5 show the results of bond interactions in curcumin found seven hydrogen bonds, namely PHE858, ASP855, LYS745, GLN791, LEU792, **THR790**, and MET793. There are five non-hydrogen bonds formed in the form of **MET766**, LEU777, LEU788, ALA743, and LEU844. Captopril as a control ligand has four hydrogen bonds, namely THR854,

THR790, ALA743, and LEU788. Two amino acid bonding interactions were found in captopril in the form of PHE856 and **MET766**.

The most dominant hydrogen bonding interaction of amino acids in this analysis is THR790. The same findings were shown in research on curcumin as an anticancer drug. This shows that curcumin analogs can be an alternative treatment through EGFR inhibition (Afzal et al., 2022). Mutations in EGFR at the THR790 MET site help the development of Non Small Cell Lung Cancer (NSCLC) cancer cells by inhibiting this mutation; curcumin can be useful as an anti-cancer NSCLC (Lu et al., 2024)). The most dominant non-hydrogen bonding interaction of amino acids in this analysis is MET766. The interaction of MET766 with EGFR can be anti-proliferative, which can help in the recovery of renal tubules in diabetic nephropathy sufferers (Ibrahim et al., 2020).

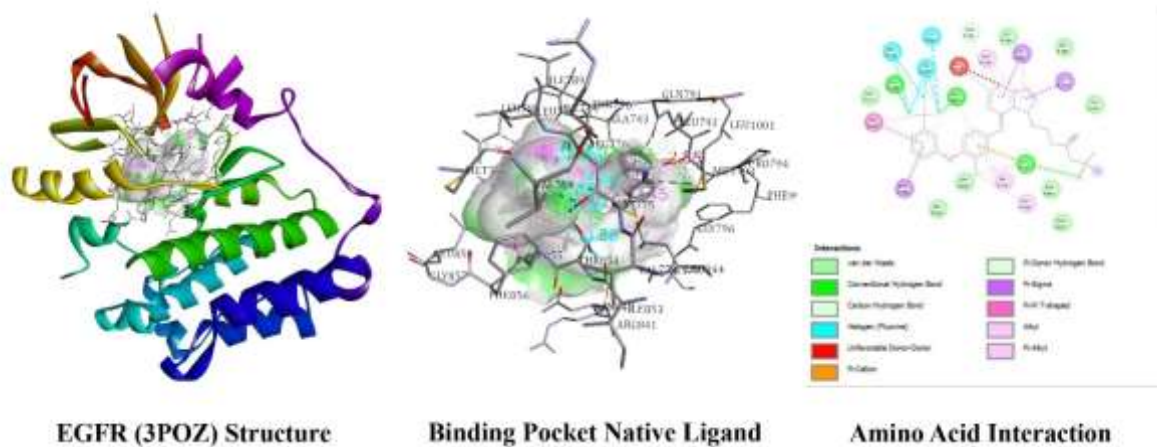


Figure 4. EGFR structure and docking analysis a native ligand

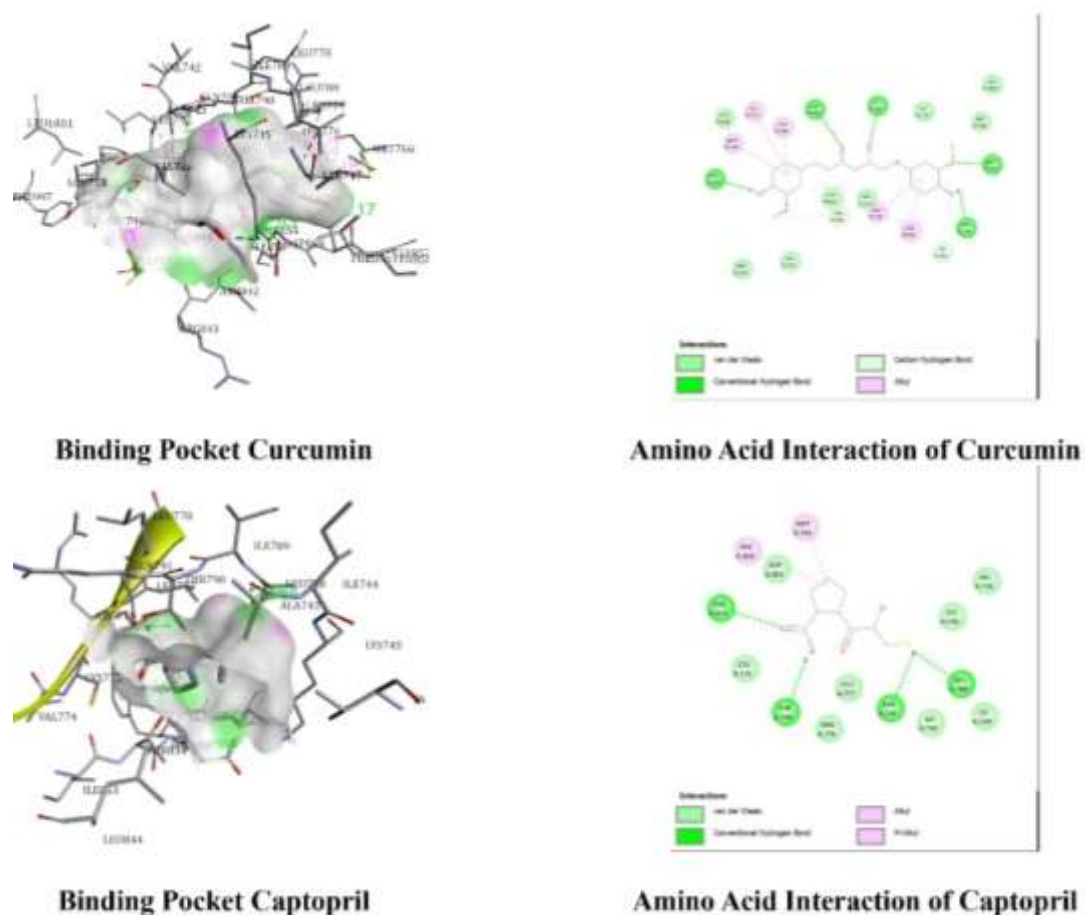


Figure 5. Visualization of the best pose docking results and amino acid interactions of ar-Curcumene and captopril

The results of this study show the potential for using *Curcuma caesia* as an alternative treatment for diabetic nephropathy patients. Research conducted by Machado et al/ (2022) showed good results in early treatment in diabetic rat renal injury with improvements in renal oxidative repercussion and hemodynamics profile (Machado et al., 2022). Aini et al.(2024) showed that

there was a decrease in serum creatinine and microalbumin in the urine of mice affected by diabetic nephropathy by administering *Curcuma caesia extract*. *Curcuma caesia* can reduce the expression of KIM-1, NGAL, and reduce toxic oxidative stress in renal tissue of mice with diabetic nephropathy (Ghasemi et al., 2019). Lee et al. (2019) showed that there was a

reduction in kidney damage by administering a curcumin analog (Dibenzoylmethane) which could reduce the risk of developing diabetic nephropathy in mice. The benefits of *Curcuma caesia* as antidiabetic, anti-inflammatory, promoting-autophagy, and antioxidant strengthen the results of this research which shows great potential in the treatment of diabetic nephropathy (Zhu et al., 2022). The role of curcumin and ar-curcumene as the active compounds in *Curcuma caesia* is significant, as they show promising binding affinities with EGFR and STAT3. However, the study could further emphasize the findings related to other species of *Curcuma*, such as *C. longa*, *C. phaecocaulis*, *C. wenyujin*, *C. aromatica*, and *C. kwangsiensis* which may also contain similar bioactive compounds and contribute to a broader understanding of the therapeutic potential of the *Curcuma* genus in treating diabetic nephropathy (Chen et al., 2023).

ADMET predictions

The similarity analysis of eight black turmeric compounds (Table 3) against existing drugs indicates that seven of them meet the criteria outlined by Lipinski's rules. Only elemene exhibits a non-compliance issue, with a LogP value exceeding 4.15. Compounds with high LogP values can demonstrate poor solubility in aqueous environments, which may lead to slow absorption and irregular bioavailability,

thereby causing problematic kinetic profiles in the body (Dong et al., 2018). Overall, the majority of black turmeric compounds show good potential as drug candidates.

The pharmacokinetic and toxicity analysis of the active compounds in black turmeric shows promising results, making them suitable candidates for drug development (Table 4). All compounds have an absorption value greater than 30%, indicating good absorption capabilities. Regarding distribution, all compounds demonstrate positive results, although they have difficulty crossing the blood-brain barrier with values below -1. The cytochrome P450 enzyme, which plays a role in metabolism, shows a tendency to be inhibited only by curcumin. CYP1A2 plays a crucial role in the metabolism of many drugs, and its inhibition may result in decreased clearance rates and prolonged drug action, which could potentially lead to accumulation and increased therapeutic effects or side effects (Bayoumi et al., 2024). Additionally, all compounds exhibit good excretion values. Toxicity analyses, including the Ames test and hepatotoxicity assessments, reveal no toxic properties in any of the compounds, further supporting the idea that black turmeric can be considered a safe and effective drug candidate.

Table 3. Lipinski analysis

Compound	Molecular Weight	Hydrogen Bond donors	Hydrogen Bond acceptors	Log-P	Violations
Camphor	152.23 g/mol	0	1	2.30	-
Curcumin	368.38 g/mol	2	6	1.47	-
Ocimen	154.25 g/mol	0	1	2.30	-
Cineole	154.25 g/mol	0	1	2.45	-
Elemene	204.35 g/mol	0	0	4.53	LOGP>4.15
Borneol	154.25 g/mol	1	1	2.45	-
Bornyl acetate	196.29 g/mol	0	2	2.76	-
ar-Curcumene	218.33 g/mol	0	1	3.37	-

Table 4. ADMET analysis

Compound	GI Absorption	BBB Permeability	CYP1A2	Total Clearance	Renal Oct2 Substrate	AMES Toxicity	Hepatotoxicity
Camphor	95.968%	0.612	No	0.109	No	No	No
Curcumin	82.19%	-0.562	Yes	-0.002	No	No	No
Ocimen	95.898%	0.436	No	1.272	No	No	No
Cineole	96.505%	0.491	No	1.009	No	No	No
Element	94.359%	0.809	No	0.251	No	No	No
Borneol	93.439%	0.646	No	1.035	No	No	No
Bornyl acetate	95.366%	0.553	No	1.029	No	No	No
ar-Curcumene	95.626%	0.66	No	1.543	No	No	No
requirement	>30%	<-1	No	Higher is better	No	No	No

CONCLUSION

This study shows that *Curcuma caesia* compounds with good ability, can even surpass control drugs against STAT3 and EGFR. While ar-curcumin with STAT3 has a binding energy of -5.04 and curcumin with EGFR has a binding energy of -9.71 which shows the best ΔG value in the docking test; these results are based on computational analysis and may not fully represent their therapeutic potential in vivo. Future in vitro and in vivo studies will provide deeper insights into the actual effectiveness and safety of these compounds, thus allowing for a more accurate evaluation of their potential as therapeutic alternatives for diabetic nephropathy.

ACKNOWLEDGMENT

We would like to express our gratitude for the opportunity to conduct this research. This work is the result of our efforts and dedication, and we appreciate the support from the academic community that has fostered our growth as researchers.

AUTHOR CONTRIBUTIONS

Conceptualization, M.F., S.A.M., S.R.; Methodology, M.F., S.A.M.; Software, M.F.; Validation, M.F., S.A.M.; Formal Analysis, S.A.M., S.R.; Investigation, M.F., S.R.; Resources, S.A.M., S.R.; Data Curation; M.F.; Writing - Original Draft, M.F., S.A.M., S.R.; Writing - Review & Editing, M.F., S.A.M., S.R.; Visualization, S.A.M., S.R.; Supervision, S.R.

CONFLICT OF INTEREST

The authors declared no conflict of interest.

REFERENCES

- Abd Allah, E. S. & Gomaa, A. M. (2015). Effects of Curcumin and Captopril on The Functions of Kidney and Nerve in Streptozotocin-Induced Diabetic Rats: Role of Angiotensin Converting Enzyme 1. *Applied Physiology, Nutrition, and Metabolism*; 40; 1061–1067. doi: 10.1139/apnm-2015-0145.
- Abdul-Hammed, M., Adedotun, I. O., Olajide, M., Irabor, C. O., Afolabi, T. I., Gbadebo, I. O., Rhyman, L. & Ramasami, P. (2022). Virtual Screening, ADMET Profiling, PASS Prediction, and Bioactivity Studies of Potential Inhibitory Roles of Alkaloids, Phytosterols, and Flavonoids Against COVID-19 Main Protease (Mpro). *Natural Product Research*;

- 36; 3110–3116. doi: 10.1080/14786419.2021.1935933.
- Abdullah, S. S., Putra, P. P., Antasionasti, I., Rundengan, G., Suoth, E. J., Abdullah, R. P. I. & Abdullah, F. (2021). Analisis Sifat Fisikokimia, Farmakokinetik dan Toksikologi pada *Pericarpium Pala* (*Myristica Fragrans*) Secara Artificial Intelligence. *Chemistry Progress*; 14; 81. doi: 10.35799/cp.14.2.2021.37112.
- Afzal, O., Yusuf, M., Ahsan, M. J., Altamimi, A. S. A., Bakht, M. A., Ali, A. & Salahuddin. (2022). Chemical Modification of Curcumin into Its Semi-Synthetic Analogs Bearing Pyrimidinone Moiety as Anticancer Agents. *Plants*; 11; 1-17. doi: 10.3390/plants11202737.
- Akalu, Y. & Birhan, A. (2020). Peripheral Arterial Disease and Its Associated Factors Among Type 2 Diabetes Mellitus Patients at Debre Tabor General Hospital, Northwest Ethiopia. *Journal of Diabetes Research*; 2020; 1-9. doi: 10.1155/2020/9419413.
- Aini, Z.Q., Wijayanti, T. & Puspitasari, A. C. (2024). Analisis Efektivitas Kunyit Hitam (*Curcuma caesia* Roxb.) dalam Penurunan Kadar Mikroalbumin dan Serum Kreatinin pada Tikus Diabetes Nefropati. *Healthy Indonesian Journal*; 3; 79-85. doi: 10.58353/jurinse.v3i2.214.
- Badal, S. S. & Danesh, F. R. (2014). New Insights Into Molecular Mechanisms of Diabetic Kidney Disease. *American Journal of Kidney Diseases*; 63; 63-83. doi: 10.1053/j.ajkd.2013.10.047.
- Bayoumi, H. H., Ibrahim, M. K., Dahab, M. A., Khedr, F. & El-Adl, K. (2024). Rationale, in Silico Docking, ADMET Profile, Design, Synthesis and Cytotoxicity Evaluations of Phthalazine Derivatives as VEGFR-2 Inhibitors and Apoptosis Inducers. *RSC Advances*; 14; 27110–27121. doi: 10.1039/d4ra04956j.
- Chen, M., Sun, J., Yao, H., Gong, F., Cai, L., Wang, C., Shao, Q. & Wang, Z. (2023). Analysis of Genetic and Chemical Variability of Five *Curcuma* Species Based on DNA Barcoding and HPLC Fingerprints. *Frontiers in Plant Science*; 14; 1-14. doi: 10.3389/fpls.2023.1229041
- Dong, J., Wang, N. N., Yao, Z. J., Zhang, L., Cheng, Y., Ouyang, D., Lu, A. P. & Cao, D. S. (2018). ADMETlab: A Platform For Systematic

- ADMET Evaluation Based on a Comprehensively Collected ADMET Database. *Journal of Cheminformatics*; 10; 1-11. doi: 10.1186/s13321-018-0283-x
- Elendu, C., John Okah, M., Fiemotongha, K. D. J., Adeyemo, B. I., Bassey, B. N., Omeludike, E. K. & Obidigbo, B. (2023). Comprehensive Advancements in the Prevention and Treatment of Diabetic Nephropathy: A Narrative Review. *Medicine (United States)*; 102; 1-6. doi: 10.1097/MD.00000000000035397.
- Ghasemi, H., Einollahi, B., Kheiripour, N., Hosseini-Zijoud, S. R. & Nezhad, M. F. (2019). Protective Effects of Curcumin on Diabetic Nephropathy Via Attenuation of Kidney Injury Molecule 1 (KIM-1) And Neutrophil Gelatinase-Associated Lipocalin (NGAL) Expression And Alleviation of Oxidative Stress In Rats With Type 1 Diabetes. *Iranian Journal of Basic Medical Sciences*, 22; 376–383. doi: 10.22038/ijbms.2019.31922.7674.
- Goyal, R., Singhal, M. & Jialal, I. (2023). Type 2 Diabetes. Treasure Island: StatPearls Publishing.
- Grover, M., Shah, K., Khullar, G., Gupta, J. & Behl, T. (2019). Investigation of the Utility Of Curcuma Caesia in the Treatment of Diabetic Neuropathy. *Journal of Pharmacy and Pharmacology*; 71; 725–732. doi: 10.1111/jphp.13075.
- Ibrahim, M. T., Uzairu, A., Shallangwa, G. A. & Uba, S. (2020). In-Silico Activity Prediction and Docking Studies of Some 2, 9-Disubstituted 8-Phenylthio/Phenylsulfinyl-9h-Purine Derivatives As Anti-Proliferative Agents. *Heliyon*; 6; 1-9. doi: 10.1016/j.heliyon.2020.e03158.
- Ibrahim, N. N. A., Wan Mustapha, W. A., Sofian-Seng, N. S., Lim, S. J., Mohd Razali, N. S., Teh, A. H., Rahman, H. A. & Mediani, A. (2023). A Comprehensive Review with Future Prospects on the Medicinal Properties and Biological Activities of Curcuma Caesia Roxb. *Evidence-based Complementary and Alternative Medicine*; 2023; 1-17. doi: 10.1155/2023/7006565.
- Kilambi, K. P. & Gray, J. J. (2017). Structure-Based Cross-Docking Analysis of Antibody-Antigen Interactions. *Scientific Reports*; 7; 1-15. doi: 10.1038/s41598-017-08414-y.
- Lee, E. S., Kwon, M. H., Kim, H. M., Kim, N., Kim, Y. M., Kim, H. S., Lee, E. Y. & Chung, C. H. (2019). Dibenzoylmethane Ameliorates Lipid-Induced Inflammation and Oxidative Injury in Diabetic Nephropathy. *Journal of Endocrinology*, 240; 169–179. doi: 10.1530/JOE-18-0206.
- Lestarinigrum, W. T., Kintoko, K. & Farid, M. (2024). Integrated Ethnomedicine Study in Silico of Medicinal Plants for Hypertension. *Journal La Lifesci*; 5; 483–501. doi: 10.37899/journallalifesci.v5i5.1656.
- Lu, J., Ji, X., Liu, X., Jiang, Y., Li, G., Fang, P., Li, W., Zuo, A., Guo, Z., Yang, S., Ji, Y. & Lu, D. (2024). Machine Learning-Based Radiomics Strategy for Prediction of Acquired EGFR T790M Mutation Following Treatment With EGFR-TKI In NSCLC. *Scientific Reports*; 14; 1-14. doi: 10.1038/s41598-023-50984-7.
- Machado, D. I., Silva, E. de O., Ventura, S. & Vattimo, M. de F. F. (2022). The Effect of Curcumin on Renal Ischemia/Reperfusion Injury in Diabetic Rats. *Nutrients*, 14; 1-10. doi: 10.3390/nu14142798.
- Majumder, P., Mazumder, S., Chakraborty, M., Chowdhury, S. G., Karmakar, S., & Haldar, P. K. (2017). Preclinical Evaluation of Kali Haldi (Curcuma Caesia): A Promising Herb to Treat Type-2 Diabetes. *Oriental Pharmacy and Experimental Medicine*; 17; 161–169. doi: 10.1007/s13596-017-0259-9.
- Ononamadu, C. J. & Ibrahim, A. (2021). Molecular Docking and Prediction Of ADME/Drug-Likeness Properties of Potentially Active Antidiabetic Compounds Isolated From Aqueous-Methanol Extracts of Gymnema Sylvestre and Combretum Micranthum. *Biotechnologia*; 102; 85–99. doi: 10.5114/bta.2021.103765
- Paudel, A., Khanal, N., Khanal, A., Rai, S. & Adhikari, R. (2024). Pharmacological Insights Into Curcuma Caesia Roxb., The Black Turmeric: A Review of Bioactive Compounds and Medicinal Applications. *Discover Plants*; 1; 1-19. doi: 10.1007/s44372-024-00076-1.
- Ramadhan, M. M., Utami, D. & Yuliani, S. (2024). In Silico Study of Purple Yam Anthocyanin Compounds (Dioscorea alata L.) As MAO-B and COMT Inhibitors in Parkinson's Disease. *Journal of Pharmaceutical Science*; 20; 13-24.

- Ramírez, D., & Caballero, J. (2018). Is It Reliable to Take the Molecular Docking Top Scoring Position as the Best Solution without Considering Available Structural Data? *Molecules*; 23; 1-17. doi: org/10.3390/molecules23051038.
- Shao, H., Xu, X., Mastrangelo, M. A. A., Jing, N., Cook, R. G., Legge, G. B., & Tweardy, D. J. (2004). Structural Requirements for Signal Transducer and Activator of Transcription 3 Binding to Phosphotyrosine Ligands Containing the YXXQ Motif. *Journal of Biological Chemistry*; 279; 18967-18973. doi: 10.1074/jbc.M314037200.
- Shivanika, C., Deepak Kumar, S., Ragunathan, V., Tiwari, P., Sumitha, A. & Brindha Devi, P. (2022). Molecular Docking, Validation, Dynamics Simulations, and Pharmacokinetic Prediction of Natural Compounds Against the SARS-Cov-2 Main-Protease. *Journal of Biomolecular Structure and Dynamics*; 40; 585-611. doi: 10.1080/07391102.2020.1815584.
- Sun, L. N., Yang, Z. Y., Lv, S. S., Liu, X. C., Guan, G. J. & Liu, G. (2014). Curcumin Prevents Diabetic Nephropathy Against Inflammatory Response Via Reversing Caveolin-1 Tyr14phosphorylation Influenced TLR4 Activation. *International Immunopharmacology*; 23; 236-246. doi: 10.1016/j.intimp.2014.08.023.
- Syahputra, R., Utami, D. & Widyaningsih, W. (2022). Studi Docking Molekuler Aktivitas Penghambatan Enzim Tirosinase Ubi Jalar (*Ipomoea batatas* L. Lam). *Pharmacon: Jurnal Farmasi Indonesia*; 19; 21-34. doi: 10.23917/pharmakon.v19i1.18295.
- Udayani, N. N. W., Putra, I. M. A. S. & Santoso, P. (2024). Effects of Black Turmeric Ethanol Extract (*Curcuma caesia* Roxb) on Blood Glucose Levels, SGOT, SGPT, Histopathology Pancreas: A Preliminary Study. *South Eastern European Journal of Public Health*; 25; 467-477. doi: 10.70135/seejph.vi.1831
- Varghese, R. T. & Jialal, I. (2023). *Diabetic Nephropathy*. Treasure Island: StatPearls Publishing.
- Wang, N. & Zhang, C. (2024). Oxidative Stress: A Culprit in the Progression of Diabetic Kidney Disease. In *Antioxidants*, 13; 1-45. doi: 10.3390/antiox13040455.
- Yu, J. T., Fan, S., Li, X. Y., Hou, R., Hu, X. W., Wang, J. N., Shan, R. R., Dong, Z. H., Xie, M. M., Dong, Y. H., Shen, X. Y., Jin, J., Wen, J. G., Liu, M. M., Wang, W. & Meng, X. M. (2023). Novel Insights Into STAT3 in Renal Diseases. *Biomedicine and Pharmacotherapy*; 165; 1-12. doi: 10.1016/j.biopha.2023.115166.
- Zhang, X., Liang, D., Guo, L., Liang, W., Jiang, Y., Li, H., Zhao, Y., Lu, S. & Chi, Z. H. (2015). Curcumin Protects Renal Tubular Epithelial Cells From High Glucose-Induced Epithelial-To-Mesenchymal Transition Through Nrf2-Mediated Upregulation of Heme Oxygenase-1. *Molecular Medicine Reports*; 12; 1347-1355. doi: 10.3892/mmr.2015.3556.
- Zheng, C., Huang, L., Luo, W., Yu, W., Hu, X., Guan, X., Cai, Y., Zou, C., Yin, H., Xu, Z., Liang, G. & Wang, Y. (2019). Inhibition Of STAT3 in Tubular Epithelial Cells Prevents Kidney Fibrosis and Nephropathy in STZ-Induced Diabetic Mice. *Cell Death and Disease*, 10; 1-14. doi: 10.1038/s41419-019-2085-0.
- Zhu, X., Xu, X., Du, C., Su, Y., Yin, L., Tan, X., Liu, H., Wang, Y., Xu, L., & Xu, X. (2022). An Examination of The Protective Effects and Molecular Mechanisms of Curcumin, a Polyphenol Curcuminoid in Diabetic Nephropathy. *Biomedicine and Pharmacotherapy*; 153; 1-18. doi: 10.1016/j.biopha.2022.113438.



Potassium Profile in Heart Failure Patients Before and After Hospitalization at Prof. Dr. I.G.N.G. Ngoerah Hospital

Kadek Indra Aryani¹, Ni Putu Ika Swastiartha², Ni Komang Ayu Krisma Suriatha Putri¹, Ni Kadek Mas Ari Pratiwi¹, Made Suta Wahyudi¹, Rini Noviyani^{1*}

¹Department of Pharmacy, Faculty of Mathematics and Science, Udayana University, Badung, Indonesia

²Department of Dentistry, Faculty of Medical, Udayana University, Denpasar, Indonesia

*Corresponding author: rini.noviyani@unud.ac.id

Orcid ID: 0000-0002-9306-2053

Submitted: 18 July 2024

Revised: 3 March 2025

Accepted: 20 March 2025

Abstract

Background: Hypokalemia in patients with heart failure is increasing, with an increasing incidence of 6.8% in Asia and 19.7% in Indonesia; globally, 63 million people suffer from heart failure. Hypokalemia is defined as a serum potassium level below 3.5 mEq/L [mmol/L], which can lead to decreased heart function, muscle weakness, arrhythmias and cardiac arrest. The use of diuretic drugs such as furosemide in heart failure patients may be a risk factor for hypokalemia. **Objective:** This study aims to determine the difference in potassium levels before and after furosemide administration as well as the possibility of hypokalemia due to furosemide administration in inpatients diagnosed with heart failure at Prof. Dr. I.G.N.G. Ngoerah Hospital. **Methods:** This is a cross-sectional observational study with retrospective medical record collection. The minimum sample size was calculated using Lemeshow's Formula of One Proportion Estimation Method with Absolute Precision Proportion, data normality test with Kolmogorov-Smirnov ($p > 0.05$) and parametric test with paired t-test ($p < 0.05$). This study included 101 patients that met the inclusion criteria with 11 patients having more than one inpatient visit, so a total 114 'patients' medical records were obtained. **Results:** Potassium levels before and after hospitalization showed a significant difference ($p < 0.05$). A total of 84 'patients' data showed a decrease in potassium levels, with 49 of them showing a reduction in $>15\%$ and 35 showing a decrease of $\leq 15\%$. **Conclusion:** Prevalence of hypokalemia in patients with a diagnosis of heart failure and furosemide therapy at Prof. Dr. I.G.N.G. Ngoerah Hospital during January 2022-December 2023 after hospitalization was 29%.

Keywords: furosemide, heart failure, hypokalemia, potassium

How to cite this article:

Aryani, K. I., Swastiartha, N. P. I., Putri, N. K. A. K. S., Pratiwi, N. K. M. A., Wahyudi, M. S. & Noviyanti, R. (2025). Potassium in Heart Failure Patients Before and After Hospitalization at Prof. Dr. I.G.N.G Ngoerah Hospital. *Jurnal Farmasi dan Ilmu Kefarmasian Indonesia*, 12(1), 37-49. <http://doi.org/10.20473/jfiki.v12i12025.37-49>

INTRODUCTION

Heart failure is caused by abnormalities in the function and structure of the heart that can interfere with the ventricles filling and pumping blood to the heart (Heidenreich et al., 2022). According to the European Society of Cardiology (ESC), by 2022, an estimated 63 million people worldwide will suffer from heart failure (Rosano et al., 2022). Indonesia has the second-highest number of heart failure patients in Asia (Savarese et al., 2022). According to Riset Kesehatan Dasar (Riskesdas), in 2018, 1.5% or nearly 4 million Indonesians suffered from heart failure. Bali is in 21st place with 1.1% of heart failure patients (Kemenkes RI, 2018). Heart disease is the second-highest cause of death after stroke in Indonesia (Donsu et al., 2020). Death in heart failure patients can be caused by several conditions, such as shortness of breath, fatigue and fluid retention (DiPiro et al., 2021). Fluid retention is the impact of the heart's compensatory response in maintaining heart function and can cause edema, difficulty breathing, and an increase in the amount of phlegm (DiPiro et al., 2021; PERKI, 2020). One way to treat fluid retention is to administer diuretic drugs such as furosemide, which prevents the reabsorption of potassium, sodium, and chloride in the henle loop thereby increasing the excretion of water and salt through the urine. However, furosemide administration in heart failure patients is associated with a 30% incidence of hypokalemia (Aimbudlop & Saengpanit, 2023).

Hypokalemia is a clinical condition when the concentration of potassium in the blood serum is less than 3.5 mEq/L (mmol/L), which can cause decreased heart function, arrhythmias, and cardiac arrest (DiPiro et al., 2021). This condition can be caused by comorbidities in heart failure patients such as kidney failure (Sarnowski et al., 2022; Thomsen et al., 2018), diabetes (Thomsen et al., 2018), and gastric bleeding (Rizos et al., 2017), as well as the use of drugs such as Angiotensin Converting Enzyme inhibitors (ACEi), Angiotensin Receptor Blocker (ARB), beta-blockers, spironolactone, and diuretics called furosemide (Chang et al., 2016; Rawal et al., 2020). One way to prevent hypokalemia in heart failure patients is by monitoring potassium levels before and after administration of diuretics such as furosemide and paying attention to the correct dosage. Therefore, this study was conducted to analyze potassium levels before and after hospitalization in heart failure patients receiving furosemide therapy and the possibility of hypokalemia in heart failure patients due to furosemide administration at Prof. Dr I.G.N.G. Ngoerah Hospital.

MATERIALS AND METHODS

Observational research with a cross-sectional design and retrospective collection of medical record data has been carried out and ethical exemption obtained from the Ethics Commission of the Faculty of Medicine, Udayana University No.1300/UN14.2.2.VII.14/LT/2024 with protocol number 2024/01/1/0602 and a research permit from Prof. Dr. I.G.N.G. Ngoerah Hospital with number DP.04.03/D.XVII.2.2.2/27373/2024. Sample data were collected from medical records of heart failure patients at Prof. Dr. I.G.N.G. Ngoerah Hospital who met the exclusion and inclusion criteria while hospitalized in the period January 2022-December 2023 using a purposive sampling method.

Materials

The tools used in this research are data collection forms, Statistical Package for the Social Sciences (SPSS) Version 29, and Microsoft Office applications for data processing. The materials used in this research comprise medical record data of patients diagnosed with heart failure at Prof. Dr. I.G.N.G. Ngoerah Hospital during the period January 2022-December 2023. The medical record data used included patient identity, patient diagnosis, hospital admission and discharge dates, patient final status (death or recovery), disease history, 'patients' laboratory data such as laboratory data such as pre- and post-hospitalization potassium data, sodium, creatinine, BUN, and eGFR; body mass index (BMI), and 'patients' medication history such as patients' daily medicine prescribed data, past medical history, and drug usage history.

Population

The population in this research included all patients who had been diagnosed with heart failure at Prof. Dr. I.G.N.G. Ngoerah Hospital during the period January 2022-December 2023. The inclusion criteria included patients with a diagnosis of heart failure who received furosemide therapy as a diuretic during their hospitalization at Prof. Dr. I.G.N.G. Ngoerah Hospital and had complete potassium data in their medical records during the period January 2022-December 2023. The exclusion criteria included patients with untraceable and unreadable medical records. The minimum sample size was calculated using the Lemeshow Formula One Proportion Estimation Method with Absolute Precision.

$$n = \frac{Z^2_{1-\alpha/2} + P(1-P)}{d^2}$$

The calculations were made with a 95% confidence level (1- α value) and an absolute precision of 0.09. The anticipated population proportion (P1) value refers to

research by Aimbudlop and Saengpanit (2023), which stated that the prevalence of hypokalemia patients is 0.3, so the minimum sample size obtained is 100 samples.

Data analysis

Data on patient characteristics, potassium levels before and after hospitalization, and data on patients with comorbid kidney failure, including potassium levels in patients diagnosed with heart failure and receiving furosemide at Prof. Dr. I.G.N.G. Ngoerah Hospital, during the period January 2022 - December 2023 have been collected for descriptive and statistical analysis. The normality test was carried out using the Kolmogorov-Smirnov method ($p>0.05$), and the parametric test using the paired t-test method ($p<0.05$) was applied only to potassium level data before and after hospitalization. Meanwhile, descriptive analysis was applied to patient characteristics data and potassium

level data in patients with comorbid kidney failure. The SPSS Version 29 application was used for statistical tests.

RESULTS AND DISCUSSION

Figure 1. Flowchart of Hospitalized Heart Failure Patients Receiving Furosemide with Available Potassium Data Before and After Hospitalization at Prof. Dr. I.G.N.G. Ngoerah Hospital from January 2022 to December 2023

Characteristics of patients

The data obtained included 101 patient medical records that met the inclusion criteria, with 11 patients having more than one inpatient visit so a total 114 'patient's medical records were obtained. Characteristics of patients are shown in Table 1.

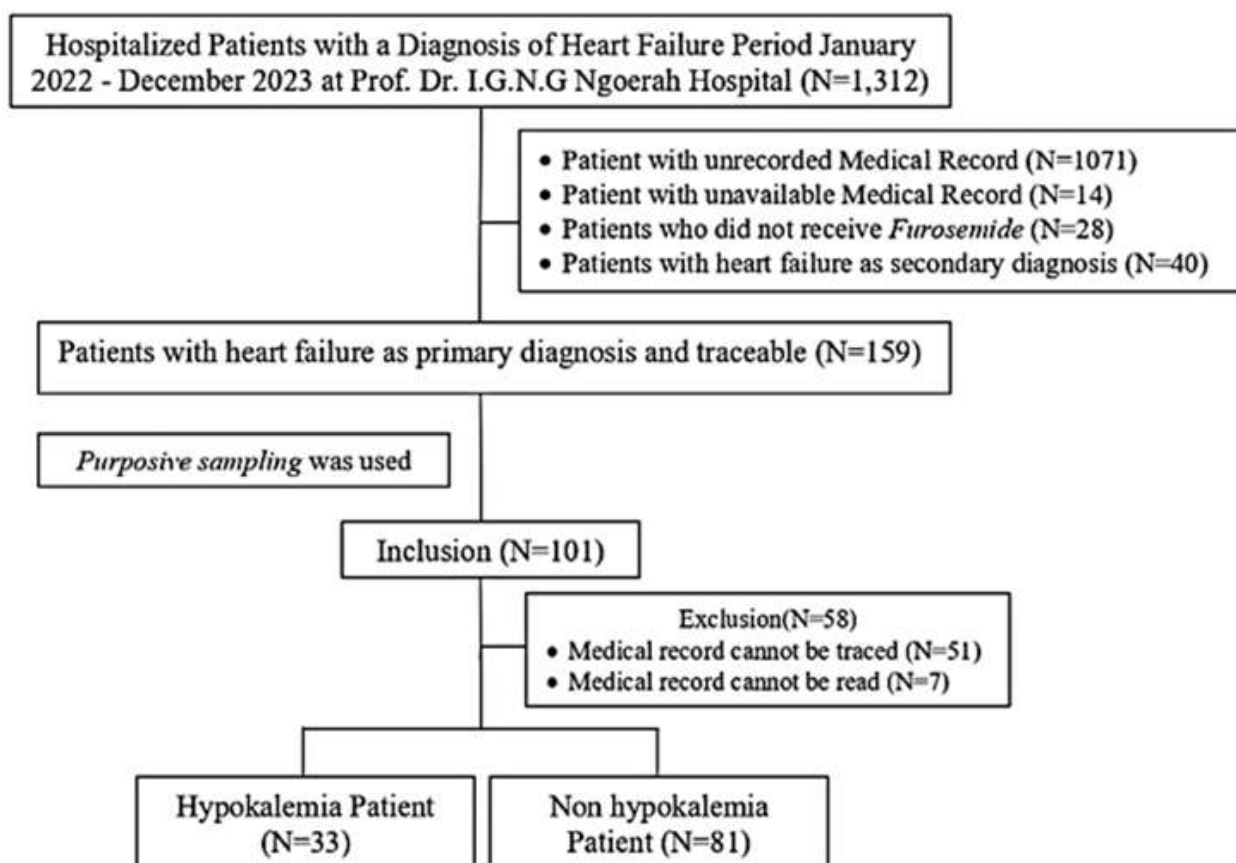


Figure 1. Flowchart of hospitalized heart failure patients receiving furosemide with available potassium data before and after hospitalization at Prof. Dr. I.G.N.G. Ngoerah Hospital from January 2022 to December 2023

Table 1. Characteristics of heart failure patients receiving furosemide with available potassium data before and after hospitalization at Prof. Dr. I.G.N.G. Ngoerah Hospital from January 2022 to December 2023

Characteristics		Number of Patients (n total = 101)	Percentage (%)
Age (years)	15-25	1	1
	26-35	7	6.9
	36-45	18	17.8
	46-55	27	26.7
	56-65	26	25.7
	> 65	22	21.8
Gender	Male	66	65.4
	Female	35	34.6
Duration of Hospitalization	0-7 days	74	64.9
	8-14 days	29	25.4
	15-21 days	4	3.5
	> 21 days	7	6.1
Patient Status	Recovered	97	85.1
	Death	17	14.9
Diagnoses	Acute Decompensated Heart Failure	98	86
	Congestive Heart Failure	11	9.6
	Chronic Heart Failure	4	3.5
	Right Heart Failure	1	0.9
Comorbidities	Kidney	62	38
	Heart	33	20.3
	Diabetic	29	17.8
	Hypertension	24	14.7
	Dyslipidemia	15	9.2
Social History	Smoking	29	28.7
	Non-Smoking	68	67.3
	Unknown	4	4
Body Mass Index (BMI)	Underweight (less than 18.5)	6	5.9
	Normal (18.5 to less than 25)	62	61.4
	Overweight (25 to less than 30)	23	22.8
	Obesity (30 or greater)	10	9.9

Abbreviations: n: Number of Patients

Table 1 shows that the majority of patients were aged 45 years and over (74.2%) and male (65.4%). This is due to a decrease in physiological function in elderly patients (Heidenreich et al., 2022), and male patients have a higher risk of experiencing heart failure than women because women can produce the hormone estrogen which acts as a heart protector by regulating lipoprotein levels (Riyadina, 2019). Furthermore, based on the characteristics of comorbidities in patients in this study, as shown in Table 1, it is known that kidney disease is the most common comorbidity experienced by patients, namely 62 (38%), followed by heart disease as many as 33 (20.3%), and diabetes as many as 29 (17.8%) in third place. These three comorbidities are risk factors for the increased incidence of heart failure (Walli-Attai et al. 2024; Bozkurt et al., 2025). In addition, smoking and excess weight can also contribute to an increased risk of cardiovascular disease, although they are not

major risk factors. Active smokers have high levels of inflammation, cardiomyocyte injury, myocardial fibrosis, and decreased left ventricular function (Gorrdiener et al., 2022), although in this study, there were fewer patients with smoking habits (29 of 114 patients (28.7%) than non-smokers and only 10 of 114 patients (9.9%) had a BMI of 30 or greater (obesity), but this needs to be considered because patients with high BMI (tend to be at higher risk of experiencing HFrEF (Heart Failure with Reduced Ejection Fraction) (Powell et al., 2021). This is because overweight patients have a greater heart workload and are at risk of developing hypertension (Rumaisyah et al., 2023).

Potassium level data

The data obtained included 114 values of potassium levels before and after hospitalization in patients with a diagnosis of heart failure at RSUP Prof. Dr. I.G.N.G. Ngoerah, who received furosemide during

the period January 2022 to December 2023. Normality test results conducted using the Kolmogorov-Smirnov method showed a p-value > 0.05 , indicating that the data were normally distributed, so it was continued with the parametric paired t-test on the value of potassium levels before and after hospitalization. Table 2 shows the results of paired t-test analysis.

Based on the results of paired t-test analysis, the p-value < 0.05 was obtained, which is < 0.001 . This

indicates a significant difference between the value of potassium levels before and after hospitalization. Next, in this study, the potassium levels of 114 patients were divided into two groups, namely the group of patients who experienced a decrease in potassium levels and the group of patients who experienced an increase in potassium levels after hospitalization.

Table 2. Results of Paired t-test analysis of potassium levels before and after hospitalization in heart failure patients receiving furosemide at Prof. Dr. I.G.N.G. Ngoerah Hospital from January 2022 to December 2023

Description	Number of patients (n total=114)	Average potassium level (mmol/L) \pm SD	p-value
Before Hospitalization	114	4.3 \pm 0.9	<0.001
After Hospitalization	114	3.9 \pm 0.7	

Abbreviations: n= number of patients; SD: Standard Deviation

Table 3. Table of increased potassium levels in 30 heart failure patients receiving furosemide before and after hospitalization at Prof. Dr. I.G.N.G. Ngoerah Hospital from January 2022 to December 2023

Potassium Level Before Hospitalization (mmol/L)	Potassium Level After Hospitalization (mmol/L)	Difference Potassium Level Before and After Hospitalization (mmol/L)	Percentage Difference Potassium Level Before and After Hospitalization (%)
4.2	4.4	0.2	4.5
3.4	3.6	0.2	5.6
2.9	3.5	0.6	17.1
3.2	3.5	0.3	8.6
3.3	3.9	0.6	15.4
3.8	3.9	0.1	2.6
3.9	4	0.1	2.5
4	4.2	0.2	4.8
3.1	4.4	1.3	29.5
3.1	3.4	0.3	8.8
3.5	4.4	0.9	20.5
4.1	5	0.9	18
3.4	4	0.6	15
4.1	4.7	0.6	12.8
3.8	4.3	0.5	11.6
3.8	3.9	0.1	2.6
3.9	4.4	0.5	11.4
3.5	3.9	0.4	10.3
4.5	5.5	1	18.2
2.9	3.6	0.7	19.4
5.5	5.6	0.1	1.8
3.4	3.8	0.4	10.5
3.6	4.1	0.5	12.2
3.5	4.3	0.8	18.6
3.8	4.7	0.9	19.1
3.2	3.5	0.3	8.6
4	5.5	1.5	27.3
3.6	4.4	0.8	18.2
3.8	5.1	1.3	25.5
3.6	4.4	0.8	18.2

The increase or decrease was calculated based on the reduction in potassium levels after hospitalization with potassium levels before hospitalization. Furthermore, the percentage difference was calculated. Patients were said to have increased potassium levels if the potassium levels after hospitalization were greater than before hospitalization. Conversely, patients were said to have decreased if the potassium levels after hospitalization were smaller than before hospitalization. Of the 114 patients, there were 30 patients who experienced an increase in potassium levels (see Table 3) and 84 patients who experienced a decrease in potassium levels after hospitalization (see Table 4).

In the group of patients who experienced increased potassium levels, the most significant percentage difference in potassium levels before and after hospitalization was 29.5%, and the smallest was 1.8%. The larger percentage difference indicates a greater

increase in potassium levels after the patient was hospitalized. Increased potassium levels can be caused by the presence of comorbid diseases such as kidney disease and diabetes mellitus as well as the use of Renin Angiotensin Aldosterone System (RAAS) and Mineralocorticoid Receptor Antagonist (MRA) inhibitor drugs. This result is in line with a cohort study in Denmark, which states that the incidence of hyperkalemia was 39% during a follow-up period of 2.2 years. The study also mentioned that kidney disease and diabetes will interfere with potassium excretion and regulation. In addition, the use of RAAS inhibitors and MRA, which are standard treatments for heart failure, can also interfere with potassium excretion, causing hyperkalemia (Thomsen et al., 2018). Although heart failure patients on therapy may have increased potassium levels, several mechanisms may also lead to decreased potassium levels during treatment.

Table 4. Table of decreased potassium levels in 84 heart failure patients received furosemide before and after hospitalization at Prof. Dr. I.G.N.G. Ngoerah Hospital from January 2022 to December 2023

Potassium Level Before Hospitalization (mmol/L)	Potassium Level After Hospitalization (mmol/L)	Difference Potassium Level Before and After Hospitalization (mmol/L)*	Percentage Difference Potassium Level Before and After Hospitalization (%)*
3.6	3.5	-0.1	-2.9
4.6	3.7	-0.9	-24.3
4.1	4	-0.1	-2.5
3.7	3	-0.7	-23.3
5.7	4.4	-1.3	-29.5
4.2	3.6	-0.6	-16.7
6.6	5.2	-1.4	-26.9
5	4.5	-0.5	-11.1
5.4	3.9	-1.5	-38.5
5.3	3.3	-2	-60.6
6.5	6.1	-0.4	-6.6
5	4.2	-0.8	-19
4.1	3.6	-0.5	-13.9
3.9	3	-0.9	-30
4	3.7	-0.3	-8.1
3.9	3.3	-0.6	-18.2
4.8	4.6	-0.2	-4.3
6.1	4.7	-1.4	-29.8
4.3	3.4	-0.9	-26.5
4.2	3.4	-0.8	-23.5
3.8	2.6	-1.2	-46.2
5.8	4.4	-1.4	-31.8
5.5	3.5	-2	-57.1
4.2	3.5	-0.7	-20
4.9	4.5	-0.4	-8.9
4	3.2	-0.8	-25
3.6	2.8	-0.8	-28.6
5.4	3.5	-1.9	-54.3

Potassium Level Before Hospitalization (mmol/L)	Potassium Level After Hospitalization (mmol/L)	Difference Potassium Level Before and After Hospitalization (mmol/L)*	Percentage Difference Potassium Level Before and After Hospitalization (%)*
3.8	3	-0.8	-26.7
4.8	3.6	-1.2	-33.3
3.5	3.2	-0.3	-9.4
5.3	4.2	-1.1	-26.2
4.3	4.2	-0.1	-2.4
4.2	4.2	0	0
4.5	4.4	-0.1	-2.3
4	3.2	-0.8	-25
3.8	3.7	-0.1	-2.7
7.9	4.5	-3.4	-75.6
3.6	2.8	-0.8	-28.6
3.5	3.1	-0.4	-12.9
3.8	3.7	-0.1	-2.7
4.5	3.9	-0.6	-15.4
5.7	4.5	-1.2	-26.7
4.2	3.5	-0.7	-20
2.9	2.5	-0.4	-16
4.4	3.6	-0.8	-22.2
6.7	4.9	-1.8	-36.7
5.1	4.6	-0.5	-10.9
4.1	3.1	-1	-32.3
4.8	4.6	-0.2	-4.3
4	3.6	-0.4	-11.1
5	4.6	-0.4	-8.7
4.2	3.7	-0.5	-13.5
3.9	3.7	-0.2	-5.4
3.9	3	-0.9	-30
3.6	3.5	-0.1	-2.9
6	4.5	-1.5	-33.3
5.1	4.8	-0.3	-6.3
5.3	3.7	-1.6	-43.2
3.8	3.5	-0.3	-8.6
4.3	4.1	-0.2	-4.9
4.4	4	-0.4	-10
4.6	3.2	-1.4	-43.8
4.6	3.3	-1.3	-39.4
5.1	3.8	-1.3	-34.2
4.4	4.1	-0.3	-7.3
5.1	4	-1.1	-27.5
4.7	4.2	-0.5	-11.9
4.7	4.4	-0.3	-6.8
4.1	3.3	-0.8	-24.2
5.5	3.8	-1.7	-44.7
4.2	3.4	-0.8	-23.5
4.7	3.8	-0.9	-23.7
3.4	3.4	0	0
4.4	4.2	-0.2	-4.8
5	2.1	-2.9	-138.1
6.2	4.2	-2	-47.6
4.9	4.7	-0.2	-4.3
4.3	3.9	-0.4	-10.3
3.5	3.4	-0.1	-2.9
3.9	3.1	-0.8	-25.8

Potassium Level Before Hospitalization (mmol/L)	Potassium Level After Hospitalization (mmol/L)	Difference Potassium Level Before and After Hospitalization (mmol/L)*	Percentage Difference Potassium Level Before and After Hospitalization (%)*
3.7	3.6	-0.1	-2.8
4	3.5	-0.5	-14.3
4.8	3.2	-1.6	-50

*: the negative value means the potassium level was decreasing after hospitalization

Table 5. Categorized potassium levels after hospitalization in heart failure patients receiving furosemide at Prof. Dr. I.G.N.G. Ngoerah Hospital from January 2022 to December 2023

Classification of Potassium Levels	Number of Patients who Increased Potassium Levels After Hospitalization (n=30)	Number of Patients who Decreased Potassium Levels After Hospitalization (n=84)
Hypokalemia (< 3,5 mmol/L)	1	32
Normal (3,5-5,1 mmol/L)	27	50
Hyperkalemia (>5,1 mmol/L)	2	2

Abbreviation: n=number of patients

In the group of patients who experienced decreased potassium levels, the percentage difference in potassium levels before and after hospitalization was 138.1%, and the smallest was 0%. The larger percentage difference indicates a greater decrease in potassium levels. The percentage showing a value of 0% in the group of patients who experienced decreased potassium levels can occur because there is no difference in potassium levels before and after hospitalization.

Decreased potassium levels in heart failure patients after hospitalization may be due to several factors such as diuretic use, RAAS activation, and insulin use. Studies have shown that 10 to 50% of patients treated with diuretics may develop hypokalemia (Ring et al., 2022). The dose or duration of the use of Furosemide as a loop diuretic (Ferreira et al., 2020). Furosemide can increase water and electrolyte excretion through urinary excretion, inhibit Na^+ , K^+ , and Ca^{2+} co-transporters in the loop of henle, and induce prostaglandin-mediated and aldosterone hormones (Felker et al., 2020).

Moreover, based on Table 4, from 84 data of patients who had decreased potassium levels, 49 patients showed a decrease of >15%, and 35 patients showed a decrease of $\leq 15\%$. Patients with a decrease in potassium levels >15% have a higher risk of arrhythmias that can trigger sudden cardiac death in heart failure patients (Aimbudlop & Saengpait, 2023). This is caused by low K^+ concentrations that can increase heart muscle excitability and delay repolarization (Ring et al., 2022). Arrhythmias often trigger sudden cardiac death in heart failure patients (Zaher et al., 2024).

Furthermore, after the potassium levels after hospitalization were obtained, we then grouped the

potassium levels into three groups: hypokalemia, normal, and hyperkalemia, as can be seen in Table 5.

Based on the results in Table 5, most patients in this study had normal potassium levels, both in the group of patients who experienced increased potassium levels after hospitalization (27 of 30 patients) and also in the group of patients who experienced decreased potassium levels after hospitalization (50 of 84). In the group of patients who experienced increased and reduced potassium levels after hospitalization, only two patients from each group had hyperkalemia, and more patients had hypokalemia (32 of 84 patients) in the group who experienced decreased potassium levels than in the group who experienced increased potassium levels after hospitalization, only 1 of 30 patients. The changes in potassium level values in patients are also influenced by several factors, such as the presence of kidney disease and the use of drugs that affect RAAS. Kidneys are responsible for 90-95% of potassium elimination, so abnormal conditions in the kidneys will interfere with the regulation of a patient's potassium levels (Ferreira et al., 2020).

One of the factors that play a role in increasing or decreasing potassium levels is the presence of kidney failure. In this study, there were more than half of the heart failure patients in this study (62 out of 114 patients) who also had comorbid kidney disorders. Moreover, for a more in-depth descriptive analysis in this study, we classified the kidney disorders experienced by patients and explored the data so that the results of Table 6 were obtained.

Based on Table 6, all heart failure patients with concomitant kidney disease experienced a decrease in potassium levels after treatment, with chronic kidney

disease (CKD) stage IIIB patients experiencing the highest reduction of potassium levels. In CKD stage IIIB, decreased potassium levels often occur due to a combination of diuretic use, relatively active renal excretion, dietary changes, and the influence of other drugs. However, as the disease progresses to advanced stages (stages IV and V), the kidneys lose their ability to excrete potassium, making patients more prone to hyperkalemia than hypokalemia (Sarnowski et al., 2022). In addition to CKD patients, changes in potassium also occur in acute kidney injury (AKI) patients, although the decrease is not as great as in CKD patients. AKI patients generally have increased serum creatinine levels and decreased urinary excretion (Kellum et al., 2021). Patients with lower glomerular filtration rate (eGFR), higher creatinine clearance, and renal failure comorbidities are more likely to develop hyperkalemia (Jun et al., 2021). In addition, patients with ACKD who have multiple bilateral cysts growing in the kidneys also have decreased potassium levels. Cysts in ACKD patients cause loss of renal tissue that triggers mitogenic signaling, changes in sodium and potassium concentrations, activation of the RAAS system, and hyperplasia of renal tubular cells (Teuwafu et al., 2023).

Based on Table 6, it also shows that heart failure patients in this study, in addition to having comorbid kidney disorders, also had other comorbidities, called diabetes, hypertension, and dyslipidemia. The presence of additional comorbidities can affect potassium levels. Where in this study, patients with additional comorbid diabetes experienced hyperkalemia, while patients with additional comorbid cancer experienced hypokalemia. Diabetic patients are at risk of hyperkalemia due to the condition of hyporeninemic hypoaldosteronism, which causes RAAS dysfunction so that there is a decrease in aldosterone secretion by the adrenal glands, which plays a role in K^+ secretion so that potassium levels in the blood increase. In addition, uncontrolled diabetic patients also generally experience hyperosmolality, which causes K^+ ions to leave the cells so that potassium levels in the blood increase (Goia-Nishide, 2022), and patients with diabetes have a prevalence ratio of 1.38 to experience hyperkalemia compared to those without diabetes because diabetes can cause diabetic nephropathy, which can reduce kidney function and potassium excretion ability. In addition, insulin deficiency in diabetes can also disrupt the distribution of potassium between intracellular and extracellular fluids so that potassium levels in the blood tend to be high (Thomsen et al., 2018).

The presence of comorbid dyslipidemia and hypertension can also affect the patient's potassium levels. Heart failure patients who also have hypertension are at risk of experiencing increased potassium levels caused by the use of antihypertensive drugs (Rakugi et al., 2021), such as the use of RAASi drugs (ACEi, ARB, ARNi), which work by inhibiting the action of angiotensin II, thereby reducing aldosterone hormone levels, which regulate potassium secretion, thereby increasing the risk of hyperkalemia (Oktaviono & Kusumawardhani, 2020; Rakugi et al., 2021). The risk of hyperkalemia associated with renin-angiotensin-aldosterone system (RAAS) inhibition ranges from 2% to 10% in patients with hypertension (Chang et al., 2016). Besides that, patients with dyslipidemia will also tend to have altered potassium levels, as patients with central obesity, hypertriglyceridemia, low HDL-C and high fasting plasma glucose tend to have lower serum potassium levels (Sun et al., 2014).

In this study, heart failure patients were also prescribed other drugs besides furosemide, which can affect potassium levels, as seen in Table 7.

Based on Table 7, instead of furosemide, patients also received other drugs such as Angiotensin Converting Enzyme inhibitors (ACEi), Angiotensin II Receptor Blockers (ARB), beta blockers, spironolactone, potassium chloride (KSR), and insulin. Those drugs can also affect potassium levels in heart failure patients. There were 84 (73.7%) prescriptions of ACEi and 23 (20.2%) prescriptions of ARB. These two groups of drugs are angiotensin II antagonists and are commonly used in heart failure patients (Heidenreich et al., 2022). Inhibition by angiotensin II will reduce levels of the hormone aldosterone, which regulates potassium secretion. The decrease in aldosterone levels due to ACEi and ARB is mostly offset by increased distal sodium so that potassium levels remain stable. However, in patients with renal perfusion, the proximal reabsorption becomes very strong, reducing distal sodium levels and increasing the risk of hyperkalemia (Oktaviono & Kusumawardhani, 2020).

There were 82 (71.9%) prescriptions using β -blocker drugs that inhibit β receptors in the cell membranes of various organs. This class of drugs induces hyperkalemia by suppressing the secretion of the hormone aldosterone from the adrenal cortex and decreasing the activities of the Na^+-K^+ ATPase pump so that potassium absorption by cells will also decrease (Rawal et al., 2020).

Table 6. Classification of comorbid kidney disease and the potassium level in 62 heart failure patients receiving furosemide before and after hospitalization at Prof. Dr. I.G.N.G. Ngoerah Hospital from January 2022 to December 2023

Classification of Comorbid Kidney Disease	Number of Patients (n total=62)	Average Potassium Before Hospitalization (mmol/L)	Average Potassium After Hospitalization (mmol/L)	Number of Patients with Hyperkalemia or Hypokalemia (n total=62)	Other Comorbidities owned by patients
Acute Kidney Injury (AKI)	32	4.2	3.7	11 Hypokalemia 0 Hyperkalemia	Diabetes Type 2 Dyslipidemia Hypertension Atrial Fibrillation
Acquired Cystic Kidney Disease (ACKD)	11	4.6	4	2 Hypokalemia 0 Hyperkalemia	Dyslipidemia Hypertension Atrial flutter Diabetes Type 2
Chronic Kidney Disease (CKD)	19				
CKD Stage II	2	4	3.9	0 Hypokalemia 0 Hyperkalemia	Diabetes Type 2 Hypertension
CKD Stage III A	6	4.8	4.1	1 Hypokalemia 1 Hyperkalemia	Diabetes Type 2 Hypertension Atrial Fibrillation
CKD Stage III B	4	6	4.5	1 Hypokalemia 1 Hyperkalemia	Diabetes Type 2
CKD Stage IV	4	4.2	4	2 Hypokalemia 0 Hyperkalemia	Diabetes Type 2 Atrial Fibrillation Paroxysmal
CKD Stage V	3	5	4.3	0 Hypokalemia 0 Hyperkalemia	Diabetes Type 2 Atrial flutter

Table 7. Drugs Used by Heart Failure Patients Who Received Furosemide During Hospitalization at Prof. Dr. I.G.N.G. Ngoerah Hospital from January 2022 to December 2023

Classification of Drugs	Number of Prescriptions	Percentage (%)
Angiotensin Converting Enzyme inhibitors (ACEi)	84	73.7
Angiotensin II Receptor Blockers (ARB)	23	20.2
Beta-Blocker	82	71.9
Spironolactone	85	74.6
Potassium Chloride (KSR)	33	29
Insulin	23	20.2

Table 7 also shows that there were 85 (74.6%) prescriptions of spironolactone. This drug works by competitively blocking the action of aldosterone, resulting in decreased sodium reabsorption and increased potassium retention (Patibandla et al., 2023). Patients with spironolactone therapy have a 10% lower risk of hypokalemia than patients with loop diuretic therapy (Ferreira et al., 2020). In addition, 33 (29%) patients received potassium supplements, namely KSR, which can increase body potassium levels (Table 7). KSR will be ionized into K^+ and Cl^- in the body. Kalium ions will then undergo reabsorption in the kidneys (Yamada & Inaba, 2021). The use of potassium supplements in patients undergoing furosemide therapy will reduce the risk of hypokalemia by 12% (Aimbudlop

& Saengpait, 2023). Based on Table 7, it is also known that there are 23 (20.2%) patients using insulin. The physiological response to insulin is the activation of the Na^+-K^+ ATPase pump, which increases the absorption of K^+ into cells, thereby providing defense against hyperkalemia (Ring et al., 2022).

This study has several strengths, including a comprehensive evaluation of potassium level fluctuations in heart failure patients receiving furosemide therapy, a large sample size that enhances the reliability of findings, and a holistic approach that considers multiple influencing factors such as comorbidities and concurrent medications. Additionally, the use of robust statistical analyses strengthens the validity of the results. However, there

are some limitations, such as the retrospective study, which relies on the availability and accuracy of medical records, and the fact that it was conducted in a single hospital, potentially limiting the generalizability of the findings. The study also does not account for the dosage of furosemide, which may influence potassium levels. Future research should focus on prospective studies to calculate the furosemide dose given to patients with renal impairment and track furosemide and potassium levels over time after dose adjustments. In addition, multicenter studies are needed to increase generalizability.

CONCLUSION

This study highlights the dynamic changes in potassium levels among heart failure patients receiving furosemide therapy during hospitalization. These findings reinforce the need for continuous potassium monitoring and individualized therapeutic strategies to reduce the risk of potassium imbalance, especially hypokalemia. Given the complexity of factors affecting potassium levels, including comorbid conditions and use of certain medications, a multidisciplinary approach is essential to optimize patient outcomes.

ACKNOWLEDGMENT

Our thanks to Ministry of Education, Culture, Research, and Technology, Directorate of Learning and Student Affairs, and Udayana University who provided research funds, so this research could be carried out properly

ETHICAL CLEARANCE

Ethical approval was not necessary for this case report. The authors provided written informed consent for the publication of this case report. All identifying information was carefully omitted in accordance with patients' wishes.

FUNDING

This research was funded by Student Creativity-Exact Research (PKM-RE) 2024, Directorate of Learning and Student Affairs, Directorate General of Higher Education, Research, and Technology, Ministry of Education, Culture, Research, and Technology and Udayana University.

AUTHOR CONTRIBUTIONS

Conceptualization, R.N., K.I.A.; Methodology, R.N., K.I.A.; Software, K.I.A., N.P.I.S., N.K.A.K.; Validation, R.N.; Formal Analysis, N.P.I.S., N.K.A.K.,

N.K.M.A., M.S.W.; Investigation, K.I.A., N.P.I.S., N.K.A.K., N.K.M.A., M.S.W.; Resources, K.I.A., N.P.I.S., N.K.A.K., N.K.M.A., M.S.W.; Data Curation; K.I.A., N.K.A.K., N.K.M.A.; Writing - Original Draft, R.N., K.I.A., N.P.I.S., M.S.W.; Writing - Review & Editing, R.N., K.I.A., N.K.A.K., N.K.M.A.; Visualization, N.K.M.A., M.S.W.; Supervision, R.N.; Project Administration, K.I.A.; Funding Acquisition, R.N., K.I.A., N.P.I.S., N.K.A.K., N.K.M.A., M.S.W.

CONFLICT OF INTEREST

The authors declared no conflict of interest.

REFERENCES

- Aimbudlop, K. & Saengpanit, D. (2023). Factors Associated with Hypokalemia after Furosemide Treatment in Hospitalized Patients with Acute Decompensated Heart Failure. *Journal of the Nephrology Society of Thailand*; 30; 57-68.
- Bozkurt, B., Ahman, T., Alexander, K., Yancy, C. & Ziaieian, B. (2025). HF STATS 2024: Heart Failure Epidemiology and Outcomes Statistics an Updated 2024 Report from the Heart Failure Society of America. *Journal of Cardiac Failure*; 31; 66-116. doi: 10.1016/j.cardfail.2024.07.001.
- Chang, A. R., Sang, Y., Leddy, J., Yahya, T., Kirchner, H. L., Inker, L. A., Matsushita, K., Ballew, S. H., Coresh, J. & Grams, M. E. (2016). Antihypertensive Medications and the Prevalence of Hyperkalemia in A Large Health System. *Hypertension*; 67; 1181-1188. doi: 10.1161/hypertensionaha.116.07363.
- DiPiro, J. S., Yee, G. C., Posey, L. M., Haines, S. T., Nolin, T. D. & Ellingrod, V. (2021). *Pharmacotherapy Handbook* (11th ed). USA: McGraw Hill.
- Donsu, R. A., Rampengan, S. H. & Polii, N. (2020). Karakteristik Pasien Gagal Jantung Akut di RSUP Prof Dr. R. D. Kandou Periode Januari-Desember 2018. *Medical Scope Journal*; 1; 30-37. doi: 10.35790/msj.v1i2.27463.
- Ferreira, J. P., Butler, J., Rossignol, P., Pitt, B., Anker, S. D., Kosiborod, M., Lund, L. H., Bakris, G. L., Weir, M. R. & Zannad, F. (2020). Abnormalities of Potassium in Heart Failure: Jacc State-Of-The-Art Review. *Journal of The American College of Cardiology*; 75; 2836-2850. doi: 10.1016/j.jacc.2020.04.021.
- Felker, G.M., Ellison, D.H., Mullens, W., Cox, Z. L. & Testani, J. M. (2020). Diuretic Therapy for

- Patients with Heart Failure: JACC State-Of-The-Art Review. *Journal of the American College of Cardiology*; 75; 1178-1195. doi: 10.1016/j.jacc.2019.12.059.
- Goia-Nishide, K., Coregliano-Ring, L. & Rangel, É.B. (2022). Hyperkalemia in Diabetes Mellitus Setting. *Diseases*; 10: 1-17. doi: 10.3390/diseases10020020
- Gorrdiener, J. S., Buzkova, P., Kahn, P. A., DeFilippi, C., Shah, S., Barasch, E., Kizer, J. R., Psaty, B. & Gardin, J. M. (2022). Relation of Cigarette Smoking and Heart Failure in Adults ≥ 65 Years of Age (From the Cardiovascular Health Study). *The American Journal Of Cardiology*; 168; 90-98. doi: 10.1016/j.amjcard.2021.12.021.
- Heidenreich, P. A., Bozkurt, B., Aguilar, D., Allen, L. A., Byun, J. J., Colvin, M. M., Deswal, A., Drazner, M. H., Dunlay, S. M., Evers, L. R., Fang, J. C., Fedson, S. E., Fonarow, G. C., Hayek, S. S., Hernandez, A. F., Khazanie, P., Kittleson, M. M., Lee, C. S., Link, M. S. & Yancy, C.W. (2022). AHA/ACC/HFSA Guideline for the Management of Heart Failure: A Report of the American College of Cardiology/American Heart Association Joint Committee on Clinical Practice Guidelines. *Circulation*; 145; 895–1032. doi: 10.1161/CIR.0000000000001063
- Jun, H.R., Kim, H., Lee, S.H., Cho, J. H., Lee, H., Yim, H. W., Yoon, K. H. & Kim, H. S. (2021). Onset of Hyperkalemia Following the Administration of Angiotensin-Converting Enzyme Inhibitor or Angiotensin II Receptor Blocker. *Cardiovascular Therapeutics*; 1; 5935149. doi: 10.1155/2021/5935149.
- Kellum, J. A., Romagnani, P., Ashuntantang, G., Ronco, C., Zarbock, A. & Anders, H. J. (2021). Acute Kidney Injury. *Nature reviews. Disease Primers*; 7; 52. doi: 10.1038/s41572-021-00284-z.
- Oktaviono, Y. H. & Kusumawardhani, N. (2020). Hyperkalemia Associated with Angiotensin Converting Enzyme Inhibitor or Angiotensin Receptor Blockers In Chronic Kidney Disease. *Acta Medica Indonesiana*; 52; 74-79.
- Patibandla, S., Heaton, J. & Kyaw, H. (2024). Spironolactone. StatPearls.
- PERKI (Perhimpunan Dokter Spesialis Kardiovaskular Indonesia). (2020). Pedoman Tatalaksana Gagal Jantung. 2nd edn. Jakarta Barat: Perhimpunan Dokter Spesialis Kardiovaskular Indonesia.
- Powell-Wiley, T. M., Poirier, P., Burke, Després, J. P., Gordon-Larsen, P., Lavie, C. J., Lear, S. A., Ndumele, C. E., Neeland, I. J., Sanders, P. & St-Onge, M. P. On Behalf of the American Heart Association Council on Lifestyle and Cardiometabolic Health; Council on Cardiovascular and Stroke Nursing; Council on Clinical Cardiology; Council on Epidemiology and Prevention; and Stroke Council (2021). Obesity and Cardiovascular Disease: A Scientific Statement From The American Heart Association. *Circulation*; 143; 984-1010. doi: 10.1161/CIR.0000000000000973
- Rawal, K.B., Chhetri, D.R., Giri, A., Girish, H.N., Luhar, M.B., Anusha, S., Ashvil, A. & Lalrinsiam, R. (2021). Metoprolol-Induced Hyperkalemia—A Case Report. *Indian Journal of Medical Sciences*; 73; 253-255. doi: 10.25259/IJMS_134_2020
- Ring, L.C., Nishide, K.G. & Rangel, E.B. (2022). Hypokalemia in Diabetes Mellitus Setting. *Medicina*; 58; 1-18. doi: 10.3390/medicina58030431
- Riskesdas. (2018). Hasil Utama Riset Kesehatan Dasar (RISKESDAS). Jakarta: Kementerian Kesehatan Republik Indonesia.
- Riyadina, W. (2019). Hipertensi pada Wanita Menopause. Jakarta: LIPI Press.
- Rizos, C.V., Milionis, H.J. & Elisaf, M.S. (2017). Severe Hyperkalemia Following Blood Transfusions: Is There a Link?. *World Journal of Nephrology*; 6; 53-56. doi: 10.5527/wjn.v6.i1.53.
- Rosano, G.M.C., Seferovic, P., Savarese, G., Spoleitini, I., Lopatin, Y., Gustafsson, F., Bayes-Genis, A., Jaarsma, T., Abdelhamid, M., Miqueo, A. G., Piepoli, M., Tocchetti, C. G., Ristić, A. D., Jankowska, E., Moura, B., Hill, L., Filippatos, G., Metra, M., Milicic, D. & Coats, A. J. S. (2022). Impact Analysis of Heart Failure Across European Countries: an ESC-HFA Position Paper. *ESC Heart Failure*; 9; 2767–2778. doi: 10.1002/ehf2.14076.
- Rumaisyah, R., Fatmawati, I., Arini, F. A. & Octaria, Y. C. (2023). Association between Types of Obesity and Hypertension in Young Adults in Indonesia. *Amerta Nutrition*; 7; 24-30. doi: 10.20473/amnt.v7i2SP.2023.24-30.
- Sarnowski, A., Gama, R.M., Dawson, A., Mason, H. & Banerjee, D., (2022). Hyperkalemia in Chronic Kidney Disease: Links, Risks and Management. *International Journal of Nephrology and Renovascular Disease*; 2; 215-228. doi: 10.2147/IJNRD.S326464.

- Savarese, G., Becher, P.M., Lund, L.H., Seferovic, P., Rosano, G.M.C. & Coats, A.J. (2022). Global Burden of Heart Failure: A Comprehensive and Updated Review of Epidemiology. *European Society of Cardiology*; 118; 3272–3287. doi: 10.1093/cvr/cvac013.
- Sun, K., Su, T., Li, M. & Xu, B. (2014). Serum potassium level is associated with metabolic syndrome: A population-based study. *Clinical Nutrition*; 2014; 521-527. doi: 10.1016/j.clnu.2013.07.010.
- Teuwafeu, D. G., Dongmo, A., Fomekong, S. D., Amougou, M., Mahamat, M., Nono, A., Kaze, F. F. & Ashuntantang, G. (2023). Acquired Cystic Kidney Disease in Patients On Maintenance Hemodialysis, Prevalence and Associated Factors: A Cross-Sectional Study. *The Pan African Medical Journal*; 45; 1-10. doi: 10.11604/pamj.2023.45.175.31773.
- Thomsen, R. W., Nicolaisen, S. K., Hasvold, P., Garcia-Sanchez, R., Pedersen, L., Adelborg, K., Egffjord, M., Egstrup, K. & Sørensen, H. T. (2018). Elevated Potassium Levels in Patients with Congestive Heart Failure: Occurrence, Risk Factors, and Clinical Outcomes: A Danish Population-Based Cohort Study. *Journal of the American Heart Association*; 7; 1-15. doi: 10.1161/JAHA.118.008912.
- Walli-Attai, M., Joseph, P., Johansson, I., Sliwa, K., Lonn, E., Maggioni, A. P., Mielniczuk, L., Ross, H., Karaye, K., Hage, C., Pogosova, N., Grinvalds, A., McCready, T., McMurray, J., Yusuf, S. & G-CHF investigators. (2024). Characteristics, Management, And Outcomes in Women And Men With Congestive Heart Failure In 40 Countries At Different Economic Levels: An Analysis From The Global Congestive Heart Failure (G-CHF) Registry. *Lancet Global Health*; 12; e396-e405. doi: 10.1016/S2214-109X(23)00557-0.
- Yamada, S. & Inaba, M. (2021). Potassium Metabolism and Management in Patients With CKD. *Nutrients*; 13; 1-19. doi: 10.3390/nu13061751.
- Zaher, W., Della Rocca, D. G., Pannone, L., Boveda, S., de Asmundis, C., Chierchia, G. B. & Sorgente, A. (2024). Anti Arrhythmic Effects of Heart Failure Guideline-Directed Medical Therapy and Their Role in the Prevention of Sudden Cardiac Death: From Beta-Blockers to Sodium-Glucose Co-transporter 2 Inhibitors and Beyond. *Journal of Clinical Medicine*; 13; 1-16. doi: 10.3390/jcm13051316.



Antiinflammatory Activity of Bangle Rhizome (*Zingiber purpureum* Roxb) Ethanol Extract on Rat Carrageenan Induced and Erythema Method

Mia Ariasti*, Muhammad Eka Putra Ramandha, Sri Winarni Sofya

Department of Pharmacy, Faculty of Health, Universitas Bumigora, Mataram, Indonesia

*Corresponding author: mia.ariasti@universitasbumigora.ac.id

Orcid ID: 0000-0002-8705-8170

Submitted: 2 August 2024

Revised: 19 April 2025

Accepted: 29 April 2024

Abstract

Background: Inflammation is a physiological response triggered by cellular damage, typically characterized by symptoms such as edema. **Objective:** This study was conducted to evaluate the anti-inflammatory activity of the ethanol extract of Bangle rhizome (*Zingiber purpureum* Roxb.) using the carrageenan-induced paw edema method and the UVB-induced erythema method. The most effective dose demonstrating significant anti-inflammatory activity was also determined. **Methods:** The bangle rhizome (*Zingiber purpureum* Roxb) was subjected to maceration using 96% ethanol. A total of 25 rats were randomly divided into five groups: negative control (0.5% CMC-Na), positive control (diclofenac sodium at 0.9 mg/200 g body weight), and treatment groups receiving ethanol extract of bangle rhizome at doses of 5, 10, and 20 mg/200 g body weight. In the carrageenan-induced method, the edema volume in the rat paw was measured following the administration of 0.8% lambda-carrageenan. In the erythema method, the degree of inflammation was assessed using UVB-induced erythema scoring. **Results and Conclusion:** Anti-inflammatory activity was observed at doses of 5, 10, and 20 mg/200 g body weight in the carrageenan model and at doses of 10 and 20 mg/200 g in the erythema model. The most potent anti-inflammatory effect was recorded at the dose of 20 mg/200 g body weight, which was comparable to the positive control in both models. The presence of flavonoids and steroids in the extract may contribute to the observed anti-inflammatory activity.

Keywords: Anti-inflammatory, bangle rhizome extract, carrageenan-induced edema, UVB-induced erythema

How to cite this article:

Ariasti, M., Ramandha, M. E. P. & Sofya, W. S. (2025). Antiinflammatory Activity of Bangle Rhizome (*Zingiber Purpureum* Roxb) Ethanol Extract on Rat Carrageenan Induced and Erythema Method. *Jurnal Farmasi dan Ilmu Kefarmasian Indonesia*, 12(1), 50-58. <http://doi.org/10.20473/jfiki.v11i32025.50-58>

INTRODUCTION

Inflammation is the body's reaction to damage or contamination (Bachtiar *et al.*, 2021). Inflammation occurs due to a nearby response from tissues or cells to the stimulus for the release of certain chemicals that will stimulate tissue changes in the reaction, including histamine, serotonin, bradykinin, leukotrienes, and prostaglandins (Garakia *et al.*, 2020). Inflammation is often thought of as a disease, when in fact it is the work of an immune response. The response that occurs is characterized by symptoms such as rubor (redness), calor (heat), dolor (pain), and tumor (swelling), so that inflammation often interferes with activities. Inflammation affects the membranes, causing leukocytes to secrete lysosomal enzymes, arachidonic acid, and various eicosanoids (Cowin 2008). The treatment of inflammation has two main goals: to relieve pain, which is the first visible symptom, and to sluggish or restrict the process of tissue destruction. Anti-inflammatory drugs have a common mechanism of action, which is inhibiting prostaglandin synthesis via the inhibition of the enzyme cyclooxygenase. Cyclooxygenase is responsible for prostaglandin biosynthesis. Based on the mechanism of action, anti-inflammatory drugs are divided into 2 groups, namely steroid groups that work by inhibiting the release of prostaglandins and their source cells, and nonsteroidal groups (NSAIDs) that work through the mechanism of cyclooxygenase inhibition that plays a role in prostaglandin biosynthesis. Drugs used as anti-inflammatories are the nonsteroidal group (AINS) and corticosteroids, where both groups have the potential to suppress signs and symptoms of irritation, but both groups of medicine regularly cause detrimental and dangerous outcomes together including gastrointestinal harm, nephrotoxicity, and hepatotoxicity (Garakia *et al.*, 2020).

In addition to drugs of the NSAID class, many plants are used as anti-inflammatories whose use is still widely favored by the community. Indonesia itself has many types of flora that may be used as a supply of herbal medicinal materials and are widely used by the community for generations to overcome health problems. One of the natural ingredients that is empirically effective as an anti-inflammatory drug is the bangle rhizome. Bangle belongs to the Zingiberaceae family and has been widely used in traditional medicine. Bangle rhizome is useful as a medicine for fever, abdominal pain, constipation, wind, worms, and gout (Ministry of Health RI 2001). The results of the phytochemical screening test of bangle rhizomes by Astarina *et al.* (2013) and Padmasari *et al.* (2013) showed that bangle rhizomes contain essential oil Compounds, flavonoids, saponins, triterpenoids, alkaloids, and tannins. Based on (Bachtiar

et al., 2021), bangle rhizomes contain bioactive compounds that are useful as medicines, one of which is essential oil.

The main components of the bangle rhizome essential oil (*Zingiber purpureum* Roxb.) consist of sabinene (48.1%), *terpinen-4-ol* (25.1%), *α-terpinene* (4.3%), and *α-phellandrene* and *Phenylmethylene* (2.7%). The utilization of plants that have anti-inflammatory activity is very necessary, especially to get alternative treatments that have small side effects, especially in efficacy as an anti-inflammatory, so in this study, tests will be carried out on the anti-inflammatory activity of ethanol extract of bangle rhizome which will be tested on male rats with two methods, namely carrageenan induction and UV radiation. The carrageenan induction method is a measurement of the volume of artificial edema in the leg of rats induced with lambda carrageenan, while the UV radiation induction method shows redness on the back of test animals due to UV light irritation, resulting in vasodilation followed by increased vascular permeability and local leukocytosis, commonly called erythema. The solvent used was 96% ethanol because it can dissolve compounds that are polar and non-polar, and is more selective. 96% ethanol can be used to remove impurities of amino acids, minerals, and proteins, which cannot be dissolved at low ethanol levels.

MATERIALS AND METHODS

Materials

The sample material used was a bangle rhizome. The chemicals used include distilled water, 96% ethanol, CMC-Na, and diclofenac sodium. The check animals used male white rats of stress with an age of 2-3 months and a body weight of about 150-300 grams.

Preparation of the ethanol extract of the bangle rhizome

The preparation of the ethanol extract of the bangle rhizome was accomplished through the maceration method using 96% ethanol solvent with a ratio of 1:10. As much as 1 kg was put into a maceration bottle, and then 96% ethanol was added to as much as 7.5 L. The maceration bottle was maintained at room temperature and was avoided while stirring repeatedly. After 5 days, the results of soaking were filtered with a flannel cloth and filter paper, then the pulp plus 96% ethanol as much as 2.5 L was filtered with flannel cloth and filter paper, and then the liquid extract was concentrated in a *rotary evaporator* at 40°C until a viscous extract was obtained.

Chemical content identification of the bangle rhizome extract

Flavonoid test. Flavonoid identification was done by dissolving 5 ml of concentrated extract of bangle rhizome into a test tube and adding 0.1 gram of Mg

powder and 5 drops of concentrated HCL, 2 ml of amyl alcohol, then shaking and letting it separate. If there is a red, yellow, or orange color in the amyl alcohol layer, the flavonoids are positive (Ciulei 1984). **Saponin test.** Identification of saponins was done by dissolving 0.05 mg of bangle rhizome sample into 20 ml of water, then.

Heat and filter, add 1 drop of HCL 2 N, shake vigorously for 10 seconds, and then leave for 10 seconds (Ciulei 1984). **Tannin Test.** A total of 0.05 mg of bangle rhizome powder was dissolved in 20 mL of distilled water. The solution was subsequently heated and filtered. To the obtained filtrate, 2–3 drops of 1% ferric chloride (FeCl_3) solution were added. The presence of tannins was indicated by the formation of a green or bluish-black coloration (Ciulei, 1984). **Essential oil.** A precipitate was formed by pipetting 1 mL of the test solution and then letting it evaporate in a porcelain cup. The positive effects of essential oils are indicated by the unique smell that the plant residue produces (Ciulei 1984). **Alkaloid Test.** Alkaloids were identified using the Mayer and Dragendorff methods. A mixture was prepared by combining 0.5 grams of concentrated bangle rhizome extract with 1 mL of 2 M hydrochloric acid (HCl) and 9 mL of distilled water. The mixture was then boiled for two minutes, allowed to cool, and subsequently filtered. The resulting filtrate was divided into three portions, and Mayer and Dragendorff reagents were added to each portion. A positive result for alkaloids was indicated by the formation of a white precipitate with the Mayer reagent and a light brown to yellow precipitate with the Dragendorff reagent (Ciulei, 1984).

Preparation of the solution

CMC-Na mucilago 0.5%. Weigh 500 mg of CMC-Na, and put 100 mL of hot water into a vaporizer cup. CMC-Na powder is sprinkled over the hot water little by little while stirring until homogeneous.

Diclofenac sodium suspension preparation 1%.

CMC-Na was weighed at 100 mg and then put little by little into a mortar containing hot water while stirring until homogeneous and fluffy. Diclofenac sodium was weighed at 100 mg, put into a mortar containing CMC-Na mucilage, and crushed while adding distilled water to a volume of 10 mL.

Preparation of the test preparations.

The extract test preparations were prepared by weighing 500 mg of CMC-Na and then sprinkling it into a vaporizer cup containing hot water and stirring until it expands. Bangle rhizome extract was weighed at 1 gram, then crushed in a mortar to shrink the particles, after which CMC-Na mucilago was added to a volume of 50 mL and stirred until homogeneous.

Anti-inflammatory test

Diclofenac sodium dose determination. The average human body weight of a 70-kg dose of diclofenac sodium is 50 mg/kg BW. The conversion factor from humans weighing 70 kg to rats with an average body weight of 200 g is 0.018, so the dose of diclofenac sodium for rats is 0.9 mg/200g BW of rats.

Anti-inflammatory test procedure of the rat paw edema method.

In this study, 5 animals were used in each experimental group. The anti-inflammatory test procedure is that rats are fed 8 hours before testing and, are still given drinking water. The rats were weighed and grouped randomly. 25 rats were divided into 5 groups. The left hind paw of each rat to be induced was marked at the ankle, then the volume was measured first by inserting the sole of the rat's foot into mercury until the mark limit. Each rat was treated according to its group. Group 1 with negative control treatment (CMC-Na), group 2 positive control (diclofenac sodium), dose of 0.9 mg/200 g BW, groups 3, 4, and 5 of the extract dose of 5 mg, 10 mg, and 20 mg/200 g BW. One hour later, a 0.8% lambda carrageenan solution was induced on the left hind paw with a volume of 0.2 ml. The volume of the paw was measured at 0.5, 1, 2, 3, 4, 5, 6, and 24 hours after lambda carrageenan induction; the paw of the rat was inserted into the seismometer until the limit mark. The DAI of the test drug is indicated by its ability to inhibit the volume of paw edema produced due to lambda carrageenan induction (Winter *et al.*, 1962). All data obtained were statistically analyzed on the volume of paw edema, and the proportion of edema inhibition was calculated.

Anti-inflammatory test procedure of the erythema method.

The mice were depilated with a size of 1.5 x 2.5 cm on the back for 18 hours. Test animals were treated orally 30 minutes before UV irradiation. The apparatus was heated for 30 minutes before use. Mice were irradiated with UV light at a distance of 10 cm for 5 hours, then the erythema formed was observed at 6, 12, 24, 48, and 72 hours.

Data Analysis

Carrageenan induction method. The effect of the administration of 96% ethanol extract of bangle rhizome on the anti-inflammatory effect with the carrageenan induction method was determined by calculating the volume of the edema.

$$V_u = V_t - V_o$$

Description:

Vu: The extent of edema rat paw on every occasion

Vt: Edema extent of the rat paw after stretching with 0.8% carrageenan at the time(t)

Vo: Edema volume of rat paw before 0.8% carrageenan

After obtaining the edema volume data, a comparison curve of edema volume versus time was made. Then the AUC (Area under the curve) is calculated, which is the average area under the curve, representing the relationship between the average edema volume per unit time. With the formula:

$$AUC_{n-1} = \frac{Vt_{n-1} + Vt_n}{2} (t_n - t_{n-1})$$

Description:

Vt_{n-1} : average edema volume in t_{n-1}

Vt_n : average volume at t_n

The anti-inflammatory power can be calculated using the following formula:

$$DAI = \frac{AUC_k - AUC_p}{AUC_k} \times 100\%$$

Description :

AUC_k : AUC curve of the mean edema volume against time for the negative control.

AUC_p : AUC curve of the mean edema volume versus time for each treatment group.

The data obtained is then analyzed with the *Kolmogorov-Smirnov test* to examine the distribution of facts and analyzed with the Levene check to peer the homogeneity of the statistics. If

the facts are typically allotted and homogeneous, it's typically analyzed with a one-way analysis of variance (ANOVA) test with a 95% confidence level and continued with the LSD test to determine whether or not there is a significant difference. If a condition for the ANOVA test is not met, the *Kruskal-Wallis* test is performed to determine if there is a difference. If there is a significant difference, the Mann-Whitney test is conducted to determine the difference between the treatment groups.

RESULTS AND DISCUSSION

The extraction of bangle rhizome powder was carried out by maceration with 96% ethanol as a solvent because it can dissolve polar and non-polar compounds. The macerate was obtained and then concentrated with a *rotary evaporator* at 40°C. The thick extract was 153.6 grams with a yield of 15.36%.

Identification of the chemical content of extracts and powders of bangle rhizomes aims to establish the truth of the chemical content contained in bangle rhizomes. The identification of compounds was carried out on flavonoids, saponins, tannins, essential oils, alkaloids, triterpenoids, and steroids. Analytical Chemistry Laboratory of the Faculty of Pharmacy, Bumigora University. The identification results can be seen in Table 1

Table 1. Compound content identification results of the bangle rhizome extract and powder

Name of Compound	Description	Extract Powder	
Flavonoid	The orange color that forms on the amyl alcohol layer shows flavonoid compounds (Ciulei 1984).	+	+
Saponin	The generation of foam for up to 10 seconds indicates saponin compounds (Ciulei 1984).	+	+
Tanin	The formation of a bluish-black shade suggests the presence of tannin compounds (Ciulei 1984).	+	-
Minyak atsiri	The generation of a characteristic odor by residues from the plant indicates essential oils (Ciulei 1984).	+	+
Alkaloid	Characterized by the formation of mild brown to yellow color precipitates on the <i>Dragendorff</i> reagent and white precipitates on the Mayer reagent (Ciulei 1984).	+	+
Triterpenoid	The formation of a brown ring (Ciulei 1984).	+	+
Steroid	Formation of a blue-green ring (Ciulei 1984).	-	-

Description :

+: Compounds were detected

-: Compounds were not detected.

The results of identifying the compound content of bangle rhizome extracts and powders showed that bangle rhizomes contain flavonoids, saponins, tannins, triterpenoids, essential oils, and alkaloids. According to Astarina, N. W. G., Astuti, K. W., Warditiani (2012), and Padmasari *et al.* (2013), bangle rhizomes are positive for flavonoids, saponins, tannins, triterpenoids, alkaloids, and essential oils. According to Safira *et al.* (2012) and Burdah (1996), the flavonoid compounds in the Bangle rhizomes are flavonol groups, aurones, and isoflavone. The essential oils in bangle rhizomes contain butyl phenols such as (E)-1-(3,4-dimethoxyphenyl) butadiene (DMPBD), *terpinen 4-ol*, and terpenoid groups (Jeenapongsa *et al.* 2003; Pattanaseree 2005).

Anti-inflammatory effect test using the carrageenan induction method

The anti-inflammatory effect test was conducted using the rat paw edema approach by injecting 0.8% λ -carrageenan as a great deal as 0.2 ml. This approach is one of the simplest, easiest to perform, and most frequently used methods of testing anti-inflammatory activity. The inflammation formed by carrageenan induction also does not cause tissue damage. The edema quantity was measured before and after management of the check substance using a plethysmometer. This test used 25 rats divided into 5 test groups, namely negative control, positive control, and ethanol extract of bangle rhizome with dose variations obtained from the orientation results, namely 5 mg/200g BW, 10 mg/200g BW, and 20 mg/200g BW. Data were obtained from observations in a subplantar volume of rats in the form of the subplantar volume of rat after the hours 0.5 to 6 hours and 24 hours after carrageenan induction

Table 2. Average edema volume

Treatment	Mean volume (mL) of edema \pm SD								
	T0	T0,5	T1	T2	T3	T4	T5	T6	T24
Negative control (CMC-Na)	0 \pm 0	0.024 \pm 0.003	0.028 \pm 0.002	0.032 \pm 0.003	0.036 \pm 0.002	0.040 \pm 0.001	0.0616 \pm 0.00167	0.0446 \pm 0.001	0.0398 \pm 0.002
Extract dose 5 mg/kg BW	0 \pm 0	0.019 \pm 0.002	0.023 \pm 0.003	0.026 \pm 0.005	0.031 \pm 0.004	0.033 \pm 0.004	0.034 \pm 0.003	0.0328 \pm 0.002	0.022 \pm 0.002
Extract dose 10 mg/kg BW	0 \pm 0	0.018 \pm 0.002	0.022 \pm 0.003	0.026 \pm 0.003	0.028 \pm 0.004	0.030 \pm 0.002	0.031 \pm 0.001	0.031 \pm 0.002	0.021 \pm 0.002
Extract dose 20 mg/kg BW	0 \pm 0	0.018 \pm 0.002	0.020 \pm 0.0007	0.023 \pm 0.001	0.025 \pm 0.002	0.026 \pm 0.002	0.026 \pm 0.002	0.025 \pm 0.002	0.013 \pm 0.002
Na Diklofenak	0 \pm 0	0.017 \pm 0.001	0.018 \pm 0.002	0.020 \pm 0.002	0.023 \pm 0.002	0.024 \pm 0.002	0.023 \pm 0.002	0.022 \pm 0.002	0.012 \pm 0.0008

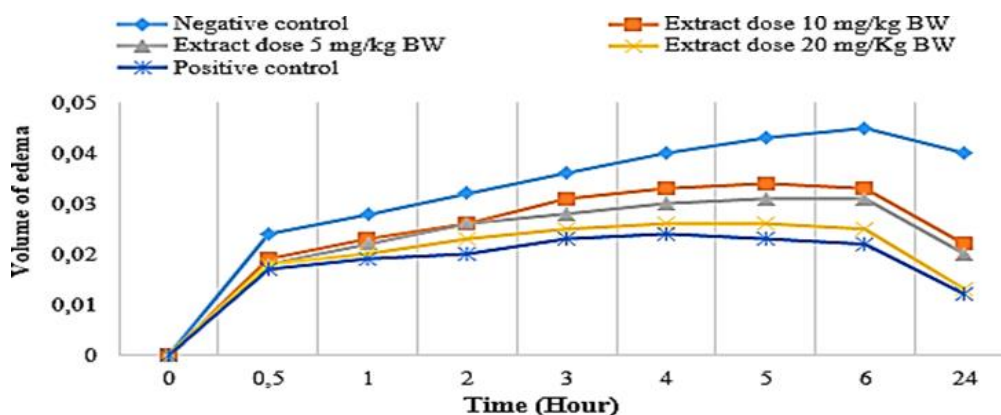


Figure 2. Results of the anti-inflammatory effect test with the carrageenan induction method

The negative control group given CMC Na experienced an increase in edema volume starting from hour 0.5, which was able to last for 6 hours due to the absence of an inhibitory process in the three processes of inflammation by carrageenan and decreased 24 hours later, where the largest edema volume formed occurred at hour 6. Based on the average edema volume in rat feet, it is known that the edema volume increases 30 minutes after induction with λ -carrageenan. According to Moris (2003), the formation of edema due to carrageenan induction consists of 3 phases. The primary segment involves the discharge of histamine and serotonin and lasts for ninety minutes. The second section involves the discharge of bradykinin and occurs 1.5-2.5 hours after induction. The 1/3 segment occurs three hours after induction, and the release decreases for up to 24 hours. The positive control group given diclofenac sodium in a dose of 4.5 mg/kg BW increased slowly, starting from hour 0.5, where the volume of leg edema formed was highest at hour 4, then the volume decreased from hour 5 to hour 24. This shows that diclofenac sodium provides a good therapeutic effect in the form of edema inhibition that occurs at hour 4. Diclofenac sodium is a phenyl acetate derivative

belonging to the AINS group with the strongest anti-inflammatory power. This drug works to inhibit cyclooxygenase, which is relatively non-selective and reduces the bioavailability of arachidonic acid (Tjay and Rahardja 2002). Diclofenac sodium is absorbed quickly and completely; its bioavailability is about 50%, with 99% bound to plasma proteins, and has a half-life of 1-3 hours, an onset of 30 minutes, and 8 hours (Katzung 2007).

The ethanol extract treatment group from the bangle rhizome increased the the edema volume at hour 0.5 after being induced with carrageenan. In the treatment group given ethanol extract of bangle rhizome as much as 5 mg/kg body weight, the increase in edema continued until the 5th hour and decreased again at the 6th hour. In the treatment of ethanol extract of bangle rhizome at a dose of 10 mg/kg BW and 20 mg/kg BW, it increased until the 4th hour and lasted until the 5th hour with a constant volume, indicating edema inhibition and decreased starting from the 6th hour. At the 6th hour, when a decrease in edema volume was experienced, the anti-inflammatory effect of the test compound could be seen through changes in edema volume.

Table 3. Average AUC total and average DAI (%)

Group	Mean AUCtotal \pm SD	Mean percentage % DAI \pm SD
Negative control (CMC-Na)	0.965 \pm 0.033b	-
Extract dose 5 mg/kg BW	0.654 \pm 0.062ab	32.36 \pm 5.867b
Extract dose 10 mg/kg BW	0.627 \pm 0.043ab	34.96 \pm 4.142b
Extract dose 20 mg/kg BW	0.495 \pm 0.061ab	48.71 \pm 5.569
Na Diklofenak	0.430 \pm 0.031a	54.65 \pm 3.738

Description:

a: Significantly different from the poor management group based on the LSD test ($p < 0.05$)

b: Significantly different from the effective management group based on the LSD test ($p < 0.05$)

The anti-inflammatory activity is expressed in the anti-inflammatory power. Based on the results of DAI (anti-inflammatory power) of ethanol extract of bangle rhizome at a dose of 20 mg/kg BW, it is assumed that this dose has more active compound content and the amount absorbed is more so that it can provide a better anti-inflammatory effect than doses of 10 mg and 5 mg/kg BW. The results of compound identification in the ethanol extract of bangle rhizome contain steroids, flavonoids, and tannins, according to previous studies. The compounds that provide anti-inflammatory effects are flavonoids and steroids, so in this study, the suspected anti-inflammatory compounds are flavonoids and steroids. Flavonoid compounds can inhibit COX

and lipooxygenase enzymes (Narayana *et al.* 2001). Inhibition of the COX and lipooxygenase pathway directly also leads to the inhibition of eicosanoid and leukotriene biosynthesis, and flavonoids can inhibit leukocyte accumulation in inflammatory areas (Panda *et al.* 2009; Kumbhare & Sivakumar 201, referenced in Zaini *et al.* 2016). The anti-inflammatory effect is also supported by its action as an antihistamine, histamine is one of the inflammatory mediators whose release is stimulated by pumping calcium into cells, flavonoids can inhibit the release of histamine from mast cells, and another mechanism of flavonoids is stabilizing Reactive Oxygen Species (ROS) reacting with reactive compounds from radicals so that the radicals become

inactive (Nijveldt *et al.* 2001, referenced in Zaini *et al.* 2016). Steroids work by inhibiting phospholipase activity, thereby preventing the release of arachidonic acid and blocking the release of arachidonic acid and blocking the cyclooxygenase and lipoxygenase pathways so that inflammatory mediators cannot be formed (Katzung 2002). Steroids inhibit the production of many important inflammatory factors such as interleukins, cytokines, and chemotaxis agents. Decreased release of these agents leads to decreased secretion of lipolytic and proteolytic enzymes, resulting in reduced leukocyte cell migration to the inflamed area (Grover *et al.* 2007).

Test of the anti-inflammatory effect with the erythema method

This study was conducted to prove the anti-inflammatory effect of ethanol extract of bangle rhizome on the back of rats characterized by the mean erythema score. This method is based on the visual observation of erythema on the skin of rats that have been shaved on the back. Erythema is formed due to UV light irritation. UV-causing erythema is an experiments for inflammatory reactions used to evaluate compounds that have anti-inflammatory activity both topically and systemically in test animals (Thompson 1990). The inducer used was an Exoterra UV B lamp

Table 4: Mean erythema score

Group	Mean \pm SD erythema score				
	T6	T12	T24	T48	T72
Negative control	1.8 \pm 0.836	2.6 \pm 0.547	3.4 \pm 0.547 ^b	3.8 \pm 0.447 ^b	3.2 \pm 0.447 ^b
Extract 5 mg/200g BW	1.6 \pm 0.894	2.4 \pm 0.547	3.4 \pm 0.547 ^b	3.2 \pm 0.836 ^b	2.6 \pm 0.547 ^b
Extract 10 mg/200g BW	1.4 \pm 0.547	2.6 \pm 0.547	3.2 \pm 0.447	2.8 \pm 0.836 ^b	2.2 \pm 0.836 ^{ab}
Extract 20 mg/200g BW	1.4 \pm 0.547	2.2 \pm 0.836	2.6 \pm 1.140	2 \pm 1.000 ^a	1.2 \pm 0.836 ^a
Positive control	1.6 \pm 0.547	2.2 \pm 0.836	2.4 \pm 0.547 ^a	1.6 \pm 0.547 ^a	0.6 \pm 0.547 ^a

Description:

a : Substantially unique from poor management

b : Substantially specific from effective management

Based on the graph above, erythema in mice appeared 6 hours after irradiation with UVB lamps. In the negative control group given CMC Na, erythema began to increase until 48 hours after irradiation with UVB lamps and decreased after 72 hours. This is to the research of Ito *et al.* (2015) that UVB-induced erythema responds after 2-24 hours of exposure, where, according to Kobayashi (2006), at 12-24 hours after induction, there is swelling and bullous formation. UVB directly damages the DNA chain, resulting in the formation of pyrimidine dimers and causing mutations. The reaction caused by UVB radiation results in the release of inflammatory mediators such as histamine, serotonin, and prostaglandins that cause the dilation of capillaries, leading to erythema and edema. UVB radiation can activate small molecules, such as melanin, tryptophan, riboflavin, and porphyrin, to form reactive oxygen species (ROS), which indirectly cause oxidative stress and activate cellular oxygen. In the positive control group given diclofenac sodium, erythema appeared 6 hours after UVB irradiation, increased until 24 hours of

exposure, and was different from the negative control, so it can be said that diclofenac sodium can inhibit the formation of erythema. At 48 hours after exposure, the erythema score decreased. This shows that diclofenac sodium provides anti-inflammatory effects with the ability to reduce the mean erythema score. According to research by Kienzler *et al.* (2005), the administration of diclofenac sodium can reduce erythema and edema due to exposure to UVA and UVB rays 48 hours after irradiation. Diclofenac sodium works to inhibit the enzyme cyclooxygenase, which plays a role in the metabolism of arachidonic acid into inflammatory mediators such as prostaglandins, thromboxane, and prostacyclin. Inside the remedy organization of ethanol extract of the bangle rhizome, erythema formed at the 6th hour after UVB exposure. In the treatment group of ethanol extract of the bangle rhizome, doses of 5, 10, and 20 mg/200 g continued to increase after 24 hours, then decreased at 48 hours. Furthermore, the mean erythema score data were statistically tested to determine significant differences between the treatment groups.

Table 5. Mean erythema score

Treatment group	Mean erythema score \pm SD
Negative control (CMC-Na)	2.96 \pm 0.77 ^b
Positive control (Natrium diklofenak)	1.68 \pm 0.70 ^a
Extract dose 5 mg/200 g BW	2.64 \pm 0.71 ^b
Extract dose 10 mg/200 g BW	2.44 \pm 0.68 ^{ab}
Extract dose 20 mg/200 g BW	1.88 \pm 0.57 ^a

Description:

a: Significantly different from the negative control group based on the LSD test results.

b: Significantly different from the positive control group based on the LSD test results.

The statistical test results show that the mean erythema score data is normally distributed with a significance value ($0.268 > 0.05$) and homogeneous with a significance value ($0.295 > 0.05$). The outcomes of the only-manner ANOVA check confirmed that there were good-sized variations among treatment corporations with a significance value ($0.000 < 0.05$), followed by the results of the LSD test, which showed that there were significant differences between the treatment groups. The results of the statistical tests showed that the ethanol extract of bangle rhizome at a dose of 10 mg/200 g BW and ethanol extract of bangle rhizome at a dose of 20 mg/200 g BW were significantly different from the negative control CMC Na, thus proving that bangle rhizome extract has an anti-inflammatory effect. Flavonoids work by inhibiting the activity of cyclooxygenase and lipooxygenase enzymes, eicosanoid biosynthesis, and neutrophil degranulation. Flavonoids inhibit the production of pro-inflammatory cytokines such as TNF- α (tumor necrosis factor- α), IL-1 β (interleukin-1 β), and IL-6 (interleukin-6). The flavonoid mechanism also inhibits the activation of transcription factors such as NF- κ B (nuclear factor- κ B), thereby interfering with the protein expression of iNOS and COX-2 (Nijveldt RJ *et al.*, 2001). Steroids reduce inflammation by blocking phospholipase A2 activity, which stops the release of arachidonic acid. Arachidonic acid is a building block for the production of pro-inflammatory mediators such as prostaglandins and leukotrienes (Barnes, 2022).

CONCLUSION

Extract Ethanol of bangle rhizome showed anti-inflammatory interest using the carrageenin induction method at doses of 5, 10, and 20 mg/200 g bw and showed anti-inflammatory activity using the erythema method at doses of 10 mg/200 g bw and 20 mg/200 g bw, ethanol extract of bangle rhizome at a dose of 20 mg/200 g bw in rats showed the highest anti-inflammatory interest and comparable to effective management in each method. The molecular

mechanisms underlying the anti-inflammatory properties of the ethanol extract of bangle rhizome should be further investigated, particularly at the most effective dose of 20 mg/200 g body weight. Pathways involving inflammatory mediators, such as pro-inflammatory cytokines, nuclear factor-kappa B (NF- κ B), and cyclooxygenase-2 (COX-2), should be examined in greater detail. Furthermore, the identification and isolation of active compounds should be conducted to support the development of standardized phytopharmaceutical formulations. To comprehensively assess the extract's efficacy and safety, studies involving chronic inflammation models, subchronic or chronic toxicity evaluations, and long-term comparisons with conventional anti-inflammatory drugs are required. Clinical trials in humans may also be considered to determine the extract's translational potential for therapeutic application.

REFERENCES

- Astarina, N. W. G., Astuti, K. W. & Warditiani, N. K. (2012). Skrining Fitokimia Ekstrak Metanol Rimpang Bangle. *Jurnal Farmasi Udayana*, 344; 1–7.
- Bachtar, K. R., Susanti, S. & Mardianingrum, R. (2021). Uji Aktivitas Antiinflamasi Senyawa dalam Minyak Atsiri Rimpang Bangle (*Zingiber Purpureum* Roxb) Secara in Silico. *Journal of Pharmacopolium*; 4; 36–43. doi: 10.36465/jop.v4i1.719.
- Barnes, P. J. (2022). Mechanisms and Molecular Targets of Corticosteroids in Inflammation. *Journal of Clinical Investigation*; 132; 76–85. doi: 10.1172/JCI148556.
- Burdah, M. (1996). Isolasi dan Identifikasi Senyawa Flavonoid dari Rimpang Bangle (*Zingiber Purpureum* Roxb). *Undergraduate thesis*; Universitas Surabaya, Surabaya.
- Ciulei, J. (1984). *Methodology for Analysis of Vegetables and Drugs*. Bucharest: Faculty of Pharmacy. Hlm 11–26.

- Garakia, C. S. H., Sangi, M. & Koleangan, H. S. J. (2020). Uji Aktivitas Antiinflamasi Ekstrak Etanol Tanaman Patah Tulang (*Euphorbia tirucalli* L.). *Jurnal MIPA*, 9; 60-63. doi: 10.35799/jmuo.9.2.2020.28709.
- Grover, V. K., Babu, R. & Bedi, S. P. S. (2007). Steroid Therapy – Current Indications in Practice. *Indian Journal of Anaesthesia*; 51; 389-393.
- Ito, I., Yoneda, T., Omura, Y., Osaki, T., Ifuku, S., Saimoto, H., Azuma, K., Iagawa, T., Tsuka, T., Murahata, Y., Ito, N., Okamoto, Y. & Minami, S. (2015). Protective Effect Of Chitin Urocanate Nanofibers Against Ultraviolet Radiation. *Marine Drugs*; 13; 7463-7475. doi: 10.3390/md13127076.
- Jeenapongsa, R., Yoovathawoen, K., Sriwatanakul, K., Sriwattanakul, M. & Pongprayoon, U. (2003). Anti-Inflammatory Activity of (E)-1-(3,4-Methoxyphenyl) Butadiene from *Zingiber Cassumunar* Roxb. Thailand: J. Ethnopharmacol. Hlm 143-148.
- Katzung, B. G. (2007). *Basic and clinical pharmacology*. Ed ke-10. McGraw-Hill Lange. 566-568.
- Kienzler, J. L., Magnette, J., Queille-Roussel, C., Sanchez-Ponton, A. & Ortonne, J. P. (2005). Diclofenac-Na Gel Is Effective in Reducing the Pain and Inflammation Associated with Exposure to Ultraviolet Light – Results of Two Clinical Studies. *Skin Pharmacology and Physiology*; 18; 144–152. doi: 10.1159/000084912.
- Kobayashi, S. (2006). UVB-Induced Skin Damage and The Protection/Treatment Effects of a Novel, Hydrophilic Gamma-Tocopherol Derivative. *Yakugaku Zasshi*; 126; 677-693. doi: 10.1248/yakushi.126.677.
- Kumbhare, M. T. & Sivakumar. (2011). Anti-Inflammatory and Antinociceptive Activity of Pods of *Caesalpinia Pulcherrima*. *Journal of Applied Pharmaceutical Science*; 1; 180-184.
- Morris, C. J. (2003). *Carragenan-Induced Paw Edema in the Rat and Mouse*. In P. G. Winyard and D. A. Willoughby (Eds). *Methods in Molecular Biology*. 225.
- Narayana, K. R., Reddy, M. S., Chaluvadi, M. R. & Khrisna, D. R. (2001). Bioflavonoids Classification, Pharmacological, Biochemical Effects and Therapeutic Potential. *Indian Journal of Pharmacology*; 33; 2-16.
- Nijveldt, R. J., Nood, E. V., Hoorn, D. E. V., Boelens, P. G., Norren, K. V. & Leuwen, P. A. V. (2001). Flavonoids: A Review of Probable Mechanisms of Action and Potential Applications. *American Journal of Clinical and Nutrition*; 74; 418-425. doi: 10.1093/ajcn/74.4.418.
- Panda, B. B., Gaur, K., Kori, M. L., Tyagi, L. K., Nema, R. K., Sharma, C. S. & Jain, A. K. (2009). Antiinflammatory and Analgesic Activity of *Jatropha gossypifolia* in Experimental Animal Models. *Global Journal of Pharmacology*; 3; 01-05.
- Pattanaseree, T. (2005). *Chemical compositions and Antioxidant activity of Zingiber cassumunar* Roxb Essential Oil. Thailand: Jurnal Ethnopharmacol.
- Safira, Fachriyah, E. & Kusriani, D. (2012). Isolasi dan Identifikasi Senyawa Flavonoid dari Ekstrak Etil Asetat Rimpang Bangle (*Zingiber cassumunar* Roxb.). *Jurnal Kimia Sains dan Aplikasi*. 36-38. doi: 10.14710/jksa.15.1.36-38.
- Thompson, E. B. (1990). *Drug Evaluation Techniques in Pharmacology*. The University of Illinois. Chicago.
- Tjay, T. H. & Rahadrja K. (2002). *Obat-obat Penting Khasiat Penggunaan dan Efek – efek Samping*. Ed ke-4. Jakarta: Elex Media Komputindo. 159.
- Winter, C. A., Risley EA, Nuss GW. 1962. Carragenan-Induced Edema in Hind Paw of the Rat as an Assay for Antiinflammatory Drugs. *Proc. Soc. Exp. Biol Med*; 111; 544-547. doi: 10.3181/00379727-111-27849.
- Zaini, M., Biworo, A. & Anwar, K. (2016). Uji Efek Antiinflamasi Ekstrak Etanol Herba Lampasau (*Diplazium Esculentum* Swartz) terhadap Mencit Jantan yang Diinduksi Karagenan-γ. *Jurnal Pharmascience*; 3; 119-130.



Assessment of Geriatrics Patients with Cardiovascular Disease Prescriptions for Appropriateness of Medications by Using Beers Criteria in Muhammadiyah Lamongan Hospital

Dyah Puspita Sari, Irma Susanti*, Anisa Zulfa Fatihah

Department of Clinical and Community Pharmacy, Faculty of Health Science, Universitas Muhammadiyah Lamongan, Indonesia

*Corresponding author: irmasusanti.apt@gmail.com

Orcid ID: 0000-0001-9216-5205

Submitted: 10 August 2024

Revised: 20 April 2025

Accepted: 29 April 2025

Abstract

Background: The number of geriatric residents has increased annually. Owing to pathological and physiological conditions, the geriatric population tends to consume more medications, thereby increasing their risk of adverse side effects and drug interactions. **Objective:** The objective of this study was to evaluate the appropriateness of therapy for outpatient geriatric patients with cardiovascular disease at Muhammadiyah Lamongan Hospital from August to October 2023. **Methods:** The American Geriatrics Society (AGS) Beers Criteria are one of the tools used to identify drugs whose potential harm outweighs the expected benefits and should be avoided in the elderly population. This study employed a descriptive method, with retrospective data collection from secondary sources, including medical records and electronic prescriptions. **Results:** The findings revealed that out of 252 prescriptions for geriatric patients with cardiovascular disease, four types of medications were potentially inappropriate according to the Beers Criteria: nifedipine with 23 prescriptions (9.13%), amiodarone with one prescription (0.40%), digoxin with 13 prescriptions (5.16%), and diltiazem with four prescriptions (1.59%). Conversely, three types of medications were deemed appropriate: aspirin (96 prescriptions, 38.10%), digoxin (30 prescriptions, 11.90%), and diltiazem (11 prescriptions, 4.37%). In conclusion, of the 252 prescriptions reviewed for geriatric patients with cardiovascular disease, three types of drugs are appropriate, while four types increase the risk of potentially inappropriate treatment (PIM) based on the Beers Criteria. **Conclusion:** These findings underscore the need for careful consideration to mitigate the risk of drug reactions. If the medication cannot be used in geriatric patients, an alternative therapy should be used or a dose adjustment may be necessary.

Keywords: Beer criteria, cardiovascular disease, potentially inappropriate medication

How to cite this article:

Sari, D. P., Susanti, I. & Fatihah, A. Z. (2025). Assessment of Geriatrics Patients with Cardiovascular Disease Prescriptions for Appropriateness of Medications by Using Beers Criteria in Muhammadiyah Lamongan Hospital. *Jurnal Farmasi dan Ilmu Kefarmasian Indonesia*, 12(1), 59-66. <http://doi.org/10.20473/jfiki.v12i12025.59-66>

INTRODUCTION

The number of elderly individuals (geriatric population) has been increasing annually, corresponding to rising life expectancy and reflecting improvements in community welfare. The global population aged ≥ 60 years is projected to grow from 1.4 billion in 2020 to 2.1 billion by 2050 (WHO, 2022). In 2021, Indonesia has reached an aging population structure, with approximately one in ten elderly residents. According to the National Socio-Economic Survey data from March 2022, 10.48% of Indonesia's population will be elderly. With advancing age, the incidence of degenerative diseases, particularly cardiovascular diseases, has increased. This trend is especially pronounced in the elderly population (Badan Pusat Statistik 2022).

Cardiovascular disease is caused by impaired heart and blood vessel function in the body (Unger et al., 2020). Cardiovascular diseases include acute coronary syndrome, hypertension, heart failure, and atrial fibrillation (AF) (Rampengan, 2014). Cardiovascular disease (CVD) is the leading cause of death worldwide. In 2019, an estimated 17.9 million people succumbed to cardiovascular disease, accounting for 32% of all global deaths. Of these deaths, 85% were attributed to heart attack and stroke. (WHO, 2021). Riskesdas (2018) also reported that the prevalence of heart disease based on doctors' diagnosis in Indonesia reached 1.5%, with the highest prevalence in North Kalimantan Province at 2.2%, Yogyakarta Special Region at 2%, and Gorontalo at 2% (Riskesdas, 2018). Based on the 2021 health profile in Lamongan District, there has been no specific prevalence of cardiovascular diseases; however, the risk factors for cardiovascular diseases such as hypertension and diabetes mellitus are quite high. The prevalence of hypertension is 48.02% in men and 51.98% in women, whereas the prevalence of diabetes mellitus is 97.2% of the existing estimates of people with diabetes mellitus. From these data, it can be concluded that the prevalence of cardiovascular diseases is high, but has not been recorded (Dinkes Lamongan, 2021).

The high prevalence of cardiovascular disease will inevitably burdens the growing geriatric population. Physiological changes accompanying aging affect cardiovascular function, pharmacokinetics, and pharmacodynamics (Julaiha, 2021). Patients with pathological and physiological conditions in geriatric populations tend to consume more drugs (polypharmacy). Geriatric patients have a greater risk of adverse side effects and drug interactions than younger

patients (Badan Pusat Statistik, 2022). One of the criteria used to identify drugs with potential harm outweighs the expected benefits and should be avoided in the elderly population (geriatrics) is the American Geriatrics Society (AGS) Beers Criteria. Several classes of drugs according to the Beers Criteria, which are potentially inappropriate for use in the elderly (geriatrics), include anticoagulants, digoxin, antiplatelets, ACEi, CCB, ARB, oral antiarrhythmic agents, and diuretics (Panel, 2023).

In Indonesia, research on the suitability of therapy for geriatric patients with cardiovascular disease is still very rare. Cases of potentially inappropriate drug use that occur in geriatric patients need special attention because they can increase the risk of adverse drug reactions (ROTD) (Julaiha, 2021). Therefore, it is necessary to conduct more comprehensive research on this issue in geriatric patients. The novelty of this research is the limited evaluation of local data, with the results potentially supporting the integration of the Beers Criteria into digital systems.

MATERIALS AND METHODS

Materials

Patient medical record data and electronic prescriptions were obtained using the purposive sampling technique. The collected data included patient profiles (age, sex, diagnosis, laboratory results, and treatment profile).

Method

This study used a descriptive method, presenting demographic data, treatment profiles, and the suitability of patient therapy based on the Beers Criteria. Data were obtained from the medical records of geriatric patients with cardiovascular disease at Muhammadiyah Hospital Lamongan from August to October 2023. Data were collected by extracting information from the hospital's information system (SIRS). This research was conducted after obtaining an ethical permit from LPPM of Universitas Muhammadiyah Lamongan (Lembaga Penelitian dan Pengabdian Masyarakat/Institute for Research and Community Service) with the number 204/EC/KEPK-S1/01/2024.

RESULTS AND DISCUSSION

This study obtained A total of 252 patients were obtained from the medical records and electronic prescriptions of geriatric patients with cardiovascular disease at Muhammadiyah Lamongan Hospital.

Table 1. Patients' Demographic Data

No	Demography	Categories	n (%)
1	Gender	Male	137 (54.4)
		Female	115 (45.6)
2	Age (Years) (Badan Pusat Statistik, 2022)	60-69	232 (92.1)
		70-79	17 (6.7)
		≥80	3 (1.2)
3	Diagnosis	Hypertension heart disease	115 (26.20)
		Ischaemic heart disease	97 (22.10)
		Heart failure	66 (15.03)
		Atherosclerosis heart disease	37 (8.43)
		Angina stable	32 (7.29)
		Atrial fibrilasi dan flutter	30 (6.83)
		Old miokard infark	25 (5.69)
		Mitral regurgitation	15 (3.42)
		Dislipidemia	11 (2.51)
		Angina pectoris	8 (1.82)
		Coronary heart disease	2 (0.46)
		Aritmia	1 (0.23)
4	Comorbidities	No comorbidities	220 (87.3)
		Diabetes mellitus type 2	20 (7.9)
		Asthma	4 (1.6)
		Osteo arthritis genus	1 (0.4)
		Neuralgia	1 (0.4)
		Hyperuricaemia asymptomatic	2 (0.8)
		Dispepsia	2 (0.8)
		Vertigo	1 (0.4)
		Ganglion	1 (0.4)

In Table 1, it was observed that the number of male patients was 137, accounting for 54.4% of the total. The high prevalence of cardiovascular disease in men is closely associated with unhealthy lifestyle choices, including smoking, alcohol consumption, poor diet, obesity, physical inactivity, and exposure to environmental pollution. These risk factors are twice as prevalent in male patients, making them more susceptible to degenerative diseases, particularly cardiovascular diseases (Handayani et al., 2018).

A total of 232 patients were classified as elderly, aged 60-74 years, representing 92.1% of the sample. Previous research indicates that individuals within this age group have the highest prevalence compared with other older age groups. This trend can be attributed to the decline in physiological function and weakened immune systems among geriatric patients, making them more susceptible to various diseases. These age-related changes affect organ function, structure, tissues, and systems, leading to deterioration of both physical and psychological health (Rokhman et al., 2020). Age is also a non-modifiable risk factor; a person over or equal

to 60 years old has a greater risk of death than a 25-49 year old (Kep et al., 2018).

The diagnosis of geriatric patients with the most cardiovascular disease was hypertensive heart disease in 115 patients (26.20%). Hypertension (HTN) is a major modifiable risk factor. Previous results showed that hypertension was associated with the incidence of coronary heart disease, in which respondents who had hypertension were 2,667 times more likely to have coronary heart disease than those who did not have hypertension (Amisi, 2018).

In addition to cardiovascular diseases, a significant number of patients had comorbidities: 7.9% had type 2 diabetes mellitus. These results indicate that type 2 diabetes mellitus was more prevalent among respondents than other comorbidities. This higher prevalence can be attributed to the metabolic disorder caused by hyperglycemia in individuals with diabetes mellitus, which leads to the production of metabolites that damage the endothelium of blood vessels, including coronary arteries (Kep et al., 2018).

As shown in Table 2, the treatment profile of geriatric patients with cardiovascular disease revealed that the β -blocker drug group, particularly bisoprolol, was the most frequently prescribed group, with 129 prescriptions (9.31%). According to Frederix and McIntosh (2017) from the European Society of Cardiology, beta-blocker therapy is effective in controlling the heart rate and preventing the

development of symptoms in stable coronary artery disease. In post-myocardial infarction conditions, beta-blockers have been shown to reduce the risk of death and heart rate by 20-25% in patients with atrial fibrillation (Arfania et al., 2023).

Table 2. Patient treatment profile

Drug Class	Medicine	n (%)
Antihypertensive		
B-Bloker	Bisoprolol	129 (9.31)
	Carvedilol	23 (1.66)
	Propranolol	10 (0.72)
	Nebivolol	2 (0.14)
	Hydrochloride	
ARB	Valsartan	21 (1.52)
	Candesartan	110 (7.94)
	Irbesartan	7 (0.51)
ACEI Inhibitor	Lisinopril	56 (4.04)
	Ramipril	25 (1.80)
CCB (Dihydropyridine)	Amlodipine	58 (4.18)
	Nifedipine	23 (1.66)
CCB (Non Dihydropyridine)	Diltiazem	15 (1.08)
Diuretic		
Potassium-sparing diuretics	Spironolactone	101 (7.29)
Loop Diuretic	Furosemide	94 (6.78)
Thiazide Diuretic	Hydrochlorothiazide	7 (0.51)
Antiplatelet dan Anticoagulants		
	Clopidogrel	81 (5.84)
	Ticagrelor	15 (1.08)
	Aspirin	96 (6.93)
	Warfarin	35 (2.53)
	Apixaban	2 (0.14)
Antianginal		
	Isosorbide dinitrate	52 (3.75)
	Glyceryl trinitrate	58 (4.18)
Anti-cholesterol		
Statin	Simvastatin	46 (3.32)
	Atorvastatin	88 (6.35)
	Rosuvastatin	3 (0.22)
Fibrate	Fenofibrate	1 (0.07)
Heart Medicine		
Heart Glycoid	Digoxin	43 (3.10)
Inhibitor Phosphodiesterase	Sildenafil	4 (0.29)
Angiotensin II Antagonist	Uperio	1 (0.07)
Antiarrhythmic	Amiodaron	1 (0.07)
Inhibitor Sodium Glucose Co-Transporter 2	Forxiga	1 (0.07)
Antigout	Allopurinol 100mg	13 (0.94)
Antidiabetics		
Sulfonylurea	Glimepiride	16 (1.15)
	Glucodex	3 (0.22)
	Gluvas M	1 (0.07)
Biguanide	Metformin	6 (0.43)
Alpha glucosidase inhibitor	Acarbose	1 (0.07)
Gastric Medicine		
Proton Pump Inhibitor	Omeprazole	11 (0.79)
	Lansoprazole	14 (1.01)
H2 Blocker	Ranitidine	3 (0.22)

Antilulcerant	Sucralfate syr	1 (0.07)
Central Nervous System Drugs		
Analgesic Opioid/Antitussive	Codeine	21 (1.52)
NSAID	Meloxicam	8 (0.58)
	Antalgin	3 (0.22)
	Kalium Diclofenac	1 (0.07)
Benzodiazepine	Alprazolam	3 (0.22)
	Valisanbe	3 (0.22)
	Analsik	6 (0.43)
Antidepressant	Amitriptilin	4 (0.29)
Anticonvulsant	Gabapentin	2 (0.14)
Antivertigo	Betahistin Mesilat	2 (0.14)
Antipyretic Analgesic	Paracetamol	1 (0.07)
Respiratory Medicine		
Decongestant	Tremenza	3 (0.22)
	Rhinos	1 (0.07)
Antihistamine	CTM	1 (0.07)
Expectorant	GG	5 (0.36)
Mucolytic	N-Acetylcysteine	4 (0.29)
Antithyroid	Thiamazole	5 (0.36)
Anti-hemorrhoid	Anadium	1 (0.07)
Antibiotic	Amoxicillin	1 (0.07)
Supplements and Vitamins	Omega-3-acid ethyl esters 90%, Folic Acid, Curcuma, Vit B comp	10 (0.72)

Table 3. Suitability of therapy based on Beers Criteria

Drug Name	Conformity (%)	
	Appropriate	Not Appropriate
Criteria 1		
Aspirin	96 (38.10)	0
Warfarin	5 (1.98)	30 (11.90)
Nifedipine	0	23 (9.13)
Amiodaron	0	1 (0.40)
Digoxin	30 (11.90)	13 (5.16)
Criteria 2		
Diltiazem	11 (4.37)	4 (1.59)
Criteria 3		
Ticagrelor	16 (6.35)	0
Criteria 4		
ARB (Candesartan, Valsartan, Irbesartan) with Potassium sparing diuretics (Spironolactone)	0	56 (22.22)
ACEI Inhibitor (Lisinopril, Ramipril) with Spironolactone	0	52 (20.63)
Opioid (Codeine) with gabapentin	0	1 (0.40)

The prescribing pattern of geriatric patients with cardiovascular disease has four criteria: criterion 1 of drugs that are potentially inappropriate for the elderly, criterion 2 of drugs that are potentially inappropriate in the elderly due to certain conditions, criterion 3 of drugs that are used with caution, and criterion 4 of potentially inappropriate drug interactions. In the first category, criterion 1 is a potentially inappropriate drug for the

elderly, which is strongly recommended for avoidance. Aspirin was used for 96 patients (38.10%) who were compliant based on the 2023 Beers Criteria. The use of aspirin in geriatric patients may result in gastric bleeding; therefore, it is only used for secondary prevention (Panel 2023). In this study, aspirin was prescribed only for secondary prevention because all patients already had cardiovascular disease.

Prophylactic aspirin in healthy elderly patients does not provide benefits and harms, and is not used for primary prevention in patients over 60 years of age with cardiovascular disease (Rory et al., 2018). Nifedipine, with 23 prescriptions (9.13%), was potentially inappropriate. The use of nifedipine in geriatric patients will result in hypotension, which results in reduced blood flow to the heart, so that the heart muscle does not receive sufficient oxygen (Panel, 2023). In cardiogenic shock, the heart is unable to pump effectively, and this situation is exacerbated by inhibiting the entry of calcium ions into heart cells (Khan, 2023). The choice of antihypertensive therapy in elderly patients is adjusted for comorbidities, because CCB is not an absolute contraindication for geriatric patients (HUA et al., 2024).

Amiodarone has only one prescription (0.40%), which is potentially inappropriate based on the 2023 Beers Criteria. Amiodarone is effective at maintaining sinus rhythm but is more toxic than other antiarrhythmic drugs used in atrial fibrillation (Stanton et al., 2020). According to the 2023 Beers Criteria, Amiodarone is only used in geriatric patients with a diagnosis of atrial fibrillation (AF) with heart failure or atrial fibrillation and left ventricular hypertrophy (LVH) (Panel, 2023). Digoxin obtained 13 prescriptions (5.16%) that were potentially inappropriate, and 30 prescriptions (11.90%) met the Beers criteria. Digoxin is not recommended as first-line therapy in geriatric patients diagnosed with atrial fibrillation (AF) and heart failure. It is used to avoid doses >0.125 mg/day, except when treating cases of atrial arrhythmia (Panel, 2023). In this study, the appropriateness of prescriptions based on the Beers criteria was assessed for patients without a diagnosis of atrial fibrillation (AF) or heart failure. However, for those diagnosed with AF and heart failure, doses exceeding 0.125 mg/day were considered. A reduced renal clearance increases the risk of toxicity. In cases where there is objective evidence of impaired heart structure or function at rest, electrocardiography should be performed on all patients with suspected heart failure. Routine laboratory examinations for such patients should include a complete blood count (hemoglobin, leukocytes, and platelets), electrolytes, creatinine, glomerular filtration rate (GFR), glucose, liver function tests, and urinalysis (Handayani et al., 2018). Warfarin in this study obtained 5 prescriptions (1.98%) which met the Beers criteria and 30 prescriptions (11.90%) which were potentially inappropriate. According to Beers, the use of warfarin for the treatment of nonvalvular atrial fibrillation or venous thromboembolism (VTE) is not

recommended. For older adults who have been on warfarin long-term, it is okay to use warfarin with a well-controlled International Normalization Ratio (INR) (i.e., >70% of the time in the therapeutic range) and no adverse effects (Panel, 2023). According to the guidelines for warfarin management in the community, the normal INR value of warfarin ranges from 2-3 (Health 2024). It states that >70% of the time in the range of being picked is the percentage of times the patient in a given period reaches the target INR 2-3. For example, in 10 INR checks, the patient must achieve an INR value of 2-3 in as many as seven checks so that the INR value is well controlled (Badawoud et al., 2024). In this study, according to the Beers criteria, patients received warfarin drugs with an INR value of 2-3, and which is potentially inappropriate if they have an INR value <2 and >3. Dabigatran or rivaroxaban can be administered to geriatric patients with atrial fibrillation who are contraindicated with warfarin (Di et al., 2023). Rivaroxaban may be reasonable in special situations, such as when once-daily dosing is necessary to facilitate medication adherence. All Direct oral anticoagulants confer a lower risk of intracranial hemorrhage than warfarin (Panel 2023).

The second category, criterion 2, includes drugs that are potentially inappropriate for the elderly owing to certain conditions that strongly recommend their avoidance. The research found that diltiazem was included in criterion 2, with four prescriptions (1.59%) deemed appropriate according to the Beers criteria and 11 prescriptions (4.37%) considered potentially inappropriate. Diltiazem is a non-dihydropyridine calcium channel blocker (CCB) that inhibits the entry of calcium ions into the heart muscle during depolarization. This decrease in intracellular calcium concentration promotes the relaxation of smooth muscles, leading to arterial vasodilation and a subsequent decrease in blood pressure (Puspitasari et al., 2022). Diltiazem should be avoided in geriatric patients with heart failure, as it will result in increased fluid and/or may worsen heart failure (Panel, 2023).

Category 3 consisted of drugs that must be used with caution. Ticagrelor is included in this category, with 16 prescriptions (6.35%) aligning with the Beers criteria. According to these criteria, ticagrelor can increase the risk of gastric bleeding when used in combination with clopidogrel, especially in adults over 70 years of age, necessitating its careful use. In this study, the use of ticagrelor adhered to the Beers criteria, as it was prescribed only to patients aged << 70 years old. Ticagrelor is a newer drug replacing clopidogrel,

demonstrating high efficacy in cases of acute coronary syndrome without ST-segment elevation or in patients with invasive interventions such as primary percutaneous coronary intervention. It works by inhibiting binding to the P2Y₁₂ receptor (Firdaus, 2016).

Category 4 includes potentially inappropriate drug interactions that are strongly recommended to be avoided. In this study, there were three groups of potentially inappropriate drug interactions, namely, the ARB group that interacted with potassium-saving diuretics; the results of 56 prescriptions (22.22%) and ACEI Inhibitor drug groups that interacted with potassium-saving diuretics were 52 prescriptions (20.63%). Avoid routinely using 2 or more RAS inhibitors, or a RAS inhibitor and potassium-sparing diuretic, concurrently in those with chronic kidney disease stage 3A or higher because of an increased risk of hyperkalemia (Panel, 2023).

The opioid group that interacted with gabapentin was prescribed 1 (0.40%). The interaction of ARB and ACEI inhibitors with potassium-sparing diuretics resulted in an increased risk of hyperkalemia. Hyperkalemia is defined as plasma/serum potassium levels that exceed the upper limit of the normal range (Linders et al., 2020). Cell damage can lead to the release of intracellular potassium (K⁺) into the extracellular space, as observed in conditions such as rhabdomyolysis from crush injuries, excessive physical exercise, and other hemolytic processes. Insulin deficiency and diabetic ketoacidosis can cause significant and rapid shifts in intracellular and extracellular K⁺ levels, resulting in elevated serum K⁺ levels despite a decrease in total K⁺ levels. Tumor lysis syndrome following chemotherapy can also cause acute hyperkalemia due to extensive death of cancer cells (Kasper et al., 2015). In addition, the interaction between opioid drugs and gabapentin increases the risk of overdose and adverse drug effects. These side effects include respiratory distress, coma, and even death (Drug.com 2024).

The limitation of this study is that it did not include follow-up on not appropriate with the Beers Criteria, as the data collection was retrospective and conducted over a limited time period.

CONCLUSION

This study showed that seven types of inappropriate drugs increased the risk of potentially inappropriate medication according to the Beers Criteria 2023. The drugs used were warfarin, nifedipine, amiodarone,

digoxin, diltiazem, the interaction between ARB/ACEi, and potassium-sparing diuretics. If medication cannot be used in geriatric patients, an alternative therapy should be used, or dose adjustment may be necessary.

ACKNOWLEDGMENT

We extend our sincere gratitude to Muhammadiyah Lamongan Hospital for permitting the data collection for this study.

AUTHOR CONTRIBUTIONS

Conceptualization: I.S.; Methodology, D.P.; Software, A.Z.F.; Validation: I.S.; Formal Analysis, D.P.S.; Investigation: D.P.S.; Resources, D.P.S.; Data Curation; D.P.S.; Writing - Original Draft, D.P.S.; Writing - Review and Editing, I.S.; Visualization: D.P.S.; Supervision: I.S.; Project Administration I.S.; Funding Acquisition, D.P.S.

CONFLICT OF INTEREST

The authors declare that they have no conflicts of interest.

REFERENCES

- Amisi, W. G., Nelwan, J. E. & Kolibu, F. K. (2018). Hubungan antara Hipertensi dengan Kejadian Penyakit Jantung Koroner pada Pasien yang Berobat di Rumah Sakit Umum Pusat Prof. Dr. R. D. Kandou Manado, *Kesmas*; 7; pp. 1–7.
- Arfania, M., Risna, K., Musa, K. A. E., Ardianti, R. & Safitri, Y. A. (2023). Literatur Review Efektivitas Beta Bloker Pada Terapi Pasien Gagal Jantung, 3; pp. 8076–8088.
- Badan Pusat Statistik (2022). Statistik Penduduk Lanjut Usia 2022.
- Badawoud, A. M., Alanizi, A., Alnakhli, A. O., Alzahrani, W., AlThiban, H. S., AlKhurayji, R. W., Alnakhli, A. M., Almoudi, J. A. & Yami, M. S. A. (2024). Appropriateness of anticoagulation level in older adult patients on Warfarin: A multicenter retrospective study, *Saudi Pharmaceutical Journal*; 32; p. 101906. doi: 10.1016/j.jsps.2023.101906.
- Di, J., Wei Y., Zhang, G., Yue, Y. & Sun, S. (2023). Comparison of clinical effects and costs among dabigatran etexilate, rivaroxaban and warfarin in elderly patients with atrial fibrillation, *American journal of translational research*; 15; pp. 3639–3646.

- Dinkes lamongan (2021). Dinas kesehatan Kabupaten lamongan, *Profil Kesehatan Kabupaten Lamongan*.
- Drug.com (2024). *Drug Interaction Report*.
- Firdaus (2016). Penggunaan Obat Anti Platelet pada Pasien Penyakit Jantung Koroner, pp. 1–3.
- Handayani, U., Alifiar, I. & Idacahyati, K. (2018). Potentially inappropriate medication among geriatric inpatients Studi ketidaksesuaian pengobatan pada pasien geriatri rawat inap, *Jurnal Ilmiah Farmasi*; 15; pp. 87–93. doi: org/10.20885/jif.vol14.iss2.art4.
- Health, Q. (2024). Guideline for Warfarin Management in the Community, (February).
- HUA, Q., Fan, L., Wang, W. W. & Li, Jing. (2024). 2023 Guideline for the management of hypertension in the elderly population in China, *Journal of Geriatric Cardiology*; 21; pp. 589–630. doi: 10.26599/1671-5411.2024.06.001.
- Julaiha, S. (2021). Faktor yang Berhubungan dengan Kejadian Potentially Inappropriate Medication Berdasarkan Kriteria STOPP START pada Pasien Geriatri dengan Gangguan Kardiovaskuler, *Jurnal Kesehatan Metro Sai Wawai*; 14; pp. 156–167.
- Kashif M. K. (2023). *Nifedipine*, *National Library Of Medicine*.
- Mutarobin. (2018). Sistem Kardiovaskuler Acute Coronary Syndrome (ACS) ; pp. 1–72.
- Panel, U. E. (2023). American Geriatrics Society 2023 updated AGS Beers Criteria® for potentially inappropriate medication use in older adults, *Journal of the American Geriatrics Society*; (March). doi: 10.1111/jgs.18372.
- Puspitasari, C. E., Widiyastuti, R., Dewi, N. M. A. R., Woro, O. Q. L. & Syamsun, A. (2022). Profil Drug Related Problems (DRPs) pada Pasien Hipertensi di Instalasi Rawat Jalan Rumah Sakit Pemerintah di Kota Mataram Tahun 2018, *Jurnal Sains dan Kesehatan*; 4; pp. 77–87. doi: 10.25026/jsk.v4ise-1.1692.
- Rampengan, S. H. (2014). *Buku praktis kardiologi*, Badan Penerbit Fakultas Kedokteran Universitas Indonesia.
- Riskesdas (2018). Laporan Riskesdas 2018 Kementerian Kesehatan Republik Indonesia, *Laporan Nasional Riskesdas 2018*; pp. 154–165.
- Sasfi, S. M. (2020). Pola Peresepan Pasien Lanjut Usia Poli Penyakit Dalam Rawat Jalan Di Rsud Dr. Soedarso Kota Pontianak Periode Desember 2018 – Juli 2019, *Jurnal Berkala Epidemiologi*; 5; pp. 90–96.
- McNeil, J. J., Wolfe, R., Woods, R. L., Tonkin, A. M., Donnan, G. A., Nelson, M. R., Reid, C. M., Lockery, J. E., Kirpach, B., Storey, E., Shah, R. C., Williamson, J. D., Margolis, K. L., Ernst, M. E., Abhayaratna, W. P., Stocks, N., Fitzgerald, S. M., Orchard, S. G., Trevaks, R. E., Beilin, L. J., Johnston, C. I., Ryan, J., Radziszewska, B., Jelinek, M., Malik, M., Eaton, C. B., Brauer, D., Cloud, G., Wood, E. M., Mahady, S. E., Satterfield, S., Grimm, R., Murray, A. M. & ASPREE Investigator Group. (2018). Effect of Aspirin on Cardiovascular Events and Bleeding in the Healthy Elderly, *New England Journal of Medicine*; 379; pp. 1509–1518. doi: 10.1056/nejmoa1805819.
- Tanton, M. M., Samii, L., Leung, G. & Pearce, P. (2020). Amiodarone-induced neuromyopathy in a geriatric patient, *BMJ Case Reports*; 13; pp. 1–3. doi: 10.1136/bcr-2020-236620.
- Unger, T., Borghi, C., Charchar, F., Khan, N. A., Poulter, N. R., Prabhakaran, D., Ramirez, A., Schlaich, M., Stergiou, G. S., Tomaszewski, M., Wainford, R. D., Williams, B. & Schutte, A. E. (2020). Practice Guidelines 2020 International Society of Hypertension Global Hypertension Practice Guidelines International Society of Hypertension; pp. 1–24. doi: 10.1161/HypertensionAHA.120.15026.



Antihypertensive Activity of Black Garlic Extract in Rats and Its Phytochemical Analysis using GC-MS

Daru Estiningsih¹, Moch. Saiful Bachri², Laela Hayu Nurani², Muhammad Ma'ruf³, Sapto Yuliani², Vivi Sofia⁴, Dian Prasasti²

¹Faculty of Health Sciences, Universitas Alma Ata, Yogyakarta, Indonesia

²Faculty of Pharmacy, Ahmad Dahlan University, Yogyakarta, Indonesia

³Sekolah Tinggi Ilmu Kesehatan ISFI Banjarmasin, Banjarmasin, Indonesia

⁴Faculty of Pharmacy, Tjut Nyak Dien University, North Sumatra, Indonesia

*Corresponding author: msaifulbachri@pharm.uad.ac.id

Orcid ID: 000-0001-9565-846X

Submitted: 26 January 2025

Revised: 17 April 2025

Accepted : 27 April 2025

Abstract

Background: Hypertension is defined as a medical condition where blood pressure rises above 140/90 mmHg. Black garlic is recognized as a natural remedy that may help lower high blood pressure, primarily due to its abundant antioxidant properties, which are believed to inhibit the function of the angiotensin-converting enzyme (ACE) that is essential for regulating blood pressure. **Objective:** This study aimed to identify the chemical composition of black garlic using GC-MS and assess its antihypertensive effects in rat models. **Methods:** This study characterized the chemical composition of black garlic using GC-MS (Agilent 7890A) and evaluated its antihypertensive effects in rats. Hypertension was induced by oral administration of NaCl at a dose of 3.75 g/20 g body weight (BW) from day 0 to day 14. Blood pressure measurements were taken on days 0, 14, and 21. Black garlic extract was administered at three dose levels—4.2 mg/20 g BW, 8.4 mg/20 g BW, and 12.4 mg/20 g BW to evaluate dose dependent antihypertensive responses. Statistical analysis included the Kolmogorov-Smirnov test for normality, homogeneity testing, One-Way ANOVA **Results:** The GC-MS analysis identified 9-octadecenoic acid as the dominant compound in black garlic, accounting for 34.53% of its total composition. The antihypertensive activity test showed that administering black garlic at a dose of 12.4 mg/20 g BW significantly lowered systolic, diastolic, and mean arterial blood pressure while enhancing nitric oxide levels in hypertensive rats. **Conclusion:** Black garlic has the potential as an effective herbal treatment to lower blood pressure.

Keywords: GC-MS, Antihypertension, Black Garlic, In Vivo

How to cite this article:

Estiningsih, D., Bachri, M. S., Nurani L. H., Ma'ruf, M., Yuliani, S., Sofia, V. & Prasasti, D. (2025). Antihypertensive Activity of Black Garlic Extract in Rats and Its Phytochemical Analysis using GC-MS. *Jurnal Farmasi dan Ilmu Kefarmasian Indonesia*, 12(1), 68-76. <http://doi.org/10.20473/jfiki.v12i12025.68-76>

INTRODUCTION

Hypertension is a condition characterized by an increase in blood pressure above the normal limit, where the systolic pressure exceeds 140 mmHg and the diastolic pressure exceeds 90 mmHg (Wahyuni et al., 2023). Hypertension is a type of multifactorial chronic disease caused by environmental and genetic factors. In addition, this disease is also influenced by various factors such as obesity, excessive stress, lack of physical activity, and excessive salt consumption (Oliveros et al., 2020). The World Health Organization (WHO) reports a global hypertension prevalence of 22%, with Africa highest at 27% and Southeast Asia third at 25%. In Indonesia, there are 63.3 million hypertension cases and 427,218 related deaths. The condition is most common in people aged 55–64. Of the 34.1% prevalence, only 8.8% are diagnosed, with many not taking or not regularly taking medication. Hypertension can be managed through synthetic drugs and lifestyle changes (Kementerian Kesehatan, 2019). The most common antihypertensive drug prescribed to hypertensive patients is captopril (60.1%), followed by amlodipine (29.7%) and hydrochlorothiazide (10.2%) (Diarmika et al., 2018).

Captopril exerts its antihypertensive effect by inhibiting the formation of angiotensin II, a hormone responsible for vasoconstriction. However, as an ACE inhibitor, captopril can lead to bradykinin accumulation, which may cause a dry cough (Straka et al., 2016). This side effect can negatively impact patient adherence to treatment by reducing motivation, lowering awareness, and diminishing willingness to comply with therapy, ultimately increasing the risk of non-compliance (Halim et al., 2015). Therefore, people prefer to use herbal medicine which is considered safer, one of which is black garlic.

Black Garlic is a processed garlic product made through fermentation with high temperatures and humidity of 70–80%. The fermentation process requires a longer fermentation time of one month (Kim et al., 2013). Garlic undergoes characteristic changes during fermentation. The non-enzymatic browning reaction that occurs during this process causes the garlic to turn black. This reaction also produces a sweet taste and gives the garlic a chewy and jelly-like texture (Yuan et al., 2016).

Additionally, black garlic is known to contain S-allyl cysteine (SAC), an active compound which is formed during the fermentation process. The compound can dissolve in water and has strong antioxidant properties (Omar & Al-Wabel, 2010). In vitro and in

vivo studies have shown that black garlic has stronger antioxidant properties than white garlic (Lee et al., 2020).

Black garlic has a significantly higher antioxidant capacity, as indicated by its TEAC (Trolox Equivalent Antioxidant Capacity) value of $59.2 \pm 0.8 \mu\text{mol/g wet}$, compared to fresh garlic, which contains only $13.3 \pm 0.5 \mu\text{mol/g wet}$. This elevated TEAC value suggests a strong potential for preventing diabetes complications. The antioxidant properties of black garlic are primarily attributed to sulfenic acid (SAC), a compound formed from the decomposition of allicin (Chang & Jang, 2021). In a study conducted by Setyawan & Muflihatin (2019), black garlic has been shown to effectively reduce both systolic and diastolic blood pressure in individuals with hypertension. In a study by Chen et al (2021), black garlic extracts and nanoemulsions alleviate DOCA-salt-induced hypertension and improve cognitive function in rats by modulating key biomarkers such as bradykinin, aldosterone, Ang II, NO, AChE, and antioxidant enzymes.

This study aims to evaluate the in vivo antihypertensive activity of black garlic (*Allium sativum* L.) in rats. The expected outcome is to provide scientific evidence on the effectiveness of black garlic as an antihypertensive agent through in vivo analysis in rats.

MATERIALS AND METHODS

Materials

The garlic used in this study was black garlic derived from Solo garlic (*Allium sativum*), obtained from Yogyakarta City, NaCl (Merck), CMC-Na (Sigma), Captopril®, N-(1-naphthyl) ethylene diaminehydrochloride (Sigma- Aldrich), Sulfanilamide (Merck), Ortho-phosphoric acid (Merck), and Sodium Nitrate (Merck).

Extract Preparation

Black garlic is produced from Solo garlic (*Allium sativum*) through a fermentation process at 60–70°C with controlled humidity for 12 days, without any additives. The temperature during fermentation was maintained within a range of 60–70°C, with some variation throughout the process. During fermentation, the garlic undergoes a color change from white to black and develops a soft texture, mild aroma, and a distinctive sweet-sour flavor profile (Yudhayanti et al., 2020). One gram of black garlic was grounded and transferred into a 10 mL volumetric flask. Distilled water was added to the mark, and the mixture was vortexed for 1 minute. The solution was then subjected to sonication for 30 minutes at room temperature to enhance extraction.

Following sonication, the mixture was centrifuged at 5000 rpm for 10 minutes. The resulting supernatant was collected and used for further analysis (Pramitha & Yani, 2020).

Analysis with Gas Chromatography-Mass Spectrometry (GC-MS)

GC-MS analysis was performed using an Agilent 7890A system coupled with an Agilent 5975C mass spectrometer and an HP-5DB capillary column (60 m \times 250 μ m \times 0.25 μ m). Helium served as the carrier gas, with an injector temperature of 250°C, an injection volume of 0.2 μ L, and a 1:200 split ratio. A temperature gradient was applied to ensure effective separation of volatile compounds. Mass spectra were recorded in the range of 35–550 *m/z*. GC-MS enables the identification of compounds based on their retention times and unique mass spectral patterns, facilitating the characterization of complex mixtures (Pratiwi et al., 2022).

Grouping of Test Animals

This research, which involved test animals, has obtained research approval from the Research Ethics Commission (KEP) of Ahmad Dahlan University (UAD) under letter number: 012401007. In the planning of administering black garlic to test animals, 3 dosage variations were made: 4.2 mg/20 g BW, 8.4 mg/20g BW, and 12.4 mg/20g BW (Pangala et al., 2022).

Antihypertensive Activity Test

Antihypertensive activity was evaluated by measuring blood pressure on days 0, 14, and 21. Hypertension was induced by oral administration of NaCl at a dose of 3.75 g/20 g body weight from day 0 to day 14 (Sadik et al., 2021). On the following day, baseline blood pressure of the rats was measured. The animals were then administered black garlic extract at doses of 4.2 mg/20 g BW, 8.4 mg/20 g BW, and 12.4 mg/20 g BW once daily for seven consecutive days. The extract was prepared by diluting the aqueous black garlic extract with distilled water to the appropriate concentrations. Fresh solutions were prepared daily and administered orally via gavage. Blood pressure measurements were repeated on day 21.

Blood Collection of Rats

Blood samples from the rats were collected on the 21st day. The procedure was performed by holding and pinching the nape of the neck with fingers. Blood was

drawn from the ophthalmic vein using a capillary tube and collected into a tube of \pm 3 cc. Then, the blood was centrifuged at a speed of 3000 rpm for 15 minutes. The centrifugation produced a serum, which was then prepared for nitric oxide (NO) levels analysis (Ma'ruf et al., 2025).

Measurement of Nitric Oxide levels

Nitric oxide levels were measured using an ELISA Reader (Asys) following the method proposed by Hunter et al (2013) with modifications. Nitric oxide levels in mouse serum were quantified using the Griess Reaction Assay. The procedure involved preparing two reagents: Griess A (0.1% w/v N-(1-naphthyl) ethylenediamine hydrochloride in distilled water) and Griess B (1% w/v sulfanilamide in 5% ortho-phosphoric acid). A sodium nitrate standard solution (69.0 mg/100 mL) was diluted to generate a nitrite calibration curve. For analysis, 100 μ L of serum sample or standard was pipetted into a 96-well plate, followed by sequential additions of 100 μ L each of Griess A and B solutions. After a 10-minute incubation for chromogenic development, absorbance was measured at 550 nm using an ELISA microplate reader, with values compared against the standard curve to determine nitrite concentrations

Data analysis

The collected data on systolic and diastolic blood pressure, heart rate pressure, and nitric oxide test, were statistically analyzed using the Kolmogorov-Smirnov test to assess normality and the homogeneity of variance test. The differences between treatment groups were then evaluated using the Tukey test.

RESULTS AND DISCUSSION

Results of Black Garlic Component Analysis with GC-MS

The chromatogram profile of the analysis results reveals the presence of seven components in black garlic. The chromatogram of black garlic is presented in Figure 1. The analysis of black garlic components with GC-MS mass spectra was performed by comparing the base peak with spectra from NIST and WILEY 9 LIB (Pratiwi et al., 2022). The chromatogram profile of black garlic that has been analyzed with GC MS is presented in Table 1 and Figure 1.

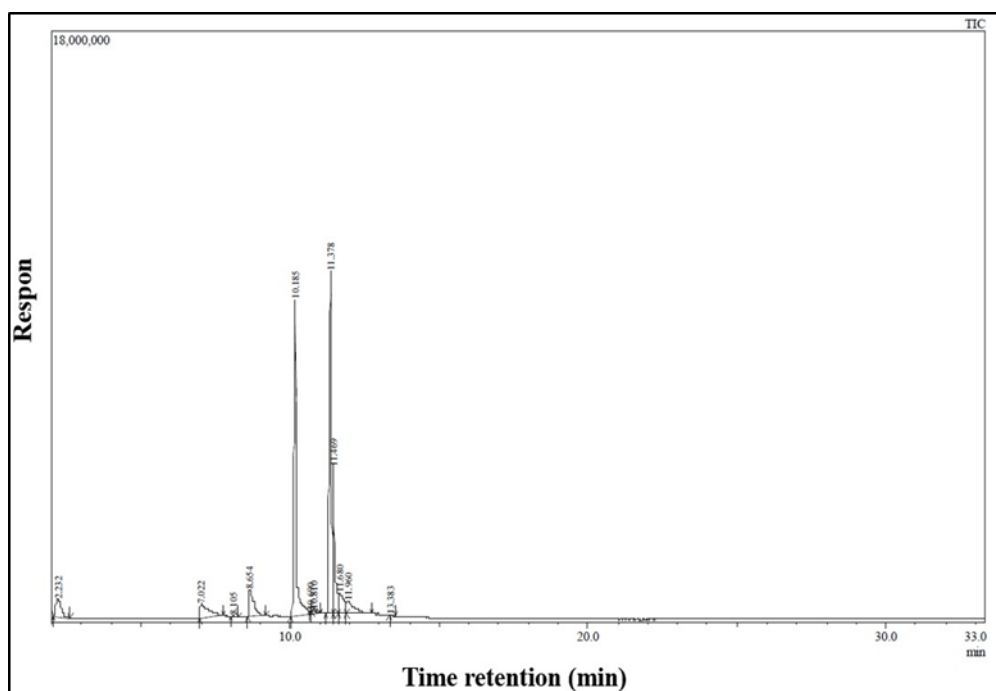


Figure 1. Chromatogram Profile of Compounds from Black Garlic

Table 1. Results of Black Garlic Component Analysis using GC-MS

No	tr (minute)	%Area	MW(g/mol)	Molecular Formula	Name
1	11.440	34.53	282.5	C ₁₈ H ₃₄ O ₂	9-Octadecenoic acid
2	11.010	32.67	256.4	C ₁₆ H ₃₂ O ₂	Hexadecanoic acid
3	11.620	9.57	284.4	C ₁₈ H ₃₆ O ₂	Octadecanoic acid
4	9.200	5.06	228.3	C ₁₄ H ₂₈ O ₂	Tetradecanoic acid
5	7.770	4.98	200.3	C ₁₂ H ₂₄ O ₂	Dodecanoic acid
6	11.910	4.88	164.2	C ₁₂ H ₂₀	Cyclododecyne
7	12.730	3.93	280.4	C ₁₈ H ₃₂ O ₂	9,12-Octadecadienoic acid

Note :

tr: Retention Time

MW: Molecular Weight

Based on Table 2 and Figure 2, the largest component of the GC-MS profile of black garlic is 9-Octadecenoic acid (34.53%), followed by Hexadecanoic acid (32.67%), Octadecanoic acid (9.57%), Tetradecanoic acid (5.06%), Dodecanoic acid (4.98%), Cyclododecyne (4.88%), and 9,12-Octadecadienoic acid (3.93%). The results of the black garlic chromatogram profile reveal that dodecanoic acid had the shortest retention time, and the longest was 9,12-Octadecadienoic acid. This is due to the influence of MW and the influence of the boiling point of each different compound (Rohman & Man, 2012).

Black garlic is the result of the fermentation of fresh garlic (*Allium sativum*) through the Maillard reaction at high temperatures (60–90 °C) and high humidity (70–90%) over a certain period. This process alters the chemical composition and enhances the content of its

bioactive compounds. The main bioactive compounds in black garlic include water-soluble sulfur compounds such as S-allyl cysteine and S-allyl-mercapto cysteine, as well as Maillard reaction products such as 5-hydroxymethylfurfural. The levels of polyphenols and volatile compounds also increase significantly compared to fresh garlic, resulting in improved antioxidant, anti-inflammatory, anticancer, hepatoprotective, and immunomodulatory activities (Ahmed & Wang, 2021).

GC-MS analysis of black garlic detects only volatile compounds, excluding non-volatile bioactives such as polyphenols, amino acids, and water-soluble sulfur compounds. Since these compounds play important biological roles, complementary techniques like LC-MS are needed for a more comprehensive chemical profile. Therefore, GC-MS provides only a

partial overview, highlighting the need for further studies using additional analytical methods (Wonorahardjo et al., 2023).

readings were recorded on the 14th and 21st days of the experiment. The findings from these measurements are presented in Tables 2, 3, and 4.

The Results of Antihypertensive Activity Test

The study involved six groups of test subjects, with each group comprising five rats. Blood pressure

Table 2. Results of Systolic Blood Pressure (SBP) Measurements on Days 14 and 21

Group	Dose (mg/gBW)	Average of SBP (mmHg) \pm SD		Decrease of SBP (mmHg)
		Day 14 (NaCl)	Day 21 (Intervention)	
Normal	-	96.4 \pm 5.12	95.6 \pm 6.98 ^b	-0.80
Control	CMC-Na	129.8 \pm 5.63 ^a	129.2 \pm 5.26	-0.60
<i>Black Garlic</i>	14	129.4 \pm 7.12 ^a	127.2 \pm 5.49 ^c	-2.20
	28	130.0 \pm 5.47 ^a	124.2 \pm 5.97 ^b	-5.80
	56	129.8 \pm 5.40 ^a	120.6 \pm 6.42 ^b	-9.20
	4,5	131.0 \pm 7.68 ^a	117.8 \pm 5.26 ^b	-13.20
Captopril	4,5	131.0 \pm 7.68 ^a	117.8 \pm 5.26 ^b	-13.20

The data presented in Table 2 revealed that black garlic administration significantly reduced systolic blood pressure, with the most effective dosage being 56 mg/g body weight. This dosage achieved a reduction in blood pressure comparable to the captopril-treated group, highlighting the potent antihypertensive effects of black garlic. These findings underscore the role of black garlic's rich antioxidant content, particularly 9-octadecenoic acid (oleic acid), in modulating blood

pressure and supporting cardiovascular health (Massaro et al., 2020).

The statistical evaluation of systolic blood pressure revealed a notable decrease ($p < 0.05$) following the administration of the test preparation. These findings suggest that black garlic demonstrates efficacy as an antihypertensive agent in male Wistar strain white rats. This significant reduction in blood pressure underscores the potential of black garlic as a natural treatment option for managing hypertension.

Table 3. Diastolic Blood Pressure (DBP) Measurement Results on Days 14 and 21

Group	Dose (mg/gBW)	Average of DBP (mmHg) \pm SD		Decreased of DBP (mmHg)
		Day 14 (NaCl)	Day 21 (Intervention)	
Normal	-	83.8 \pm 6.30	83.0 \pm 5.56 ^b	-0.80
Control	CMC-Na	89.4 \pm 5.94 ^a	88.0 \pm 6.20	-1.40
<i>Black Garlic</i>	14	91.0 \pm 5.43 ^a	87.6 \pm 5.72 ^c	-3.40
	28	89.2 \pm 5.89 ^a	82.4 \pm 6.73 ^b	-6.80
	56	89.6 \pm 7.89 ^a	81.8 \pm 5.40 ^b	-7.80
	4,5	96.0 \pm 6.20 ^a	80.4 \pm 5.41 ^b	-15.60
Captopril	4,5	96.0 \pm 6.20 ^a	80.4 \pm 5.41 ^b	-15.60

The data on diastolic blood pressure presented in Table 3 indicated that the administration of black garlic significantly reduced diastolic blood pressure levels. Notably, the most effective dosage identified in this study was 56 mg per gram of body weight, which resulted in a decrease that was almost comparable to the reduction observed in the group treated with captopril.

The present study demonstrated that black garlic exhibits an antihypertensive effect, which is attributed

to 9-octadecenoic acid (oleic acid), a compound with high antioxidant activity (Massaro et al., 2020). The statistical analysis of systolic blood pressure revealed a significant result ($p < 0.05$), indicating a marked reduction in systolic blood pressure after the administration of the test preparation. Therefore, it can be concluded that black garlic serves as an effective antihypertensive agent in male Wistar strain white rats.

This finding highlights the potential of black garlic as a natural alternative for the management of hypertension.

Table 4. Mean Arterial Blood Pressure (ABP) Measurement Results on Days 14 and 21

Group	Dose (mg/gBW)	Average of ABP (mmHg) \pm SD		Decreased of ABP (mmHg)
		Day 14 (NaCl)	Day 21 (Intervention)	
Normal	-	88.0 \pm 5.69	87.2 \pm 5.65 ^b	-0.80
Control	CMC Na	102.8 \pm 5.68 ^a	101.7 \pm 5.87	-1.10
Black Garlic	14	103.8 \pm 5.93 ^a	100.8 \pm 5.62 ^c	-3.00
	28	102.8 \pm 5.55 ^a	96.3 \pm 6.40 ^b	-6.50
	56	103.0 \pm 7.05 ^a	94.7 \pm 5.73 ^b	-8.30
Captopril	4,5	107.66 \pm 5.31 ^a	93.1 \pm 5.52 ^b	-15.60

Table 4 highlights the mean arterial blood pressure scores, showing that black garlic administration effectively lowered blood pressure. The optimal dose of black garlic was 56 mg/g BW, producing results nearly comparable to captopril, the standard antihypertensive drug. This study confirmed the antihypertensive effects of black garlic, attributed to its high antioxidant content, particularly 9-Octadecenoic acid (oleic acid). Statistical analysis showed a significant reduction in systolic blood pressure ($p < 0.05$) after treatment, indicating that black garlic effectively lowers blood pressure in male Wistar rats. This finding supports the potential of black garlic as a natural antihypertensive agent (Massaro et al., 2020).

GC-MS analysis revealed that black garlic contains fatty acids such as 9-octadecenoic acid, hexadecanoic acid, and 9,12-octadecadienoic acid, which contribute to its biological effects, including antiproliferative activity and modulation of lipid metabolism. The fermentation process also reduces the pungent odor of fresh garlic and

results in a chewy texture and a distinct sweet flavor. Therefore, black garlic holds therapeutic potential in the prevention and management of various chronic diseases through its strong antioxidant and anti-inflammatory mechanisms (Binici et al., 2025).

The fatty acid, 9-octadecenoic acid has been shown to exhibit anti-inflammatory and vasodilation properties, which may contribute to its effects on blood pressure regulation. Its ability to modulate endothelial function and reduce oxidative stress could play a key role in lowering blood pressure (Villaño et al., 2023).

Nitric Oxide (NO) Level Measurement

In determining the NO levels in hypertensive male rats, measurements were made at a wavelength of 550 nm. The average value of NO absorption level in male Wistar rats, measured using ELISA Reader, is listed in Table 5.

Table 5. Results of Nitric Oxide (NO) Level Measurements on Day 21

Group	Dose (mg/gBW)	Nitrit Oxide Concentration (μ M/L)
Normal	-	10.3 \pm 2.73
Control	NaCMC	5.6 \pm 2.11 ^a
Black Garlic	14	6.1 \pm 2.44 ^a
	28	8.8 \pm 2.06 ^b
	56	10.1 \pm 2.52 ^b
Captopril	4.5	11.1 \pm 2.50 ^b

The measurement of nitric oxide (NO) levels on the 21st day revealed statistically significant differences among the groups. However, no significant difference was observed between the black garlic 28 mg/gBW, 56

mg/gBW, and Captopril 4.5 mg/gBW groups. This indicates that black garlic at doses of 28 mg/gBW (8.8 \pm 2.06 μ M/L) and 56 mg/gBW (10.1 \pm 2.52 μ M/L) can effectively increase NO levels, achieving results

comparable to Captopril at a dose of 4.5 mg/gBW ($11.1 \pm 2.50 \mu\text{M/L}$).

According to Astutik et al (2014), nitric oxide (NO) levels in the blood are related to systolic and diastolic blood pressure because NO has vasodilator properties. This may be attributed to endothelial damage due to excessive oxidative stress. As endothelial damage worsens, NO production decreases, and blood pressure increases. As a result, decreased NO availability leads to endothelial-dependent vasodilation disorders in hypertensive patients.

Increased expression of nitric oxide (NO) in hypertensive rats indicates involvement in the regulation of Hexadecanoic acid or palmitic acid on myocardial contractility. Palmitic acid supplementation, followed by the addition of NO inhibitors, significantly increase contractility. NO affects myocardial function through mitochondrial protein regulation, reduction of mitochondrial oxygen consumption, and modulation of cardiac metabolism. The combination of NO with mitochondrial protein inhibitors has the potential to inhibit the positive inotropic effect of palmitic acid on hypertensive cardiomyocytes (Tan et al., 2021).

CONCLUSION

The GC-MS analysis identified 9-Octadecenoic acid as the dominant compound in black garlic, comprising 34.53% of its composition. Furthermore, administering black garlic at a dose of 12.4 mg/20 g BW significantly reduced systolic, diastolic, and mean arterial blood pressure in hypertensive rats, while also increasing nitric oxide levels. These findings highlight the potential of black garlic as an effective natural remedy for managing high blood pressure. Given its promising effects, further clinical studies are necessary to validate its therapeutic efficacy and explore its potential incorporation into clinical practice as a safe and accessible antihypertensive treatment.

ACKNOWLEDGMENT

We would like to express our deepest gratitude to the individuals and institutions whose support and contributions have been instrumental in this research. Special appreciation is extended to the Dean of the Faculty of Health Sciences of Alma Ata University for supporting the completion of this research.

AUTHOR CONTRIBUTIONS

Conceptualization: DE, MSB, LHN, MM, SY, VS, DP; Methodology: DE, MSB, LHN; Software : MSB, LHN, MM.; Validation : DE, MSB, LHN, MM, SY;

Formal Analysis : DE, MSB, LHN, MM.; Investigation : DE, MSB, SY, VS, DP ; Resources : DE, MSB, LHN, MM, SY; Data Curation : DE, MSB, LHN, MM, SY, VS, DP ; Writing - Original Draft : DE, MSB, LHN, MM; Writing - Review &Editing : DE, MSB, SY, VS, DP; Visualization : DE, MSB, LHN, MM, SY, VS, DP; Supervision : DE; Project Administration : DE; Funding Acquisition : DE.

REFERENCE

- Ahmed, T. & Wang, C. K. (2021). Black Garlic and Its Bioactive Compounds on Human Health Diseases: A Review. *Molecules*; 26; 1–38. doi: 10.3390/molecules26165028.
- Astutik, P., Adriani, M. & Wirjatmadi, B. (2014). Kadar Radikal Superoksid (O_2^-), Nitric Oxide (NO) dan Asupan Lemak pada Pasien Hipertensi dan Tidak Hipertensi. *Jurnal Gizi Indonesia*; 3; 1–6. doi: 10.14710/jgi.3.1.90-95.
- Binici, H. I., Savas, A. & Erim, B. (2025). Processing-Induced Modifications in Bioactive Compounds of Black Garlic: A Comparative Analysis with White Garlic. *Italian Journal of Food Science*; 37; 432–440. doi: 10.15586/ijfs.v37i1.2877.
- Chang, T. C. & Jang, H. D. (2021). Optimization of Aging Time for Improved Antioxidant Activity and Bacteriostatic Capacity of Fresh and Black Garlic. *Appl Sci*; 11; 1–16. doi: 10.3390/app11052377.
- Chen, C. Y., Tsai, T. Y. & Chen, B. H. (2021). Effects of Black Garlic Extract and Nanoemulsion on the Deoxy Corticosterone Acetate-Salt Induced Hypertension and Its Associated Mild Cognitive Impairment in Rats. *Antioxidants*; 10; 1–21. doi: 10.3390/antiox10101611.
- Diarmika, I. K. D. P., Artini, G. A., & Ernawati, D. K. (2018). Profil Efek Samping Kaptopril pada Pasien Hipertensi di Puskesmas Denpasar Timur I Periode Oktober 2017. *Jurnal Medika Udayana*; 7; 221–225.
- Halim, M. C., Andrajari, R. & Supardi, S. (2015). Risiko Penggunaan ACEi Terhadap Kejadian Batuk Kering pada Pasien Hipertensi di RSUD Cengkareng dan RSUD Tarakan DKI Jakarta. *JMKI*; 5; 113–122. doi: 10.22435/jki.v5i2.4406.113-122.
- Hunter, R. A., Storm, W. L., Coneski, P. N. & Schoenfisch, M. H. (2013). Inaccuracies of Nitric Oxide Measurement Methods in

- Biological Media. *Anal Chem*; 85; 1957–1963. doi: 10.1021/ac303787p.
- Kementerian Kesehatan. (2019). *Hari Hipertensi Dunia 2019: "Know Your Number, Kendalikan Tekanan Darahmu dengan CERDIK."* Kementerian Kesehatan RI. <https://p2ptm.kemkes.go.id/tag/hari-hipertensi-dunia-2019-know-your-number-kendalikan-tekanan-darahmu-dengan-cerdik>
- Kim, J. S., Kang, O. J. & Gweon, O. C. (2013). Comparison of Phenolic Acids and Flavonoids in Black Garlic at Different Thermal Processing Steps. *Journal of Functional Foods*; 5; 80–86. doi: 10.1016/j.jff.2012.08.006.
- Lee, C. H., Chen, Y. T., Hsieh, H. J., Chen, K. T., Chen, Y. A., Wu, J. T., Tsai, M. S., Lin, J. A. & Hsieh, C. W. (2020). Exploring Epigallocatechin Gallate Impregnation to Inhibit 5-Hydroxymethylfurfural Formation And The Effect On Antioxidant Ability Of Black Garlic. *LWT-Food Science and Technology*; 117; 1–6. doi: 10.1016/j.lwt.2019.108628.
- Ma'ruf, M., Bachri, M. S. & Nurani, L. H. (2025). Antihypertensive Activities of Peronema Canescens Jack Extract: An In Vivo Study. *Scripta Medica*; 56; 61–68. doi: 10.5937/scriptamed56-52947.
- Massaro, M., Scoditti, E., Carluccio, M. A., Calabriso, N., Santarpino, G., Verri, T. & Caterina, R. D. (2020). Effects of Olive Oil on Blood Pressure: Epidemiological, Clinical, and Mechanistic Evidence. *Nutrients*; 12; 1–22. doi: 10.3390/nu12061548.
- Oliveros, E., Patel, H., Kyung, S., Fugar, S., Goldberg, A. & Madan, N. (2020). Hypertension in Older Adults: Assessment, Management and Challenges. *Journal of Clinical Cardiology*; 43; 99–107. doi: 10.1002/clc.23303.
- Omar, S. H. & Al-Wabel, N. A. (2010). Organosulfur Compounds and Possible Mechanism of Garlic in Cancer. *Saudi Pharmaceutical Journal*, 18; 51–58. doi: 10.1016/j.jsps.2009.12.007.
- Pangala, G. B., Mahendra, A. N., Jawi, I. M. & Dewi, N. W. S. (2022). Ekstrak Etanol Bawang Hitam (*Allium sativum* L.) Menurunkan Kadar Asam Urat Mencit Jantan Model Hiperurisemia. *Jurnal Medika Udayana*, 11(8), 89–93.
- Pramitha, D. A. I. & Yani, N. N. A. K. (2020). Perbedaan Kadar Flavonoid Total dari Black Garlic Tunggal dan Majemuk dengan Metode Spektrofotometri UV-Vis. *Chimica et Natura Acta*; 8; 84–88. doi: 10.24198/cna.v8.n2.27274.
- Pratiwi, H. K., Guntarti, A., Nurani, L. H. & Ginandjar, I. G. (2022). Authentication of Lemongrass Oil By Gas Chromatography-Mass Spectroscopy (GC-MS) Combination Chemometrics. *Indonesian Journal of Pharmaceutical Science and Technology*; 9; 174–180. doi: 10.24198/ijpst.v9i3.32558.
- Rohman, A., & Man, Y. B. C. (2012). The chemometrics approach applied to FTIR spectral data for the analysis of rice bran oil in extra virgin olive oil. *Chemometric and Intelligent Laboratory Systems*, 110(1), 129–134.
- Sadik, F., Bachri, M. S. & Nurkhasanah. (2021). Uji Efektivitas Ekstrak Etanol Daun Jarak Pagar (*Jatropha Curcas* L) Sebagai Antihipertensi Pada Tikus. *Kieraha Medical Journal*, 3(2), 74–81. doi: 10.33387/kmj.v3i2.3949.
- Setyawan, A. B., & Muflihatin, S. K. (2019). Efektivitas Black Garlic Untuk Menurunkan Tekanan Darah pada Pasien Hipertensi. *Media Ilmu Kesehatan*; 8; 126–132.
- Straka, B. T., Ramirez, C. & Byrd, J. (2016). Effect of Bradykinin Receptor Antagonism on ACE Inhibitor-Associated Angioedema. *Clin Allergy Clin Immunol*; 2; 28–32. doi: 10.1016/j.jaci.2016.09.051.
- Tan, H., Song, W., Liu, S., Song, Q., Zhou, T., Wang, Y. & Hou, Y. (2021). Molecular Mechanism of Palmitic Acid on Myocardial Contractility in Hypertensive Rats and Its Relationship with Neural Nitric Oxide Synthase Protein in Cardiomyocytes. *BioMed Research International*; 1–8. doi: 10.1155/2021/6657476.
- Villaño, D., Marhuenda, J., Arcusa, R., Moreno-Rojas, J. M., Cerda, B., Pereira-Caro, G. & Zafrilla, P. (2023). Effect of Black Garlic Consumption on Endothelial Function and Lipid Profile: A Before-and-After Study in Hypercholesterolemic and Non-Hypercholesterolemic Subjects. *Nutrients*; 15; 1–13. doi: 10.3390/nu15143138.
- Wahyuni, Majid, Y. A., & Pujiana, D. (2023). Pengaruh Senam Hipertensi Terhadap Tekanan Darah Lansia Penderita Hipertensi. *Jurnal Inspirasi Kesehatan*, 1(1), 65–71.

- Wonorahardjo, S., Sari, D. P., Salsabila, A., Estiyawati, E., Yuliani, D., Wijaya, A. R., Suharti, S., Kusumaningrum, I. K., Maharani, C. A. & Noviyanti, T. A. (2023). Physicochemical Changes and Role of Analytical Chemistry in Black Garlic (*Allium sativum* L.) Processing. *Makara Journal of Science*; 27; 148–159. doi: 10.7454/mss.v27i2.1333.
- Yuan, H., Sun, L., Chen, M., & Wang, J. (2016). The Comparison of the Contents of Sugar, Amadori, and Heyns Compounds in Fresh and Black Garlic. *Journal of Food Science*; 81; 1662–1668. doi: 10.1111/1750-3841.13365.
- Yudhayanti, P. E., Permana, I. D. G. M., & Nocianitri, K. A. (2020). Stability of Black Garlic Extract on Various pH and Temperature. *Scientific Journal of Food Technology*; 7; 17–26. doi: 10.24843/MITP.2020.V07.I01.P03.



Formulation and Physical Evaluation of Kratom (*Mitragyna speciosa* Korth.) Leaf Extract Emulgel as an Analgesic in Mice (*Mus musculus*)

Iqmal Zulhakim*, Kathina Deswiasa, Jane Arantika

Department of Pharmacy, Sambas College of Health Sciences, Sambas, Indonesia

*Corresponding author: iqmalzulhakim@gmail.com

Orcid ID: 0009-0009-4020-8424

Submitted: 23 January 2025

Revised: 18 April 2025

Accepted: 28 April 2025

Abstract

Background: Kratom leaves contain major alkaloid compounds, particularly mitragynine and 7-hydroxymitragynine which have demonstrated anti-pain or analgesic properties. **Objective:** This study aims to evaluate the effectiveness of kratom leaf extract emulgel in reducing pain when applied topically in mice. **Methods:** This study was conducted on male mice that had been induced with acetan acid intraperitoneally. Following induction, emulgel formulations were applied topically and pain responses were recorded every five minutes over 30 minutes period. Group 1 (emulgel base without active ingredient), Group 2 (voltaren emulgel), Group 3 (emulgel with 5.6% extract concentration), Group 4 (emulgel with 11.6% extract concentration) and Group 5 (emulgel with 17.6% extract concentration). **Results:** The results of physical evaluations of emulgel formulations met the applicable standards. Observations of pain responses indicated optimal analgesic effect in the emulgels containing 11.6% and 17.6% extract concentration with analgesic values of 51.52% and 63.06% respectively. An active substance is considered to have analgesic activity when it demonstrates $\geq 50\%$ effectiveness. **Conclusion:** This study concluded that emulgels formulated with kratom leaf extract exhibited analgesic activity as evidenced by the decreased in the writhing response of mice every five minutes.

Keywords: analgesic, emulgel, kratom leaf, *Mitragyna speciosa*, physical evaluation

How to cite this article:

Zulhakaim, I., Deswiasa, K. & Arantika, J. (2025). Formulation and Physical Evaluation of Kratom (*Mitragyna speciosa* Korth.) Leaf Extract Emulgel as an Analgesic in Mice (*Mus musculus*). *Jurnal Farmasi dan Ilmu Kefarmasian Indonesia*, 12(1), 77-84. <http://doi.org/10.20473/jfiki.v12i12025.77-84>

INTRODUCTION

Pain is a common and significant health issue, particularly among middle-aged and elderly individuals. It is often caused by severe tissue damage or necrosis, which leads to discomfort during daily activities (Raja et al., 2020). Therefore, pain management is necessary. However, the use of non-steroidal drugs or analgesics may result in adverse side effects, such as gastrointestinal disorders, nausea, increased blood pressure, and melena. Acute or chronic pain conditions, such as musculoskeletal pain, can also be managed with the use of topical drugs, which offer potential benefits by reducing systemic side effects (Wang et al., 2018). Traditionally, kratom leaves have been used to boost stamina, relieve pain, and treat conditions such as rheumatism, gout, hypertension, stroke symptoms, diabetes, insomnia, wounds, diarrhea, cough, cholesterol, typhoid, and to increase appetite (Wahyono et al., 2019). The primary compound in kratom leaves is mitragynine, which has a strong affinity for opioid receptors and exhibits opioid-like analgesic activity (Nugraha et al., 2018). Research conducted by Anindita (2023) on kratom leaf ethanol extract cream formulations at concentrations of 0.26 grams, 0.56 grams, and 0.86 grams showed that the cream containing 0.86 grams of kratom leaf ethanol extract demonstrated the strongest antinociceptive activity (Anindita et al., 2023).

An emulgel is a topical preparation composed of two phases: a gel phase and an emulsion phase (Vanpariya et al., 2021). Emulgels can serve as formulations with a prolonged-action mechanism as they are suitable for both hydrophobic and hydrophilic active ingredients and are advantageous for active ingredients with a short half-life (Patel et al., 2022). Other advantages of emulgel formulations include ease of spreading, easy removal, non-staining, acceptability, transparency, and long-lasting effects (Vanpariya et al., 2021).

Based on the aforementioned descriptions, there has been limited research on topical formulations of kratom leaf extract, with most studies focusing only on the antinociceptive or analgesic activity of the extract itself. Therefore, this study aims to develop and physically evaluate kratom (*Mitragyna speciosa* Korth.) leaf extract emulgel formulations as an anti-pain or analgesic agent in mice (*Mus musculus*). The concentrations of the kratom leaf extract used in the emulgel formulations (*Mitragyna speciosa* Korth.) were adapted from Anintida's research (2023) in which initial extract amounts of 0.26, 0.56 and 0.86 grams corresponded to

concentrations of 2.6%, 5.6% and 8.6% and were adjusted to 5.6%, 11.6% and 17.6%.

MATERIALS AND METHODS

Material

The chemical materials used included kratom leaf extract, Carbopol 940 (Arcypol, Ahmehabad, India), propylene glycol (SamirasChem, Indonesia), liquid paraffin (Rofa Laboratorium Centre, Bandung, Indonesia), Span 80 (KOLB, Swiss), Tween 80 (LG H&H, Korea), TEA (Methan Tirta Kimia, Bekasi, Indonesia), methylparaben (Golden Era, India), propylparaben (UENO, Japan), distilled water (Rofa Laboratorium Centre, Bandung, Indonesia), peppermint essential oil, 95% ethanol (JK Care, Indonesia), glacial acetic acid (Merck, Germany), Mayer's reagent (Merck, Germany), FeCl₃ (Merck, Germany), and NaOH (Merck, Germany).

Method

Extraction

The extraction process began by weighing 100 g of dried powdered leaves, which was then placed in a previously prepared round bottom flask. A 96% ethanol solvent was added to the flask up to 500 ml and a boiling stone was inserted to keep the temperature stable. The soxhlet process was then carried out for three hours at 78°C. Due to the limited availability of soxhlet apparatus, the extraction was repeated several times to obtain the desired quantity of extract. The resulting extract was filtered and the filtrate collected was concentrated using a rotary evaporator at a temperature of $\pm 45^{\circ}\text{C}$ (Mutiarra et al. 2023). The thickened extract was then subjected to several evaluations including: organoleptic test, extract yield, total ash content, drying shrinkage and phytochemical screening.

Phytochemical screening

a. Alkaloid Tests

The kratom leaf extract was dissolved in chloroform and placed into a test tube. Subsequently, one or two drops of ammonia were added, then mixture was shaken and filtered. Following this, 1-3 ml of 2N sulfuric acid was added. The upper layer formed was collected using a dropper pipette and distributed into three separate test tubes, each treated with a different reagent Wagner, Mayer and Dragendorff's reagents. The presence of alkaloids was indicated by the formation of a white precipitates with Mayer's reagent, a red to orange precipitate with Wagner's reagent, and a reddish brown precipitates with Dragendorff's reagent (Tiaravista et al., 2019).

b. Flavonoid Test

The kratom leaf extract was dissolved in ethanol, followed by the addition of Mg and concentrated HCL solution. The presence of flavonoid compounds in the extract was indicated by a red color change (Tiaravista et al., 2019).

c. Steroid Test

The kratom leaf extract was dissolved in ethanol, and glacial acetic acid and concentrated sulfuric acid were added. A positive result for steroids was indicated by the appearance of a green to blue color (Tiaravista et al., 2019).

d. Quinone Test

A total of 5 ml of extract dissolved in ethanol was mixed with 1N NaOH. A sample positive result for quinone compounds was indicated by the appearance of a red color (Sofia et al., 2022).

e. Tannin Test

A total of 0.5 g of extract was added to hot water, followed by a few drops of 1% FeCl₃. The presence of tannin compounds was indicated by the formation of a dark blue or blackish green color (Sofia et al., 2022).

f. Saponin Test

A total of 0.5 g of kratom leaf extract was dissolved in distilled water, shaken and left for 10 minutes. Then one drop of 1% hydrochloric acid was added. A positive for saponins was indicated by the formation of a stable foam (Sofia et al., 2022).

Formulation Optimization

The formulations of kratom leaf extract emulgel were modified from the methods described by Firmansyah et al., (2023).

Preparation of Emulgel

Carbopol 940 was dispersed in a mortar containing preheated distilled water (70–80°C) for 30 minutes, followed by trituration for 15 minutes until fully dispersed. TEA was added to the gel base in the mortar and stirred for 15 minutes until a clear gel base was formed. Separately, nipagin, nipasol, and Na EDTA were dissolved in propylene glycol using a porcelain dish and then mixed into the gel base. The emulsion base preparation began with the oil phase (Span 80 and liquid paraffin), which was melted in a porcelain dish at 60–70°C. The aqueous phase was prepared by melting Tween 80 and distilled water at 70°C in a porcelain dish. Both phases were combined by pouring the oil phase into the aqueous phase and stirred until a homogeneous emulsion mass was formed. The prepared emulsion mass was immediately mixed into the gel base in the mortar, followed by the addition of kratom leaf extract at varying concentrations and peppermint essential oil. The mixture was triturated until homogeneous, resulting in the emulgel mass. The final emulgel was then transferred into appropriate containers and subjected to evaluation (Firmansyah et al., 2023).

Table 1. Kratom leaf extract emulgel formulations

Materials	Concentration (%)					Function of Materials
	K-*	F1	F2	F3	K+*	
Kratom leaf extract	-	5.6%	11.6%	17.6%	Voltaren emulgel containing diclofenac diethylamine	Active ingredient
Carbopol 940	0.5%	0.5%	0.5%	0.5%		Gelling agent
Propylene glycol	10%	10%	10%	10%		Humectant
Liquid paraffin	5%	5%	5%	5%		Emollient
Span 80	5%	5%	5%	5%		Emulsifying agent
Tween 80	5%	5%	5%	5%		Emulsifying agent
Na EDTA	0.1%	0.1%	0.1%	0.1%		Chelating agent
TEA	2%	2%	2%	2%		Emulgator
Methyl paraben	0.1%	0.1%	0.1%	0.1%		Preservative
Propyl paraben	0.1%	0.1%	0.1%	0.1%		Preservative
Peppermint essential oil	2 drips	2 drips	2 drips	2 drips		Perfume
Aquadest	Ad 10 gr	Ad 10 gr	Ad 10 gr	Ad 10 gr		Solvent

Evaluation Parameters of Emulgel

a. Organoleptic Test

The organoleptic test was conducted by directly observing the emulgel formulation in terms of its appearance, color, and odor. Gel formulations are expected clear with a semi-solid consistency.

b. Homogeneity Test

This test involved applying the emulgel onto a glass slide and observing its color distribution to ensure uniformity and the absence of fine granules. According to SNI standards, a good gel formulation should not contain coarse particles or clumps (Firmansyah et al., 2023).

c. Spreadability Test

The spreadability test was performed by weighing 0.5 grams of the emulgel, placing it on a transparent glass surface, and covering it with another glass plate. A 150-gram weight was applied for one minute, and the increase in spread diameter was measured. The spreadability of a semi-solid formulation is considered good if it meets the standard requirement of 3–5 cm (Voigt., 1994).

d. Adhesion Test

The adhesion test was conducted using an adhesion testing device by spreading the emulgel on a glass slide, covering it with another glass slide, and applying a 250-gram weight for five minutes. After releasing the lever, a stopwatch was used to measure the time taken for the glass slides to separate. An adhesion value greater than four seconds is considered good (Firmansyah et al., 2023).

e. pH Test

The pH test was conducted by diluting 0.5 grams of the emulgel in 5 ml of distilled water, and the pH was

measured using a pH meter. According to SNI standards, a good gel formulation should have a pH suitable for the skin, which is 4.5–8 (Chandra & Rahmah, 2022).

Analgesic Test

A total of 25 mice were prepared and fasted for 18 hours, with free access to water. The mice were weighed and divided into five groups. Pain induction was performed by intraperitoneally administering 1% glacial acetic acid at a dose of 10 ml/kg body weight or 0.2 ml/20g body weight. The mice were left for 10 minutes before treatment. Group 1 received emulgel without active ingredients, group 2 received voltaren emulgel containing diclofenac diethylamine, group 3 received with emulgel containing 5.6% kratom leaf extract, group 4 received emulgel containing 11.6% kratom leaf extract and group 5 received emulgel containing 17.6% kratom leaf extract. Observations were conducted over a 30 minutes at 0, 5, 10, 15, 20, 25, and 30 minutes. Each group consisted of five mice, and each treatment was repeated five times, to obtain an average response value. The analgesic response of the mice in this test was evaluated based on their behavior, specifically writhing movements characterized by pulling both legs backward and pressing their abdomen against the surface of the cage. The percentage of pain relief activity was then calculated.

This study was declared ethically appropriate according to the seven 2011 WHO standards. The animal experiment ethics approval number is No.3088 /UN22.9/PG/2023.

$$\text{Analgesic Activity} = 100 - \left[\frac{\text{Treatment groups}}{\text{Negative control}} \times 100 \right] \%$$

RESULTS AND DISCUSSION

Table 3. Organoleptic test results of kratom leaf extract emulgel

Formula	Organoleptic			
	Color	Form	Odor	Homogeneity
FI (5.6%)	Soft brown	Semisolid	Peppermint	Homogenous
F2 (11.6%)	Brown	Semisolid	Peppermint	Homogenous
F3 (17.6%)	Dark brown	Semisolid	Peppermint	Homogenous

Table 4. Physical evaluation results of kratom leaf extract emulgel

Test	Formula	Result \pm SD	Requirement	Sig ANOVA ($p < 0.05$)
Spreadability Test	F1 (5.6%)	5 ± 0.37	3–5 cm	0.008
	F2 (11.6%)	4.76 ± 0.60		
	F3 (17.6%)	4.32 ± 0.63		
Adhesion Test	F1 (5.6%)	14.24 ± 0.90	> 4 seconds	0.092
	F2 (11.6%)	15.098 ± 0.74		
	F3 (17.6%)	15.876 ± 0.32		
pH Test	F1 (5.6%)	7.4 ± 0.203411	4.5-8	0,001
	F2 (11.6%)	7.1 ± 0.127373		
	F3 (17.6%)	6.7 ± 0.232499		

Non-Specific Parameter Tests

The concentrated extract obtained weighed 75.8 g after processing with a rotary evaporator. The results of the non-specific parameter tests were as follows yield of 25.27%, drying shrinkage of 0.56% and total ash content of 0.7171%. Phytochemical screening indicated that the kratom leaf extract contained alkaloids, flavonoids, steroids, quinones, tannins and saponins. These non-specific parameter tests were carried out to determine the quality of the extract to ensure suitability.

Phytochemical Screening

The purpose of this test was not only to identify the class of compounds present in the extract but also to evaluate the effect of the hot extraction methods (soxhletation) on the extraction chemical compounds in kratom leaves. This is consistent with the findings of Mutiara et al., (2023) who reported that heat-assisted extraction methods such as reflux and soxhlet can extract more secondary metabolite compounds. Heating facilitates the extraction of compound that are difficult to dissolve at room temperature by activating low-molecular-weight polymer subunits into high-molecular-weight, thereby improving extraction efficiency (Mutiara et al., 2023). The results shows that the kratom leaf extract tested positive for alkaloids, flavonoids, steroids, quinones, saponins and tannins. These findings are consistent with the studies by Anindita et al., (2023) which also reported the presence of these compounds in kratom leaves positive for alkaloid, flavonoids, tannins and saponins.

Organoleptic Test

Observations of the emulgel formulations containing kratom leaf extract revealed that F1 was light brown in color, with a characteristic peppermint aroma, and a semi-solid consistency. F2 produced a dark brown, emulgel with a slight blackish tint, retaining the

characteristic peppermint aroma, and exhibiting a semi-solid consistency. Meanwhile, F3 resulted in a blackish-brown emulgel, maintaining the characteristic peppermint aroma, and also presenting a semi-solid consistency. Homogeneity testing was conducted to assess the uniformity of the emulgel components. The results indicated that the formulations were homogeneous, as evidenced by the absence of coarse particles or clumps.

Spreadability Test

The spreadability of the emulgel formulations was assessed over one month, encompassing five cycles. The average spreadability ranged from 4.3 to 5 cm, meeting the requirements for effective spreadability. The spreadability of formulation is influenced by its consistency; specifically, as the consistency increases, its spreadability decreases (Bagiana & Kresnawati, 2020).

Statistical analysis was conducted to evaluate the spreadability data. The Shapiro-Wilk normality test indicated that spreadability data were normally distributed, as evidenced by a significance value greater than 0.05. Homogeneity testing of the three formulations also show homogeneous data, as indicated by a significance value of 0.456 ($p > 0.05$). Additionally, the ANOVA test yielded, a significance value of 0.008 ($p > 0.05$), suggesting no significant differences among the three formulations.

Adhesion Test

The adhesion test results over one month with five cycles presented in Table 4. The adhesion capability of the emulgel formulation in this study exceeded four seconds, meeting the criteria for good adhesion. A high adhesion value of a formulation enhances the absorption of active substances into the skin by increasing the contact time between the skin and the formulation.

The Shapiro-Wilk normality test revealed that the adhesion data were normally distributed, as evidenced by a significance value greater than 0.05. Homogeneity testing of the three formulations also showed homogeneous data, as indicated by a significance value of 0.092 ($p > 0.05$). In the ANOVA test, a significance value of 0.000 ($p < 0.05$), indicating a significant difference among the three formulations. Duncan's test identified that the third formulation, containing 17.8% emulgel concentration, exhibited significant differences compared to F1 and F2.

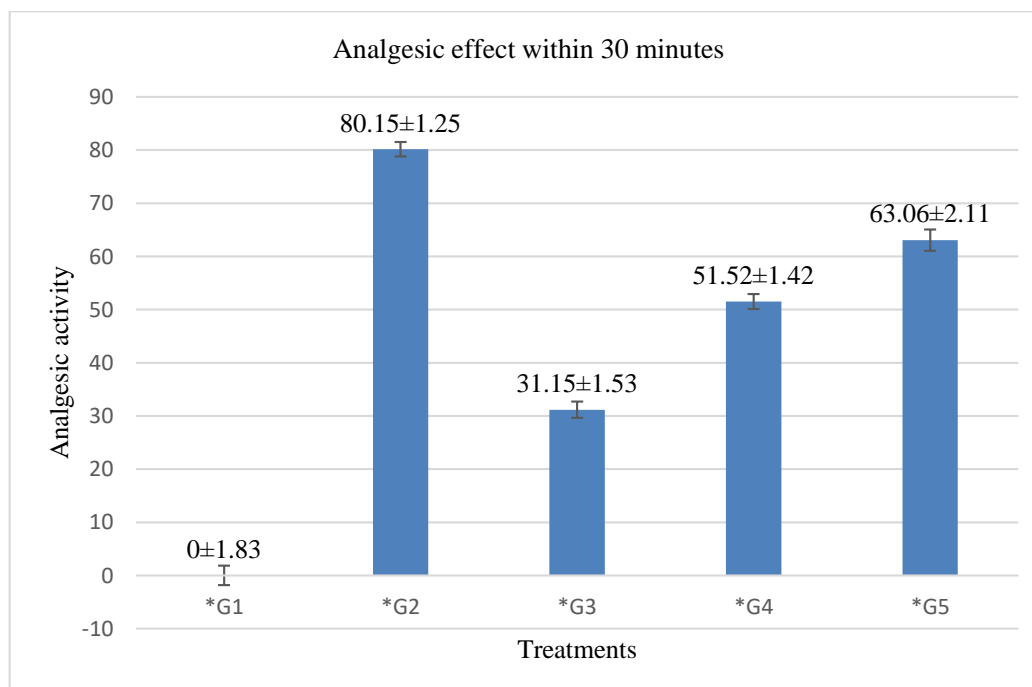
pH Test

The pH test result, conducted over one month yielded an average value ranging from 6.74 to 7.41, indicating that the emulgel formulation maintained a good pH value in accordance with the Indonesian National Standard SNI 16-3499-1996. This standard stipulates that a good pH range for emulgel formulations intended for use on the skin is 4.5-8 (Chandra & Rahmah, 2022). Throughout the one-month testing period, changes in pH were observed weekly, likely influenced by factors such as storage temperature and exposure to light.

The Shapiro-Wilk normality test for the pH values confirmed a normal distribution, with a significance

value greater than 0.05. Homogeneity testing of the three formulations also showed homogeneous data, as indicated by a significance value of 0.786 ($p > 0.05$). In the ANOVA test, a significance value of 0.001 ($p < 0.05$), indicating a significant difference among the formulations. Furthermore, post-hoc testing revealed that F3 exhibited significant differences when compared to F1 and F2.

The results presented in Figure 1 indicated in F1, with a concentration of 5.6%, provided a relatively weaker analgesic effect, whereas F2 and F3, with concentrations of 11.6% and 17.6% respectively, achieved analgesic protection rates of 51.25% and 63.06%. These values can be classified as demonstrating analgesic effects, with the percentage of pain relief increasing with higher concentrations of the extract. This trend indicated that the effectiveness of the formulation is positively correlated with the concentration of the kratom leaf extract, suggesting that higher extract concentrations lead to greater analgesic efficacy. A test substance is considered to possess analgesic or pain-relieving properties if it achieves a percentage value of $\geq 50\%$ when tested on laboratory animals (Lara et al., 2021).



*G1 = group 1 mice treated with emulgel without active ingredients

*G2 = group 2 mice treated with voltaren emulgel containing diclofenac diethylamine

*G3 = group 3 mice treated with emulgel containing 5.6% kratom leaf extract

*G4 = group 4 mice treated with emulgel containing 11.6% kratom leaf extract

*G5 = group 5 mice treated with emulgel containing 17.6% kratom leaf extract

Figure 1. Analgesic test in mice within 30 minutes

Kratom leaves contain at least 66% alkaloid compounds (Rybarczyk, 2019). The compounds responsible for the analgesic activity in the kratom leaf emulgel are alkaloids, which play a role in inhibiting the formation of prostaglandins, particularly in the cyclooxygenase (COX) enzymatic pathway of the arachidonic acid route (Tamimi et al. 2020). According to Kruegel (2019), in vitro evaluations of mitragynine and 7-hydroxymitragynine in kratom leaves (*Mitragyna speciosa*) on mouse liver preparations suggested a potential interaction with mu-opioid receptors mediated by cytochrome P450 3A. This study found high concentrations of mitragynine in the brains of mice; however, it did not directly activate opioid receptors. Kruegel further stated that the analgesic effects of these compounds may vary depending on the route of administration (Kruegel et al., 2019).

The principle underlyings topical medications or drug administration through the skin is passive diffusion, wherein active substances move from one area to another. The absorption process occurs when drug molecules penetrate the skin into the tissue, subsequently entering the bloodstream through passive diffusion (Bagiana & Kresnawati, 2020). Based on this mechanism, it can be concluded that alkaloid compounds in kratom leaves extract emulgel serve as analgesics by moving, from the skin into the bloodstream.

The Shapiro-Wilk normality test for pain relief data confirmed a normal distribution, with a significance value greater than 0.05. Homogeneity testing of the three formulas also showed homogeneous data, as indicated by a significance value of 0.013 ($p > 0.05$). The ANOVA testing yielded a significance value of 0.000 ($p < 0.05$), indicating significant differences among the three formulas. Subsequent tests were conducted identify the formulas exhibiting differences. The follow-up test demonstrated significant differences among all emulgel formulations of kratom leaf extract, as evidenced by each formulation occupying different locations in Duncan test. The results confirmed that the 17.6% kratom leaf extract emulgel concentration differed from the other two formulas. These findings are consistent with those of Anindita et al., (2023), who suggested that higher doses of kratom leaf extract administered to experimental animals are associated with decreasing response rates, reflected by smaller responses from the test subjects (Anindita et al., 2023). This study has limitations regarding the writhing response given by mice, which if the researcher is a

different person then maybe the results obtained will be different, because this study was only visually observed for the writhing response by mice. So, it is suggested that future research to use a more advanced analgesic method that is not only limited to being observed visually.

CONCLUSION

Based on the physical evaluations conducted, the emulgel formulation has met the requirements of a good emulgel, as evidenced by succesful outcome in the organoleptic test, homogeneity test, spreadibility test, adhesion test, and pH test. The efficacy of an emulgel formulation containing kratom leaf extract at three different concentrations was evaluated for its analgesic properties. Notably, the formulation with a concentration of 17.6% demonstrated a significant analgesic effect, achieving an efficacy rate of 63.06%. This was followed by the formulation with a concentration of 11.6%, which exhibited an analgesic effect of 51.52%. These findings suggest that the concentration of kratom leaf extract directly influences its analgesic capacity, highlighting its potential as a therapeutic agent in pain management.

ACKNOWLEDGMENT

The researchers express gratitude to Supervisor 1 and Supervisor 2 for their guidance throughout the research process, as well as to all parties who assisted during the research, whose names cannot be mentioned individually.

AUTHOR CONTRIBUTIONS

Conceptualization: I.Z., K.D. & J.D.; Methodology, I.Z., K.D. & J.D.; Software, I.Z.; Validation, I.Z., J.A. & K.D.; Formal Analysis, I.Z., K.D. & J.D.; Investigation: I.Z., K.D. & J.D.; Resources, I.Z., K.D. & J.D.; Data Currantion; I.Z., K.D. & J.D.; Writing - Original Draft, I.Z., K.D. & J.D.; Writing - Review and Editing, I.Z., K.D. & J.D.; Visualization, I.Z., K.D. & J.D.; Supervision: I.Z., K.D. & J.D.; Project Administration, I.Z., K.D. & J.D.; Funding Acquisition, I.Z., K.D. & J.D.;

CONFLICT OF INTEREST

The authors declare that they have no conflicts of interest.

REFERENCES

- Anindita, P.R., Setyawati, H., Wahyuni, K.I., Putri, D.O. & Ambari. (2023). Uji Sediaan Krim Ekstrak Daun Kratom (*Mitragyna Speciosa* Korth.) yang Berpotensi sebagai Antinosiseptif pada Mencit Jantan Galur DDY. *Jurnal Pharmascience*; 10; 1-13. doi: org/10.20527/jps.v10i1.12146.
- Bagiana, I.K. & Kresnawati, Y. (2020). Pengaruh Konsentrasi Campuran DMSO dan Olive Oil pada Jalur Transfor Natrium Diklofenak Melewati Kulit Secara In Vitro Menggunakan Pemodelan WimSAM. Laporan Kemajuan Penelitian. Sekolah Tinggi Ilmu Farmasi, Semarang.
- Chandra, D. & Rahmah, R.. (2022). Uji Fisikokimia Sediaan Emulsi, Gel, Emulgel Ekstrak Etanol Goji Berry (*Lycium barbarum* L.). *MEDFARM: Jurnal Farmasi dan Kesehatan*; 11; 219–228. doi: org/10.48191/medfarm.v11i2.142.
- Firmansyah., Temarwut, F.F., Topile, N.K. & Sudirman. (2023). Formulasi Dan Uji Efek Analgetik Emulgel Minyak Kayu Putih (*Oleum melaleuca cajeputi*) dengan Gelling Agent Carbopol 940. *PAPS JOURNALS*; 2; 75–84. doi: 10.51577/papsjournals.v2i2.467.
- Kruegel, A. C., Uprety, R., Grinnell, S. G., Langreck, C., Pekarskaya, E. A., Le Rouzic, V., Ansonoff, M., Gassaway, M. M., Pintar, J. E., Pasternak, G. W., Javitch, J. A., Majumdar, S. & Sames, D. (2019). 7-Hydroxymitragynine Is an Active Metabolite of Mitragynine and a Key Mediator of Its Analgesic Effects. *ACS Central Science*; 5; 992–1001. doi: 10.1021/acscentsci.9b00141.
- Lara, A.D., Elisma. E. & Kusnadi, .F.S., (2021). Uji Aktivitas Analgesik Infusa Daun jeruju (*Acanthus ilicifolius* L.) Pada Mencit Putih Jantan (*Mus musculus*). *Indonesian Journal of Pharma Science*; 3; 71–80. doi: 10.22437/ijps.v3i2.15383.
- Mutiara, S.N.I., Masriani., Muharini, R., Sapar, A. & Rasmawan, R. (2023). Comparison of Extraction Variations on Mitragynine Level of Three Variants of Kratom leaves (*Mitragyna speciosa* Korth). *EduChemia (Jurnal Kimia dan Pendidikan)*; 8; 113–129. doi: 10.30870/educhemia.v8i1.21184.
- Nugraha, W.I., Robiyanto, R. & Luliana, S. (2018). Aktivitas Antinosiseptif Fraksi Air Daun Kratom (*Mitragyna speciosa* Korth.) pada Mencit Jantan Swiss. *Traditional Medicine Journal*; 23; 91–96. doi: 10.24198/jf.v17i1.18839.
- Patel, N., Chaudhary, S. & Chaudhary, A. (2022). Emulgel –Emerging as a Smarter Value-Added Product Line Extension for Topical Preparation. *Indo Global Journal of Pharmaceutical Sciences*; 12; 92–103. doi: 10.35652/IGJPS.2022.12008.
- Rybarczyk, K.S. (2019). Quantitative Analysis of Mitragynine in Consumer Products Labeled as Kratom. *Thesis*. University of Illionis, Chicago.
- Sofia, N., Yuniarti, Y. & Rosidah, R. (2022). Uji Fitokimia Terhadap Tanaman Obat Kratom (*Mitragyna speciosa*) di KHDTK ULM. *Jurnal Sylva Scientae*; 5; 218–224. doi: 10.20527/jss.v5i2.5356.
- Tamimi, A.A., De Queljoe, E. & Siampa, J.P. (2020). Uji Efek Analgesik Ekstrak Etanol Daun Kelor (*Moringa oleifera* Lam.) pada Tikus Putih Jantan Galur Wistar (*Rattus norvegicus*). *Pharmacon*; 9; 325. doi: 10.35799/pha.9.2020.30015.
- Tiaravista, A.G., Robiyanto, R. & Luliana, S. (2019). Aktivitas Antinosiseptif Fraksi N-Heksan Daun Kratom (*Mitragyna speciosa* Korth.) Melalui Rute Oral pada Mencit Jantan Swiss. *Farmaka*; 17; 40–51. doi: 10.24198/jf.v17i1.18839.
- Vanpariya, F., Shiroya, M. & Malaviya, M. (2021). Emulgel: A Review. *International Journal of Science and Research (IJSR)*; 10; 847. doi: 10.21275/SR21311095015.
- Voigt, R. (1994). Buku Pelajaran Teknologi Farmasi (Edisi V). *Penerjemah*: Soendari Noerono. Yogyakarta: *Gajah Mada University Press*.
- Wahyono, S., Widowati, L., Handayani, L., Sampurno, O. D., Haryanti, S., Fauzi, F., Ratnawati, G. & Budiarti, M. (2019). Kratom: Prospek Kesehatan dan Sosial Ekonomi, Jakarta: Lembaga Penerbit Badan Penelitian dan Pengembangan Kesehata (LBP).
- Wang, K., LaBeff, L., Thomas, A. & Rouf, M. (2018). Topical Analgesics for Chronic Pain Conditions. *Pract Pain Manag*; 18; 5.



***In Vitro* Evaluation of Antidiabetic and Anti-Inflammatory Activities of Five Selected *Syzygium* Leaves Ethanolic Extract as Alpha-Glucosidase Inhibitors and Anti-denaturation of Bovine Serum Albumin (BSA)**

Meiliza Ekayanti*, Feri Setiadi, Siti Aminah, Alam Almaaz Afandi
Department of Pharmacy, STIKes Prima Indonesia, Bekasi, Indonesia

*Corresponding author: meilizaekayanti@gmail.com

Orcid ID: 0000-0002-5541-8610

Submitted: 10 September 2024

Revised: 13 April 2025

Accepted: 24 April 2024

Abstract

Background: Diabetes mellitus (DM) has become the main health problem in the world with a continuous increase in mortality due to complications caused by hyperglycemia. The chronic hyperglycemia is often associated with inflammation due to increase production of free radicals. **Objective:** This study's main objective is to assess antidiabetic and anti-inflammatory properties in vitro of five particular *Syzygium* leaves extract (*S. cumini*, *S. aqueum*, *S. malaccense*, *S. polyanthum*, and *S. aromaticum*) using alpha-glucosidase and Bovine Serum Albumin (BSA). **Methods:** The five of selected *Syzygium* leaves were macerated by using ethanol 96%, each extract was assessed in vitro for antidiabetic activity by analyzing the inhibitory of alpha-glucosidase using acarbose as strandard, and anti-inflammatory activity by analyzing the inhibitory denaturation of BSA Heat-induced and BSA induced by 2,2-diphenyl-1-picrylhydrazine (DPPH) with Sodium diclofenac as standard. **Result:** The result of the greater IC_{50} of α -glucosidase inhibition was *S. malaccense* 76.235 $\mu\text{g/mL}$ (strong) and acarbose standard was 0.241 $\mu\text{g/mL}$ (very strong). The greater IC_{50} of antidenaturation of BSA with heat-induced was *S. polyanthum* (95.7 $\mu\text{g/mL}$) and sodium diclofenac standard (59.25 $\mu\text{g/mL}$) both were strong inhibitor. Along with greater antidenaturation of BSA DPPH-induced was *S. malaccense* (90.320 $\mu\text{g/mL}$) and sodium diclofenac standard (43.301 $\mu\text{g/mL}$) both were strong inhibitor. **Conclusion:** Ethanol extraxt of *Syzygium* leaves were potential to be developed as an antidiabetic and anti-inflammatory herbal medicine, particularly *S. malaccense* and *S. polyanthum* leaves extract which provide greater activity on this study.

Keywords: Antidiabetic, *Syzygium*, α -glucosidase, Anti-denaturation, Bovine Serum Albumin.

How to cite this article:

Ekayanti, M., Setiadi, F., Aminah, S. & Afandi, A. A. (2025). *In Vitro* Evaluation of Antidiabetic and Anti-Inflammatory Activities of Five Selected *Syzygium* Leaves Ethanolic Extract as Alpha-Glucosidase Inhibitors and Anti-denaturation of Bovine Serum Albumin (BSA). *Jurnal Farmasi dan Ilmu Kefarmasian Indonesia*, 12(1), 85-94. <http://doi.org/10.20473/jfiki.v11i32025.85-94>

INTRODUCTION

The increasing prevalence and continuity of Diabetes Mellitus (DM) has become the main health problem in the world with a consistent increase in mortality due to complications of the disease (Zimmet *et al.*, 2016). The IDF was reported 463 million adults are diabetes and the projection in 2045 will estimated 700 million (International Diabetes Federation, 2019). The DM complications were predicted to be the cause of death of 4.2 million adults and its comparable to one mortality every eight seconds (Zimmet *et al.*, 2016). The progress of Type-2 diabetes mellitus (T2DM) complications in chronic hyperglycemia induces oxidative stress and inflammation, its simultaneously promoting complications including renal and cardiovascular diseases (Charlton *et al.*, 2021; Yuan *et al.*, 2019).

The increase in global spending on DM is reported to be more than 700 billion USD (International Diabetes Federation, 2019). The side effects of prolonged consumption of conventional drugs as well as the less invasive prevention and therapeutics using natural medicine are one of the problems in the success of DM therapy. The COVID-19 pandemic has also contributed to the increase in T2DM, so it is necessary to develop easy and inexpensive natural ingredient therapies to overcome the increased inflammation of T2DM so as to reduce diabetes complications (Salleh *et al.*, 2021). Most T2DM therapies are reported to have side effects of gastrointestinal disorders including the use of α -glucosidase Inhibitor (AGI) drugs due to the degradation of undigested carbohydrates by colon bacteria, causing excessive gas formation with a case percentage of 78% (Kumar *et al.*, 2018). The result of Riset Kesehatan Dasar (Riskesdas) (2018) reported that based on the doctor's diagnosed the prevalence of DM in Indonesia at the aged over 15 years was 2%, an increase from the previous research results in 2013 of 1.5%. Based on blood sugar test findings, the prevalence of diabetes mellitus increased from 6.9% (2013) to 8.5% (2018). The pattern of increase of DM showed higher in the age ranged 56-64 years and 66-74 years (Kemenkes RI, 2020).

Increased production of free radicals, particularly reactive oxygen species (ROS), can result from hyperglycemia and lead to oxidative stress. The disproportion between ROS and antioxidant defenses not only causes direct cell damage but also inflammation that results in tissue damage. Diabetes is often associated with inflammation when biochemical changes in diabetes affect the increase of TNF- α and IL-1 β which leads to an increase in ROS by mitochondria. Emerging therapeutic strategies address this pathway in a different way, ranging from enhancing free radical scavenging

(antioxidants and Nrf2 activators) to reduce ROS production such as NADPH oxidase inhibitors and XO inhibitors or inhibiting associated inflammatory pathways (NLRP3 inflammation inhibitors, lipoxins, GLP, receptor -1 agonists and AT-1 receptor antagonists) (Asmat *et al.*, 2016; Oguntibeju, 2019; Zhang *et al.*, 2021). The oxidative stress reported to trigger the development of micro- and macro-vascular damage complications in T2DM and hyperglycemia, as well as being responsible for DNA, lipid and protein damage associated with ROS production (Oguntibeju, 2019).

Natural ingredient therapy is currently in great demand because it is relatively cheaper and easier to obtain to become one of the options in the treatment of DM, especially T2DM. Natural medicine is projected to play a role in overcoming DM complications and the problem of side effects of conventional drug consumption, especially if used for a long period of time. *Syzygium*, a genus of plants from the *Myrtaceae* family is one of the largest genera of flowering plants with a total of 1800 species and is distributed in areas that mainly have a tropical climate including Indonesia (Abdullah *et al.*, 2021; Kavitha & Poonguzhali, 2021). Plants of the *Myrtaceae* family are reported to be the 20 largest ethnomedicinal families in Indonesia with 5 (five) species of the *Syzygium* genus (Hidayat, 2021). Some of the species of the genus *Syzygium* studied are *S. polyanthum*, *S. aromaticum*, *S. aqueum*, *S. cumini* and *S. malaccense*. The *Syzygium* group of plant species is reported to have been used for generations in traditional Ayurvedic medicine in India (Cock & Cheesman, 2018).

Studies conducted by Zaen & Ekayanti (2022) and Aklimah & Ekayanti (2022) on antioxidants from leaf extracts of several *Syzygium* genus plants showed very strong antioxidants in ethanol extracts of *Syzygium* plant leaves with IC₅₀ values *Syzygium aromaticum* 3.026 \pm 1.699 μ g/ml, *Syzygium polyanthum* 3.555 \pm 2.776 μ g/ml, *Syzygium aqueum* 5.416 \pm 2.588 μ g/mL, *Syzygium malaccense* 3.297 \pm 2.595 μ g/mL and *Syzygium cumini* 2.416 \pm 1.543 μ g/mL (Aklimah & Ekayanti, 2022; Zaen & Ekayanti, 2022). The phenetic study of each five *Syzygium* was conducted as an initial screening for the further investigation of pharmacological activities with ROS-related mechanisms. The purpose of this study was to analyze the α -glucosidase inhibition test and anti-denaturation of Bovin Serum Albumin (BSA) protein of several *Syzygium* leaf extracts as a therapy for T2DM and inflammation through the mechanism of increasing antioxidant defense, regulating carbohydrate metabolism and inhibiting inflammatory pathways. The novelty of this study is anti-denaturation BSA induced 2,2-diphenyl-1-picrylhydrazil (DPPH) of five *Syzygium* leaves extract. This study is expected to support and

improve references in the development of herbal medicine therapy as antidiabetes and anti-inflammatory. The α -glucosidase enzyme inhibition and protein anti-denaturation of *Syzygium* genus plant species that has been done before is limited to one activity test while diabetes is associated with inflammation so it is necessary to analyze the potential of natural medicine with antidiabetic and anti-inflammatory activities.

MATERIALS AND METHODS

Materials

Alpha-glucosidase from *Bacillus stearothermophilus*, 4-Nitrophenyl α -D-glucopyranoside and Bovine Serum Albumin (BSA) purchased from Sigma-Aldrich; Ethanol, Aluminum trichloride, Potassium acetate, Methanol, Citric acid, Ethyl acetate, Formic acid, silica gel F254 TLC Plates were from Merck; and DPPH (2,2-Diphenyl-1-picryl hydrazine) was from Himedia. Leaves of five grounded of *Syzygium* (*S. aromaticum*, *S. polyanthum*, *S. aqueum*, *S. malaccense*, and *S. cumini*) were collected from Balai Penelitian Tanaman Rempah dan Obat (Bogor, Indonesia). Each five plants of *Syzygium* were conducted for the identification of plant species at the Research Center of Biosystematics and Conservation (Bogor, Indonesia).

Methods

Plant extraction

Five *Syzygium* leaves powder were weighed 500 g and extracted by maceration method with 96% ethanol (1:10 w/v), soaked for three days, and stirred periodically. The filtrate of the first maceration was filtered and repeated two replication. The filtrate from maceration and repetition was evaporated at 50 °C by using a vacuum rotatory evaporator (DLAB Rotary Evaporator RE-100 Pro) (Wahyulianingsih *et al.*, 2016).

Determination of anti-diabetic activity by inhibition of α -glucosidase (Akmal & Roopma, 2023)

Initial enzyme activity assay: A total of 60 μ L of 0.1M phosphate-buffered saline (pH6.8) was added to 50 μ L of 0.07 U/mL enzyme solution and incubated in a 96 well micro plate at 37 °C for 20 minutes. After preincubation 50 μ L of 2mM pNPG was added into the microplate and then incubated again at 37 °C. The last stage was stopped by adding 160 μ L of sodium carbonate solution to the micro-plate well and evaluating the absorbance with a wavelength of 425 nm. Enzyme activity

assay - *Syzygium* leaf extract: A total of 60 μ L of 0.1M of each *Syzygium* leaves ethanol extract were added with 50 μ L of 0.07 U/mL enzyme solution and incubated in a 96 well micro plate at 37 °C for 20 minutes. After preincubation 50 μ L of 2mM pNPG was added into the microplate and then incubated again at 37 °C. The last stage was stopped by adding 160 μ L of sodium carbonate solution to microplate and reading the absorbance with a wavelength of 425 nm.

Acarbose-enzyme activity assay: A total of 60 μ L acarbose was added to 50 μ L of 0.07 U/mL enzyme solution and incubated in a 96 well micro plate at 37 °C for 20 minutes. After preincubation 50 μ L of 2mM pNPG was added into the micro plate and incubated again at 37 °C. The last stage was stopped by adding 160 μ L of sodium carbonate solution to the cuvette and reading the absorbance with a wavelength of 425 nm. The assay of initial enzyme blank activity and enzyme inhibition (BEA and BIE): A total of 60 μ L of phosphate solution of each *Syzygium* leaves extract and acarbose standard was added to 50 μ L of 0.07 U/mL enzyme solution and incubated in a 96 well micro plate at 37 °C for 20 minutes. After preincubation 50 μ L of 2mM PNPNG was added into the micro plate and then incubated again at 37 °C. The last stage was stopped by adding 160 μ L of sodium carbonate solution and reading the absorbance with a wavelength of 425 nm by using Biotek Epoch Microplate Spectrophotometer.

Determination of anti-inflammatory activity by inhibition denaturation of heat-induced bovine serum albumin (Williams *et al.*, 2008)

The assay of anti-inflammatory activity five selected *Syzygium* extracts were conducted using a heat-induced Bovine Serum Albumin (BSA) denaturation assay. Tris-buffer Saline 0.05 M was used to create the stock solutions of BSA 5% (w/v), which was then adjusted to pH 6.8 using glacial acetic acid. 100 μ L-aliquots of the BSA stock solution and distilled water were mixed with varying test tube of the extract to create 1.0 mL sample that included the extract at different dilutions. The samples were heated in a waterbath for seven minutes at 70°C to cause protein denaturation. The solutions cooled to room temperature. Spectrophotometry UV-Vis (PG-Instrument) was used to quantify the turbidity of the solutions at wavelength of 517 nm. As controls, solutions with distilled water in place of the extract were used; values obtained with these

preparations were interpreted as indicating 100% protein denaturation. BSA-free samples served as blanks and Diclofenac's anti-denaturing properties served as positive control in concurrent studies. The following formula was used to determine the percentage inhibition of denaturation, where Abs control is the absorbance of the controls, Absorbance (Abs) of sample of the *Syzygium* leaves extract or diclofenac samples, and Abs blank of the blank.

$$\% \text{ inhibition of denaturation} = \left[\frac{\text{Abscontrol} - (\text{Abssample} - \text{Absblank})}{\text{Abscontrol}} \right] \times 100\%$$

Determination of anti-inflammatory activity by inhibition denaturation of DPPH-induced bovine serum albumin (Alam *et al.*, 2022)

The anti-inflammatory activity of five selected *Syzygium* extracts was analyzed by a modified method using a DPPH-induced BSA denaturation assay. The radical scavenging activity (RSA) adopted to measure anti-inflammatory activity using the DPPH method. Briefly, 2 mL of extract solution (1–100 µg/mL) in methanol and BSA stock solutions (prepared as the same method above) was added to 2 mL of DPPH (0.1 mM) solution. The mixtures were kept aside in a dark area for 30 min and absorbance was measured at λ_{max} 517 nm against an equal amount of DPPH and methanol as a blank. The percentage of DPPH• scavenging (% Scavenging of DPPH) was estimated using the equation:

$$\% \text{ Scavenging of DPPH} \bullet = \left[\frac{(A_0 - A_1)}{A_0} \right] \times 100$$

Statistical Analysis

All the experiments for the determination of inhibitory activity of alpha-glucosidase and denaturation of BSA Heat-induced, and denaturation of BSA by using DPPH-induced have been conducted triplet (n=3). The values are expressed as the mean ± standard deviation (SD).

RESULTS AND DISCUSSION

Syzygium is a genus of plants from Myrtaceae family which is one of the largest genera of flowering plants with total 1800 species and distributed in regions mainly have a tropical climate including Indonesia (Abdullah *et al.*, 2021). The five fresh leaves of *Syzygium* were determined at the Research Center of Biosystematics and Conservation (Bogor, Indonesia) and it was validated as *Syzygium aromaticum*, *S. polyanthum*, *S. aqueum*, *S. malaccense*, and *S. cumini*. The extract of five leaves of *Syzygium* was done by cold extraction method (maceration). The crude extract of five leaves of *Syzygium* was obtained green-brownish with a distinctive aroma of leaves and the result of the higher yield percentage was *Syzygium aromaticum* (32.90%) and *Syzygium polyanthum* (30.19%) shown in Table 1. The yield percentages of five *Syzygium* extracts obtained fulfilled the quality requirements of the extraction standard as values above 10% (Kementrian Kesehatan RI, 2017).

Table 1. Yield Percentages of Five *Syzygium* Leaves Extracts

Sample	Yield (%)
<i>Syzygium cumini</i>	24.380
<i>Syzygium aqueum</i>	18.556
<i>Syzygium malaccense</i>	23.756
<i>Syzygium polyanthum</i>	30.19
<i>Syzygium aromaticum</i>	32.90

Several species of *Syzygium*, including *S. cumini*, *S. polyanthum*, *S. aqueum*, *S. aromaticum*, and *S. malaccense*, have been shown to exhibit enzymatic inhibitory action (Zulcafli *et al.*, 2020). The absorbance measurement results then calculate to percentage inhibition value. The activity of the *Syzygium* extracts mostly inhibited 50% of the enzyme activity at 100–200 µg/mL unless *S. malaccense* inhibited <100 µg/mL. The result of the α-glucosidase enzyme inhibition study showed *S. malaccense* was the greater inhibitory activity with IC₅₀ value 76.235 µg/mL (Table 2). The

concentration 200 µg/mL of *Syzygium cumini* obtained percentage of inhibition 63.261±0.178% (Figure 1). The inhibitory activity of acarbose is greater compared to each *Syzygium* extracts with IC₅₀ values 0.241 µg/mL. Acarbose acts by competitive and reversible inhibition of α-amylase and α-glucosidase from the pancreas (Glittenberg, 2012). It is well known that flavonoids derived from plants have antidiabetic effects (Najafian *et al.*, 2012; Yoshikawa *et al.*, 1998). Ethanolic extract of *Syzygium* leaves reported have high flavonoid content (Aklimah & Ekayanti, 2022;

Zaen & Ekayanti, 2022). Flavonoid and other polyphenols are reported potentially inhibit α -amylase and α -glucosidase without adverse gastrointestinal effects and useful to T2DM therapy (Barber *et al.*, 2021). Many flavonoids have a higher inhibition of α -glucosidase and leading to slow-release effect that of α -amylase which may be favoured over acarbose to decrease postprandial glucose without uncomfortable side effects (Barber *et al.*, 2021). The active substances myricetin-3-O-rhamnoside and europetin-3-O-rhamnoside, which were separated from *S. aqueum*, inhibited α -glucosidase (Manaharan *et al.*, 2012). Maslinic acid (MA) and Oleanolic acid (OA) produced from *S. aromaticum* were observed to decrease the expression of α -glucosidase, and α -amylase in the small intestines of STZ-induced diabetic rats (Khathi *et al.*, 2013). The active component of *S. cumini* and *S. malaccense*, myricitrin, was found to inhibit α -glucosidase and α -amylase (Khathi *et al.*, 2013).

The strong antioxidant activity of some *Syzygium* leaves extract reported in the previous study (Aklimah & Ekayanti, 2022; Zaen & Ekayanti, 2022), a problem-solving approach as well as a therapeutic strategy for DM and inflammation through the mechanism of increasing antioxidant defenses, improving carbohydrate metabolism profiles and inhibiting

inflammatory pathways so as to reduce the risk of hyperglycemia complications (Akmal & Roopma, 2023; Shaw *et al.*, 2017). According to Ekayanti *et al.* (2018) Phenolic components in natural materials are known to bind to proteins of enzymes and form enzyme-inhibitor bonds, thereby reducing enzyme activity (Ekayanti *et al.*, 2018). Polyphenols are also reported to have therapeutic effects on DM vascular dysfunction (Nor *et al.*, 2022). The antioxidant activity of ethanol extract of *Syzygium* plant leaves is expected to overcome the ROS imbalance that triggers oxidative stress in T2DM (Oguntibeju, 2019). Further studies in the development of T2DM and inflammation therapy need to be carried out by analyzing the α -glucosidase enzyme inhibitory activity and anti-denaturation of Bovine Serum Albumin (BSA) protein in ethanol extracts of the leaves of several *Syzygium* plants. Alpha Glucosidase Inhibitor (AGI) is one of the effective therapeutic groups used as T2DM treatment in improving metabolic profiles and potentially reducing the risk of long-term hyperglycemia complications (Akmal & Roopma, 2023). The α -glucosidase is an enzyme secreted from the epithelium of the small intestine that is responsible for carbohydrate degradation by hydrolyzing complex carbohydrates into simple glucose that can eventually be absorbed (Syabana *et al.*, 2022).

Table 2. Inhibitory percentages and IC₅₀ values of α -glucosidase

Sample	Inhibitor Percentages (%)					IC ₅₀ values (μ g/mL)
	1	2	3	4	5	
Acarbose	36.057	61.305	70.687	93.731	96.930	0.241 \pm 0.478
<i>S. cumini</i>	6.667	17.609	29.457	44.094	63.261	123.239 \pm 0.224
<i>S. aqueum</i>	28.659	37.391	43.804	48.225	56.087	169.676 \pm 0.237
<i>S. malaccense</i>	35.000	43.841	49.638	54.565	60.870	76.235 \pm 0.234
<i>S. polyanthum</i>	31.486	38.261	43.768	48.949	52.790	198.222 \pm 0.392
<i>S. aromaticum</i>	2.826	17.283	27.971	40.109	58.370	144.698 \pm 0.186

Values are mean \pm SD (n=3). Acarbose concentrations (0.1, 0.5, 1.0, 5.0, and 10.0 ppm), Sample extract concentrations (25, 50, 75 100, 200 ppm)

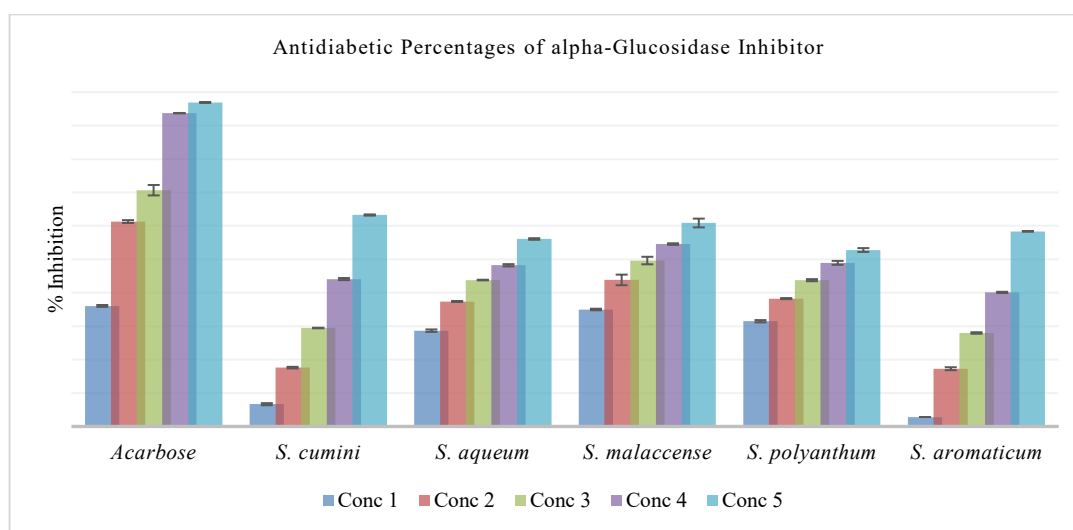


Figure 1. α -Glucosidase Inhibitor of Five Leaves *Syzygium* Extract

The production of free radicals leads to protein denaturation in the body, which triggers the release of inflammatory mediators and triggers inflammatory pathways (Shaw *et al.*, 2017). The method used to reduce BSA volume and stock solution of compound or extract for assessing anti-denaturation (anti-inflammatory) activity. The results presented at Table 3 and Figure 2 are representation of *Syzygium* ethanolic extracts and Sodium diclofenac as a control positive. Anti-denaturation protein assay using heat induction was increase kinetic energy and cause the molecules vibrating and move quickly, disrupting hydrogen bond and non-polar hydrophobic interactions of the protein. Sodium diclofenac is a non-steroidal anti-inflammatory drug works non-selectively and has better solubility in water and organic solvents. The concentration of sodium

diclofenac is 5, 15, 25, 50, and 75 $\mu\text{g/mL}$. The concentrations of *Syzygium* ethanolic extracts is 25, 50, 75, 100, and 200 $\mu\text{g/mL}$. The concentrations of *Syzygium* leaves extract can inhibit protein denaturation by >50% at range 100-200 $\mu\text{g/mL}$. The inhibition activity of protein denaturation due to the presence of bioactive compounds. The inhibition of BSA denaturation induce by heating resulted the higher IC_{50} for *Syzygium polyanthum* (95.7 $\mu\text{g/mL}$) compared to standard (sodium diclofenac) was 59.25 $\mu\text{g/mL}$. *Syzygium* extract was reported rich of polyphenol compound (Sobeh *et al.*, 2018). Polyphenol, phenyl propanoids and the disulphides interacting with the aliphatic regions around the lysine residue on the BSA and reported suitable as an anti-oxidants, anticancer, and anti-glycation (Williams *et al.*, 2008).

Table 3. Inhibitory percentages and IC_{50} values of Anti-denaturation BSA protein heat-induced

Sample	Anti-Denaturation Percentages BSA Protein Heat-Induced (%)					IC_{50} ($\mu\text{g/mL}$)
	1	2	3	4	5	
Sodium diclofenac	22.459	26.089	47.289	63.771	82.720	59.25 \pm 0.557
<i>S. cumini</i>	6.968	17.608	33.380	40.301	50.964	200.270 \pm 1.331
<i>S. aqueum</i>	8.061	13.724	32.054	41.363	51.727	198.26 \pm 0.398
<i>S. malaccense</i>	13.876	28.469	40.072	50.598	55.801	182.73 \pm 0.143
<i>S. polyanthum</i>	20.754	34.330	42.883	58.194	65.670	95.7 \pm 0.448
<i>S. aromaticum</i>	27.213	39.533	43.002	44.797	59.988	164.15 \pm 0.717

Values are mean \pm SD (n=3), Sodium diclofenac concentrations (5, 15, 25, 50, and 75 ppm), Sample extract concentrations (25, 50, 75, 100, 200 ppm)

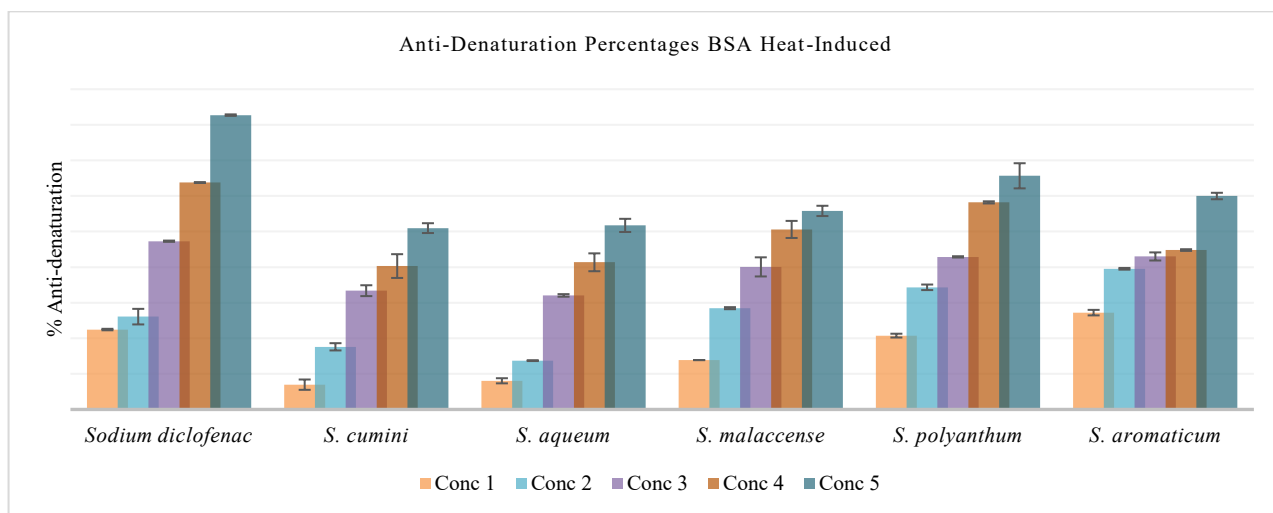


Figure 2. Anti-Denaturation BSA of Five Leaves *Syzygium* Extract Heat-Induced

Table 3. Inhibitory percentages and IC₅₀ values of Anti-denaturation BSA protein DPPH-induced

Sample	Anti-Denaturation Percentages (%)					IC ₅₀ (µg/mL)
	1	2	3	4	5	
Sodium diclofenac	13.427	31.841	49.916	56.432	61.338	43.301±0.422
<i>S. cumini</i>	20.103	27.890	36.710	49.066	63.886	117.233±1.120
<i>S. aqueum</i>	16.530	29.006	35.322	43.353	56.179	180.320±1.282
<i>S. malaccense</i>	8.782	18.306	40.198	52.628	62.400	90.320±1.076
<i>S. polyanthum</i>	13.417	22.075	28.900	44.150	51.404	196.470±0.405
<i>S. aromaticum</i>	11.817	18.760	32.722	45.008	59.165	171.596±0.479

Values are mean ± SD (n=3), Sodium diclofenac concentrations (5, 15, 25, 50, and 75 ppm), Sample extract concentrations (25, 50, 75, 100, 200 ppm)

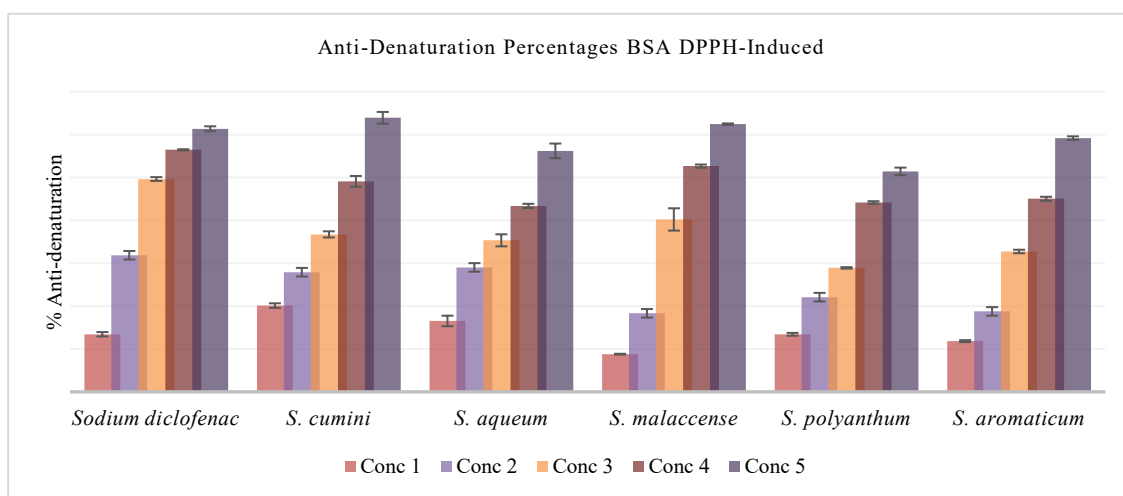


Figure 3. Anti-Denaturation BSA of Five Leaves *Syzygium* Extract DPPH-Induced

Low doses of BSA have been found as a channel for broad-spectrum *in vitro* study to analyze possible therapeutic prototypes (Williams *et al.*, 2008). The modified method of anti-denaturation BSA was designed relevant to hyperglycemia chronic conditions which inflammatory caused by increasing free radicals and stress oxidative. In this method, BSA was denaturated by DPPH-inducing and plays role as free radicals and denaturing agent as well. DPPH compound is used as a substrate to evaluate antioxidant activity, it was the stable free radical has an ability to accept one electron or Hydrogen. The greater anti-denaturation BSA DPPH-induced was *Syzygium malaccense* with IC₅₀ values is 90.320 µg/mL (Table 3) and the percentage chart showed at Figure 3. *Syzygium* leaves extract can inhibit BSA denaturation which induced by DPPH at range 100-200 µg/mL >50% inhibition percentage. The IC₅₀ value less than 50 Sodium diclofenac (positive control) is categorized as having a very strong inhibitory effect on protein denaturation. The ability of blocking the Cyclooxygenase (COX) and Lipoxygenase-5 (LOX-5) pathways was one of the pathway to overcome inflammation. Flavonoid substances are known to have anti-inflammatory properties while tannin and saponin compounds maintain membranes by attaching to cations, flavonoid and saponin compounds have been shown to have anti-inflammatory properties via scavenging free radicals. The erythrocyte membranes from hypotonic solutions could be stabilized by free radical inhibitors (Shalihah *et al.*, 2021).

CONCLUSION

Diabetes mellitus (DM) is has become the main health problem in the world with a consistent increase in mortality due to complications of the disease. The chronic hyperglycemia is often associated with inflammation due to increase production of free radicals thus lead to oxidative stress. *Syzygium* leaves were potential to be developed as antidiabetic and anti-inflammatory candidates of drugs. The greater result of IC₅₀ of α-glucosidase inhibition was *Syzygium malaccense* was 76.235 µg/mL (strong) and acarbose standard was 0.241 µg/mL (very strong). The greater antidenaturation of BSA with heat-induced was *Syzygium polyanthum* (95.7 µg/mL) and sodium diclofenac standard was 59.25 µg/mL both were strong inhibitor. Along with antidenaturation of BSA DPPH-induced was *Syzygium malaccense* 90.320 µg/mL and

sodium diclofenac standard was 43.301 µg/mL both were strong inhibitor. Further research is needed to confirm the antidiabetic and anti-inflammatory activities of *Syzygium* extract using different methods *in vitro* and *in vivo*.

ACKNOWLEDGMENT

The authors are grateful to Ministry of Education Culture, Research, and Technology of the Republic of Indonesia whom funded the study. Acknowledgment is also due to all the colleagues in accomplishing this study.

REFERENCES

- Abdullah, M., Priyono, B., Kartijono, N. E. F. & Bodijantoro, P. M. H. (2021). Medicinal Plant of Gunung Prau, Indonesia: Exploration and Ethno-Botanical Study. *Journal of Physics: Conference Series*; 1918; 1–4. doi: 10.1088/1742-6596/1918/5/052046.
- Aklimah, M. & Ekayanti, M. (2022). Penetapan Flavonoid Total dan Uji Aktivitas Antioksidan Ekstrak Etanol Daun Cengkeh (*Syzygium aromaticum* (L). Merr) dan Daun Salam (*Syzygium polyanthum* Thwaites). *Jurnal Kedokteran Universitas Palangka Raya*; 10; 11–14. doi: 10.37304/jkupr.v10i2.5536.
- Akmal, M., Patel, P. & Roopma, W. (2023). Alpha Glucosidase Inhibitors. *StatPearls Publishing LLC*. <https://www.ncbi.nlm.nih.gov/books/>
- Alam, T., Ekayanti, M., Permana, N., Hadissabil, Z. & Prima Indonesia, S. (2022). Potensi Aktivitas Antioksidan Ekstrak Etanol dan Fraksi Ciplukan (*Physalis angulata*) pada DPPH (1,1-difenil-2-pikrihidrazil) Potential Antioxidant Activity of Ethanol Extract and Fraction of Ciplukan (*Physalis angulata*) on DPPH (1,1-diphenyl-2-picrylhydrazyl). *Jurnal Farmasi Indonesia*; 19; 193–199. doi: 10.31001/jfi.v19i1.1490.
- Asmat, U., Abad, K. & Ismail, K. (2016). Diabetes Mellitus and Oxidative Stress a Concise Review. In *Saudi Pharmaceutical Journal*; 24; 547–553. Elsevier B.V. doi: 10.1016/j.jsps.2015.03.013.
- Barber, E., Houghton, M. J. & Williamson, G. (2021). Flavonoids as Human Intestinal α-glucosidase Inhibitors. *Foods*; 10; 1–22. doi: 10.3390/foods10081939.

- Charlton, A., Garzarella, J., Jandeleit-Dahm, K. A. M., & Jha, J. C. (2021). Oxidative Stress and Inflammation in Renal and Cardiovascular Complications of Diabetes. *In Biology*; 10; 1–18. MDPI AG. doi: 10.3390/biology10010018.
- Cock, I. E. & Cheesman, M. (2018). Plants of The Genus *Syzygium* (Myrtaceae): A Review on Ethnobotany, Medicinal Properties and Phytochemistry. In *Bioactive Compounds of Medicinal Plants: Properties and Potential for Human Health*; 35–85.
- Ekayanti, M., Sauriasari, R. & Elya, B. (2018). Dipeptidyl peptidase IV Inhibitory Activity of Fraction from White Tea Ethanolic Extract (*Camellia sinensis* (L.) Kuntze) ex vivo. *Pharmacognosy Journal*; 10; 190–193. doi: 10.5530/pj.2018.1.32.
- Glittenberg, D. (2012). Starch-Based Biopolymers in Paper, Corrugating, and Other Industrial Applications. *Polymer Science: A Comprehensive Reference*; ;1–10; 165–193. doi: 10.1016/B978-0-444-53349-4.00258-2.
- Hidayat, S. (2021). Pemanfaatan Tumbuhan Obat oleh Beberapa Etnis di Indonesia. *Prosiding Seminar Nasional PMEI Ke-V*, 177–185. <https://jte.pmei.or.id/index.php/jte/article/view/141>
- International Diabetes Federation. (2019). IDF Diabetes Atlas 9th Ed. In *Diabetes Atlas* (9th ed.). <https://www.diabetesatlas.org>.
- Kavitha, V. & Poonguzhali, T. V. (2021). Phylogenetic Analysis on Different Species of *Syzygium*. *International Research Journal of Plant Science*; 12; 1–03. doi: 10.14303/irjps.2021.001
- Kemenkes RI. (2020). InfoDatin (Pusat Data dan Informasi Kementerian Kesehatan RI): Tetap Produktif, Cegah, dan Atasi Diabetes Melitus. *Kementerian Kesehatan RI*, 4–5. <https://www.kemkes.go.id/downloads/resources/download/pusdatin/infodatin/Infodatin%202020%20Diabetes%20Melitus.pdf>
- Kementerian Kesehatan RI. (2017). *Farmakope Herbal Indonesia Edisi II*.
- Khathi, A., Serumula, M. R., Myburg, R. B., Van Heerden, F. R. & Musabayane, C. T. (2013). Effects of *Syzygium aromaticum*-Derived Triterpenes on Postprandial Blood Glucose in Streptozotocin-Induced Diabetic Rats Following Carbohydrate Challenge. *PLoS ONE*; 8; 1–8. doi: 10.1371/journal.pone.0081632.
- Kumar, Y., Goyal, R. K. & Thakur, A. K. (2018). Pharmacotherapeutics of Miglitol: An α -Glucosidase Inhibitor. *Journal of Analytical & Pharmaceutical Research*; 7; 617–619. doi: 10.15406/japlr.2018.07.00292.
- Manaharan, T., Appleton, D., Cheng, H. M., & Palanisamy, U. D. (2012). Flavonoids isolated from *Syzygium aqueum* Leaf Extract as Potential Antihyperglycaemic Agents. *Food Chemistry*; 132; 1802–1807. doi: 10.1016/j.foodchem.2011.11.147.
- Najafian, M., Jahromi, M. Z., Nowrozejjhad, M. J., Khajeaian, P., Kargar, M. M., Sadeghi, M. & Arasteh, A. (2012). Phloridzin Reduces Blood Glucose Levels and Improves Lipids Metabolism in Streptozotocin-Induced Diabetic Rats. *Molecular Biology Reports*; 39; 5299–5306. doi: 10.1007/s11033-011-1328-7.
- Nor, N. A., Budin, S. B., Zainalabidin, S., Jalil, J., Sopian, S., Jubaidi, F. F. & Anuar, N. N. (2022). Review: The Role of Polyphenol in Modulating Associated Genes in Diabetes-Induced Vascular Disorders. *International Journal of Molecular Sciences*; 23; 6936–6960. doi: 10.3390/ijms23126396.
- Oguntibeju, O. O. (2019). Type 2 Diabetes Mellitus, Oxidative Stress and Inflammation. *Int J Physiol Pathophysiol Pharmacol*; 11; 45–63.
- Oguntibeju, O. O. (2019). Review Article Type 2 Diabetes Mellitus, Oxidative Stress and Inflammation: Examining the Links. *Int J Physiol Pharmacol*; 11; 45–63.
- Salleh, N. H., Zulkipli, I. N., Mohd Yasin, H., Ja' Afar, F., Ahmad, N., Wan Ahmad, W. A. N. & Ahmad, S. R. (2021). Systematic Review of Medicinal Plants Used for Treatment of Diabetes in Human Clinical Trials: An ASEAN Perspective. *Evidence-Based Complementary and Alternative Medicine*; 2021; 1–10. doi: 10.1155/2021/5570939.
- Shalihah, A., Christianty, F. M. & Fajrin, F. A. (2021). Anti-inflammatory Activity of the Ethanol Extract of Cinnamon (*Cinnamomum burmannii*) Bark using Membrane Stabilization Method and Protein Denaturation. *In Indonesian Journal of Pharmaceutical Science and Technology*

- Journal Homepage*; 1; 9-14 doi: 10.24198/ijpst.v1i1.36323.
- Shaw, Y., Williams, L., Green, C., Rodney, S. & Smith, M. (2017). In-Vitro Evaluation of the Anti-Inflammatory Potential of Selected Jamaican Plant Extracts using the Bovine Serum Albumin Protein Denaturation Assay. *Int. J. Pharm. Sci. Rev. Res*; 47; 145–153.
- Sobeh, M., Mahmoud, M. F., Petruk, G., Rezq, S., Ashour, M. L., Youssef, F. S., El-Shazly, A. M., Monti, D. M., Abdel-Naim, A. B. & Wink, M. (2018). *Syzygium Aqueum*: A Polyphenol-Rich Leaf Extract Exhibits Antioxidant, Hepatoprotective, Pain-Killing and Anti-Inflammatory Activities in Animal Models. *Frontiers in Pharmacology*; 9; 1-14. doi: 10.3389/fphar.2018.00566.
- Syabana, M. A., Yuliana, N. D., Batubara, I. & Fardiaz, D. (2022). α -Glucosidase Inhibitors from *Syzygium polyanthum* (Wight) Walp Leaves as Revealed by Metabolomics and in silico Approaches. *Journal of Ethnopharmacology*, 282. 1-13. doi: 10.1016/j.jep.2021.114618
- Wahyulianingsih, W., Handayani, S. & Malik, Abd. (2016). Penetapan Kadar Flavonoid Total Ekstrak Daun Cengkeh (*Syzygium aromaticum* (L.) Merr & Perry). *Jurnal Fitofarmaka Indonesia*; 3; 188–193. doi: 10.33096/jffi.v3i2.221.
- Williams, L., O'Connar, A., Latore, L., Dennis, O., Ringer, S., Whittaker, J., Conrad, J., Volger, B., Rosner, H. & Kraus, W. (2008). The in vitro Anti-denaturation Effects Induced by Natural Products and Non-steroidal Compounds in Heat Treated (Immunogenic) Bovine Serum Albumin is Proposed as a Screening Assay for the Detection of Anti-inflammatory Compounds, without the use of Animals, in the Early Stages of the Drug Discovery Process. *West Indian Medical Journal*; 57; 327–378. doi: 10.1215/9780822388630-010
- Yoshikawa, M., Shimada, H., Nishida, N., Li, Y., Toguchida, I., Yamahara, J. & Matsuda, H. (1998). Antidiabetic Principles of Natural Medicines II. Aldose Reductase and Alpha-Glucosidase Inhibitors from Brazilian Natural Medicine, The Leaves of *Myrcia multiflora* DC. (Myrtaceae): Structures of Myrciacitrins I and II and Myrciaphenones A and B. *Chemical and Pharmaceutical Bulletin*; 46; 113–119. doi: 10.1248/cpb.46.113
- Yuan, T., Yang, T., Chen, H., Fu, D., Hu, Y., Wang, J., Yuan, Q., Yu, H., Xu, W. & Xie, X. (2019). New Insights into Oxidative Stress and Inflammation During Diabetes Mellitus-Accelerated Atherosclerosis. *In Redox Biology*; 20; 247–260. Elsevier B.V. doi: 10.1016/j.redox.2018.09.025.
- Zaen, D. M. & Ekayanti, M. (2022). Penetapan Flavonoid Total dan Uji Aktivitas Antioksidan Ekstrak Etanol Daun Jambu Air (*Syzygium aqueum*), Daun Jambu Bol (*Syzygium malaccense*) dan Daun Jamblang (*Syzygium cumini*). *Jurnal Kedokteran Universitas Palangka Raya*; 10; 15–18. doi: 10.37304/jkupr.v10i2.5531.
- Zhang, C., Wang, X., Du, J., Gu, Z. & Zhao, Y. (2021). Reactive Oxygen Species-Regulating Strategies Based on Nanomaterials for Disease Treatment. *In Advanced Science*; 8; 1-34. doi: 10.1002/advs.202002797.
- Zimmet, P., Alberti, K. G., Magliano, D. J. & Bennett, P. H. (2016). Diabetes Mellitus Statistics on Prevalence and Mortality: Facts and Fallacies. *Nature Reviews Endocrinology*; 12; 616–622. doi: 10.1038/nrendo.2016.105.
- Zulcafli, A. S., Lim, C., Ling, A. P., Chye, S. & Koh, R. (2020). Antidiabetic Potential of *Syzygium* sp.: An Overview. *The Yale Journal of Biology and Medicine*; 93; 307–325.



***In Silico* Study of Green Tea (*Camellia sinensis*) Compound as Potential Anxiolytic Drug Material Targeting Estrogen Alpha Receptor**

Harfiah Nur Aini, Susanti, Richa Mardianingrum*

Department of Pharmacy, Faculty of Health Sciences, Universitas Perjuangan Tasikmalaya, Tasikmalaya, Indonesia

*Corresponding author: richamardianingrum@unper.ac.id

Orcid ID: 0000-0002-2327-363X

Submitted: 10 September 2024

Revised: 16 April 2025

Accepted: 22 April 2025

Abstract

Background: The prevalence of anxiety disorders has significantly increased each year but has not been matched by the availability of adequate treatments. Estrogen receptor alpha (ER α) is known to induce anxiety through the activation of a complex system in the body, and drugs that inhibit ER α activity are predicted to have anxiolytic potential. **Objective:** This study aims to evaluate 50 compounds derived from green tea leaves to discover potential anxiolytic candidates that act by inhibiting ER α . **Methods:** The research methods used include toxicity screening, pharmacokinetic screening, drug scan, molecular docking, and molecular dynamics. **Results:** Based on the screening results, quercetin was identified as non-carcinogenic, non-hepatotoxic, easily absorbed, evenly distributed, non-interfering with CYP2D6 enzyme metabolism, and potentially effective as an oral drug. In molecular docking results, quercetin showed a ΔG value of -7.54 kcal/mol and K_i of 2.97 μM , which are better than the reference drug with a ΔG value of -7.20 kcal/mol and K_i of 5.24 μM . Quercetin also shown more stable interactions with the ER α binding site, indicated by amino acids Glu353 and Arg394 in RMSD and RMSF analysis during molecular dynamics simulation. **Conclusion:** From the study result it can be concluded that quercetin has potential as a good candidate for anxiolytic drug material by inhibiting ER α activity.

Keywords: anxiolytic, anxiety disorder, estrogen receptor alpha, green tea, in silico

How to cite this article:

SafitAini, H. N., Susanti, S. & Mardianingrum, R. (2025). *In Silico* Study of Green Tea (*Camellia sinensis*) Compound as Potential Anxiolytic Drug Material Targeting Estrogen Alpha Receptor. *Jurnal Farmasi dan Ilmu Kefarmasian Indonesia*, 12(1), 95-105. <http://doi.org/10.20473/jfiki.v12i12025.95-105>

INTRODUCTION

Anxiety disorders involve intense and excessive fear and worry, accompanied by physical tension and cognitive symptoms, which significantly impact daily life if untreated (WHO, 2023). As many as 301 million people worldwide were known to suffer from anxiety disorders in 2019 and that number increased significantly due to the COVID-19 pandemic, but only 27.6% of anxiety disorder sufferers received treatment due to limited availability (WHO, 2022). Meanwhile, in Indonesia, the prevalence of anxiety disorders reached 31.9% among children, adults, and the elderly with or without prior mental disorders in 2022 (Atmawati, 2022).

Estrogen alpha (ER α) is known to influence anxiety by increasing glucocorticoid secretion through the Hypothalamic-Pituitary-Adrenal (HPA) axis activity, enhancing Adrenocorticotrophic Hormone (ACTH) response to stress, and regulating Corticotropin-Releasing Hormone (CRH) gene expression via histone acetylation (Borrow & Handa, 2017). Therefore, drugs that inhibit ER α receptor activity are predicted to have promising potential in treating anxiety disorders. Clonazepam, a benzodiazepine-class anxiolytic drug, has been shown through in vitro research on hER α -HeLa-99035 cells to exhibit antagonistic activity against ER α (Kenda et al., 2022).

Many studies have been conducted to discover anxiolytic drug candidates including research on green tea plants. Clinical studies indicate that consumption of decaffeinated green tea beverages positively contributes to reducing anxiety levels in adolescents who stutter (Almudhi & Gabr, 2022). *In vivo* studies also show positive effects of green tea on neurobiological behaviors, including anxiety in lead-induced mice (Al-Qahtani et al., 2022). Meanwhile, *in silico* studies were conducted to investigate the molecular interactions of green tea compounds. The ER α was chosen as the target due to its known involvement in anxiety pathophysiology through modulation of the HPA axis and stress hormone regulation.

MATERIALS AND METHODS

Materials and tools

The hardware used in this research include a Lenovo ThinkPad laptop with an Intel® Core™ i5-6200U CPU @ 2.30GHz (4 CPUs) ~2.40GHz; 8GB RAM; 64-bit system type; operating system Windows 10 Pro, and a computer with specifications featuring an Intel® Core™ i5-8400 CPU @ 2.80 GHz x 6, Nvidia Geforce GTX 970/PCIe/SSE2 GPU, 64-bit operating

system type, and 245.1 GB RAM. The software utilized in this study includes MarvinSketch, Molegro Molecular Viewer, AutodockTools, Desmond, and BIOVIA Discovery Studio. Additionally, the research utilized websites such as KNApSACk, PubChem, PDBsum, RCSB PDB, and pkCSM. The materials used comprise 50 compounds found in green tea from websites

http://www.knapsackfamily.com/KNApSACk_Family/ the reference drug clonazepam, and the ER α with PDB ID 7UJM (Hosfield et al., 2022).

Method

Preparation of receptor and compound ligands

The crystallographic structure of the ligand binding domain of the ER α was downloaded from the RCSB PDB website (<https://www.rcsb.org/>) at a resolution of 1.80 Å (Hosfield et al., 2022). The receptor was subsequently analyzed on the PDBsum website (<https://www.ebi.ac.uk/thornton-srv/databases/pdbsum/>), which provides detailed receptor structure information, schematic diagrams of molecules within each structure, and their interactions with ligands (Mardianingrum et al., 2021). Further receptor preparation involved removing solvent molecules, separating the receptor from natural ligands and other residues, and adding hydrogen atoms (Mardianingrum et al., 2023).

The 50 green tea compound ligands were sourced from the KNApSACk database (http://www.knapsackfamily.com/KNApSACk_Family/), by entering the plant name *Camellia sinensis* (green tea) as the query. The search results were filtered to include only naturally occurring compounds reported specifically in the leaves of *Camellia sinensis*, which are commonly used in tea preparations and known to contain bioactive phytochemicals with potential pharmacological effects. Their structures are obtained from the PubChem website (<https://pubchem.ncbi.nlm.nih.gov/>). The compound ligands were then prepared through protonation at physiological pH conditions and conformational search using Marvin Sketch (Mardianingrum et al., 2023).

Validation of the docking method

The validation process of the docking method was conducted by redocking the ligand to the previously separated receptor. Parameters considered included the RMSD value, which is deemed acceptable if ≤ 2 Å (Mardianingrum et al., 2023). Interactions occurring between the natural ligand and amino acid residues on the receptor were then assessed based on 2D visualization. Additionally, comparisons between the

natural ligand before and after the docking method validation process were also examined through 3D overlays.

Prediction of toxicity aspects, pharmacokinetic aspects and drug scans

The prediction of toxicity and pharmacokinetic aspects was conducted by entering the SMILES notation of the compound ligands on the pkCSM website (<https://biosig.lab.uq.edu.au/pkcsm/prediction>).

Meanwhile, drug scanning, which refers to predicting the potential of compound ligands as orally-based drugs, was performed considering drug absorption characteristics and effectiveness through parameters such as molecular weight, log P, partition coefficient, number of hydrogen bond donors and acceptors, and molar refractivity, following Lipinski's rule of five (Mardianingrum et al., 2023).

Analysis and visualization of molecular docking results

Molecular docking was performed using AutoDockTools with the Lamarckian Genetic Algorithm (LGA) settings. Each docking was replicated three times to ensure consistency of the results. The best binding pose was selected based on the lowest binding free energy (ΔG) and inhibition constant (K_i) to proceed to molecular dynamics simulation (Mardianingrum et al., 2022). 2D visualization was conducted on natural ligands, reference drugs, and the best compound ligands from the molecular docking results to analyze amino acid residue contacts and hydrogen bond interactions (Mardianingrum et al., 2022).

Simulation and Analysis of Molecular Dynamics (MD) Results

MD were performed on the reference drug as well as on the test compound ligands using Desmond. The

simulation system was set at 300⁰K temperature, 1 bar pressure, 100 ns duration, with data recorded every 100 ps that resulting in a total of 1,000 frames (Lv et al., 2022). The results obtained included trajectory files analyzed based on Root Mean Square Deviation (RMSD) and Root Mean Square Fluctuation (RMSF) (Lv et al., 2022).

RESULTS AND DISCUSSION

Receptor Analysis

The 7UJM receptor is a ligand-binding domain classified as a transcription factor involved in regulating estrogen-related gene expression in Homo sapiens organisms (Hosfield et al., 2022). The receptor was analyzed using a Ramachandran plot, a statistical representation of amino acid residues in the protein structure based on ϕ and ψ dihedral angles (Ruswanto et al., 2018). The analysis results indicate that the 7UJM receptor meets the criteria for good structural quality, with 0.0% of residues in disallowed regions and 94.7% of residues in most favored regions, as shown in Figure 1 (a).

The binding sites of natural ligands on the receptor were analyzed using LigPlot, which automatically generates 2D schematic representations of all interactions formed between the ligand and protein molecule residues (Wadapurkar et al., 2018). Binding sites on the natural ligand are characterized by hydrogen bonds (Ruswanto et al., 2018). Therefore, based on LigPlot analysis results, it was found that the binding site of the natural ligand on receptor 7UJM involves hydrogen bonding with residues Glu353 and Arg394, as depicted in Figure 1 (b).

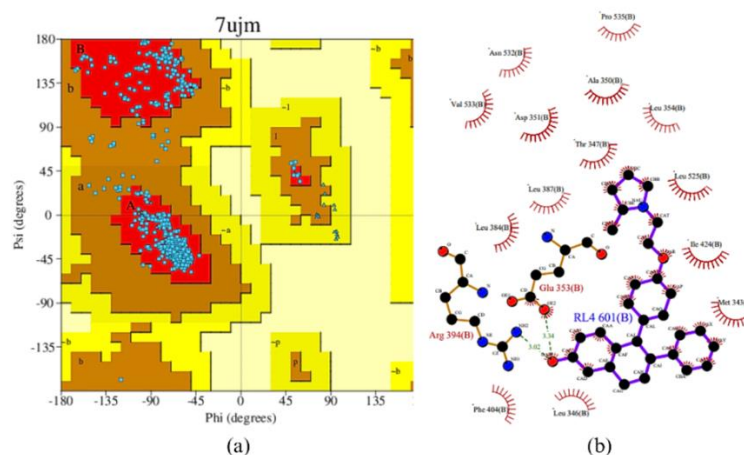


Figure 1. (a) Ramachandran statistical plot of 7UJM receptors, (b) LigPlot schematic of natural ligands on the 7UJM receptor

Docking method validation

The docking method validation was conducted using a grid box coordinate setup that encompassed the receptor binding site area and allowed sufficient space for ligand rotation and translation (Gopinath & Kathiravan, 2021). The docking method in this study was deemed valid with an RMSD value $< 2 \text{ \AA}$ because the lower RMSD value indicating the more similar docking ligand positions to the natural ligand positions

from crystallography and the more effective docking method (Mardianingrum et al., 2023). Additionally, the selected receptor structure (PDB ID: 7UJM) had previously been validated through Ramachandran plot analysis, with 94.7% of residues located in the most favored regions and 0.0% in disallowed regions, confirming its structural reliability. The validation results of the docking method can be seen in Figure 2 and Table 1.

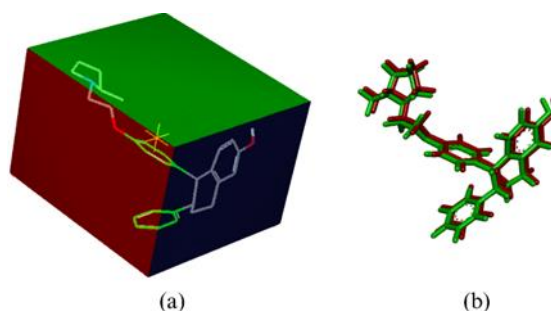


Figure 2. (a) natural ligands in a grid box, (b) 3D overlay of ligands before redocking (green) and after redocking (red)

Table 1. Validation results of the 7UJM receptor docking method along with grid box coordinate settings

Grid dimension			Grid center			Spacing	RMSD	ΔG	Ki
x	y	z	x	y	z				
30	24	34	-0.944	18.643	18.988	0.375 \AA	0.72 \AA	-13.74 kcal/mol	85.02 pM

Table 2. Prediction results of toxicity and pharmacokinetic aspects of 50 compound ligands from green tea

No	Compound name	Toxicity Aspects			Pharmacokinetic Aspects				
		Ames Toxicity	LD ₅₀ (mol/Kg)	Hepato-toxicity	Caco2 (Log 10 ⁻⁶)	HIA (%)	VDss (log L/Kg)	CYP2D6 inhibitor	Renal OCT2 substrate
+	Clonazepam	No	3.08	No	0.98	98.58	0.14	No	No
1.	Indole	No	2.40	No	1.54	93.30	0.26	No	No
2.	Adenine	No	2.07	No	1.37	88.74	-0.08	No	No
3.	Caffeine	No	2.80	Yes	1.11	99.27	-0.59	No	No
4.	Cytosine	No	1.94	No	0.47	83.05	-0.15	No	No
5.	Theobromine	Yes	2.38	Yes	0.51	98.37	-0.15	No	No
6.	Theophylline	No	2.30	Yes	0.62	100	0.84	No	No
7.	Xanthine	Yes	2.08	No	-0.17	63.92	-0.51	No	No
8.	Methyl anthranilate	No	1.74	No	1.18	87.46	0.01	No	No
9.	7-Methylxanthine	Yes	2.14	Yes	0.45	89.90	-0.26	No	No
10.	Paraxanthine	No	2.18	Yes	0.46	93.97	-0.24	No	No
11.	7-Methylxanthosine	No	1.93	Yes	0.63	39.33	0.04	No	No
12.	AMP	No	2.06	No	-0.66	35.80	0.57	No	No
13.	L-Theanine	No	2.06	No	-0.25	42.53	-0.56	No	No
14.	Xanthosine	No	1.85	Yes	0.19	44.83	-0.02	No	No
15.	IMP	No	2.03	No	-0.68	25.94	-0.27	No	No
16.	Xanthosine 5'-monophosphate	No	2.04	No	-0.57	22.49	-0.11	No	No
17.	7-Methyl-XMP	No	2.57	Yes	-0.97	20.89	0.37	No	No

18.	N,N-Dibutylacetamide	No	2.03	No	1.48	93.43	0.09	No	No
19.	1-Methylxanthine	No	2.48	Yes	1.12	83.63	0.21	No	No
20.	(+)-Catechin	No	2.42	No	-0.28	68.82	1.02	No	No
21.	(+)-Epicatechin	No	2.42	No	-0.28	68.82	1.02	No	No
22.	(+)-Gallocatechin	No	2.49	No	-0.37	54.12	1.30	No	No
23.	(-)-Catechin	No	2.42	No	-0.28	68.82	1.02	No	No
24.	(-)-Epiafzelechin	No	2.36	No	1.07	91.48	0.56	No	No
25.	(-)-Epicatechin 3-O-gallate	No	2.55	No	-1.26	62.09	0.66	No	No
26.	(-)-Epigallocatechin	No	2.92	No	-0.37	54.12	1.30	No	No
27.	(-)-Epitheaflavic acid	No	2.48	2.48	-1.59	45.17	0.13	No	No
28.	(-)-Gallocatechin gallate	No	2.52	No	-1.52	47.39	0.80	No	No
29.	Catechin-3-gallate	No	2.55	No	-1.26	62.09	0.66	No	No
30.	Epicatechin 3,5-di-O-gallate	No	2.48	No	-1.25	54.04	-0.04	No	No
31.	Epicatechin 3-O-(3-O-methylgallate)	No	2.55	No	-0.27	80.84	0.71	No	No
32.	Epigallocatechin 3,3',-di-O-gallate	No	2.48	No	-1.25	39.04	0.14	No	Yes
33.	Epigallocatechin 3-O-(3-O-methylgallate)	No	2.55	No	-1.78	71.28	1.00	No	No
34.	Epigallocatechin 3-O-cafeate	No	2.55	No	-1.36	51.08	0.68	No	No
35.	Ampelopsin	No	2.43	No	0.11	58.92	1.66	No	No
36.	Astragalin	No	2.54	No	0.30	48.05	1.44	No	No
37.	Cinnamate	No	1.75	No	1.60	81.81	-1.07	No	No
38.	Cyanidin	No	2.46	No	-0.35	87.30	0.95	No	No
39.	Delphinidin chloride	No	2.54	No	-0.32	61.91	0.96	No	No
40.	Dihydroquercetin	No	2.26	No	0.92	64.70	1.63	No	No
41.	Isomyricitrin	No	2.54	No	-1.34	33.39	1.54	No	No
42.	Leucocyanidin	No	2.39	No	-0.25	56.71	1.81	No	No
43.	Naringenin	No	1.79	No	1.02	91.31	-0.01	No	No
44.	Pollenitin	No	2.36	No	-0.27	74.72	0.61	No	No
45.	Quercetin	No	2.47	No	-0.22	77.20	1.55	No	No
46.	Tricetinidin	No	2.60	No	-0.98	75.64	0.27	No	No
47.	3-O-Caffeoylquinic acid	No	1.97	No	No	-0.84	36.37	0.58	No
48.	Peonidin chloride	No	2.39	No	No	-0.04	73.69	0.62	No
49.	Malvidin	No	2.34	No	No	-0.38	88.78	0.76	No
50.	Luteoliflavan	No	2.48	No	No	0.98	90.00	0.96	No

*highlight: Not eligible

Prediction of toxicity aspects, pharmacokinetic aspects and drug scans

Prediction of toxicity and pharmacokinetic aspects was conducted using the pkCSM website based on graphical structural features (Pires et al., 2015). Parameters considered in toxicity aspects include Ames toxicity as widely used method to assess the mutagenic

potential of a compound using bacteria, rat LD₅₀ as the amount of a compound that causes 50% mortality in test animal groups, and hepatotoxicity which involves chemical-induced liver damage (Pires et al., 2015). Meanwhile, parameters considered in pharmacokinetic aspects include Caco-2 permeability as an in vitro cell model that predicting oral drug absorption, intestinal absorption (human) as percentage of compound

absorbed by the human intestine, VDss that indicating drug distribution in body tissues relative to blood plasma, CYP2D6 inhibitor as an enzyme crucial in drug metabolism, and renal OCT2 substrate that predicting compound transport potential via kidney transporters affecting drug elimination (Pires et al., 2015). Based on the results in Table 2, 35 compounds meeting the criteria for predicting both toxicity and pharmacokinetic aspects.

Drug scan was conducted on 35 compounds that had passed the prediction stage for pharmacokinetic and toxicity aspects. The drug scan stage refers to the process of scanning or analyzing test compounds using Lipinski's rule of five. Lipinski's rule of five consists of guidelines used to evaluate the pharmacokinetic properties of a compound, particularly its absorption and permeability characteristics (Chen et al., 2020). First, molecular weight < 500 Da because smaller molecules tend to be absorbed better. Second, Log P value < 5 indicating a balance between lipophilicity and hydrophilicity crucial for optimal absorption. Third, hydrogen bond donors < 5 (NH or OH groups) to minimize membrane permeability. Fourth, hydrogen bond acceptors < 10 to avoid excessive membrane permeability. Fifth, molar refractivity reflecting molecule size and polarity ideally between 40-130 (Chen et al., 2020). Based on the results of the drug scan in Table 3, 17 test compounds were found to meet all drug scan parameters. This indicates that these compounds have the potential for effective use as oral drugs, capable of being well-absorbed through the digestive tract, efficiently distributed throughout the body, and able to reach drug targets with adequate concentrations. The drug scan results can be seen in Table 3.

Analysis and visualization of molecular docking results

Molecular docking process was conducted on 17 test compounds that had passed prediction for toxicity aspects, pharmacokinetic aspects, and drug scan. The results of molecular docking were analyzed based on ΔG and K_i values. ΔG measures the ligand's ability to bind to the receptor, where more negative values indicate stronger binding affinity (Mardianingrum et al., 2022). K_i represents the affinity of the compound and its decomposition, directly proportional to ΔG , which mean the more negative the ΔG value and the K_i value, indicating more effective inhibition of ligand activity on the protein (Mardianingrum et al., 2022). The results of molecular docking can be seen in Table 4.

Based on the results of molecular docking in Table 4, two compounds were selected that showed more negative ΔG and K_i values compared to clonazepam. These compounds are (+)-epicatechin with ΔG -7.55 kcal/mol and K_i 2.93 μM , and quercetin with ΔG -7.54 kcal/mol and K_i 2.97 μM . Both compounds are anticipated to have potential as promising candidates for anxiolytic drug materials targeting the $Er\alpha$.

Further visualization was performed as a graphical representation stage of the molecular docking results to analyze molecular interactions including the types of interactions that occur, binding distances, atoms in the ligand bound to the receptor, and amino acid residues involved in the interaction (Thahara et al., 2022). 2D visualization provides important insights into the interactions between ligands and amino acid residues, indicating the active site on the receptor (Thahara et al., 2022). The 2D visualization results can be seen in Figure 3 and Table 5.

Table 4. Results of molecular docking of 17 compounds from green tea against the 7UJM receptor

No	Compound Name	ΔG (kcal/mol)	K_i (μM)
(+)	Clonazepam	-7.20	5.24
1.	Methyl anthranilate	-6.05	166.34
2.	N,N-Dibutylacetamide	-4.51	493.02
3.	(+)-Catechin	-7.00	7.42
4.	(+)-Epicatechin	-7.55	2.93
5.	(-)-Catechin	-7.42	3.64
6.	(-)-Epiafzelechin	-7.18	5.50
7.	Ampelopsin	-6.83	9.93
8.	Cyanidin	-7.44	3.51
9.	Delphinidin chloride	-7.42	3.64
10.	Dihydroquercetin	-7.12	6.09
11.	Pollenitin	-6.94	8.18
12.	Quercetin	-7.54	2.97

13.	Tricetinidin	-7.47	3.32
14.	3-O-Caffeoylquinic acid	-6.23	26.93
15.	Peonidin chloride	-7.34	4.14
16.	Malvidin	-6.73	11.65
17.	Luteoliflavan	-7.52	3.07

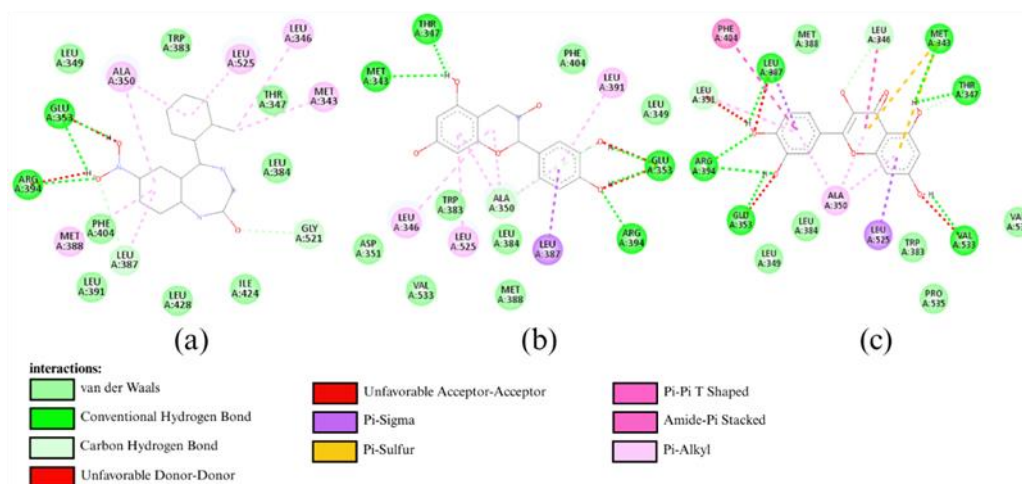


Figure 3. 2D visualization (a) clonazepam, (b) epicatechin, (c) quercetin

Table 5. Ligand interactions with 7UJM receptor amino acid residues

Compound Name	Hydrogen Bond	Hydrogen distance (Å)	bond	Hydrophobic Bond
Clonazepam	Glu353	1.79		Leu387, Gly521, Leu346, Leu525,
	Arg394	2.20		Ala350, Met343, Met388
(+)-Epicatechin	Met343	2.83		Leu346, Ala350, Leu387, Leu391,
	Thr347	2.05		Leu525
	Glu353	1.74		
	Arg394	1.97		
Quercetin	Met343	2.75		Met343, Leu346, Ala350, Leu391,
	Thr347	2.05		Phe404, Leu525
	Glu353	1.71		
	Leu387	2.00		
	Arg394	2.45		
	Val533	2.98		

Parameters considered in the visualization stage include amino acid residue contacts, particularly the presence of hydrogen bonds that indicating interaction stability. The more hydrogen bonds present, the better and more stable the interaction between the compound ligand and amino acid residues on the receptor (Mardianingrum et al., 2022). Hydrogen bonds are considered stable and strong when they are within a distance of < 2.7 Å, because distances exceeding 2.7 Å are deemed weak and easily disrupted (Thahara et al., 2022). Therefore, based on the visualization results, quercetin is predicted to have more hydrogen bonds at qualifying distances and to exhibit compatibility with

amino acid residues comparable to natural ligands and clonazepam.

In this study, the Era is known to be a ligand-binding domain with an active site on helix 12 (Lv et al., 2022). Compounds are said to have agonistic properties if they interact through hydrogen bonding with His524 that causing helix 12 open and bind with coactivators (Mardianingrum et al., 2022). (+)-epicatechin and quercetin are predicted to be antagonistic to the Era because they do not form hydrogen bonds with His524.

Molecular dynamic analysis and simulation

Molecular Dynamics (MD) simulation is a method that integrates techniques from physics, mathematics, and chemistry to study protein movement processes by tracking protein conformations over time (Lv et al., 2022). The RMSD graph in Figure 4 (a) shows conformational changes of three protein complexes over 100 ns (100,000 ps) for clonazepam, (+)-epicatechin and quercetin. Based on analysis of the graph, quercetin that represented by the green trendline, appears stable with RMSD around 3-3.5 Å and low fluctuations starting at

80 ns (80,000 ps) until the end of the simulation which indicating attainment of dynamic equilibrium in the protein complex. Compared to clonazepam and (+)-epicatechin which exhibit unstable fluctuation movements, quercetin is predicted to have better interaction potential with the protein molecule and selected as the top candidate compound. Meanwhile average, minimum, and maximum RMSD values during the 100 ns (100,000 ps) MD simulation can be observed in Table 6.

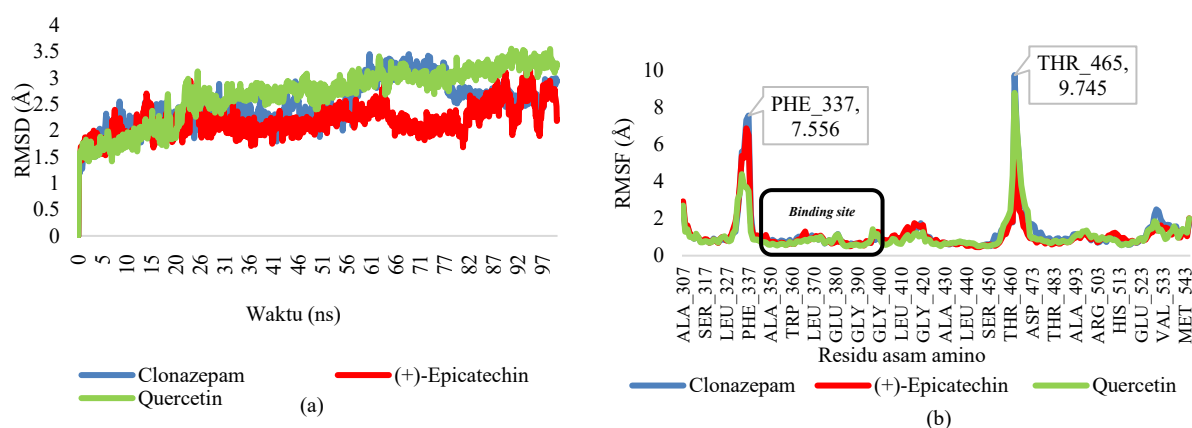


Figure 4. (a) RMSD graph, (b) RMSF graph

Table 6. Table of RMSD values during MD simulation

Complex	RMSD (Å)		
	Average	Minimum	Maximum
Clonazepam	2.48	1.13	3.45
(+)-Epicatechin	2.19	1.30	3.29
Quercetin	2.69	1.14	3.56

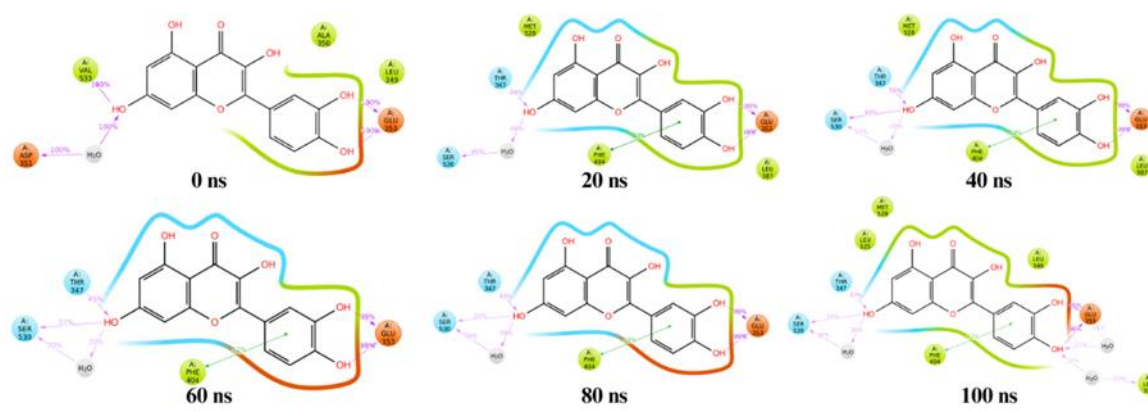


Figure 5. Conformational changes of quercetin compounds during MD simulations

Overall, the fluctuation movements exhibited by the test compounds and reference drugs based on the RMSF graph in Figure 4 (b) appear nearly identical. Residues Thr465 and Phe337, which showed the highest fluctuations, are predicted not to be active sites of the Er α due to their significant positional changes during the MD simulation. Quercetin exhibits the lowest fluctuation at residue Glu353 with an RMSF value of 0.54 Å and at amino acid residue Arg394 with an RMSF value of 0.65 Å, which are binding sites of the 7UJM receptor. The higher stability of these two residues indicates that quercetin interacts more stably and strongly with the Er α compared to clonazepam and (+)-epicatechin.

From Figure 5, it can be observed that the conformational changes in quercetin during the MD simulation are accompanied by alterations in its contacts with amino acid residues. The conformation at 100 ns shows the best stability, as it exhibits similarity with the amino acids from the molecular docking results. The presence of more identical amino acids before and after the MD simulation indicates that the compound is stable and resistant to thermodynamic changes. The amino acid residues with the highest similarity are Glu353, Thr347, Leu387, and Phe404.

Quercetin is an abundant flavonoid in nature, found in various plants, fruits, and vegetables such as onions, cabbage, tea, apples, nuts, and berries (Hasan et al., 2022). Quercetin is also known as 3,3',4',5,7-pentahydroxyflavone, characterized chemically as an

aglycone or glycoside bound to sugars like glucose, rhamnose, or rutinose (Hasan et al., 2022).

The biosynthesis of quercetin begins with the conversion of 4-coumaroyl-CoA, which is condensed by Chalcone Synthase (CHS) with three molecules of malonyl-CoA to produce naringenin (Hasan et al., 2022). The closure of the heterocyclic C ring is catalyzed by Chalcone Isomerase (CHI), resulting in naringenin. Then, with the assistance of Naringenin 3-Dioxygenase (N3DOX), naringenin produces dihydrokaempferol, which is then converted into quercetin through the action of Flavonol Synthase 1 (FLS1). Dihydrokaempferol also serves as a substrate for Flavonoid 3'-Hydroxylase (F3'H), producing dihydroquercetin, which is ultimately converted into quercetin by Flavonol Synthase 1 (FLS1) (Marín et al., 2018).

The MMGBSA calculations indicated that the Clonazepam and Quercetin complexes had nearly identical total binding free energy (ΔG_{TOTAL}) values, at -29.2558 kcal/mol and -29.1441 kcal/mol, respectively. Despite significant differences in electrostatic energy (EEL) and solvation contributions (EGB), where Clonazepam had a positive EEL and negative EGB, while Quercetin showed the opposite, the substantial contribution from Van der Waals (VdW) interactions dominated, bringing the total stability of both complexes closer. This indicated that the VdW energy component had the most significant impact on the system (Mardianingrum et al., 2022).

Table 7. Calculation results of bond energy method of molecular mechanics-generalized born surface area (MM-GBSA)

Energy Component (kcal/mol)	Clonazepam	Quercetin
Van der Waals Interaction (VdW)	-37.7244	-36.5924
Electrostatic Energy (EEL)	106.1903	-131.2730
Electrostatic Contribution to Solvation Free Energy (E _{GB})	-93.6150	142.5944
Non-Polar Contribtio to Solvation Free Energy (E _{SURF})	-4.1067	-3.8731
ΔG_{gas} (VdW + EEL)	68.4659	-167.8654
ΔG_{solv} (E _{GB} + E _{SURF})	-97.7217	138.7213
ΔG_{TOTAL} (VdW + EEL + E _{GB} + E _{SURF})	-29.2558	-29.1441

CONCLUSION

This study identified quercetin as a promising anxiolytic drug material through the inhibition of *Era* using *in silico* studies. Screening results revealed that quercetin is non-carcinogenic, non-hepatotoxic, easily absorbed, evenly distributed, non-interfering with CYP2D6 enzyme metabolism, and potentially effective as an oral drug. Molecular docking analysis showed that quercetin has a ΔG value of -7.54 kcal/mol and a K_i of 2.97 μM , which are better than the reference drug with a ΔG value of -7.20 kcal/mol and K_i of 5.24 μM . Quercetin also demonstrated more stable interactions with the $ER\alpha$ binding site, indicated by Glu353 and Arg394 amino acid in RMSD and RMSF analysis during molecular dynamic simulations.

This study is limited by its *in silico* nature, which requires further validation through *in vivo* experiments. Future studies will focus on confirming quercetin's anxiolytic effects in animal models and exploring its formulation into a suitable delivery system. The findings of this study support the traditional use of green tea for mental health and may pave the way for its development into a standardized phytopharmaceutical.

ACKNOWLEDGMENT

We thank Mrs. Arini Aprilliani and Mr. Muhammad Zaky, who helped and guided the research implementation.

AUTHOR CONTRIBUTIONS

Conceptualization: H.N.A., R.M., S.; Methodology: H.N.A., R.M., S.; Software, (N/A); Validation, H.N.A., R.M., S.; Formal Analysis, H.N.A.; Investigation, H.N.A.; Resources, R.M., S.; Data Curation: H.N.A.; Writing - Original Draft, H.N.A.; Writing - Review and Editing, H.N.A., R.M., S.; Visualization, H.N.A.; Supervision, R.M., S.; Project administration, R.M., S.; Funding Acquisition, No funding was received for this research.

CONFLICT OF INTEREST

The authors declare that they have no conflicts of interest.

REFERENCES

Almudhi, A. & Gabr, S. A. (2022). Green tea consumption and the management of adrenal stress hormones in adolescents who stutter. *Biomedical Reports*; 16; 32. doi: 10.3892/BR.2022.1515.

Al-Qahtani, A., Ajarem, J., Okla, M. K., Rubnawaz, S., Alamri, S. A., Al-Qahtani, W. H., Al-Himaidi, A. R., Elgawad, H. A., Akhtar, N., Maodaa, S. N. & Abdel-Maksoud, M. A. (2022). Protective Effects of Green Tea Supplementation against Lead-Induced Neurotoxicity in Mice. *Molecules*; 27; 993. doi: 10.3390/molecules27030993.

Atmawati, E. (2022). *Masalah Kesehatan Mental pada Penyintas Covid-19*. Kementerian Kesehatan.

Borrow, A. P. & Handa, R. J. (2017). Estrogen Receptors Modulation of Anxiety-Like Behavior. In *Vitamins and Hormones*; 103, 27–52. doi: 10.1016/bs.vh.2016.08.004.

Chen, X., Li, H., Tian, L., Li, Q., Luo, J. & Zhang, Y. (2020). Analysis of the Physicochemical Properties of Acaricides Based on Lipinski's Rule of Five. *Journal of Computational Biology*; 27; 1397–1406. doi: 10.1089/cmb.2019.0323.

Gopinath, P. & Kathiravan, M. K. (2021). Docking studies and molecular dynamics simulation of triazole benzene sulfonamide derivatives with human carbonic anhydrase IX inhibition activity. *RSC Advances*; 11; 38079–38093. doi: 10.1039/d1ra07377j.

Hasan, A. A., Tatarskiy, V. & Kalinina, E. (2022). Synthetic Pathways and the Therapeutic Potential of Quercetin and Curcumin. In *International Journal of Molecular Sciences*; 23; 22. doi: org/10.3390/ijms232214413.

Hosfield, D. J., Weber, S., Li, N. S., Sauvage, M., Joiner, C. F., Hancock, G. R., Sullivan, E. A., Ndukwe, E., Han, R., Cush, S., Lainé, M., Mader, S., Greene, G. L. & Fanning, S. W. (2022). Stereospecific Lasofoxifene Derivatives Reveal the Interplay between Estrogen Receptor Alpha Stability and Antagonistic Activity in ESR1 Mutant Breast Cancer Cells. *ELife*; 11; 72512. doi: 10.7554/eLife.72512.

Kenda, M., Zore, T. & Sollner Dolenc, M. (2022). Effects of central nervous system drugs on androgen, estrogen α , glucocorticoid, and thyroid receptors. *Chemico-Biological Interactions*; 25; 363. doi: 10.1016/j.cbi.2022.110030.

Lv, S., Dai, W., Zheng, Y., Dong, P., Yu, Y., Zhao, Y., Sun, S., Bi, D., Liu, C., Han, F., Wu, J., Zhao, T., Ma, Y., Zheng, F. & Sun, P. (2022). Anxiolytic effect of YangshenDingzhi granules: Integrated network pharmacology and hippocampal metabolomics. *Frontiers in Pharmacology*; 13; 966218. doi: 10.3389/fphar.2022.966218.

- Mardianingrum, R., Endah, S. R. N., Suhardiana, E., Ruswanto, R. & Siswandono, S. (2021). Docking and molecular dynamic study of isoniazid derivatives as anti-tuberculosis drug candidate. *Chemical Data Collections*; 32; 100647. doi: 10.1016/j.cdc.2021.100647.
- Mardianingrum, R., Lestary, M. S. R., Aji, N. & Ruswanto, R. (2023). Potential of Prenylated Flavonoid Derivatives from Jackfruit Roots (*Artocarpus heterophyllus* Lam.) as Liver Anticancer Candidates: In Silico Study. *Jurnal Kimia Sains Dan Aplikasi*; 26; 57–63. doi: 10.14710/jksa.26.2.57-63.
- Mardianingrum, R., Susilawati, D. & Ruswanto, R. (2022). Computational Study of 1-(3-Nitrobenzoyloxymethyl)-5-Fluorouracil Derivatives as Colorectal Cancer Agents. *Jurnal Kimia Valensi*; 8; 211–220. doi: 10.15408/jkv.v8i2.25489.
- Mardianingrum, R., Yusuf, M., Hariono, M., Mohd Gazzali, A. & Muchtaridi, M. (2022). α -Mangostin and its derivatives against estrogen receptor alpha. *Journal of Biomolecular Structure and Dynamics*; 40; 2621–2634. doi: 10.1080/07391102.2020.1841031.
- Marín, L., Gutiérrez-del-Río, I., Entrialgo-Cadierno, R., Claudio, Villar, J. & Lombó, F. (2018). De novo biosynthesis of myricetin, kaempferol and quercetin in *Streptomyces albus* and *Streptomyces coelicolor*. *PLoS ONE*; 13; e0207278. doi: 10.1371/journal.pone.0207278.
- Pires, D. E. V., Blundell, T. L. & Ascher, D. B. (2015). pkCSM: Predicting small-molecule pharmacokinetic and toxicity properties using graph-based signatures. *Journal of Medicinal Chemistry*; 58; 4066–4072. doi: 10.1021/acs.jmedchem.5b00104.
- Ruswanto, R., Mardianingrum, R., Lestari, T., Nofianti, T., Tuslinah, L. & Nurmali, D. (2018). In silico study of the active compounds in bitter melon (*Momordica charantia* L.) as antidiabetic medication. *Pharmaciana*; 8; 194. doi: 10.12928/pharmaciana.v8i2.8993.
- Thahara, C. A., Rizarullah*, R., Atika, R. A. & Wahab, A. (2022). Potensi Pendekatan in Silico Sebagai Penghambat Aktivitas Protein Protease Utama SARS-CoV-2 dari Tiga Senyawa Tanaman Obat Jahe Merah. *Jurnal IPA & Pembelajaran IPA*; 6; 207–218. doi: 10.24815/jipi.v6i3.24914.
- Wadapurkar, R. M., Shilpa, M. D., Katti, A. K. S. & Sulochana, M. B. (2018). In silico drug design for *Staphylococcus aureus* and development of host-pathogen interaction network. *Informatics in Medicine Unlocked*; 10; 58–70. doi: 10.1016/j.imu.2017.11.002.
- World Health Organization. *Mental Disorders*. June 8, 2022. <https://www.who.int/news-room/fact-sheets/detail/mental-disorder>. Accessed: January 22, 2024.
- World Health Organization. *Anxiety disorders*. Published September 27, 2023. <https://www.who.int/news-room/fact-sheets/detail/anxiety-disorder>. Accessed: January 22, 2024.



Influence of Hesperetin Concentration in Poloxamer P84 and TPGS Mixed Micelles on Physical Characteristics and Cytotoxicity in T47D Cell Line

Nanda Intan Aulia¹, Muh. Agus Syamsur Rijal^{2*}, Helmy Yusuf²

¹Magister of Pharmaceutical Sciences, Faculty of Pharmacy, Universitas Airlangga, Surabaya, Indonesia

²Department of Pharmaceutical Sciences, Faculty of Pharmacy, Universitas Airlangga, Surabaya, Indonesia

*Corresponding author: muh-a-s-r@ff.unair.ac.id

Orcid ID: 0000-0001-6881-1684

Submitted: 17 January 2025

Revised: 10 February 2025

Accepted : 5 March 2025

Abstract

Background: Hesperetin is a natural compound that has several properties including anticancer, but has limitation on low solubility in water. In this case, the development of a hesperetin delivery system using the micellar system is carried out. **Objective:** The current study aims to determine the effect of drug concentration on the physical characteristics and cytotoxicity of the mixed micelle. **Methods:** In this study, mixed micelles were formulated with D- α -tocopheryl polyethylene glycol 1000 succinate (TPGS) and poloxamer P84 as polymers through the thin film method, with hesperetin loaded at four different concentrations, i.e., 5 mg (F1), 10 mg (F2), 20 mg (F3), and 40 mg (F4). The mixed micelles were formulated using thin film hydration method. The evaluation of micelle's physical characteristics was the measurement of particle size, Critical Micelle Concentration (CMC) value, drug loading, and drug entrapment efficiency. The evaluation of cytotoxicity used the T47D cell line and Micro Tetrazolium (MTT) method. **Results:** The CMC value of the mixed micelle was 0.0029% w/v, which was lower than the CMC of TPGS and poloxamer P84 only. The particle size of the micelles produced was between 17.07–20.37 nm. Among the various formulations, F3 showed relatively small particle size and has homogeneous particle size, high drug loading and encapsulation efficiency, and low IC₅₀. Based on the study, particle size of F3 was 17.93 ± 0.32 nm with polydispersity index (PDI) of 0.256 ± 0.034 . The drug loading percentage of F3 was $4.0092 \pm 0.0048\%$ with an encapsulation efficiency of $94.5492 \pm 0.0013\%$. Based on cytotoxicity test using MTT method, F3 has low IC₅₀, there was 4.036 ppm. **Conclusion:** Hesperetin-loaded mixed micelles offer the potential as an anticancer drug that provides improvement of hesperetin efficacy. The result showed that F3 was the most potent formulation to be an anticancer based on physical characteristics and cytotoxicity test.

Keywords: Hesperetin, mixed micelles, physical characteristics, cytotoxicity

How to cite this article:

Aulia, N. I., Rijal, M. A. S. & Yusuf, H. (2025). Influence of Hesperetin Concentration in Poloxamer P84 and TPGS Mixed Micelles on Physical Characteristics and Cytotoxicity in T47D Cell Line. *Jurnal Farmasi dan Ilmu Kefarmasian Indonesia*, 12(1), 106-115. <http://doi.org/10.20473/jfiki.v12i12025. 106-115>

INTRODUCTION

Cancer is one of the diseases characterized by abnormal, uncontrolled, fast, and continuous cell growth caused by mutation of genes that control proliferation (Kumbhar et al., 2017). Cancer cells can cause damage to surrounding tissues and can metastasize, which spreads to other tissues. Cancer cells grow from the body tissue cells that grow abnormally and can be malignant (Arafah & Notobroto, 2017). Chemotherapy is one of the most commonly used cancer treatments (Kumbhar et al., 2017). Chemotherapy is a cancer treatment using a chemical compound but has adverse side effects, besides killing cancer cells, it can also kill normal cells in the body especially those that have rapid cell division (Setiawan, 2015). To overcome this, an anticancer was developed with a drug delivery system to deliver drugs to cancer cells without affecting normal cells. Hesperetin is one of the chemical compounds that can be used as an anticancer. Hesperetin is an aglycone of hesperidin which is included in flavonoid compounds (Stanisic, 2018). Based on research by Choi (2007), hesperetin can inhibit cell proliferation, induce cell rest in the G1 phase, and induce cell apoptosis (Choi, 2007). Hesperetin is classified under BCS class 2 due to it is high permeability but low water solubility, which leads to reduced bioavailability in the body when taken orally (Shete et al., 2015). A micelle system can be utilized to enhance solubility (Choi, 2007).

Micelles are self-assembling microstructures of surfactants in water and generally have small particle sizes of < 50 nm in diameter. Micelles can protect drugs that have low water solubility or hydrophobic drugs and can be carriers to deliver drugs to target cells (Lu et al., 2019). Micelles have a relatively small particle size, namely nanoparticle size, this causes the micelles system to avoid detection and destruction by the endoplasmic reticulum so that can have longer circulation time in systemic. However, micelles should not be too small as they can be easily filtered by the kidneys and excreted in the urine (Saxena & Hussain, 2013). Generally, the micelle structure of block copolymers is spherical and block copolymers have larger hydrophilic blocks than hydrophobic blocks with the core encapsulating the active compounds (Croy & Known, 2006; Lombardo et al., 2015). The spherical shape has low free energy so it can reduce the hydrophobic block to interact with the aqueous environment. This can increase the stability of the micelles system in water (Croy & Known, 2006; Lombardo et al., 2015).

Poloxamer is a polymer that is commonly used in micellar systems. Poloxamer is a block copolymer composed of ethylene oxide (EO) and propylene oxide (PO). Generally, the structure is $EO_x - PO_y - EO_x$. Poloxamer is a self-assembly system with PO as the hydrophobic core and EO as the hydrophilic tail. The drugs will be encapsulated within the hydrophobic core, while the hydrophilic tail will help maintain the stability of micelles (Gao et al., 2008; Saxena & Hussain, 2012). One of the poloxamers that can be used is the poloxamer P84. Poloxamer can be used as a carrier of cancer drugs but it has low encapsulation capacity and high CMC value (Zarrintaj et al., 2020). To improve the low encapsulation capacity and high CMC value, poloxamer P84 will be combined with other micelle-forming compounds, which can be D- α -tocopheryl polyethylene glycol 1000 succinate (TPGS) (Zhang et al., 2014). TPGS is a natural compound that is a derivative of vitamin C (α -tocopheryl) and polyethylene glycol 1000 succinate which can improve solubility and absorption. It can be a carrier form of a lipid-based drug delivery system. The combination of poloxamer and TPGS will produce a mixed micelle system (Gao et al., 2008; Saxena & Hussain, 2012). TPGS and poloxamer will interact at the hydrophobic block by hydrogen bonding. The aromatic ring on hesperetin will interact with the hydrocarbon group of poloxamer P84 and the aromatic ring of TPGS. The phenolic hydroxyl of hesperetin will make hydrogen bonds with TPGS and poloxamer P84 (Liu et al., 2019). TPGS and poloxamer P84 mixed micelles have low CMC value, small particle size, and high encapsulation efficiency. It can be used to entrap anticancer drugs that have low water solubility. The drug release will be maintained so that the bioavailability will be maintained for some time. Mixed micelles of poloxamer P84 and TPGS have a synergistic effect to inhibit p-glycoprotein (P-gp) thus increasing the effectiveness of hesperetin and can deliver high concentrations of the drug to cancer cells (Saxena & Hussain, 2012).

Based on research by Arifah (2019), the mixed micelles of TPGS and poloxamer P84 in the ratio 1:4 had good stability and physical characteristics but the formulation had a low concentration of hesperetin about 5 mg (Arifah, 2019). Further research is needed to increase the concentration of hesperetin by considering its stability and physical characteristics. Changes in the level of drug encapsulated in mixed micelles can change the physical characteristics but have the same CMC value (Mandal et al., 2017). An increase in the loading capacity can increase the levels of hesperetin that can be

encapsulated in the micelle system. An increase in the hesperetin can enhance the interaction of drugs with micelle-forming polymers and can improve the kinetic stability of micelles (Zhou et al., 2016).

The method of micelle preparation is based on the physicochemical properties of micelle-forming polymer which have an effect on the physicochemical properties of micelles. In addition, the amount of polymer can also influence to physical properties of micelles such as particle size, homogeneity, drug loading capacity, encapsulation efficiency, and micelle stability, so it is necessary to optimize the micelle preparation with good physicochemical properties. Generally, micelle systems are fabricated using physical methods such as solvent evaporation, dialysis, direct dissolution, and thin film hydration. Thin film hydration is a commonly used method because it is easy, simple, and produces small and uniform particle sizes (Ai et al., 2014).

One evaluation of the effectiveness of the micelle system is cytotoxicity testing. The size, charge, shape, and structure of micelles can affect the interaction of micelles and the biological environment (Adjei & Sharma, 2014). The cytotoxicity test is a method to determine the potential of a compound that can induce cell damage (Damiani et al., 2009). Micro tetrazolium (MTT) is a commonly used method in cytotoxicity testing (Cancer Chemoprevention Research Center, 2012). The micro tetrazolium assay has a colorimetry principle, namely tetrazolium salt (3 - (4,5 - dimethylthiazole - 2 - il) - 2,5 - diphenyltetrazolium bromide) which is yellow salt will dissolve and turn into purple formazan which cannot be dissolved by membrane reductase and cell plasma. In this study, an ELISA reader was used (Cancer Chemoprevention Research Center, 2012; Nga et al., 2020; Raveendran, 2012). IC_{50} is a cytotoxicity outcome parameter. A low IC_{50} value correlates with high cytotoxicity (Damiani et al., 2009). According to in vitro studies, hesperetin is believed to have a higher IC_{50} value compared to hesperetin loaded in mixed micelles. This is because mixed micelles enhance the delivery of hesperetin to cancer cells, leading to increased accumulation within the cells and correlates with increased efficacy as an anticancer (Zarrintaj et al., 2020). However, increasing the content of the drug loaded in the micelle system cannot always increase its cytotoxicity effect because micelles have a maximum capacity to load drugs (Callari et al., 2017). This research aims to determine the

effect of increasing the level of hesperetin loaded in mixed micelles of poloxamer P84 and TPGS on the physical characteristics and effectiveness of mixed micelles as carriers by cytotoxicity test.

MATERIALS AND METHODS

Materials

Hesperetin was purchased from Xi'an Xiaocao Botanical Development, China. D- α -tocopheryl polyethylene glycol 1000 succinate (TPGS) was purchased from Sigma Aldrich, Singapore. Poloxamer P84 was purchased from BASF, Germany. Potassium Iodide (KI) was purchased from Merck, Germany. Iodine (I_2) was purchased from Merck, Germany. Ethanol 96% was purchased from Merck, Germany. 3-(4,5-Dimethylthiazole-2-yl)-2,5-diphenyltetrazolium bromide was purchased from Biobasic Inc. Dimethyl Sulfoxide (DMSO) and Phosphate Buffer Saline (PBS) was purchased from Invitrogen, USA. SDS 10% in 0,01 N HCl, Culture Medium (CM) (1% penicillin - streptomycin, 10% FBS (*Fetal Bovine Serum*), Trypsin-EDTA, and ad 100% *Gibco Roswell Park Memorial Institute* (RPMI) 1640 Medium) was purchased from Gibco, USA. Sodium Bicarbonate was purchased from Nacalai, Tesque.

Method

Micelle preparation by thin film hydration method

Micelle preparation with this method was done by dissolving the polymers and active compounds into an organic solvent, such as 96% ethanol, then followed by the solvent's evaporation and reconstitution to make the formation of the micelles (Bodratti & Alexandridis, 2018). Hesperetin, TPGS, and poloxamer P84 were dissolved in 5.0 mL 96% ethanol in a round bottom flask and mixed. Then 96% ethanol was removed using rotary vacuum evaporation (Buchi R-100) at 50°C for 1 hour to form a drug-containing thin film and further dried in a vacuum desiccator for 24 hours to remove the residue. The 10.0 mL distilled water was added to the drug-containing thin film and the solution was mixed by rotary evaporation at 50°C for 30 min without vacuum and allowed to reach room temperature. The micelle solution was prepared by passing it through a 0.2 μ m filter to distribute the micelles structures and remove free hesperetin. The micelles form flowed through the membrane filter. Micelles were prepared in four different formulas as in Table 1:

Table 1. Mixed micelles of TPGS and poloxamer P84 with hesperetin loading at various concentrations

Materials	Function	Amount (mg)			
		F1	F2	F3	F4
Hesperetin	Active compound	5.0	10.0	20.0	40.0
TPGS (2,5 mM)	Polymer	37.825	37.825	37.825	37.825
Poloxamer P84 (10 mM)	Polymer	420.0	420.0	420.0	420.0
Distilled water	Hydration media	10.0 ml	10.0 ml	10.0 ml	10.0 ml

Particle size and polydispersity index (PDI)

Dynamic Light Scattering (Delsa™ Nano Beckman Coulter) was used to measure the particle size and polydispersity index. Each sample was taken as much as 2.5 ml. The measurements were repeated three times. The reported experimental result of each sample was expressed as a mean size \pm SD and PDI \pm SD.

Critical micelles concentration

CMC value test used iodine as the hydrophobic probe. Iodine storage was carried out in a dark place and protected from direct sunlight because iodine can decompose if exposed to light (Fallah et al., 2020). First, the standard solution of KI/I₂ was made from 0.5 g of I₂ and 1 g of KI in 50.0 ml of distilled water. The polymer solution was made with a concentration of 0.0001% w/v - 0.0055 % w/v (1 – 55 ppm). Then standard KI / I₂ was added as much as 25 μ L. Incubation was carried out for 12 hours with room temperature conditions and a dark environment before measurement. Before absorbance measurement was carried out, the maximum wavelength of absorbance was determined using a UV-Vis Spectrophotometer (Double Beam Spectrophotometer HITACHI UH5300). The CMC value corresponds to the concentration that undergoes a sharp increase in the observed absorbance (Gao et al., 2008).

Drug loading and encapsulation efficiency

UV-Vis spectrophotometry (Double Beam Spectrophotometer HITACHI UH5300) was used to measure the percent of drug loading and encapsulation efficiency at a measurement wavelength of 288.5 nm. A linear regression was established before conducting the formula analysis, which then served as the basis for determining the hesperetin content loaded in the micelle system. First, each sample was diluted with 96% ethanol to disrupt the micelle system, allowing the measurement of hesperetin content within the micelles. The drug loading and encapsulation efficiency percentage were determined using the following equations.

$$\% \text{ Drug Loading} = \frac{\text{Weigh of hesperetin in micelle}}{\text{Weigh of the feeding copolymer and hesperetin}} \times 100\%$$

$$\% \text{ Encapsulation Efficiency} = \frac{\text{Weigh of hesperetin in micelle}}{\text{Weigh of the feeding hesperetin}} \times 100\%$$

In vitro cytotoxicity study

In vitro cytotoxicity of hesperetin-loaded mixed micelles was evaluated using the MTT assay. Briefly, T47D cells were seeded to 96-well culture plates at a density of 5×10^3 cells/well with 100 μ L/well each formulation, then incubated for 24 h at 37°C under 5% CO₂. The medium was replaced with fresh medium, and 100 μ L of samples containing free hesperetin, blank micelles, and hesperetin-loaded micelles at different concentrations (20 ppm, 30 ppm, 40 ppm, 60 ppm, 100 ppm, 150 ppm, and 200 ppm) were added. The cells were then incubated for an additional 24 h at 37°C under 5% CO₂. After the incubation, the media was removed and the cells were washed twice with 100 μ L PBS. Then, 100 μ L MTT solution was added, and the cells were incubated for 4 h at 37°C under 5% CO₂. To stop reaction, 10% SDS in 0,01 N HCl was added to each well, followed by incubation for 24 hours in a dark. Cell viability was assessed by measuring absorbance at 570 nm using an ELISA reader (Thermo Fisher), and concentration at which 50% cell viability is inhibited (IC₅₀) was calculated using the following equations then the IC₅₀ value was obtained using Probit analysis.

$$\% \text{ Viability cells} = \frac{\text{Absorbance of the formulation} - \text{Absorbance of control medium}}{\text{Absorbance of control cells} - \text{Absorbance of control medium}} \times 100\%$$

RESULTS AND DISCUSSION

The mixed micelles result in a liquid formulation with clear organoleptic characteristics, being transparent, odorless, colorless, and tasteless. The occurrence of turbidity during storage indicates instability of the formulation, which is observed in F4.

Particle size and polydispersity index (PDI)

The particle size of micelles must be controlled because can affect the solubility. It can be determined by dynamic light scattering (DLS), also referred to as photon correlation spectroscopy or quasi-elastic light scattering. DLS can detect the Brownian motion of the particles which can be correlated with particle size. Brownian motion is based on random particles scattering due to collisions between molecules so that translation occurs and can be detected by DLS. Larger molecules have a slower Brownian motion. The result of particle size and PDI value can be seen in Table 2.

Table 2. Particle size and PDI value of micelles

Formulations	Particle Size (nm)	PDI
F1	17.07 ± 0.47	0.262 ± 0.034
F2	20.37 ± 0.25	0.266 ± 0.011
F3	17.93 ± 0.32	0.256 ± 0.034
F4	18.20 ± 0.36	0.170 ± 0.019

Based on the study, all the formulations have small particles and uniform size. The uniform particle size can be described by the polydispersity index (PDI), in which the uniform particle has a range between 0.170 – 0.266. PDI values smaller than 0.7 indicate the particles has a narrow size distribution. In drug delivery system applications, a PDI of 0.3 and below indicates a homogenous population of the particles (Danaei et al., 2018). F2 has the biggest particle size, it is 20.37 ± 0.25 nm and the smallest particle size was F1, which is 17.07 ± 0.47 nm. Based on analytical studies of one way ANOVA, it can be known increasing hesperetin concentration has an impact on particle size of all formulations ($P < 0.005$).

In this study, the decreasing particle size of F3 caused increasing the interaction of the drugs and micelle-forming compounds. It has been reported that increasing the hydrophobic drug into micelles enhances the hydrophobic forces during micellization, strengthening in the interaction between the drug and micelle-forming compounds while also improving

kinetic stability (Zhou et al., 2016). On the other hand, F4 precipitation caused by the level of hesperetin loaded in micelle has exceeded the capacity. Based on research by Liu et al. (2006), if the drug concentration is increased to a level that surpasses the solubilization capacity of the micelles, it can affect to precipitation (Liu et al., 2006).

Critical micelle concentration

Based on the study the maximum wavelength obtained is 351.5 nm. The results of the I₂ absorption measurement can be seen in Table 3.

Based on the results, a log curve of polymer concentration and I₂ absorption is then carried out as shown in Figure 1. A sharp spike in absorption was obtained in polymer solutions at 30.041 ppm, which is 0.378. Then calculations were carried out to obtain the intersection of the two regression equations before and after the absorbance with the substitution method so that the critical concentration of micelles was 28.99 µg/mL or equal to 0.0029% w/v.

Table 3. I₂ absorbance results at a maximum wavelength of 351.5 nm

Polymer concentration (ppm)	Log of polymer concentration (Log C)	Absorbance I ₂
1.001	0.000	0.261
5.007	0.700	0.298
7.510	0.876	0.323
10.014	1.001	0.325
15.020	1.177	0.339
20.027	1.302	0.337
25.034	1.398	0.327
30.041	1.478	0.378
35.048	1.545	0.343
40.054	1.603	0.358
45.061	1.654	0.372
50.068	1.700	0.384
55.075	1.741	0.397

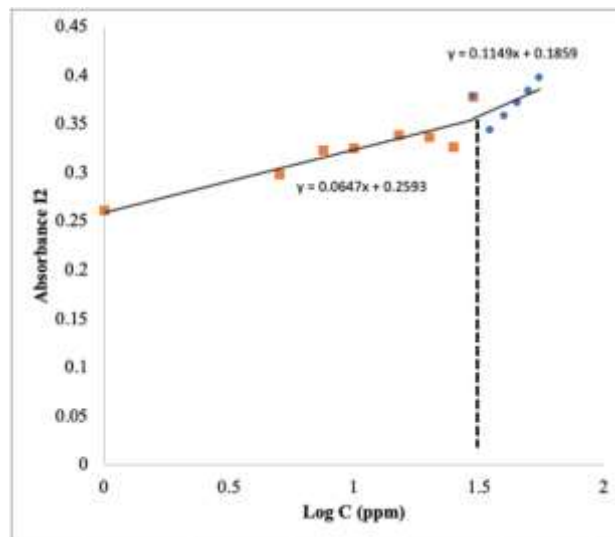


Figure 1. Curve of log concentration and absorbance I2

Table 4. Drug loading and encapsulation efficiency of mixed micelles (n=3)

Formulations	Drug Loading \pm SD (%)	Encapsulation Efficiency \pm SD (%)
F1	1.0094 \pm 0.0000	93.7111 \pm 0.0000
F2	2.2649 \pm 0.0081	97.4781 \pm 0.0035
F3	4.0092 \pm 0.0048	94.5492 \pm 0.0013
F4	5.0789 \pm 0.0035	62.5231 \pm 0.0004

The CMC value obtained is below the CMC value of its single polymer. Based on research by Bodratti and Alexandridis (2018), it is known that the CMC value of a single poloxamer P84 is 2.6% w/v and single TPGS value is 0.02% w/w (Zhang et al., 2012).

TPGS and poloxamer P84 mixed micelles can decrease the CMC value which can affect to increasing the hydrophobicity of the polymer and the interaction strength of the drug with the polymer to improve the thermodynamic and kinetics stability of micelles (Zhou, et al., 2016). A low CMC value indicates that a low concentration of polymer can make micelle form. When the surfactant concentration is below the CMC value, the micelle will dissociate to establish thermodynamic balance (Croy & Known, 2006). In this case, the advantage of micelles with low CMC values is that they can maintain their stability by still forming a micelle system when dilution occurs, so it can be concluded that the use of a combination of TPGS and poloxamer P84 has a synergistic effect so that its stability is better than its single polymer.

Drug loading and encapsulation efficiency

Observations of encapsulation efficiency were made to determine the amount of hesperetin that can be trapped in the micelle system. Based on the study, it is known that F2 has the highest encapsulation efficiency

and F4 has the lowest encapsulation efficiency, this is because the micellar system is no longer able to contain hesperetin in it. Entrapment efficiency data can be seen in Table 4. Based on the statistical analysis of one way ANOVA obtained, it is known that there is an effect of increased levels of hesperetin loaded in the micellar system on drug loading and encapsulation efficiency of all formulations ($P < 0.005$).

The drug loading increases but the encapsulation efficiency of F3 and F4 decreases; this is due to the presence of hesperetin compounds that cannot be loaded in the micelle system. According to the encapsulation efficiency data, the hydrophobic part of the micelle-forming polymer can no longer load hesperetin. As a result, any hesperetin that is not bound to the hydrophobic portion of the micelle-forming polymer will be removed during the filtration process.

Based on the study, F3 is the best formulation because has high drug loading despite a decrease in the encapsulation efficiency. The drug loading can affect the amount of drug present in the preparation so it will affect the dosage dose given. The higher the drug loaded in the micellar system, the smaller the dose given so that acceptability, effectiveness, and efficiency of using the preparation can be achieved.

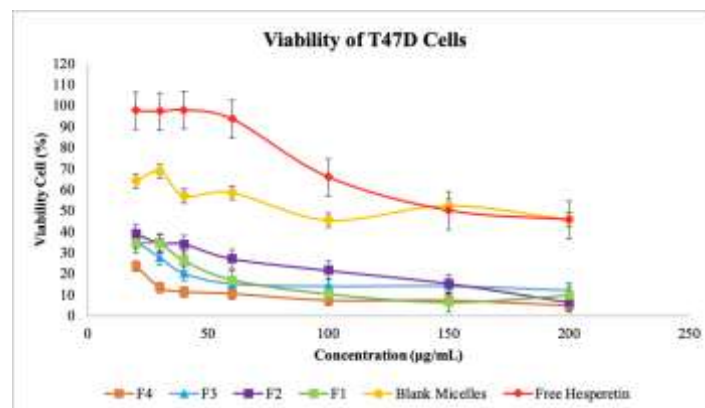


Figure 2. Graph of T47D cell viability in sample treatment (n=3)

Table 5. IC₅₀ value with Probit analysis

Formulations	IC ₅₀ (ppm)
Blank Micelles	126.161
Free Hesperetin	165.767
F1	10.621
F2	13.200
F3	4.036
F4	1.759

In vitro cytotoxicity

Data related to cell viability were obtained which were then graphed the results of observations of cell viability as shown in Figure 2.

From the graph, it can be seen that the four formulas have effectiveness against cell death which is indicated by a lower cell viability value when compared to the free micellar and hesperetin. From the results of cell viability data, calculations were then made on the IC₅₀ value of each formulation. Free hesperetin exhibits the highest levels of T47D cell viability due to its low solubility causing it to precipitate during in vitro evaluation based on organoleptic observation. As a result, it is unable to penetrate cancer cells, leading to reduced effectiveness. Blank micelles have lower levels of T47D cell viability than free hesperetin because poloxamer P84 and TPMS has synergistic effect in inhibiting P-glycoprotein thus can inhibit the cancer cells growth (Saxena & Hussain, 2012). To obtain the concentration value of the 50% resistance of the population, calculations were carried out using Probit analysis so that the prediction of the IC₅₀ value was obtained as in Table 5.

It is known that the four formulas have a lower IC₅₀ value when compared to the blank micelles and free hesperetin. The use of a combination of poloxamer P84 and TPMS as a combination micellar system has a

synergistic effect on the inhibition of p-glycoprotein (p-gp) to increase the permeation of hesperetin into cancer cells which correlates with an increase in its effectiveness. Free hesperetin has the highest IC₅₀ value due to the effect of p-gp on cancer cells which causes the ejection of hesperetin from the cells so that levels in cancer cells become small (Saxena & Hussain, 2012). Based on the cytotoxicity study, increasing the levels of hesperetin can decrease the IC₅₀ value because higher levels of hesperetin can be inside the cancer cell and caused the death of cancer cell. It is known that the formula that has the potential for further testing is F3 because it has a low IC₅₀ value. F4 is unsuitable for use because hesperetin precipitates in the micelle formulation. This occurs when the micelle system exceeds its loading capacity, preventing effective delivery of hesperetin to cancer cells (Fares et al., 2017).

CONCLUSIONS

The usage of poloxamer P84 and TPMS as combination micellar-forming polymers can reduce the CMC value, which will increase its effectiveness. The use of these two polymers has a synergistic effect so that it can produce a smaller CMC value when compared to the single polymer. Increased levels of hesperetin influence the physical characteristics of micelles, which

by increasing these levels can improve the physical properties of the micelle system. Based on this study, it is known that the most optimal formula is F3 with an amount of hesperetin about 20.0 mg because has a small particle size and is homogeneous which is characterized by a PDI value. F3 has high drug loading and encapsulation efficiency. In tests on cytotoxicity using T47D cells, the four formulas have lower IC₅₀ values when compared to blank micelles and free hesperetin. This is due to the increased ability of drug permeation into cancer cells and the inhibition of p-gp which causes accumulation in cancer cells so that it is more effective to kill cancer cells. Of the four formulas, F3 has an optimal effect on cytotoxicity testing with low IC₅₀ value.

ACKNOWLEDGMENTS

The authors wish to express their gratitude to the Faculty of Pharmacy, Universitas Airlangga for the research grant from Penelitian Unggulan 2022.

ETHICAL CONSIDERATIONS

Ethical approval was not necessary for this case report. The authors provided written informed consent for the publication of this case report. All identifying information was carefully omitted in accordance with patients' wishes.

AUTHOR CONTRIBUTIONS

Conceptualization, M.A.S.R., N.I.A., H.Y.; Methodology, M.A.S.R., N.I.A.; Software, M.A.S.R., N.I.A.; Validation, M.A.S.R., N.I.A.; Formal Analysis, M.A.S.R., N.I.A.; Investigation, M.A.S.R., N.I.A.; Resources, M.A.S.R., N.I.A.; Data Curation; M.A.S.R., N.I.A.; Writing - Original Draft, M.A.S.R., N.I.A., H.Y.; Writing - Review & Editing, M.A.S.R., N.I.A., H.Y.; Visualization, N.I.A.; Supervision, M.A.S.R.; Project Administration, M.A.S.R.; Funding Acquisition, M.A.S.R.

CONFLICT OF INTEREST

The authors declared no conflict of interest.

REFERENCES

- Adjei, I. M. & Sharma, B. (2014). Nanoparticles : Cellular Uptake and Cytotoxicity. *Nanomaterials, Advance in Experimental Medicine and Biology*; 811; 73-91. doi: 10.1007/978-94-017-8739-0_5.
- Ai, X., Niu, L. Z. H. & He, Z. (2014). Thin-film Hydration Preparation Method and Stability Test of DOX-Loaded Disulfide-Linked Polyethylene Glycol 5000-Lysine-Di-Tocopherol Succinate Nanomicelles. *Asian Journal of Pharmaceutical Sciences*; 9; 244–250. doi: org/10.1016/j.ajps.2014.06.006.
- Arafah, A. B. R. & Notobroto, H. B. (2017). Faktor Yang Berhubungan Dengan Perilaku Ibu Rumah Tangga Melakukan Pemeriksaan Payudara Sendiri (Sadari). *The Indonesian Journal of Public Health*; 12; 143-153. doi: org/10.20473/ijph.v12i2.2017.
- Arifah, I. F. (2019). Pengaruh Perbandingan D-A-Tocopheryl Polyethylene Glycol 1000 Succinate dan Poloksamer P84 terhadap Karakteristik Fisik dan Stabilitas Misel Kombinasi (Mixed Micelles). *Skripsi*. Fakultas Farmasi Universitas Airlangga. Surabaya.
- Bodratti, A. M. & Alexandridis, P. (2018). Formulation of Poloxamers for Drug Delivery. *Journal of Functional Biomaterials*; 9; 1-24. doi: 10.3390/jfb9010011.
- Bruer, J. D. (2020). Determining Particle Size of Polymeric Micelles in Thermo-thickening Aqueous Solutions. *MSU Graduate Thesis*; Missouri State University. Master of Science, Chemistry. United States.
- Callari, M., Souza, P. L. D., Rawal, A. & Stenzel, M. H. (2017). The Effect of Drug Loading on Micelle Properties: Solid-State NMR as a Tool to Gain Structural Insight. *Journal of Angewandte Chemie International Edition*; 56; 8441-8445. doi: 10.1002/anie.201701471.
- Cancer Chemoprevention Research Center. (2012). *Protokol Uji Sitotoksik Metode MTT*. Yogyakarta. Fakultas Farmasi Universitas Gajah Mada.
- Choi, E. J. (2007). Hesperetin Induced G1-Phase Cell Cycle Arrest in Human Breast Cancer MCF-7 Cells: Involvement of CDK4 and p21. *Nutrition and Cancer*; 59; 115–119. doi: 10.1080/01635580701419030.
- Croy, S. R and Kwon, G. S. (2006) Polymeric Micelles for Drug Delivery. *Journal of Current Pharmaceutical Design*; 12; 4669–4684. doi: 10.2174/138161206779026245.
- Damiani, E., Solorio, J. A., Doyle, A. P. & Wallace, H. M. (2009). How Reliable are In Vitro IC₅₀ Values? Values Vary with Cytotoxicity Assays in Human Glioblastoma Cells. *Toxicology Letters*; Sep 302; 28–34. doi: 10.1016/j.toxlet.2018.12.004.

- Danaei, M., Dehghankhold, M., Ataei, S., Davarani, F. H., Javanmard, R., Dokhani, A., Khorasani, S. & Mozafri, M. R. (2018). Impact of Particle Size and Polydispersity Index on the Clinical Applications of Lipidic Nanocarrier Systems. *Journal of Pharmaceutics*; 10; 1–17. doi: 10.3390/pharmaceutics10020057.
- Fallah, S. H., Khalilpour, A., Amouei, A., Rezapour, M. & Tabarinia, H. (2020). Stability of Iodine in Iodized Salt Against Heat, Light and Humidity. *International Journal of Health and Life Sciences*; 6; 1–6. doi: org/10.5812/ijhls.100098
- Fares, A. R., Elmeshad, A. N. & Kassem, M. A. (2017). Enhancement of Dissolution and Oral Bioavailability of Lacidipine via Pluronic P123/F127 Mixed Polymeric Micelles : Formulation, Optimization Using Central Composite Design, and In Vivo Bioavailability Study. *Journal of Drug Delivery*; 25; 132–142. doi: 10.1080/10717544.2017.1419512.
- Gao, Y., Li, L. B. & Zhai, G. (2008). Preparation and Characterization of Pluronic / TPGS Mixed Micelles for Solubilization of Camptothecin. *Journal of Elsevier*; 64; 194–199. doi: 10.1016/j.colsurfb.2008.01.021.
- Kumbhar, P. S., Patil, N. J., Patil, A. B., Sambamoorthy, U., Disouza, J. I. & Manjappa, A. S. (2017). Simvastatin Loaded Nano Mixed Micelles: An Approach to Treat Hormone Dependent Carcinomas. *International Journal of Pharmaceutical Sciences and Research*; 12; 546–554. doi: 10.13040/IJPSR.0975-8232.10(2).
- Liu, J., Lee, H. & Allen, C. (2006). Formulation of Drugs in Block Copolymer Micelles: Drug Loading and Release. *Current Pharmaceutical Design*; 12; 4685–4701. doi: 10.2174/138161206779026263.
- Liu, X., Jiang, H. & Shen, Y. (2019). Enhanced Water Solubility, Antioxidant Activity, and Oral Absorption of Hesperetin by D- α -Tocopheryl Polyethylene Glycol 1000. *Journal of Zhejiang Universitt-SCIENCE B(Biomedicine & Biotechnology)*; 20; 273–281. doi: 10.1631/jzus.B1800346.
- Lombardo, D., Kiselev, M. A., Magazu, S. & Calandra, P. (2015). Amphiphiles Self-Assembly : Basic Concepts and Future Perspectives of Amphiphiles Self-Assembly : Basic Concepts and Future Perspectives of Supramolecular Approaches. *Journal of Cindensed Matter Physics*; 2015; 1–21. doi: org/10.1155/2015/151683
- Lu, Y., Zhang, E., Yang, J. & Cao, Z. (2019) Strategies to Improve Micelle Stability for Drug Delivery. *HHS Public Access*; 11; 4985–4998. doi: 10.1007/s12274-018-2152-3
- Mandal, A., Bisht, R., Rupenthal, I. D. & Mitra, A. K. (2017). Polymeric Micelles for Ocular Drug Delivery: From Structural Frameworks to Recent Preclinical Studies. *Journal of Controlled Release*; 248; 96–116. doi: org/10.1016/j.jconrel.2017.01.012
- Nga, N. T. H., Ngoc, T. T. B., Trinh, N. T. M., Thuoc, T. L. & Thao, D. T. P. (2020). Optimization and Application of MTT Assay in Determining Density of Suspension Cells. *Journal of Analytical Biochemistry*; September 610; 1–11. doi: org/10.1016/j.ab.2020.113937.
- Rajeshwar, B. R., Gatla, A., Rajesh, G., Arjun, N. & Swapna, M. (2011). Polymeric Micelles : A Nanoscience Technology. *Indo Amerixan Journal of Pharmaceutical Research*; 1; 351–363.
- Raveendran, R., Bhuvaneshwar, G. S. & Sharma, C. P. (2012). In Vitro Cytotoxicity and Cellular Uptake of Curcumin-Loaded Pluronic/Polycaprolactone Micelles in Colorectal Adenocarcinoma Cells. *Journal of Biomaterials Applications*; 2; 811–827. doi: 10.1177/0885328211427473.
- Saxena, V. & Hussain, M. D. (2012). Poloxamer 407/TPGS Mixed micelles for Delivery of Gambogic Acid to Breast and Multidrug-Resistant Cancer. *International Journal of Nanomedicine*; 7; 713–721. doi: 10.2147/IJN.S28745.
- Saxena, V. & Hussain, M. D. (2013). Polymeric Mixed Micelles for Delivery of Curcumin to Multidrug Resistant Ovarian Cancer. *Journal of Biomedical Nanotechnology*; 9; 1146–1154. doi: 10.1166/jbn.2013.1632.
- Setiawan, D. (2015). The Effect of Chemotherapy in Cancer Patient To Anxiety. *Jurnal Majority*; 4; 94–99.
- Shete, G., Pawar, Y. B., Thanki, K., Jain, S. & Bansal, A. K. (2015). Oral Bioavailability and Pharmacodynamic Activity of Hesperetin Nanocrystals Generated Using a Novel Bottom-Up Technology. *Journal of Molecular Pharmaceutics*; 12(4); 1158–1170. doi: 10.1021/mp5008647.

- Stanisic, D., Costa, A. F., Făvaro, W. J., Tasic, L., Seabra, A. B. & Duran, N. (2018). Anticancer Activities of Hesperidin and Hesperetin In vivo and their Potentiality against Bladder Cancer. *Journal of Nanomedicine & Nanotechnology*; 09; 4-6. doi: 10.4172/2157-7439.1000515.
- Zarrintaj, P., Ramsey, J. D., Samadi, A., Atoufi, Z., Yazdi, M. K., Ganjali, M. R., Amirabad, L. M., Zangene, E., Farokhi, M., Formela, K., Saeb, M. R., Mozafari, M. & Thomas, S. (2020). Poloxamer: A Versatile Tri-Block Copolymer for Biomedical Applications. *Journal of Acta Biomaterialia*; 110; 37–67. doi: 10.1016/j.actbio.2020.04.028.
- Zhang, J., Li Y., Zhou, D., Wang, Y. & Chen, M. (2014). TPGS-G-PLGA/Pluronic F68 Mixed Micelles for Tanshinone IIA Delivery In Cancer Therapy. *International Journal of Pharmaceutics*; 476(1); 185–198. doi: 10.1016/j.ijpharm.2014.09.017.
- Zhang, Z., Tan, S. and Feng, S. (2012). Vitamin E TPGS as a Molecular Biomaterial for Drug Delivery. *Journal of Biomaterials*; 33; 4889–4906. doi: 10.1016/j.biomaterials.2012.03.046.
- Zhou, W., Li C., Wang, Z., Zhang, W. & Liu, J. (2016). Factors Affecting The Stability of Drug-Loaded Polymeric Micelles and Strategies for Improvement. *Journal of Nanoparticle Research*; 18; 1-18. doi: 10.1007/s11051-016-3583-y.



Formulation, Characterization, and In Vitro Evaluation of Sunscreen Cream Containing Kenikir (*Cosmos caudatus* Kunth.) Extract and Chicken Bone Collagen Hydrolysate

Annisa Zukhruf*, Ika Qurrotul Afifah

Chemistry Department, Faculty of Science and Technology, Sunan Kalijaga State Islamic University, Yogyakarta, Indonesia

*Corresponding author: annisazukhruf3@gmail.com

Orcid ID: 0009-0006-1338-5327

Submitted: 9 November 2024

Revised: 19 April 2025

Accepted: 28 April 2025

Abstract

Background: Sunlight is a major contributor to skin damage, including erythema, pigmentation, premature aging, and other related conditions. Kenikir extract contains flavonoid derivatives, which have the potential to act as sunscreen due to the presence of chromophore groups that can reduce the intensity of sun exposure on the skin. In this study, sunscreen was made from kenikir extract with the addition of collagen hydrolysate. **Objective:** This study aims to assess the effectiveness and characteristics of various sunscreen cream formulations produced. **Methods:** Kenikir extract was obtained through ethanol-based maceration, while collagen hydrolysate was prepared by isolating chicken bone collagen using acetic acid solvent, followed by enzymatic hydrolysis with bromelain. Four sunscreen cream formulations were developed using various concentrations of kenikir extract and collagen hydrolysate. The creams were characterized by evaluating sun protection factor (SPF), percent erythema, percent pigmentation, organoleptic properties, acceptance testing, homogeneity, pH, viscosity, centrifugation, and spreadability. **Results:** The cream containing kenikir extract was effective as sunscreen with an SPF of 45.59, erythema of 1.96%, and pigmentation of 1.27%. It also exhibited homogeneity, with a pH of 7.83 and a viscosity of 46,700 cps, which met the permissible range for sunscreen use. The stability test indicated that it was stable, with no separation observed. **Conclusion:** Sunscreen cream containing kenikir extract has the potential to protect the skin from excessive sun exposure due to the effectiveness and good characteristics according to the Indonesian National Standard (SNI).

Keywords: sunscreen, SPF, kenikir extract, collagen hydrolysate

How to cite this article:

Zukhruf, A. & Afifah I. Q. (2025). Formulation, Characterization, and In Vitro Evaluation of Sunscreen Cream Containing Kenikir (*Cosmos caudatus* Kunth.) Extract and Chicken Bone Collagen Hydrolysate. *Jurnal Farmasi dan Ilmu Kefarmasian Indonesia*, 12(1), 117-127. <http://doi.org/10.20473/jfiki.v12i12025.117-127>

INTRODUCTION

The primary cause of skin damage, including erythema, pigmentation, premature aging, and skin cancer, is ultraviolet (UV) radiation (Ahmad & Agus, 2013). Cosmetics are used to protect the skin both physically and chemically. Sunscreen is a component contained in topical formulations that has the ability to interact with UV radiation (Pasha, 2021). Synthetic chemicals are typically used in the cosmetic industry to produce sunscreens. However, the use of synthetic sunscreens sometimes causes irritation with a burning or stinging sensation and allergic photocontact reactions. As a result, natural ingredients are now being developed as sunscreens (Savira & Iskandar, 2020). To ensure effective photoprotection, natural sunscreens must contain at least one active ingredient with antioxidant properties (Ismail, 2013). Antioxidants in sunscreen formulations function to prevent or minimize UV-induced oxidative damage, increase the effectiveness of photoprotection, and reduce skin aging (Jesus *et al.*, 2023).

Kenikir (*Cosmos caudatus* Kunth.) extract is rich in flavonoids derivatives such as quercetin, kaempferol, myricetin, catechin, luteolin, apigenin, quercetin 3-O-rhamnpside (quercitrin, quercetin 3-O-glucoside, quercetin 3-O-xyloside, quercetin 3-O-arabinofuranoside), and rutin that have the potential as sunscreen agents. Phenolic compounds, especially flavonoids, contain chromophore groups that can absorb UV radiation, thereby reducing the intensity of exposure to the skin (Lisnawati *et al.*, 2019). Chromophore groups are unsaturated covalent structures that can absorb radiation in the ultraviolet and visible regions (Wardani *et al.*, 2020).

Another ingredient that can be added to sunscreen formulations is collagen hydrolysate, which has been widely used as a substitute for synthetic antioxidants because it is safer, more nutritious, and therapeutically beneficial (Aguirre-Cruz *et al.*, 2020). Collagen hydrolysate has the ability to inhibit the tyrosinase enzyme activity, which leads to skin pigmentation. In addition, when applied topically, it can hydrate the skin, increase skin elasticity, and eliminate wrinkles (Prokopova *et al.*, 2021). Chicken bone waste is a potential and underutilized raw material source for collagen hydrolysate production.

A previous study has indicated that a nanocream prepared from kenikir leaves exhibited an SPF of 7.26 (Rahman & Herdaningsih, 2021). However, the study did not involve any viscosity tests, centrifugation tests, or determination of erythema and pigmentation values.

In addition, a study by Wang *et al.* (2019) showed that collagen hydrolysate derived from chicken skin can increase the viability and production of pro-collagen 1, reduce the levels of reactive oxygen species (ROS), MMP-1, and MMP-9, induce phosphorylation of the discoidin domain receptor 2 (DDR2), and inhibit UV-induced phosphorylation of Akt and ERK1/2. Thus, kenikir extract and collagen hydrolysate derived from chicken bone are potential natural ingredients for sunscreen.

In this study, sunscreen creams were prepared using kenikir extract and collagen hydrolysate. Four cream formulations were developed, including a control cream, a kenikir extract cream, a collagen hydrolysate cream, and a combination cream. These formulations were evaluated in accordance with SNI 16-4399-1996 standards. The analyses carried out included tests for homogeneity, viscosity, pH, and SPF. In addition, the creams were subjected to quality assessments through organoleptic and acceptance tests, spreadability tests, centrifugation tests, and determination of erythema and pigmentation values.

MATERIALS AND METHODS

Materials

The materials used in this study were kenikir leaves obtained from Telagareja Market, Yogyakarta, chicken bones, 96% ethanol (technical grade), ethanol (Merck), glacial acetic acid (Merck), NaOH (Merck), aquades, bromelain enzyme (HIMEDIA), disodium hydrogen phosphate (Merck), sodium dihydrogen phosphate (Merck), stearic acid (technical grade), cetyl alcohol (technical grade), mineral oil (technical grade), glycerin (technical grade), dimethicone (technical grade), triethanolamine (TEA) (technical grade), and methyl paraben (technical grade).

Equipment

The tools used in this study were a set of glassware, an analytical balance, a grinder, a 30-mesh sieve, an oven, a basic equipment set consisting of a waterbath, condenser, and vacuum pump to replace a rotary vacuum evaporator, a shaker incubator (Witeg Wisd Shaking Incubator WIS-30), fume hood, mortar and pestle, magnetic stirrer, centrifuge (Labogene 406), Brookfield viscometer (DV-II+ Pro), freeze dryer, UV-Vis spectrophotometer (Hitachi U-1800), and FTIR spectrophotometer (Thermo Scientific Nicolet Is10).

Methods

Maceration of kenikir leaves

Kenikir leaves were cleaned, dried, and ground using a grinder and sieved through a 30-mesh sieve. A

total of 250 grams of kenikir leaf powder was macerated in 96% ethanol solvent at a ratio of 1:4 for 3 x 24 hours. The extract was then filtered using a filter paper. The filtrate obtained was then evaporated using a substitute apparatus for a rotary evaporator (Widiyantoro & Harlia, 2020).

Preparation of collagen hydrolysate

The preparation of collagen hydrolysate was adapted from the method described by Putri and Ningsih (2018). Cleaned chicken bones were ground using a blender and air-dried. A total of 100 grams of chicken bone powder was demineralized by soaking in 1N acetic acid solvent using a shaker incubator for five hours at room temperature. The demineralized bone was then neutralized with 10% NaOH and rinsed with distilled water. The mineral-free chicken bone powder was then extracted with acetic acid solvent at a ratio of 1:5 using a shaker incubator for five hours at 40°C. The filtrate and residue from the extraction were then filtered using a filter paper. Furthermore, the filtrate was neutralized with 10% NaOH. The filtrate was then decanted, and only the white precipitate was collected. The white precipitate was then centrifuged at a speed of 4,000 rpm and the wet solid was oven-dried at 40°C for three days to produce dry collagen. Chicken bone collagen was then hydrolyzed using bromelain enzyme at a concentration of 0.002 grams/ml in 600 ml phosphate buffer solution at 55°C for four hours in a shaker incubator. The enzyme was then inactivated by heating at 100°C for 10 minutes, then centrifuged. Finally, the resulting wet solid was dried using a freeze dryer.

Sunscreen Cream Formulation

The oil phase in beaker I containing stearic acid, cetyl alcohol, mineral oil, and dimethylcone, was heated at 75°C. In beaker II, the water phase containing TEA, glycerin, methyl paraben, and distilled water was prepared. The water phase was gradually added to the oil phase with continuous stirring until the mixture was homogeneous. Following the formation of the oil-in-water emulsion, the active ingredients were added to the mixture as specified in Table 1, and the mixture was stirred for 25 minutes until homogeneous (Elcistia & Zulkarnain, 2018).

Table 1. Sunscreen cream formulations in gram

Material	Formula			
	A	B	C	D
Kenikir Extract	-	-	0.3	0.3
Hydrolyzed Collagen	-	2	-	2
Stearic Acid	7.5	7.5	7.5	7.5

Cetyl Alcohol	2	2	2	2
Mineral Oil	2.2	2.2	2.2	2.2
Dimethylcone	4	4	4	4
TEA	1.5	1.5	1.5	1.5
Glycerin	1.8	1.8	1.8	1.8
Methyl Paraben	0.2	0.2	0.2	0.2
Aquadest	Add	Add	Add	Add
	100	100	100	100

*A: basic cream; B: collagen hydrolysate cream; C: kenikir extract cream; D: collagen hydrolyzate-kenikir extract cream.

Organoleptic and Acceptance Tests

Organoleptic tests were performed through direct observation of the shape, color, and odor of the sunscreen cream formulations (Prastya, 2019). Acceptance tests were conducted by 27 panelists by assessing the color, odor, and texture of the cream using a 7-point scale, where 7 indicated very much like, 6 much like, 5 like, 4 neutral, 3 dislike, 2 somewhat dislike, and 1 very much dislike (Guttifera *et al.*, 2020).

Homogeneity Test

The cream was applied to a glass slide, spread, and observed visually by touch. A homogeneous cream formulation was indicated by the absence of coarse grains in the cream (Prastya, 2019).

pH Test

A pH meter was used to measure the dissolved cream (1 g) in 100 ml of distilled water (Prastya, 2019).

Spreadability Test

A 500 mg sample of the cream was placed at the center of a graduated round glass and another weighed round glass was placed on top of the cream for one minute. The diameter of the cream that spread after adding a load of 100 grams, 150 grams, or 200 grams was then recorded (Prastya, 2019).

Viscosity Test

The cream was put into a container, and spindle No. 64 was installed. The rotor was operated at a speed of 12 rpm with a torque percentage of 11%. After the reading of the Brookfield viscometer stabilized, the value was recorded and multiplied by the spindle correction factor (Suhery *et al.*, 2023).

Centrifugation Test

The cream was put into a centrifuge tube and centrifuged at 3,700 rpm for five hours. This test aimed to detect the presence of phase separation in the cream formulation (Pratasik *et al.*, 2019).

Determination of SPF value, % Erythema, and % Pigmentation

A total of 2 grams of cream was dissolved in 10 ml of ethanol PA and mixed until homogeneous and then

filtered using a filter paper. Subsequently, the absorbance at a wavelength of 290-400 nm and its transmittance at a wavelength of 292.5-372.5 nm were measured at intervals of 5 nm. The results of absorbance and transmittance were used to calculate SPF, percentage of erythema, and percentage of pigmentation (Syahrani, 2015).

Data Analysis

The pH, viscosity, spreadability, SPF, and percentage transmission for erythema and pigmentation were analyzed using IBM SPSS Statistics version 29.0.1.0. The data obtained were tested for normality (using the Saphiro-Wilk test) and homogeneity (using the Levene's test). If the data were normally distributed, analysis was continued with one-way ANOVA. However, if the data were not normally distributed, it was continued with the Kruskal-Wallis test. Data from the homogeneity, organoleptic, and stability tests were analyzed descriptively. Acceptance test data (color, odor, and texture) were analyzed statistically using univariate analysis, followed by Duncan's post-hoc test if significant differences were found (Mayangsari *et al.*, 2022).

RESULTS AND DISCUSSION

Kenikir Extract

The maceration process of kenikir leaves used ethanol as a solvent due to its polarity and ability to dissolve flavonoid compounds. In addition, ethanol has good absorption capacity, neutrality, resistance to microbial growth, non-toxicity, and relatively low evaporation temperature. During maceration, the ethanol solvent penetrated the cell walls of kenikir leaves and entered the cell cavity containing active compounds. These compounds dissolved into the solvent and moved out of the cell due to the difference in concentration between the solution inside and outside. The process was repeated until a balanced concentration between the solution outside and inside the cell was reached (Najib, 2018). The resulting kenikir extract had a yield of 4.168% and a texture similar to blackish brown cotton candy, with a unique aroma.

Hydrolyzed Chicken Bone Collagen

Chicken bone collagen was obtained through the process of reducing the size of chicken bones, drying, acid-based demineralization, and extraction (Nurjanah, 2020). To increase the bone surface during the extraction process, it is necessary to cut the chicken bones (Rahmawati & Nurjanah, 2020). The addition of acid in the demineralization process aims to remove minerals (impurities) and loosen the bone structure. The

demineralization process results in a highly acidic pH, thereby necessitating neutralization with NaOH. During the extraction process with acid solvents, the triple helix structure of the collagen is broken down (Putri & Ningsih, 2018). Following re-neutralization and decantation, collagen was obtained with a yield of 4.802%. The collagen was then hydrolyzed using the bromelain enzyme to produce short peptides. The resulting collagen hydrolysate was then analyzed using an FTIR spectrophotometer to compare its functional group profile with that of collagen and commercially available collagen hydrolysates.

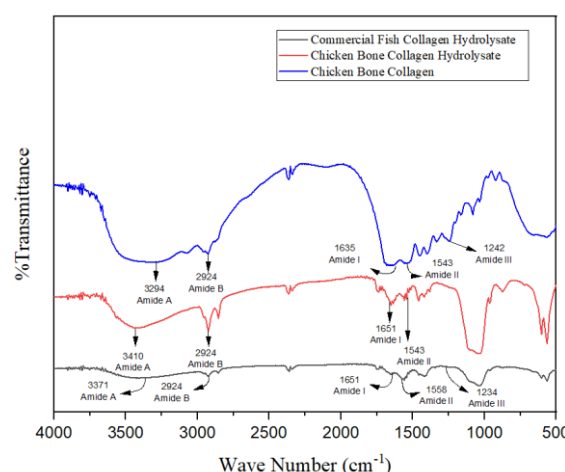


Figure 1. FTIR of chicken bone collagen, commercial collagen hydrolysate, and chicken bone collagen hydrolysate

Collagen has standard absorption peaks in the regions of the amide bands A and B as well as I, II and III. Figure 1 shows that chicken bone collagen had an absorption peak in the amide III region at 1234 cm^{-1} . After hydrolysis using bromelain, this peak was no longer observed within the amide III range (1229 cm^{-1} -1301 cm^{-1}), while commercial fish collagen hydrolysate showed a low-intensity admide III absorption. The absence or reduction in intensity of amide III confirmed that the triple helix structure of the collagen transformed into a random coil shape due to the dissociation of hydrogen bonds during hydrolysis. Schmidt *et al.* (2020) compared the FTIR spectra of collagen and collagen hydrolysate produced by treatment with the flavourzyme and alcalase enzyme. The spectrum of collagen hydrolyzed with the flavourzyme enzyme had a low-intensity amide III absorption peaked at 1450 cm^{-1} , and the absorption disappeared in hydrolysate produced using the alcalase enzyme. Enzymatic treatment can break the bonds in polypeptide chains, thereby generating a higher yield of peptides (León-López *et al.*, 2019).

SPF Test

According to Figure 2, cream A containing no active ingredients was ineffective as a sunscreen because the SPF was below the minimum protection value. Cream B also lacked sunscreen efficacy, with an SPF of 1.539 ± 0.001 , while cream C containing kenikir extract was a good sunscreen because the SPF value met the ultra protection category. Cream D, comprised of active ingredients such as kenikir extract and collagen hydrolysate, was also effective as a sunscreen although it exhibited a lower SPF of 38.91 ± 0.799 .

Table 2. SPF test results

Code	Formula	SPF Value	Standard Deviation
A	Base Cream	1.139	0.001
B	Hydrolyzed Collagen Cream	1.539	0.018
C	Kenikir Extract Cream	45.59	4.049
D	Combination Cream	38.91	0.799

After determining the SPF, the Saphiro-Wilk normality test and the homogeneity test were conducted using SPSS. The results indicated that the SPF data were not normally distributed ($p = 0.009 < 0.005$) and not homogeneous ($p < 0.001$). Therefore, the analysis was continued with a non-parametric test, namely the Kruskal-Wallis test, whose results showed no significant differences among the four sunscreen formulations ($p = 0.080 > 0.05$).

The hydrolyzed collagen cream was not effective as a sunscreen because of the presence of peptides with varying molecular weights resulting from the lack of a purification process. Song *et. al* (2017) reported that the molecular weight of collagen peptides affects the effectiveness in repairing photoaging on the skin. The administration of collagen peptides with low molecular weights ($0.5 \text{ kDa} < \text{BM} < 1 \text{ kDa}$) demonstrated greater efficacy in repairing photoaging on mouse skin than collagen peptides with high molecular weights ($>1 \text{ kDa}$). This is attributed to the greater availability of electron donors and enhanced free radical scavenging capacity of low molecular weight collagen peptides. The composition and sequence of their amino acids also play a role in the effectiveness of collagen peptides. A high composition of hydrophobic amino acids is present in collagen peptides with high antioxidant activity, including pro, his, tyr, trp, met, and cys amino acids. In

addition, hydrophobic amino acids at the C and N terminals such as Ala, Phe, Leu, and Prp contribute significantly to antioxidant activity (Li *et al.*, 2021).

Compared to the base cream, adding kenikir extract alone significantly increased the SPF. This is attributed to the presence of flavonoid compounds in the kenikir extract. According to Rafi *et al.* (2023), kenikir contains isoquercitrin, quercetin-3-O-rutinoside, avicularin, rutin, quercitrin, vitexin compounds which are known for their antioxidant properties. These compounds can protect the skin from sun exposure due to the chromophore groups in the form of an aromatic ring that has the ability to absorb UV radiation and emit light with lower energy. This mechanism helps prevent the adverse effects of exposure to UV radiation.

The combination cream, which contains both kenikir extract and collagen hydrolysate, offered excellent protection against UV rays, but its SPF (38.9075) was lower than that of the cream containing only kenikir extract. The UV absorption capacity of the combination cream may be compromised possibly due to the antagonistic interactions between kenikir extract and collagen hydrolysate, resulting in lower SPF. Such interactions have been reported in previous studies, including between soy protein hydrolysate and polyphenolic flavonoid cyanidine-3-ortho-glucoside, which was found to reduce antioxidant activity against ABTS and DPPH free radicals (Wu *et al.*, 2021).

Similarly, Peres *et al.* (2017) formulated a sunscreen with active ingredients, namely octocrylene, avobenzene, titanium dioxide, and collagen hydrolysate. The SPF was 41% lower than the formulation without the addition of collagen hydrolysate to the sunscreen cream. Furthermore, the addition of collagen hydrolysate to a combination of octocrylene, avobenzene, and titanium dioxide caused a decrease in SPF by 38%. These findings support the notion that negative interactions between natural ingredients, excipients, and sunscreen carriers can reduce the effectiveness of the sunscreen formulation.

Percentage of Erythema

Redness following UV exposure is a symptom of an acute inflammatory reaction known as erythema. When the skin is exposed to UVB radiation, the skin sensitizer absorbs the radiation and undergoes excitation to generate ROS. These ROS interact with mast cells to release mediators (such as histamine) which can induce vasodilation of blood vessels, causing skin redness (Pratama *et al.*, 2020). The percentage of erythema transmission indicates the proportion of sunlight that

penetrates the sunscreen formulation and can lead to erythema or redness on the skin.

As shown in Table 3, cream A had a high erythema percentage of $77.351\% \pm 0.001$, indicating its ineffectiveness in protecting the skin from UVB-induced erythema. Cream B also lacked effectiveness in protecting the skin from UVB-induced erythema, but it transmitted less UVB radiation than the base cream, with a percentage of $39.98\% \pm 0.018$. Cream C offered additional protection and was successful in preventing erythema, as it transmitted UVB radiation to the skin at $1.965\% \pm 4.049$. Cream D was capable of preventing erythema, as it transmitted less UV radiation to the skin than the kenikir extract cream. This is possible because the active compounds in cream C absorbed more light at the transmittance wavelength of 317.5-372.5 nm than at the erythema-inducing wavelength of 292.5-317.5 nm.

Table 3. Percentages of erythema transmittance

Code	Formula	Percentage of Erythema (%)	Standard Deviation
A	Base Cream	77.351	0.001
B	Hydrolyzed Collagen Cream	39.98	0.018
C	Kenikir Extract Cream	1.965	4.049
D	Combination Cream	1.648	0.799

The erythema data obtained were tested using the Shapiro-Wilk normality test and the homogeneity test using SPSS. The results indicated that the data were normally distributed ($0.057 > 0.05$), allowing for parametric testing using one-way ANOVA. The ANOVA test revealed a significant difference among the four formulations ($p = 0.002 < 0.005$), indicating the need for further analysis. The homogeneity test showed that the data were not homogeneously distributed ($p = 0.001 < 0.005$). Therefore, the Games-Howell test was employed. The additional examination revealed no difference between two formulas.

Percentage of Pigmentation

Melanin production is directly affected by UV radiation, which causes skin pigmentation, through the stimulation of various keratinocyte cytokines such as interleukin-1, α -MSH, and ACTH. These cytokines bind to melanocortin-1 receptors, thereby stimulating tyrosinase activity. Increased tyrosinase activity leads to the proliferation of melanocytes and an increase in melanin production. Melanin that accumulates in keratinocytes causes skin to darken or tanning (Mamoto *et al.*, 2013). Additionally, UV radiation can damage the

sulphydryl groups present in the epidermis. These groups function as inhibitors by binding to Cu ions essential for the tyrosinase enzyme. Damage to the sulphydryl groups can lift the inhibition of the tyrosinase enzyme, allowing the enzyme to function optimally and triggering melanogenesis (Fajriah, 2021).

The percentage of pigmentation transmittance refers to the amount of UV radiation that penetrates the skin despite the application of sunscreen, which can result in skin pigmentation or darkening. As shown in Table 4, the base cream transmitted $94.04\% \pm 0.549$ of UVA radiation at a wavelength of 320-375 nm, indicating that it was ineffective in preventing UVA-induced pigmentation. Cream B was able to protect the skin from the effects of pigmentation, placing it in the fasttanning category, by transmitting $75.484\% \pm 2.52$ of UVA radiation. Sunscreens in the fast-tanning category allow significant UVA penetration, which can rapidly darken the skin without causing erythema. Cream B had the ability to prevent pigmentation from UVA radiation, but its protective ability was minimal. In contrast, creams C and D had very good ability to protect the skin from UVA-induced pigmentation by only transmitting $1.274\% \pm 0.057$ and $1.585\% \pm 0.042$ of UVA radiation, respectively, classifying them in the sunblock category.

Table 4. Percentages of pigmentation transmittance

Code	Formula	Percentage of Pigmentation (%)	Standard Deviation
A	Base Cream	94.004	0.549
B	Hydrolyzed Collagen Cream	75.484	2.52
C	Kenikir Extract Cream	1.274	0.057
D	Combination Cream	1.585	0.042

Based on the Shapiro-Wilk normality test, the percentage of pigmentation transmittance data were not normally distributed ($p = 0.007 < 0.05$). In addition, the homogeneity test showed that the data were not homogeneous ($p < 0.001$). Therefore, the Kruskal-Wallis test, a non-parametric test, was used for further analysis. The results showed no significant differences among the four sunscreen formulations ($p = 0.083 > 0.05$).

Organoleptic and Acceptance Tests

As shown in Table 6, the highest average preference score (5.11 ± 1.07) was recorded for cream A, which

was classified as “like” by panelists due to its extra white color indicating a clean cream formulation. Cream B, with a color ranging from pure white to milky white, showed a decrease in brightness due to the addition of collagen hydrolysate. This change affected the panelists’ preference, resulting in a score of 4.67 ± 1.02 within the neutral category. Cream D exhibited a pure bone white color with low brightness, which reduced its preference score (4.33 ± 1), falling under the neutral category. Cream C with kenikir extract displayed a creamy texture, which influenced its preference score, which was the lowest (3.74 ± 1.35), placing it in the “dislike” category. According to the univariate analysis, the preference scores for cream color showed a significant difference ($p = 0.01 < 0.05$). Therefore, further analysis was carried out using the Duncan’s test. This test revealed that the preference score level for the kenikir extract cream was significantly different from the other three formulations.

Table 6 also illustrates that the panelists had nearly identical preferences for the aroma of the four creams. According to Table 5, all four creams exhibited an aroma similar to stearic acid because of its high concentration following aquadest in the formulation. The univariate test yielded a significance level greater than 0.05 ($p = 0.721$), suggesting no difference in the preference level for the aroma of the four creams.

As illustrated in Table 6, the panelists had similar preferences for the texture of the four creams. The texture of all four creams was semi-solid (Table 5). According to the univariate test, no significant differences in texture preferences were observed ($p = 0.117 > 0.005$).

Table 5. Organoleptic test results

Formula	Color	Aroma	Texture
Base Cream	Extra White	Stearic Acid	Semi Solid
Hydrolyzed Collagen Cream	Pure White	Stearic Acid	Semi Solid
Kenikir Extract Cream	Cream	Stearic Acid	Semi Solid
Combination Cream	Cottage White	Stearic Acid	Semi Solid

Table 6. Acceptance test results

Parameter	Code	Likeability Score	Standard Deviation
Color	A	5.11	1.07
	B	4.67	1.02
	C	3.74	1.35
	D	4.33	1
Aroma	A	4.37	1.04

P-ISSN: 2406-9388
E-ISSN: 2580-8303

Teksture	B	4.15	0.95
	C	4.3	1.03
	D	4.07	0.83
	A	4.93	0.96
	B	4.89	1.12
	C	4.41	1.47
	D	4.33	1

Homogeneity Test

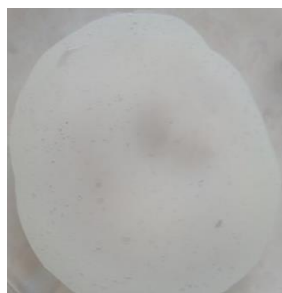
Cream A



Cream B



Cream C



Cream D



Figure 2. Homogeneity test results. Red circles indicate unmixed collagen hydrolysate granules

To determine the uniformity of ingredient dispersion in the cream formulations, a homogeneity test was conducted. A good cream is defined by the absence of coarse grains and a uniform color distribution. The cream formulation must be homogeneous to prevent irritation when applied to the skin surface, and so that each gram of cream contains ingredients with the same levels and effectiveness. According to the test results, the base cream and kenikir extract cream exhibited homogenous mixtures with evenly distributed color. This indicated the effective performance of the emulsifier agents used in the formulation. The emulsifier, a non-ionic surfactant, causes all ingredients to be evenly dispersed, resulting in a homogenous cream formulation (Hendrawan *et al.*, 2020). Non-ionic surfactants such as cetyl alcohol and stearic acid can be used as emulsifying agents and contribute to the physical stability of the formulation (Devi *et al.*, 2019). In contrast, the collagen hydrolysate cream and combination cream failed to achieve homogeneity because of the presence of coarse collagen hydrolysate grains (Figure 6). Proteins that contain more

hydrophobic amino acids have less water solubility than those that contain more hydrophilic amino acids. Collagen consists of approximately 80% of non-polar amino acids such as glycine, alanine, valine, and proline. The composition of collagen chains is made up of thousands of amino acids that have repeating Gly-X-Y sequences, where X and Y sequences are mostly occupied by proline and hydroxyproline (Cherim *et al.*, 2019).

pH Test

Table 7. pH test results

Code	Formula	pH	Standard Deviation
A	Base Cream	7.874	0.059
B	Hydrolyzed Collagen Cream	7.03	0.014
C	Kenikir Extract Cream	7.833	0.007
D	Combination Cream	6.964	0.041

A cream that is too acidic may cause skin irritation, while a cream that is too alkaline may result in itching and flaking of the skin (Sari, 2014). All four cream formulations had pH values within the range permitted by SNI 16-4399-1996 (4.5-8), indicating they are safe for use.

The Shapiro-Wilk normality test and homogeneity test showed that the pH data were not normally distributed ($p = 0.006 < 0.05$) and not homogeneous. Therefore, the analysis was continued with the non-parametric Kruskal-Wallis test. The results showed no significant differences among the four sunscreen formulas ($p = 0.083 > 0.05$).

Cream A had a pH of 7.874 ± 0.059 , which was a weak base. Cream C had a lower pH than its base cream, which was 7.833 ± 0.007 . Kenikir extract lowers the pH of the formulation because it contains phenolic compounds that can release H^+ ions from their hydroxyl groups (Tambun *et al.*, 2016). Cream B had a lower pH than the base cream, which was 7.03 ± 0.014 . This is because the added collagen hydrolysate is composed of amino acids. Amino acids contain both hydroxyl ($-COOH$) and amine ($-NH$), allowing them to behave as acids or bases depending on the surrounding environment (amphoteric). If the amino acid is in a strong acidic environment, the substance will be basic, but if the substance is in a basic environment, the substance will be acidic (Wahyudiati, 2017). When collagen hydrolysate is added to a weak base cream, the

amino acid will act as an acid and release H^+ ions, resulting in a decrease in the pH of the formulation.

Cream D was prepared by adding kenikir extract first, followed by collagen hydrolysate. The addition of kenikir extract caused a slight decrease in the pH, although the cream remained weakly alkaline. When collagen hydrolysate was added, the amino acids released H^+ and further decrease the pH.

Viscosity Test

Table 8. Viscosity test results

Code	Formula	Viscosity (Cps)	Standard Deviation
A	Base Cream	43,500	25
B	Hydrolyzed Collagen Cream	19,100	100
C	Kenikir Extract Cream	46,700	50
D	Combination Cream	41,550	550

The viscosity test was conducted to assess the thickness of the cream formulation, which directly influences its ease of application to the skin. A cream is considered good when its viscosity is neither too thick nor too runny. According to SNI 16-4399-1996, a high-quality sunscreen cream should have a viscosity between 2,000 and 50,000 cps. As shown in Table 8, the four creams met this standard with viscosities above 2000 cps and below 50,000 cps.

The Shapiro-Wilk normality test and homogeneity test showed that the viscosity data were not normally distributed ($p = 0.003 < 0.05$) and not homogeneous. Therefore, further analysis was conducted using the non-parametric Kruskal-Wallis test, whose results showed no significant differences among the four sunscreen formulations ($0.083 > 0.05$).

The addition of collagen hydrolysate resulted in decreased viscosity, while the addition of kenikir extract resulted in increased viscosity. The base cream had a viscosity of $43,525 \pm 25$ cps. The presence of hydroxyl groups in kenikir extract can increase viscosity because of the high number of hydroxyl groups present in its flavonoid compounds, particularly quercetin. These hydroxyl groups can interact with similar groups in the components of the cream formulations, such as stearic acid, TEA, cetyl alcohol, glycerol, methyl paraben, and aquadest by forming hydrogen bonds. These hydrogen bonds occur when hydrogen atoms in both kenikir extract and cream components bind to more

electronegative atoms, specifically oxygen atoms. The increase in hydrogen bonds strengthens the interactions among components, leading to a higher viscosity. Kuncari and Praptiwi (2014), citing Contreras and Sanchez, noted that hydrogen bonds can increase cross-linking between chains, thereby increasing viscosity. In contrast, the addition of active ingredients such as collagen hydrolysate decreases the viscosity of the base cream. Collagen hydrolysate can act as a natural humectant (Sionkowska *et al.*, 2020) which can reduce the viscosity of the cream and make its consistency more liquid. Humectants are utilized to minimize water loss from the formulation, helping to prevent dryness and increase spreadability.

Centrifugation Test

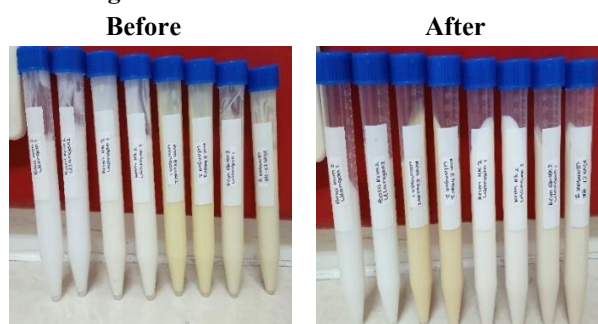


Figure 3. Centrifugation test. The four creams did not experience phase separation after centrifugation.

The stability of an emulsion is determined by its ability to resist changes in its properties over time. The more stable the emulsion, the slower its properties change (Del Río-Ortuño *et al.*, 2022). The centrifugation technique, which operates based on Stokes' law, is used to determine cream stability. Under increased gravitational force, phase separation occurs more rapidly, thereby accelerating the creaming process. Creaming is a process where layers with different concentrations form within an emulsion. Gravitational force causes the raising of particles with lower densities to the surface, and vice versa. Centrifuging a cream formulation for five hours at a speed of 3,700 rpm is equivalent to the effect of gravitational force for one year (Dewi *et al.*, 2014).

Figure 4 shows that the four cream formulations did not separate, indicating that they were stable over a one-year storage period. By combining stearic acid and triethanolamine, the molecules on the surface will be packed more tightly, increasing the strength of the interfacial layer and enhancing the stability. The stability of the preparation can be improved with the use of cetyl alcohol as a cosurfactant, which can increase the density of the emulsifier molecules at the emulsion interface. Cetyl alcohol also functions to increase

P-ISSN: 2406-9388
E-ISSN: 2580-8303

consistency and as a non-ionic surfactant (Sari *et al.*, 2021).

Spreadability Test

Table 9. Spreadability test results

Code	Formula	Spread Power Test (cm)	Standard Deviation
A	Base Cream	4.55	0.167
B	Hydrolyzed Collagen Cream	4.183	0.033
C	Kenikir Extract Cream	4.967	0
D	Combination Cream	4.042	0.075

The spreadability test was conducted to evaluate the ability of the cream formulation to spread when applied to the skin surface. Greater spreadability allows the active ingredients to be dispersed evenly, enhancing their therapeutic effects. A good spreadability range of the cream is approximately 5-7 cm (Syarif *et al.*, 2015). As shown in Table 10, the four formulas demonstrated poor spreadability.

A normal distribution was observed in the spreadability test data, as shown by the Shapiro-Wilk normality and homogeneity test. Therefore, a one-way ANOVA parametric test was conducted. The ANOVA test revealed a significant difference ($p = 0.190 > 0.005$), indicating that further analysis was required. The homogeneity test showed that the data were not homogeneous ($p < 0.001$), so the Games-Howell test was employed. The additional examination revealed a difference in spreadability between collagen hydrolysate cream and kenikir extract cream. This may be attributed to the high viscosity of the formulations. In addition, the poor spreadability of the collagen hydrolysate cream and the combination cream is likely due to the uneven mixing of hydrolyzed collagen during formulation. Greater pressure is required when applying creams with low spreadability to the skin so that it is evenly distributed (Sari & Susiloningrum, 2022).

CONCLUSION

The kenikir extract cream and combination cream were effective in protecting the skin from UV radiation with ultra protection indicated by the SPF and percentages of erythema and pigmentation. Meanwhile, the base cream and collagen hydrolysate cream were less effective as sunscreens. Based on the characterization tests, the four creams were stable with no phase separation during the centrifugation test and

met the standards for viscosity and pH. However, the four creams had poor spreadability which can affect the ease of application. The panelists had similar preferences for the aroma and texture of the four creams and favored formulations with a clean white color.

ACKNOWLEDGEMENT

The authors would like to thank the Faculty of Science and Technology, UIN Sunan Kalijaga Yogyakarta for providing assistance in the laboratory and LPPM UIN for funding some of the research and publication needs under the scheme Capacity Building Research 2022.

REFERENCES

- Aguirre-Cruz, G., Leon-Lopez, A., Cruz-Gomez, V., Jimenez-Alvarado, R., & Aguirre-Alvarez, G. (2020). Collagen Hydrolysates for Skin Protection: Oral Administration and Topical Formulation. *National Library of Medicine*, 9.
- Ahmad, I., & Agus, ASR (2013). Uji Stabilitas Formula Krim Tabir Surya Ekstrak Umbi Bawang Dayak (Eleutherine Americana L. Merr.). *J. Trop. Pharm*, 2 (3), 159–165.
- Cherim, M., Mustafa, A., Cadar, E., Lupaşcu, N., Paris, S., & Sirbu, R. (2019). Collagen Sources and Areas of Use. *European Journal of Medicine and Natural Sciences*, 2 (2 SE-Articles), 8–13. <https://doi.org/10.26417/ejis.v4i1.p122-128>
- Del Río-Ortuño, Y., Streitenberger-Jacobi, S., Bermejo-Fernández, R., & Marin-Iniesta, F. (2022). Estabilidad en cremas con ingredientes de origen vegetal. *Anales de Veterinaria de Murcia*, 36, 1–21. <https://doi.org/10.6018/analesvet.541121>
- Devi, IGASK, Mulyani, S., & Suhendra, L. (2019). Pengaruh Nilai Hydrophile-Liphophile Balance (HLB) dan Jenis Ekstrak terhadap Karakteristik Krim Kunyit-Lidah Buaya (Curcuma domestica Val.-Aloe Vera). *Jurnal Ilmiah Teknologi Pertanian Agrotechno*, 4, 56.
- Dewi, R., Anwar, E., & Yunita, KS (2014). Uji Stabilitas Fisik Formula Krim yang Mengandung Ekstrak Kacang Kedelai (Glycine max) Abstrak . *Pharma Schi Res*, 1 (3), 194–208.
- Elcistia, R., & Zulkarnain, AK (2018). Optimasi Formula Sediaan Krim o / w Kombinasi Oksibenzon dan Titanium Dioksida serta Uji Aktivitas Tabir Suryanya secara In Vivo. *Majalah Farmasetika*, 14.
- Emma Sri Kuncari, I., & Praptiwi. (2014). Evaluasi, Uji Stabilitas Fisik Dan Sineresis Sediaan Gel Yang Mengandung Minoksidil, Apigenin Dan Perasan Herba Seledri (Apium graveolens L.). *Buletin Penelitian Kesehatan*, 42(4), 213–222.
- Fajriah, L. (2021). Hubungan Perilaku Penggunaan Tabir Surya Dengan Derajat Keparahan Melasma. In *Paper Knowledge . Toward a Media History of Documents*. UIN Syarif Hidayatullah Jakarta.
- GuttiFERA, Sari, S. R., Pratama, F., Widowati, T. W., & Prariska, D. (2020). Karakteristik Sensori Mikrowaveable Kemplang Palembang dengan Perbedaan Ketebalan dan Level Daya pada Proses Pematangan. *Jurnal Ilmu Perikanan Air Tawar*, 1.
- Hendrawan, I. M. O., Suhendra, L., & Putra, G. P. G. (2020). Pengaruh Perbandingan Minyak dan Surfaktan serta Suhu terhadap Karakteristik Sediaan Krim. *Jurnal Rekayasa Dan Manajemen Agroindustri*, 8.
- Ismail, I. (2013). Potensi Bahan Alam Sebagai Bahan Aktif Kosmetik Tabir Surya. *JF UINAM*, 1(1), 45–55.
- Jesus, A., Mota, S., Torres, A., T. Cruz, M., Sousa, E., Almeida, IF, & Cidade, H. (2023). Antioxidants in Sunscreens: Which and What For? *Antioxidants*, 12.
- León-López, A., Morales-Peñaloza, A., Martínez-Juárez, V.M., Vargas-Torres, A., Zeugolis, D.I., & Aguirre-Álvarez, G. (2019). Hydrolyzed collagen-sources and applications. *Molecules*, 24 (22), 1–16. <https://doi.org/10.3390/molecules24224031>
- Li, C., Fu, Y., Dai, H., Wang, Q., Gao, R., & Zhang, Y. (2021). Recent Progress In Preventive Effect Of Collagen Peptides On Photoaging Skin And Action Mechanism. *Science Direct*, 11.
- Lisnawati, N., N.U, M. F., & Nurlitasari, D. (2019). Penentuan Nilai SPF Ekstrak Etil Asetat Daun Mangga Gedong Menggunakan Spektrofotometri UV-VIS. *Jurnal Riset Kefarmasian Indonesia*, 1.
- Mamoto, N., Kalangi, S., & Karundeng, R. (2013). The Role of Melanocortin in Melanocytes. *Biomedical Journal (Jbm)*, 1 (1). <https://doi.org/10.35790/jbm.1.1.2009.805>
- Mayangsari, FD, Kusumo, DW, & Muarifah, Z. (2022). Uji Karakteristik Fisik dan Hedonik dari Antiaging Sleeping Mask dengan Ekstrak Kulit Buah Delima Merah. *Jurnal Ilmiah Manutung Sains Farmasi Dan Kesehatan*, 8.
- Najib, A. (2018). *Ekstraksi Senyawa Bahan Alam*. Deepublish.
- Pasha, FF (2021). *Kajian Bahan Alam Berpotensi Sebagai Tabir Surya*. Universitas Ngudi Waluyo.
- Peres, DD, Hubner, A., Oliveira, CA de, Almeida, TS de, Kaneko, TM, Consiglieri, VO, Pinto, CAS de O., Velasco, MVR, & Baby, AR (2017). Hydrolyzed Collagen Interferes with in Vitro Photoprotective Effectiveness of Sunscreen. *Brazilian Journal of Pharmaceutical Science*, 2.
- Prastya, G. (2019). *Pengaruh Emulgator Tween 80 Dan Span 80 Terhadap Stabilitas Fisik Sediaan Krim Anti-Aging Minyak Vco (Virgin Coconut Oil)*. Sekolah Tinggi Ilmu Kesehatan Tulungagung.
- Pratama, G. M. C. T., Gusti B R M Hartawan, I. N., Gusti T Indriani, I. A., Yusrika, M. U., A Suryantari, S. A., S Satyarsa, A. B., & S Sudarsa, P. S. (2020). Potensi Ekstrak Spirulina platensis sebagai Tabir Surya terhadap Paparan Ultraviolet B. *Journal of Medicine and Health Potensi Ekstrak Spirulina Platensis*, 2(6), 205–217.

- Pratasik, MCM, Yamlean, PVY, & Wiyono, WI (2019). Formulasi Dan Uji Stabilitas Fisik Sediaan Krim Ekstrak Etanol Daun Sesewanua (*Clerodendron squamatum* Vahl.). *PHARMACON*, 8, 263.
- Prokopova, A., Pavlackova, J., Mokrejs, P., & Gal, R. (2021). Collagen hydrolyzate prepared from chicken by-product as a functional polymer in cosmetic formulation. *Molecules*, 26 (7), 1–19. <https://doi.org/10.3390/molecules26072021>
- Putri, SL, & Ningsih, LA (2018). *Pembuatan Sapi (Bovine Collagen) Dengan Metode Ekstraksi Solvent Sebagai Bahan Aditif Kosmetik*. Institut Teknologi Sepuluh Nopember.
- Rafi, M., Hayati, F., Umar, AH, Septaningsih, DA, & Rachmatiah, T. (2023). LC-HRMS-based metabolomics to evaluate the phytochemical profile and antioxidant capacity of *Cosmos caudatus* with different extraction methods and solvents. *Arabian Journal of Chemistry*, 16 (9), 105065. <https://doi.org/10.1016/j.arabjc.2023.105065>
- Rahman, IR, & Herdaningsih, S. (2021). Formulation And Physical Properties Test Of Nano Cream Preparation Purified Extract Of Kenikir Leaf (Etdk) And Tampoi Fruit Peel Extract (Ekbt). *Jurnal Ilmiah Farmako Bahari*, 12, 160–167.
- Rahmawati, R., & Nurjanah, S. (2020). Pengaruh Konsentrasi Enzim Papain terhadap Mutu Gelatin Bubuk dari Tulang dan Cakar Ayam. *Jurnal Konversi*, 9, 41.
- Sari, DEM, & Susiloningrum, D. (2022). Penentuan Nilai SPF Krim Tabir Surya Yang Mengandung Ekstrak Temu Mangga (*Curcuma mangga* Valetton & Zijp) Dan Titanium Dioksida. *Cendekia Journal of Pharmacy*, 6(1), 102–111.
- Sari, MP (2014). *Formulasi Krim Tabir Surya Fraksi Etil Asetat Kulit Pisang Ambon Putih [Musa (AAA Group)] Dan Penentuan Nilai Faktor Perlindungan Surya (FPS) Fraksi Etil Asetat Secara In Vitro*. Universitas Islam Bandung.
- Sari, N., Samsul, E., & Narsa, A.C. (2021). Pengaruh Trietanolamin pada Basis Krim Minyak dalam Air yang Berbahan Dasar Asam Stearat dan Setil Alkohol. *Proceeding of Mulawarman Pharmaceuticals Conferences*, 14, 70–75. <https://doi.org/10.25026/mpc.v14i1.573>
- Savira, D., & Iskandar, D. (2020). Pemanfaatan Ekstrak Daun Kitolod (*Hippobroma longiflora* (L) G.Don) Sebagai Bahan Aktif Sediaan Tabir Surya. *Jurnal Kimia Riset*, 5(1), 44. <https://doi.org/10.20473/jkr.v5i1.19680>
- Sionkowska, A., Adamiak, K., Musial, K., & Gadowska, M. (2020). Collagen Based Materials in Cosmetic Applications: A Review. *MDPI*, 13 (19).
- Suhery, W. N., Muhtadi, W. K., Yenny, R. F., & Risma, A. T. (2022). Formulation and Evaluation of Anti-Acne Cream of Fennel Oil (*Foeniculum vulgare* Mill.) Againsts *Propionibacterium Acnes* Bacteria. *Pharmauho: Jurnal Farmasi, Sains, dan Kesehatan*, 8(2), 39–45.
- Syahrani. (2015). *Formulasi Dan Uji Potensi Krim Tabir Surya Dengan Bahan Aktif Ekstrak Etanol Kulit Nanas (Ananas comosus (L.) Merr)*. Universitas Islam Negeri Alauddin Makassar.
- Syarif, UIN, Jakarta, H., Ilyas, NZ, Kedokteran, F., Ilmu, D. A. N., & Farmasi, P. S. (2015). *Uji Stabilitas Fisik Dan Penentuan Nilai Sun Protection Factor (SPF) Krim Rice Bran Oil Uji Stabilitas Fisik Dan Penentuan Nilai Sun Protection Factor (SPF)*. Uin Syarif Hidayatullah Jakarta.
- Tambun, R., Limbong, HP, Pinem, C., & Manurung, E. (2016). Pengaruh Ukuran Partikel, Waktu Dan Suhu Pada Ekstraksi Fenol Dari Jahe. *Jurnal Teknik Kimia USU*, 5(4), 53–56.
- Wahyudiati, D. (2017). *Biokimia*. LEPPIM Mataram.
- Wang, X., Hong, H., & Wu, J. (2019). Hen collagen hydrolyzate alleviates UVA-induced damage in human dermal fibroblasts. *Journal of Functional Foods*, 63 (September), 103574. <https://doi.org/10.1016/j.jff.2019.103574>
- Wardani, GA, Abiya, SL, & Setiawan, F. (2020). Analysis of the Lead on Lip Tint Cosmetics on the Market Using UV-Vis Spectrophotometry Method. *EduChemia (Jurnal Kimia Dan Pendidikan)*, 5 (1), 87. <https://doi.org/10.30870/educhemia.v5i1.7598>
- Warnis, M., Aprilina, L. A., & Maryanti, L. (2020). Pengaruh Suhu Pengeringan Simplisia terhadap Kadar Flavonoid Total Ekstrak Daun Kelor. 265.
- Widiyantoro, A., & Harlia. (2020). Aktivitas Antioksidan Ekstrak Daun Kenikir (*Cosmos Caudatus* Kunth) Dengan Berbagai Metode Ekstraksi. *Indonesian Journal of Pure and Applied Chemistry*, 3(1), 9–14.
- Wu, Y., Yin, Z., Qie, X., Chen, Y., Zeng, M., Wang, Z., Qin, F., Chen, J., & He, Z. (2021). *Interaction of Soy Protein Isolate Hydrolysates with Cyanidin-3- O -Glucoside and Its Effect on the In Vitro Antioxidant Capacity of the Complexes under Neutral Condition*.



Formulation of Lip Balm Extract of Temu Mangga Rhizome (*Curcuma mangga* Val) as Moisturizer

Rina Andriani¹, Mus Ifaya^{1*}, Rismayanti Fauziah¹, Dian Rahmانيar Trisnaputri¹, Wa Ode Ida Fitriah¹, Qur'ani²

¹Department of Pharmacy, Faculty of Science and Technology, Mandala Waluya University, Kendari, Indonesia

²Student, Department of Pharmacy, Faculty of Science and Technology, Mandala Waluya University, Kendari, Indonesia

*Corresponding author: andrianyrina@gmail.com

Orcid ID: 0000-0002-5456-8131

Submitted: 1 January 2025

Revised: 15 April 2025

Accepted: 22 April 2025

Abstract

Background: Lip balm moisturizes the lips and can be made from natural ingredients such as mango rhizome extract (*Curcuma mangga* Val), which is rich in antioxidants. **Objective:** This study aims to evaluate the formulation of lip balm with varying concentrations of mango rhizome extract and determine its optimal concentration. **Methods:** The research employs a qualitative and quantitative approach using 1 Kg of mango rhizome simplisia from Southeast Sulawesi. The lip balm formulations include extract concentrations of 0%, 5%, 10%, and 15%, involving ingredients such as mango rhizome extract, cera alba, olive oil, glycerin, BHT, nipasol, strawberry essence, D & C Red 6, and vaseline album. Evaluation was conducted through organoleptic tests, pH, homogeneity, adhesion, spreadability, melting point, cycling test, moisture, irritation, and panelist preference. All formulations demonstrated stability in color, texture, and aroma at room temperature and during the cycling test. Consistency, homogeneity, and pH of all formulas remained stable. **Results:** Spreadability and adhesion improved with the concentration of the extract, with Formula F3 (15% extract) showing the best results, including an increased melting point indicating thermal stability. All formulas were safe and did not cause irritation. Preference tests indicated that F3 was preferred for moisture, while F1 and F2 were favored for aroma and color. **Conclusion:** The mango rhizome extract lip balm is stable, safe, and effective as a lip moisturizer, with Formula F3 being the most effective. Future research is expected to develop other formulations from mango rhizome to enhance moisturizing effects while maintaining the stability of the preparation.

Keywords: lip balm, mango rhizome extract (*curcuma mangga val*), lip moisturizer, stability

How to cite this article:

Andriani, R., Ifaya, M., Fauziah, R., Trisnaputri D. R., Fitriah, W. O. I. & Qur'ani. (2025). Formulation of Lip Balm Extract of Temu Mangga Rhizome (*Curcuma mangga* Val) as Moisturizer. *Jurnal Farmasi dan Ilmu Kefarmasian Indonesia*, 12(1), 128-144. <http://doi.org/10.20473/jfiki.v12i12025.128-144>

INTRODUCTION

The development of cosmetics in the modern era has become a daily necessity for people to enhance their appearance. The use of cosmetics serves not only beauty but also health (Tranggono, 2007). Cosmetics are substances applied to the outer parts of the human body, such as the skin, hair, nails, lips, and external genital organs, as well as the teeth and mucous membranes of the mouth. They are primarily intended to cleanse, improve body odor, protect, or care for the body. Skin care cosmetic products, or skincare, are utilized to cleanse the skin (cleanser), moisturize the skin (moisturizer), and protect the skin (sunscreen) (Pusmarani, 2023).

Lips are a part of the body that need protection to maintain moisture. Lips do not have sweat glands or hair follicles, and they possess a thinner stratum corneum (Rasyadi et al., 2022). Damage to the lips can also be caused by exposure to UV rays from the sun, which harm the keratin cells in the lips that serve to protect them. When keratin cells are damaged, the lips may peel, appearing chapped, dry, and dull in color. Additionally, chapped lips can cause pain, appear less attractive, and make the skin of the lips even more unhealthy (Ambari et al., 2020).

Lip balm is a product that is applied to the lips that serves as a moisturizer by forming a protective layer of unmixed oil on the surface. The primary purpose of using lip balm is to enhance lip moisture (Kase et al., 2023). While the use of lip balm has become a lifestyle choice for many, it has also evolved into a necessity. However, numerous manufacturers incorporate hazardous chemicals as fundamental components of lip balm, which can irritate the lips and undermine the very purpose of the product. These synthetic ingredients may lead to side effects and even compromise the natural shape of the lips (Tampubolon, 2023).

Natural ingredients offer a safe alternative for formulating lip balm. One such ingredient is the rhizome of temu mangga (*Curcuma mangga* Val). This rhizome is rich in compounds such as curcumin, flavonoids, polyphenols, and p-hydroxycinnamic acid. The presence of flavonoids and curcumin in temu mangga is believed to be closely associated with its antioxidant activity (Zulkarnain et al., 2023). These antioxidants can help address lip issues by delaying or inhibiting the oxidation reactions of free radicals, which can lead to cellular damage (Erwan et al., 2022).

Research conducted by Susiloningrum and Mugita Sari (2021) evaluated the antioxidant activity and total flavonoid content in *temu mangga* rhizomes, with optimal results achieved using a 96% ethanol solvent.

Under these conditions, the flavonoid content was measured at $10.22 \pm 0.11\%$, and the IC₅₀ value was determined to be 75.06 ppm, indicating strong antioxidant activity. According to Zulkarnain (2023), temu mangga rhizomes are rich in flavonoids and curcumin, both of which exhibit antioxidant properties.

Pujumulyani (2020) stated that *temu mangga* rhizome can reduce oxidative stress caused by excessive exposure to free radicals and disruptions in the antioxidant system, which can accelerate the aging process. Additionally, *temu mangga* rhizome extract can also protect collagen from degradation and inhibit the activity of pro-inflammatory enzymes such as MMP1, MMP3, and MMP13. Furthermore, it helps maintain the health of human skin fibroblast cells that have been induced by free radicals, serving as a model for cellular aging.

In this study, the concentrations of *temu mangga* rhizome extract to be used in the lip balm preparation were 5%, 10%, and 15%. Based on research by Susiloningrum and Mugita Sari (2021), the cream preparation with a combination of temu mangga rhizome and zinc oxide showed the best results at a concentration of 5%. Additionally, Zulkarnain et al. (2023) found that a concentration of 10% also produced favorable outcomes, while Widyastuti (2017) reported that a concentration of 15% achieved optimal results in the formulation. Based on the background provided, the researcher is interested in conducting a study entitled "Lip Balm Formulation of Mango Ginger Rhizome Extract (*Curcuma mangga* Val) as a Lip Moisturizer. a lip balm using mango ginger rhizome extract and to compare different concentrations to determine which formulation exhibits the best characteristics.

MATERIALS AND METHODS

Materials

The materials used in this study included turmeric extract, 96% alcohol (Brataco), ammonia (Mitra Muda Berkah), BHT (Advent), magnesium metal powder (Mitra Muda Berkah), cera alba (Making Cosmetic), CI 15850, strawberry essence (Spectra), FeCl₃, glycerin (Palapa Muda Perkasa), HCl (Supelco), H₂SO₄ (Supelco), chloroform (Mitra Muda Berkah), nipasol (Mitra Muda Berkah), Mayer's reagent, Wagner's reagent, Dragendorf, and Vaseline album (Brataco), olive oil (NHR), and aquadest.

Tools

The tools utilized in this study included a stirring rod (Pyrex), glass beaker (Pyrex), porcelain cup (Pyrex), measuring cup (Pyrex), hand scoop (latex examination), hot plate (IKA C-MAG HS 7), watch glass (Pyrex),

object glass (Pyrex), filter cloth, oven (Memmert), universal pH meter (Nesco), dropper pipette (Pyrex), rotary evaporator (Stuart), skin moisture analyzer, test tube (Pyrex), and digital scales (Ohaus).

Method

Sampling

The samples used in this study were mango ginger rhizomes (*Curcuma mangga* Val) that were ready for harvest. These samples were obtained from Penanggo Jaya Village in the Lambandia District of East Kolaka Regency, Southeast Sulawesi.

Sample determination

The plant specimens were identified at Mandala Waluya University in Kendari. The purpose of this identification is to verify the authenticity of the samples used in the study. Plant identification is conducted by comparing the morphological characteristics of the specimens with descriptions found in existing literature (Ekayani et al., 2021).

Sample processing

The temu mangga rhizome samples were sorted to remove impurities, washed, and cut into pieces. They were then dried in the sun until completely dry, crushed using a blender, and sieved with a 60 mesh sieve to produce temu mangga powder (Bintoro et al., 2017).

Sample extraction

Extraction of temu mangga rhizome employing the maceration method involves soaking. Temu mangga powder is placed in a dark container, and 96% ethanol is added until the simplicia is fully submerged. The simplicia is stirred evenly, and then the vessel is tightly sealed. The maceration process is conducted for 3 x 24 hours, replacing the solvent daily and stirring several times, keeping it in a location protected from sunlight. The resulting macerate is filtered using filter paper with the assistance of a vacuum pump to separate it from the filtrate. The resulting filtrate is evaporated with a rotary evaporator at a temperature of 40°C to produce a thick extract (Ambari et al., 2020).

Phytochemical screening of mango rhizome extract (*Curcuma mangga* Val)

Alkaloid testing

A weighing 4 g was combined with an adequate amount of chloroform. Subsequently, 10 mL of ammonia was added, and the solution was filtered. The filtrate was then transferred to an Erlenmeyer flask, followed by the

addition of 10 drops of 2 N H₂SO₄. The mixture was shaken gently and allowed to sit until two distinct layers formed. The upper layer was carefully transferred to a test tube. The solution was then tested with Mayer, Wagner, and Dragendorff reagents. The formation of a precipitate indicates the presence of alkaloids: Meyer's reagent produces a white precipitate, Wagner's reagent yields a brown precipitate, and Dragendorff's reagent results in an orange precipitate (Rahmi et al., 2021).

Flavonoid test

The flavonoid test was conducted using 0.5 g of extract, to which 5 mL of ethanol was added. The mixture was then heated for approximately 5 minutes, after which 10 drops of concentrated hydrochloric acid (HCl) and 0.2 grams of magnesium powder were introduced. The formation of a reddish-black, yellow, or orange color indicates a positive result for flavonoids (Septia Ningsih et al., 2020).

Phenol test

The phenol test was conducted by adding 0.5 g of the extract to 3-4 drops of FeCl₃. A color change from bluish black to dark black indicates the presence of phenolic compounds (Septia Ningsih et al., 2020).

Saponin test

A total of 0.5 grams of extract was placed into a test tube, followed by the addition of 10 mL of previously heated distilled water. The mixture was shaken vigorously for approximately one minute. It was then allowed to sit for 10 minutes, during which the formation of foam was observed, indicating a positive result for saponins (Septia Ningsih et al., 2020).

Tannin test

The tannin test was conducted by adding 0.5 grams of extract to 10 mL of hot water, followed by with the addition of 1% FeCl₃. The formation of a blackish-green color indicates the presence of tannins (Septia Ningsih et al., 2020).

Steroid and terpenoid testing

A total of 0.5 g of extract was placed into a test tube, followed by the addition of 2 mL of concentrated H₂SO₄. The solution was gently shaken and allowed to sit for a few minutes. A blue to green color indicates a positive result for steroids, while a brownish red to purple color indicates a positive result for terpenoids (Septia Ningsih et al., 2020).

Table 1. Formula design of lip balm extract from mango ginger rhizome (*Curcuma mangga* Val)

Material	Function	F0	F1	F2	F3
Mango ginger rhizome extract	Active Substance	0%	5%	10%	15%
Glycerin	Humectant	8%	8%	8%	8%
Cera alba	Stiffening agent	15%	15%	15%	15%
Olive Oil	Oil	5%	5%	5%	5%
Nipasol	Preservative	0.2%	0.2%	0.2%	0.2%
BHT	Antioxidant	0.05%	0.05%	0.05%	0.05%
Strawberry Essence	Fragrance	1%	1%	1%	1%
CI 15850	Coloring	0.5%	0.5%	0.5%	0.5%
Vaseline album	Mass gainer/Base	ad 100%	ad 100%	ad 100%	ad 100%

Making lip balm preparations from mango ginger rhizome extract (*Curcuma mangga* Val.)

Melt the base of Vaseline, cera alba, and olive oil at a temperature of 60-65°C (Mixture A). In a separate container, mix Nipasol, BHT, and glycerin to create Mixture B. Gradually incorporate Mixture A into Mixture B while continuously stirring at a temperature of 50-55°C. Once the mixture is not too hot, add strawberry essence and CI 15850. While stirring, incorporate the extract of mango ginger (*Curcuma mangga* Val). Pour the mixture into a mold that has been coated with glycerin. Allow it to set at room temperature (Sholehah et al., 2022).

Physical evaluation of mango turmeric extract lip balm

Organoleptic test

Organoleptic testing utilizes human senses as the primary means of assessing the acceptability of a preparation. The types of tests conducted include evaluations of color, taste, smell, and shape (Ambari et al., 2020).

pH Test

The pH measurement was conducted using a Universal pH Indicator tool, with each formula replicated three times. The Universal pH Indicator was immersed in the lip balm preparation and allowed to sit for a few seconds. Subsequently, the color on the paper was compared to the comparator provided on the packaging. The pH of the lip balm preparation ranged from 4.5 to 6.5 (Ambari et al., 2020).

Homogeneity test

Each lip balm preparation containing the active ingredient, temu mangga rhizome extract, was evaluated for homogeneity by applying 1 gram of the formulation to a glass surface. The coarse particles were then assessed by touch, ensuring that the preparation exhibited a homogeneous composition with no visible coarse grains are visible (Ministry of Health of the Republic of Indonesia, 2020).

Spreadability test

A sample of lip balm weighing 0.5 grams was placed on a spreadability tester, which consisted of a glass plate with a scale paper base. The sample was covered with a previously weighed glass plate and allowed to rest for 1 minute. The diameter of the lip balm spread was measured from various angles, and the average was calculated. This process was repeated three times, with incremental loads added periodically (50 g, 100 g, 150 g, 200 g) (Ambari et al., 2020). Good spreadability for lip balm preparations is between 3 and 5 cm (Pawestri et al., 2024).

Adhesive power test

The lip balm preparation sample was weighed to a mass of 0.25 grams and then placed on a glass object. Two glass objects were joined together until they were united. A load of 1 kg was applied for 5 minutes, after which it was removed. Subsequently, a load of 80 grams was applied, and the time was recorded until the two glass objects were separated. This procedure was replicated three times (Ambari et al., 2020). A good adhesive power is defined as lasting more than 4 seconds (Pawestri, et al 2024).

Melting point test

The method for determining the melting point of lip balm involves placing the lip balm in an oven set to an initial temperature of 50°C for 15 minutes to observe whether it melts. After this initial period, the temperature is increased by 1°C every 15 minutes, and observations are made to identify the temperature at which the lip balm begins to melt. The melting point specifications for lip balm are based on SNI 5769-1998, which stipulates a range of 50-70°C, with the experiment being replicated three times under the same conditions. According to Pertiwi (2020), a quality lip balm should have a melting point above 50°C (Tampubolon, 2023).

Stability test (cycling test)

The cycling stability test evaluates the stability of the preparation by storing it at specific temperatures and

humidity levels over designated intervals. The temperature storage is conducted at 4°C and 40°C for 24 hours (one cycle), with three replicates for each condition. The test is performed for a total of six cycles, and each cycle is monitored for physical changes (Abdul et al., 2022)

Moisture test

This test involved 20 panelists, divided into four groups. Five researchers utilized formula 0, while five panelists each used formulas F1, F2, and F3. The moisture test for the lip balm preparation was conducted by applying the product to the panelists' lower arms every morning and evening. This test was carried out for 12 days, with measurements taken daily. Observations of the results were made by directly assessing physical changes and measuring skin moisture with a skin moisture analyzer. The skin moisture analyzer (U-trac Model: CR-302) employs sensor technology to gauge the skin's moisture levels. It analyzes the skin's ability to conduct electrical signals, which are then processed to determine whether the skin is dry, normal, or hydrated. The measurement results are presented in numerical form or as graphs, indicating the percentage of skin moisture (Imani, 2022).

Irritation test of preparations

The technique employed in this irritation test is an open patch test conducted on the inner lower arm of 20 panelists who have provided written consent. The open patch test involves applying the preparation to a designated area (2.5 x 2.5 cm) and leaving it uncovered to observe any reactions (ethical clearance 004/KEP/UMW/II/2024). This test is performed three times a day over two consecutive days (Ambari et al., 2020). The inclusion criteria for the irritation test are as follows: female participants aged 20 to 30 years, who are physically and mentally healthy, have no history of allergic diseases, and have expressed their willingness to participate. The preparation is deemed acceptable if the researcher does not observe any irritation reactions, such as erythema, papules, vesicles, or edema (Sariwating and Wass, 2020).

Preference test (hedonic test)

The preference test was conducted visually with 20 panelists. Each panelist was instructed to apply the prepared formula to the skin on their wrist. Subsequently, the panelists selected the formula variation they preferred the most. They rated their preferences using a scale: 1 for strong dislike, 2 for dislike, 3 for like, and 4 for strong like. Panelists completed the provided questionnaire, which assessed

observation parameters in the preference test, including ease of application (texture), aroma, color, and the level of moisture felt on the skin (Tampubolon, 2023).

RESULTS AND DISCUSSION

This study commenced with the collection and processing of 1,000 grams of temu mangga (*Curcuma mangga* Val) rhizome samples from Penanggo Jaya Village, Lambandia District, East Kolaka Regency, Southeast Sulawesi. The initial procedure involved wet cleaning to eliminate dirt from the rhizomes, followed by cutting to reduce the sample size for easier drying. The samples were then sun-dried using a black cloth until completely dry, after which they were crushed using a blender. The identity of this plant was verified at the Pharmacognosy-Phytochemistry Laboratory of Mandala Waluya University in Kendari, confirming it as the *Curcuma mangga* Val species.

Rhizome extraction is performed using the maceration method, which involves soaking powdered *simplicia* in a solvent. This method was selected for its simplicity and its ability to preserve thermolabile compounds. Ethanol is utilized as the solvent due to its universal, polar nature and its availability (Asworo and Widwastuti, 2023). A 96% ethanol solution was chosen for its selective properties, non-toxicity, effective absorption, and high extraction capacity, enabling it to extract non-polar, semi-polar, and polar compounds (Wendersteyt et al., 2021).

The ginger mango rhizome powder is placed in a dark container, and 96% ethanol is added until the herbal material is fully submerged. The mixture is stirred thoroughly, and the vessel is sealed tightly. The maceration process is conducted for three days, with periodic stirring, and is kept in a location protected from sunlight. Stirring is intended to facilitate a more rapid equilibrium of the extracted material's concentration in the solvent. Subsequently, the initial brown macerate is filtered. The residue is then soaked again in the solvent during the remaceration process, which involves adding fresh solvent to the remaining herbal material to optimize the extraction of active compounds. Remaceration continues until a clear-colored macerate is obtained, indicating that no more soluble compounds remain (Alviola Bani et al., 2023).

After the maceration process, the filtrate was separated using a vacuum pump to eliminate any remaining liquid. Subsequently, the filtrate was evaporated with a rotary evaporator at a temperature of 40°C to prevent damage to the compounds from

excessive heat, while also concentrating the extract and removing 96% ethanol solvent from the rhizome of temu mangga (*Curcuma mangga* Val) through the principle of solvent evaporation. The concentration process continued until a constant weight was achieved over three days (Ambari et al., 2020).

The yield of *temu mangga* rhizome extract was measured at 11.21%, as presented in Table 2. This extract is characterized by its brown color, thick consistency, distinctive odor, and bitter taste. The yield exceeds the minimum requirement of 10.7% set by the Indonesian Ministry of Health (2017). Table 3 displays the results of the phytochemical screening, indicating that the *temu mangga* rhizome extract contains various compounds. The extract also yielded positive results for several phytochemical constituents: flavonoids (indicated by a reddish-black color when treated with HCl and Mg), phenols (dark red color with FeCl₃), saponins (stable foam formation with hot distilled water), tannins (blackish-green color with 1% FeCl₃), and terpenoids (brownish-red color with concentrated H₂SO₄) (Septia Ningsih et al., 2020).

Based on the standard formula proposed by Sholehah et al. (2022), the lip balm formulation incorporating ethanol extract of *temu mangga* rhizome was modified to enhance physical stability and moisturizing properties, attributed to its antioxidant content. This formulation includes ethanol extract of *temu mangga* rhizome at concentrations of 5%, 10%, and 15%, along with additional ingredients such as cera alba (15%), glycerin (8%), olive oil (5%), nipasol

(0.2%), BHT (0.05%), strawberry essence (1%), CI 15850 dye (0.5%), and vaseline album, totaling 100%. Cera alba is utilized to improve consistency at a concentration of 15%, glycerin serves as a humectant at 8%, olive oil acts as an oil base at 5%, nipasol functions as a preservative at 0.2%, BHT is included as an antioxidant at 0.05%, strawberry essence provides fragrance at 1%, and CI 15850 dye (D&C Red 6) is used at 0.5%. Vaseline album is incorporated as a fat base, with a total weight of up to 5 grams.

A physical stability evaluation was conducted on days 0, 7, 14, 21, and 28 at room temperature. The evaluation included a Cycling Test consisting of 6 cycles to assess the stability of the lip balm. Various parameters were examined, including organoleptic properties, homogeneity, pH, spreadability, adhesion, melting temperature, humidity, irritation, and preference tests (hedonic).

The room temperature stability test and temperature cycle test are crucial for ensuring the stability and effectiveness of mango ginger rhizome extract lip balm. The room temperature stability test evaluates the performance of the lip balm at ambient conditions, confirming that there are no changes in color, texture, or efficacy. In contrast, the temperature cycle test simulates extreme temperature fluctuations to verify that the quality of the lip balm is preserved during storage. Both tests are essential for ensuring that the lip balm retains its optimal moisturizing benefits as a lip moisturizer under various conditions (Pertiwi and Unggul, 2023).

Table 2. Results of extraction of mango ginger rhizome (*Curcuma mangga* val)

Solvent	Powder Weight(gram)	Extract Color	Extract Weight (gram)	% Yield
Etanol 96 %	1000	Brown	112.1	11.21

Table 3. Phytochemical screening results

No	Type of testing	Reagen	Result	Information
1	Alkaloid Test	Mayer	No sediment	(-)
		Dragendoff	There is orange sediment	(+)
		Wagner	There is brown sediment	(+)
2	Flavonoid Test	Concentrated HCl and Powder Mg	Blackish red color	(+)
3	Fenol Test	FeCl ₃	Dark black color	(+)
4	Tanin Test	FeCl ₃ 1%	Greenish black color	(+)
5	Saponin Test	Aquadest Hot	Forms a stable foam	(+)
6	Triterpenoid Test	H ₂ SO ₄ Pekat	Brownish red color	(+)

The organoleptic test revealed that F0 (without extract) was pink, F1 was pink, F2 was red, and F3 was brick red. After 4 weeks, there was no change in shape, color, or aroma, indicating the stability of the preparation. Organoleptic testing during the Cycling Test showed that the F0, F1, F2, and F3 preparations maintained their original color, with no change before and after the Cycling Test. The correlation between the results of room temperature storage and the Cycling Test indicated that the preparation exhibited high stability against various environmental conditions. Thus, the resulting lip balm demonstrates good quality and can be relied upon during storage and use.

The observation results regarding the consistency of all lip balm formulas indicate that all samples have a soft texture, making them easy to apply to the lips. This softness is attributed to the use of a cera alba base, which is one of the components in oil-in-water (o/w) preparations, ensuring ease of application, good spreadability on the skin, and a soft texture. Additionally, the inclusion of Vaseline album as a mass enhancer and softener further contributes to the softness and ease of application of the product (Sholehah et al., 2022).

The homogeneity test was conducted by applying 1 gram of the preparation to a glass object, demonstrating that all formulas (F0, F1, F2, F3) did not contain coarse grains for 28 days, both before and after storage, indicating good homogeneity (Ambari et al., 2020). Homogeneity testing during the Cycling Test also revealed no changes in all preparations. This is attributed to the method of making lip balm, which employs a melting technique where the ingredients are heated until completely melted to ensure a homogeneous

mixture (Desnita et al., 2022). Research by Nurul Afriyanti Yusuf (2019) also indicated that the use of cera alba base in lip balm formulations produced good homogeneity, confirming that the cera alba base influences the homogeneity of the preparation (Sholehah et al., 2022).

The pH test was conducted using universal pH paper. The results of the test, shown in Table 4, indicate that preparations F0, F1, F2, and F3 maintained a pH of 5 for 28 days, both before and after storage. The pH cycling test of lip balm preparations F0, F1, F2, and F3 also showed a pH of 5 before and after the cycling test. This indicates a stable pH, meeting the requirements for a good lip balm pH, which is 4.5-6.5 according to Tranggono (2007).

Based on the results of the spreadability test of the lip balm preparation using the ethanol extract of temu mangga rhizome (*Curcuma mangga* Val), there was an increase in spreadability over 28 days. The F0 preparation increased from 3.39 cm to 3.72 cm; F1 went from 3.35 cm to 3.75 cm; F2 rose from 3.31 cm to 3.48 cm; and F3 improved from 3.38 cm to 3.50 cm. In the cycling test for spreadability, results were gathered for all formulations (F0-F3). Formulation F0 (without temu mangga rhizome) exhibited the smallest increase, from 3.51 ± 0.21 cm to 3.59 ± 0.09 cm. Meanwhile, formulation F1, which contains 5% temu mangga rhizome, showed a more significant increase, rising from 3.53 ± 0.20 cm to 3.79 ± 0.19 cm. Formulations F2 (10%) and F3 (15%) also demonstrated an increase in spreadability. This increase suggests that higher extract concentrations enhance the stability of spreadability (Pawestri et al., 2024).

Table 4. Organoleptic examination

Preparation	Inspection	Day-to-Day Observations				
		0	7	14	21	28
F0 (0%)	Color	Pink	Pink	Pink	Pink	Pink
F1 (5%)		Pink	Pink	Pink	Pink	Pink
F2 (10%)		Red	Red	Red	Red	Red
F3 (15%)		Brick red	Brick red	Brick red	Brick red	Brick red
F0 (0%)	Aroma	Strawberry	Strawberry	Strawberry	Strawberry	Strawberry
F1 (5%)		Strawberry	Strawberry	Strawberry	Strawberry	Strawberry
F2 (10%)		Strawberry	Strawberry	Strawberry	Strawberry	Strawberry
F3 (15%)		Strawberry	Strawberry	Strawberry	Strawberry	Strawberry
F0 (0%)	Consistency	Semi Solid	Semi Solid	Semi Solid	Semi Solid	Semi Solid
F1 (5%)		Semi Solid	Semi Solid	Semi Solid	Semi Solid	Semi Solid
F2 (10%)		Semi Solid	Semi Solid	Semi Solid	Semi Solid	Semi Solid
F3 (15%)		Semi Solid	Semi Solid	Semi Solid	Semi Solid	Semi Solid

The adhesion test indicated that all formulas (F0, F1, F2, and F3) satisfied the adhesion requirements of over 4 seconds after being stored for 28 days. Increased adhesion was also observed in all formulas following the Cycling Test. Formula F0 (without extract) improved from 12.47 seconds to 13.47 seconds, F1 (with 5% extract) from 12.50 seconds to 13.98 seconds, F2 (10% extract) from 13.92 seconds to 14.40 seconds, and F3 (15% extract) from 14.03 seconds to 14.68 seconds. The most significant increase was noted in F3. All formulations met the criteria for good adhesion testing, defined as exceeding 4 seconds. During six cycles of stability testing, the adhesion test values showed a trend of increasing, suggesting that the active substance was strongly retained within the formulation base, thereby enhancing the adhesion duration. Augmenting the concentration of temu mangga rhizome extract in lip balm led to an improved adhesion capacity.

The test results show that all lip balm formulas meet the criteria for a good adhesion test, which is more than 4 seconds. During the six cycles of stability testing, the adhesion value tends to increase. After the cycling test, the adhesion duration becomes longer because the active substance is strongly bound in the formulation base, affecting the increase in adhesion time. Higher concentrations of temu mangga rhizome extract in the formulation produce greater adhesion, increasing the duration of contact between the preparation and the skin, as well as the effectiveness of the delivery of active substances (Ridhani et al., 2022). Adhesion is greatly influenced by the viscosity of the preparation base (Priawanto, 2017). Vaseline album, which is used in the formulation, can reduce the consistency of the preparation, making it thinner (Alfilaili et al., 2021). In the formulation, the concentration of vaseline album in F0 yields the thinnest preparation consistency or the lowest viscosity. A decrease in the viscosity of the preparation can lead to a decrease in adhesive power (Lumentut et al., 2020).

At room temperature, the melting point of lip balm gradually increased for all formulas, indicating enhanced thermal stability over time. An increase in melting point was also observed after the cycling test, but this change was not as pronounced as that seen during room temperature storage. There was a positive relationship between extract concentration and the increase in melting point, both at room temperature and during the cycling test. The effect of room temperature storage appeared to be more significant than the cycling test regarding the increase in melting point.

The addition of ethanol extract from temu mangga rhizome increases the melting point of lip balm, with a more significant increase occurring during room temperature storage compared to the cycling test. This indicates that the formulation containing the extract is more thermally stable, particularly at room temperature. The higher the concentration of the extract, the higher the melting point of the lip balm preparation (Hayati et al., 2024). The obtained melting point meets the SNI 16-5769-1998 standard (50-70°C), although the ideal melting temperature for lip balm should be close to body temperature (36-38°C). A higher temperature (55-75°C) was chosen to enhance resistance to tropical conditions and maintain shape during distribution, storage, and use (Tampubolon, 2023).

The results of the humidity test demonstrated the impact of the concentration of the preparation on the changes in the parameters measured over several days of observation, both in the morning and evening. Group F0 (0%) exhibited minimal changes in parameters, with differences ranging from 1.2 to 3.6. Group F1 (5%) experienced a greater increase in the difference compared to F0, ranging from 4.2 to 6.2. Group F2 (10%) showed a more substantial increase, with a difference reaching up to 9.0. Meanwhile, group F3 (15%) displayed the most dramatic increase, with a difference reaching 20.4 in the morning and 19.2 at night.

Lip balm moisture testing was conducted in the morning and evening to obtain a comprehensive understanding of the product's effectiveness in various situations. In the morning, lips are typically drier after waking up, while at night, they have been exposed to various environmental factors throughout the day. By testing at these two times, researchers can assess the lip balm's ability to retain moisture and provide maximum protection, both during activities and while resting. This test also reflects daily usage patterns, where lip balm is usually applied in the morning and evening, making the test results more relevant and applicable (Bielfeldt et al., 2019).

These findings can be explained by the skin hydration theory, which highlights the importance of balancing water content in the stratum corneum with the rate of water evaporation from the skin surface (Mojumdar et al., 2017). Mango turmeric extract in lip balm works to enhance hydration through two mechanisms: creating a barrier to reduce water evaporation (occlusive effect) and attracting moisture from the environment into the skin (Azmin et al., 2020).

The effectiveness of this lip balm can be understood through the theory of active ingredient penetration. Increasing the concentration of temu mangga extract creates a greater concentration gradient, facilitating the penetration of active ingredients into the skin layers of the lips. This explains why Formula 3, with the highest concentration, showed the most significant moisturizing effect. Although the increased concentration of the extract resulted in enhanced moisturizing properties, the right formulation must consider the overall balance and stability of the preparation (Dal'Belo et al., 2006).

A study by Yuandanandi et al. (2021) on Curcuma mango extract showed high antioxidant activity, which may contribute to skin protection from oxidative damage. This aligns with the findings of this study, where increasing the concentration of the extract resulted in a better moisturizing effect, which may also provide additional skin protection benefits.

A study by Zang et al (2024) investigated the dose-response relationship between the concentration of natural active ingredients in skincare products and their effectiveness. The researchers discovered that higher concentrations did not always correlate linearly with increased effectiveness, highlighting the significance of

formula optimization. This finding is pertinent to the results of the current study, as Formula 3 demonstrated the best outcomes; however, further optimization may still be necessary.

A lip balm irritation test was conducted to ensure that the lip balm does not irritate the lips. Irritation is categorized into primary irritation, which occurs immediately after contact with the skin, and secondary irritation, which occurs several hours later. The irritation test employed an open patch test on the forearms of 20 panelists who consented to participate. The preparation was applied to an area measuring 2.5 x 2.5 cm, left uncovered, and observed three times a day for two days. Inclusion criteria required participants to be women aged 20-30 years, physically and mentally healthy, with no history of allergies, and willing to serve as panelists. The reactions monitored included erythema, papules, vesicles, and edema. The test results indicated that all formulations (F0, F1, F2, and F3) did not elicit irritation reactions in the panelists, as they had a pH of 5, which is within the skin's normal pH range of 4.5-6.5. A preparation is considered safe if it does not cause irritant reactions on the skin.

Table 5. Homogeneity test results

Preparation	Day to Day Observations				
	0	7	14	21	28
F0 (0%)	Homogen	Homogen	Homogen	Homogen	Homogen
F1 (5%)	Homogen	Homogen	Homogen	Homogen	Homogen
F2 (10%)	Homogen	Homogen	Homogen	Homogen	Homogen
F3 (15%)	Homogen	Homogen	Homogen	Homogen	Homogen

Table 6. Results of pH test

Preparation	Day-to-Day Observations					Acceptance Parameter
	0	7	14	21	28	
F0 (0%)	5.00±0,00	5.00±0,00	5.00±0,00	5.00±0,00	5.00±0,00	4.5-6.5
F1 (5%)	5.00±0,00	5.00±0,00	5.00±0,00	5.00±0,00	5.00±0,00	
F2 (10%)	5.00±0,00	5.00±0,00	5.00±0,00	5.00±0,00	5.00±0,00	
F3 (15%)	5.00±0,00	5.00±0,00	5.00±0,00	5.00±0,00	5.00±0,00	

Table 7. Spreading power test results

Preparation	Day-to-Day Observations				
	0 (cm)	7 (cm)	14 (cm)	21 (cm)	28 (cm)
F0 (0%)	3.31±0.15	3.31±0.16	3.34±0.14	3.47±0.20	3.72±0.17
F1 (5%)	3.35±0.19	3.32±0.17	3.41±0.15	3.45±0.13	3.75±0.17
F2 (10%)	3.38±0.13	3.41±0.18	3.43±0.16	3.47±0.19	3.48±0.13
F3 (15%)	3.39±0.17	3.44±0.20	3.46±0.19	3.46±0.16	3.50±0.17

Table 8. Results of adhesion power test

Preparation	Day-to-Day Observations				
	0 (det)	7 (det)	14 (det)	21 (det)	28 (det)
F0 (0%)	12.45±1.64	12.50±0.61	12.57±1.54	13.47±0.57	13.65±0.59
F1 (5%)	12.47±1.05	12.55±0.84	12.74±0.39	10.84±0.33	13.82±0.44
F2 (10%)	12.50±0.70	12.70±1.93	12.77±0.92	10.83±0.37	14.51±1.02
F3 (15%)	12.59±0.87	13.01±1.67	13.92±0.56	14.06±0.17	14.63±1.00

Table 9. Melting point test results

Preparation	Day-to-Day Observations				
	0 (°C)	7 (°C)	14 (°C)	21 (°C)	28 (°C)
F0 (0%)	54.0±0.00	55.1±0.00	56.5±0.00	57.0±0.00	58.5±0.00
F1 (5%)	59.0±0.00	60.0±0.00	61.1±0.00	63.0±0.00	64.0±0.00
F2 (10%)	60.0±0.00	61.0±0.00	61.5±0.00	62.0±0.00	63.0±0.00
F3 (10%)	61.0±0.00	62.0±0.00	63.0±0.00	63.5±0.00	64.0±0.00

Table 10. Organoleptic cycling test results

Formula	Inspection	Observation Cycling Test	
		Before	After
F0 (0%)	Color	Pink	Pink
F1 (5%)		Pink	Pink
F2 (10%)		Red	Red
F3 (15%)		Brick red	Brick red
F0 (0%)	Aroma	Strawberry	Strawberry
F1 (5%)		Strawberry	Strawberry
F2 (10%)		Strawberry	Strawberry
F3 (15%)		Strawberry	Strawberry
F0 (0%)	Dosage Form	Semi Solid	Semi Solid
F1 (5%)		Semi Solid	Semi Solid
F2 (10%)		Semi Solid	Semi Solid
F3 (15%)		Semi Solid	Semi Solid

Table 11. Cycling test homogeneity test results

Formula	Homogeneity Examination Result	
	Before	After
F0 (0%)	Homogen	Homogen
F1 (5%)	Homogen	Homogen
F2 (10%)	Homogen	Homogen
F3 (15%)	Homogen	Homogen

Table 12. pH cycling test results

Formula	Observation Cycling Test		Acceptance Parameter
	Before	After	
	Accelerated	Accelerated	
F0 (0%)	5.00±0.00	5.00±0.00	4.5-6.5
F1 (5%)	5.00±0.00	5.00±0.00	
F2 (10%)	5.00±0.00	5.00±0.00	
F3 (15%)	5.00±0.00	5.00±0.00	

Table 13. Spreadability test results cycling test storage

Formula	Spread Power Test Observation	
	Before (cm)	After (cm)
F0 (0%)	3.53±0.25	3.59±0.09
F1 (5%)	3.51±0.21	3.79±0.19
F2 (10%)	3.60±0.23	3.70±0.10
F3 (15%)	3.53±0.20	3.75±0.16

Table 14. Cycling test storage adhesion test results

Formula	Observation of Adhesion Test	
	Before (det)	After (det)
F0 (0%)	12.47±1.05	13.47±0.57
F1 (5%)	12.50±0.61	13.98±0.37
F2 (10%)	13.92±0.56	14.40±0.15
F3 (15%)	14.03±0.84	14.68±0.40

Table 15. Melting point test results storage cycling test

Formula	Before (°C)	After (°C)
F0 (0%)	59.7±0.00	62.0±0.00
F1 (5%)	61.0±0.00	62.8±0.00
F2 (10%)	62.0±0.00	63.0±0.00
F3 (15%)	63.0±0.00	64.0±0.00

Table 16. Humidity Test Results

Formula	Day Ke-	Before (SD)	After (SD)	Difference (SD)
F0 (0%) Morning	1	36.8 ±2.59	38.6±2.07	1.8 ±3.32
	2	39.0±4.06	41.2±4.21	2.2 ±5.85
	3	37.4±2.51	39.2±2.39	1.8 ±3.47
	4	36.4±1.14	39.2±1.10	2.8 ±1.59
	5	39.8±2.39	42.2±3.27	2.4 ±4.05
	6	38.2±2.49	40.0±2.24	1.8 ±3.35
	7	37.0±1.00	39.4±0.55	2.4 ±1.14
	8	35.0±3.16	38.6±2.30	3.6 ±3.91
	9	40.8±1.30	43.6±2.61	2.8 ±2.92
	10	37.6±3.05	40.4±2.61	2.8 ±4.01
	11	38.6±2.88	41.8±2.59	3.2 ±3.87
	12	37.4±2.07	40.4±1.52	3.0 ±2.57
F1 (5%) Morning	1	35.4±2.61	41.6±2.88	6.2 ±3.88
	2	37.6±2.07	42.4±3.65	4.8 ±4.20
	3	37.0±1.41	42.2±1.79	5.2 ±2.28
	4	37.0±1.00	41.6±2.07	4.6 ±2.30
	5	37.8±2.59	42.2±3.77	4.4 ±4.58
	6	35.8±2.86	40.0±3.67	4.2 ±4.65
	7	34.4±2.30	40.4±3.13	6.0 ±3.88
	8	37.6±1.82	43.2±1.64	5.6 ±2.45
	9	37.2±1.10	43.0±1.22	5.8 ±1.64
	10	36.6±1.67	42.2±1.79	5.6 ±2.45
	11	38.0±2.74	43.8±2.05	5.8 ±3.42
	12	38.4±0.55	43.8±0.84	5.4 ±1.01
F2 (10%) Morning	1	38.0±2.24	47.0±5.15	9.0 ±5.61
	2	38.4±1.95	44.2±2.49	5.8 ±3.16
	3	37.2±1.79	44.0±1.58	6.8 ±2.39
	4	38.0±2.12	45.4±3.21	7.4 ±3.84
	5	35.0±1.87	41.6±1.95	6.6 ±2.70
	6	37.6±2.41	43.6±3.36	6.0 ±4.14
	7	37.0±1.22	44.4±2.61	7.4 ±2.88
	8	35.6±2.51	42.6±2.97	7.0 ±3.88
	9	38.6±3.91	44.8±3.35	6.2 ±4.83

F3 (15%) Morning	10	39.2±2.49	47.6±1.14	8.4 ±2.74
	11	36.8±2.95	44.6±3.85	7.8 ±4.85
	12	37.0±1.58	44.4±1.95	7.4 ±2.51
	1	39.6±2.30	57.6±5.37	18.0 ±5.84
	2	39.8±2.39	59.0±2.24	19.2 ±3.28
	3	40.2±1.64	58.0±3.46	17.8 ±3.83
	4	40.8±1.92	60.0±0.00	19.2 ±1.92
	5	39.6±5.32	54.6±5.55	15.0 ±7.69
	6	38.4±1.34	55.8±4.55	17.4 ±4.74
	7	38.6±1.52	59.0±2.24	20.4 ±2.71
	8	39.6±1.67	58.2±3.49	18.6 ±3.87
	9	39.2±1.48	59.6±0.89	20.4 ±1.73
F0 (0%) Evening	10	40.0±1.58	55.8±4.38	15.8 ±4.66
	11	39.0±3.67	57.8±4.92	18.8 ±6.13
	12	39.8±3.03	56.0±4.18	16.2 ±5.16
	1	37.2±3.56	39.2±3.03	2.0 ±4.67
	2	37.4±2.30	38.6±2.41	1.2 ±3.33
	3	37.8±2.17	40.2±2.28	2.4 ±3.15
	4	38.4±1.82	39.8±1.64	1.4 ±2.45
	5	40.2±2.95	42.2±2.59	2.0 ±3.93
	6	36.0±1.73	37.8±2.17	1.8 ±2.78
	7	38.6±1.14	41.2±0.84	2.6 ±1.42
	8	37.2±1.48	40.6±1.14	3.4 ±1.87
	9	39.2±2.59	41.4±2.61	2.2 ±3.68
F1 (5%) Evening	10	39.6±2.07	42.2±2.05	2.6 ±2.91
	11	37.2±1.79	40.4±1.52	3.2 ±2.35
	12	39.6±0.89	42.4±1.14	2.8 ±1.45
	1	36.4±1.67	41.8±1.48	5.4 ±2.23
	2	36.8±1.64	41.6±1.14	4.8 ±2.00
	3	37.0±3.39	41.4±3.97	4.4 ±5.22
	4	39.0±0.71	43.8±1.10	4.8 ±1.31
	5	38.6±1.52	43.6±1.52	5.0 ±2.15
	6	38.0±2.35	43.4±2.30	5.4 ±3.29
	7	37.8±1.79	42.4±2.30	4.6 ±2.91
	8	38.0±3.16	42.8±3.03	4.8 ±4.38
	9	39.0±2.24	44.2±2.17	5.2 ±3.12
F2 (10%) Evening	10	38.6±1.67	42.8±3.56	4.2 ±3.93
	11	37.4±1.82	43.2±2.95	5.8 ±3.47
	12	40.0±1.22	45.6±1.14	5.6 ±1.67
	1	36.4±0.55	42.8±3.11	6.4 ±3.16
	2	38.0±2.35	46.8±2.17	8.8 ±3.20
	3	37.6±1.95	43.6±2.88	6.0 ±3.48
	4	37.0±1.58	44.4±4.04	7.4 ±4.34
	5	38.2±1.79	43.8±3.03	5.6 ±3.52
	6	36.8±1.48	42.6±1.95	5.8 ±2.45
	7	36.6±2.19	41.8±1.48	5.2 ±2.64
	8	37.4±1.14	44.2±1.30	6.8 ±1.73

	9	36.6±2.30	45.6±2.61	9.0 ±3.48
	10	37.6±1.67	43.8±1.64	6.2 ±2.34
	11	37.8±2.17	46.0±1.87	8.2 ±2.87
	12	37.8±1.10	44.2±1.48	6.4 ±1.84
	1	42.2±3.49	59.0±2.24	16.8 ±4.15
	2	42.0±3.24	59.4±1.34	17.4 ±3.51
	3	40.6±2.70	57.0±4.80	16.4 ±5.51
	4	40.0±2.65	56.6±4.72	16.6 ±5.41
	5	40.0±1.22	58.8±1.79	18.8 ±2.17
F3 (15%)	6	41.8±2.59	59.4±1.34	17.6 ±2.92
Evening	7	40.6±0.89	57.4±3.71	16.8 ±3.81
	8	38.8±2.49	58.0±2.74	19.2 ±3.70
	9	40.4±2.51	59.0±2.24	18.6 ±3.37
	10	38.6±2.07	57.0±4.00	18.4 ±4.50
	11	41.2±0.84	57.6±2.19	16.4 ±2.35
	12	40.8±1.79	59.2±1.79	18.4 ±2.53

Table 17. Preparation Irritation Test Results

Formula	Eritema	Eritema and Papula	Eritema, Papula, and Vesikula	Edema and Vesikula
F0 (0%)	-	-	-	-
F1 (5%)	-	-	-	-
F2 (10%)	-	-	-	-
F3 (15%)	-	-	-	-

Table 18. Hedonic test results

Formula	Indicator			
	Texture	Aroma	Color	Hummadity
F0 (0%)	63	71	67	54
F1 (5%)	62	72	72	62
F2 (10%)	65	68	64	68
F3 (15%)	72	65	65	73

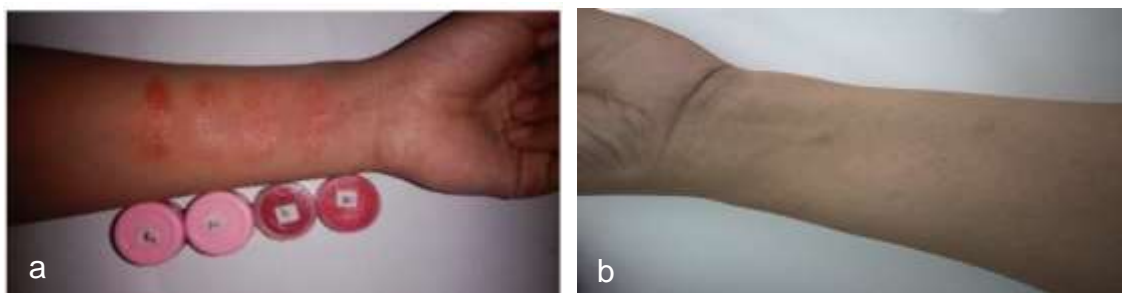


Figure 1. Irritation test on the formulation (a) application of the formulation (b) test results showing no irritation reaction

Description:

Erythema (Redness)	: +
Erythema & Papules (Redness & Small solid bumps in red)	: ++
Erythema, Papules & Vesicles (Redness, small solid bumps in red and small blisters containing fluid)	: +++
Edema & Vesicles (Swelling and small blisters containing fluid)	: ++++
No reaction	: -

CONCLUSION

The lip balm containing temu mangga rhizome extract from all formulations demonstrated good stability regarding color, aroma, consistency, homogeneity, and pH. Formula F3, which contains 15% extract, excelled in spreadability, adhesion, and thermal stability, making it the most preferred option for moisture retention. Formulas F1 and F2 were favored for their pleasant aroma and appealing color. All formulations were found to be safe and non-irritating.

The lip balm containing turmeric rhizome extract (*Curcuma mangga* Val) in formulations F1, F2, and F3 significantly enhanced moisture levels, with F3 (15%) demonstrating the highest effectiveness in moisture retention. The effectiveness of the extract in moisturizing the lips increases with higher concentrations. Future research should aim to develop additional formulations that incorporate turmeric rhizome (*Curcuma mangga* Val) for moisturizing benefits, thereby broadening its applications. Furthermore, increasing the concentration of the extract in the formulation may yield a more optimal moisturizing effect while maintaining product stability.

ACKNOWLEDGEMENTS

We would like to express our gratitude to Mandala Waluya University and all parties who contributed to this research, particularly the supervisors, colleagues, respondents, and institutions that provided support and resources. This research was made possible through their assistance and the support of product stability.

REFERENCES

- Ambari, Y., Rahmawati, M., Andayani, R., & Zulkifli, M. (2020) 'Studi Formulasi Sediaan *Lip balm* Ekstrak Kayu Secang (*Caesalpinia sappan* L.) dengan Variasi Beeswax', *Journal of Islamic Pharmacy*, 5(2), pp. 36–45. Available at: <https://doi.org/10.18860/jip.v5i2.10434>.
- Bani, A., Ilham, F., Rahman, A., & Muchtar, A.. (2023) 'Rasio Nilai Rendamen dan Lama Ekstraksi Maserat Etanol Daging Buah Burahol (*Stelecocharpus burahol*) Berdasarkan Cara Preparasi Simplisia', *Makassar Natural Product Journal*, 1(3), pp. 176–184. Available at: <https://journal.farmasi.umi.ac.id/index.php/mnpj>.
- Arizona, M. and Zulkarnain, A.K. (2018) 'Optimasi Formula dan Uji Aktivitas Secara In Vitro Lotion O/W Ekstrak Etanolik Rimpang Temu Mangga (*Curcuma mangga* Val. dan van Zijp) sebagai Tabir Surya', *Majalah Farmaseutik*, 14(1), p. 29. Available at: <https://doi.org/10.22146/farmaseutik.v14i1.41926>.
- Aulia, M.I., Rustikawati and Inorihah, E. (2020) 'Respon temu putih dan temu mangga dengan pemberian BA dan 2,4-D secara in vitro', *Gema Agro*, 25(2), pp. 92–102.
- Azmin, S.N.H.M., Jaïne, N.I.M. and Nor, M.S.M. (2020) 'Physicochemical and sensory evaluations of moisturising *Lip balm* using natural pigment from *Beta vulgaris*', *Cogent Engineering*. Edited by H. Arellano-Garcia, 7(1), p. 1788297. Available at: <https://doi.org/10.1080/23311916.2020.1788297>.
- Badaring, D.R., Sumarsa, J., & Pratama, R. (2020) 'Uji Ekstrak Daun Maja (*Aegle marmelos* L.) terhadap Pertumbuhan Bakteri *Escherichia coli* dan *Staphylococcus aureus*', *Indonesian Journal of Fundamental Sciences*, 6(1), p. 16. Available at: <https://doi.org/10.26858/ijfs.v6i1.13941>.
- Bielfeldt, S., Götz, S., Meier, M., Kapp, A., & Schaller, M. (2019) 'Deposition of plant lipids after single application of a lip care product determined by confocal raman spectroscopy, corneometry and transepidermal water-loss', *International Journal of Cosmetic Science*, 41(3), pp. 281–291. Available at: <https://doi.org/10.1111/ics.12533>.
- Bintoro, A., Ibrahim, A.M. and Situmeang, B. (2017) 'Analisis Dan Identifikasi Senyawa Saponin Dari Daun Bidara (*Zhizipus mauritania* L.)', *Jurnal Itekima*, 2(1), pp. 84–94.
- Butler H (2000) 'Poucher's perfumes, cosmetics, and soaps', in. London: Kluwer Academic Publisher.
- Chandra, D., Tandiono, S. and Irianto Tampubolon, M. (2023) 'Pelembab Bibir *Lip balm* dengan Memanfaatkan Ekstrak Daun Anggur (*Vitis vinifera* L.)', *Jurnal Ilmu Farmasi dan Kesehatan*, 1(2), pp. 143–158. Available at: <https://doi.org/10.59841/an-najat.v1i2.189>.
- Dal'Belo, S., Gaspar, L. and Campos, P. (2006) 'Moisturizing effect of cosmetic formulations containing Aloe vera extract in different concentrations assessed by skin bioengineering techniques', *Skin research and technology: official journal of International Society for*

- Bioengineering and the Skin (ISBS) [and] International Society for Digital Imaging of Skin (ISDIS) [and] International Society for Skin Imaging (ISSI), 12, pp. 241–246. Available at: <https://doi.org/10.1111/j.0909-752X.2006.00155.x>.
- Depkes RI (2020) Farmakope Indonesia edisi VI, Departemen Kesehatan Republik Indonesia.
- Ekayani, M., Juliantoni, Y. and Hakim, A. (2021) 'Uji efektivitas larvasida dan evaluasi sifat fisik sediaan losio antinyamuk ekstrak etanol daun kirinyuh (*Chromolaena odorata* L.) terhadap nyamuk *aedes aegypti*', Jurnal Inovasi Penelitian, 2(4), pp. 1261–1270. Available at: <https://stp-mataram.e-journal.id/JIP/article/view/802>.
- Elfariyanti, Zarwinda, I. and Dewi Safrida, Y. (2022) 'Gambaran Pengetahuan Masyarakat Tentang Macam Rimpang Temu Sebagai Jamu Di Indonesia', E-proceeding 2 nd SENRIABDI 2022, 2, pp. 17–23. Available at: <https://jurnal.usahidsolo.ac.id/>.
- Erwan, F., Ahmad, R., Nurul, R., & Dian, M. (2022) 'Experimental Design of Lip Moisturizer as a Patchouli-Based Innovation Product', Journal of Patchouli and Essential Oil Products, 1(1), pp. 14–17. Available at: <https://doi.org/10.24815/jpeop.v1i1.23748>.
- Hayati, M., Nusantara, C.S. and Shinta, W. (2024) 'Formulasi Dan Uji Fisik Sediaan *Lip balm* Dari Ekstrak Biji Alpukat (*Persea americana* Mill) Sebagai Pelembab', INPHARNMED Journal (Indonesian Pharmacy and Natural Medicine Journal), 7(2), p. 84. Available at: <https://doi.org/10.21927/inpharmmed.v7i2.3875>.
- Hendrika, Y. and Sandi, N.H. (2021) 'The Antidiabetic Activity of *Curcuma mangga* Val. Rhizome Ethyl Acetate Fraction against Mice Induced by Alloxan', JPK : Jurnal Proteksi Kesehatan, 10(1), pp. 55–61. Available at: <https://doi.org/10.36929/jpk.v10i1.348>.
- Imani, C.F. (2022) '(Aloe vera L .) Moisture Test Of Aloe Vera (Aloe Vera L .) Leaf Extract *Lip balm* Cahaya Firdausi Imani , 1 Fenita Shoviantari *', Jurnal Pharma Bhakta, 2(44), pp. 44–51.
- Jacobsen, P.. (2011) The little Lip Book. USA: Carma Laboratories Incorporated.
- Kadbane, N. et al. (2023) 'International Journal of Research Publication and Reviews Formulation and Evaluation of *Lip balm* by Using Moringo Oleifera', International Journal of Research Publication and Reviews, 4(6), pp. 391–398. Available at: <https://ijrpr.com/uploads/V4ISSUE6/IJRPR14064.pdf>.
- Kadu, M., Vishwasrao, S. and Singh, S. (2015) 'Review on Natural *Lip balm*', International Journal of Research in Cosmetic Science, 5(1), pp. 1–7. Available at: <http://www.urpjournals.com>.
- Karim Zulkarnain, A. et al. (2023) 'Formulasi Dan Stabilitas Fisik Sediaan Cream Ekstrak Rimpang Temu Mangga (*Curcuma mangga* Val.) Dan Uji Aktivitas Sebagai Tabir Surya Secara In Vitro', Majalah Farmaseutik, 19(2), pp. 164–170. Available at: <https://doi.org/10.22146/farmaseutik.v19i2.84915>.
- Kase, M.G., Prasetyaningsih, A. and Aditriyarni, D. (2023) 'Antioxidant and Antibacterial Activity of Pomegranate Extract (*Punica granatum* L.) in *Lip balm* Formulation', Biology, Medicine, & Natural Product Chemistry, 12(1), pp. 109–117. Available at: <https://doi.org/10.14421/biomedich.2023.121.109-117>.
- Latifah dan Tranggono RI (2007) Buku Pegangan Ilmu Pengetahuan Kosmetik. Jakarta: PT. Gramedia Pustaka Utama.
- Lestari, U. (2021) 'Formulasi lipstick pelembab bibir berbahan dasar Minyak Tengkawang (*Shorea sumatrana*) dengan perwarna alami Resin Jernang(*Daemonorops didymophylla*)', Chempublish Journal, 6(1), pp. 12–21. Available at: <https://doi.org/10.22437/chp.v6i1.12544>.
- Mojumdar, E., Chattopadhyay, A., Ghosh, A., & Mandal, M. (2017) 'Skin hydration: Interplay between molecular dynamics, structure and water uptake in the stratum corneum', Scientific Reports, 7. Available at: <https://doi.org/10.1038/s41598-017-15921-5>.
- Permenkes, 2010 (2010) 'Peraturan Menteri Kesehatan RI. Nomor 1175/Menkes/Per/VIII/2010'.
- Pawestri Ardhana, C., Y Yamlean, P. V and Sumantri Abdullah, S. (2024) 'Uji Stabilitas Fisik Sediaan Pelembab Bibir (*Lip balm*) Ekstrak Etanol Buah Tomat (*Solanum lycopersicum* L.)', Jurnal Pharmacon, 13(1), pp. 434–447. Available at: <https://doi.org/10.35799/pha.13.2024.49321>.

- Pertiwi, R.D. and Unggul, U.E. (2023) 'Formulation and Evaluation of *Lip balm* from Rambutan Fruit Extract Formulasi dan Evaluasi Sediaan *Lip balm* dari Ekstrak Kulit Buah Rambutan (*Nephelium lappaceum* L .) Formulation and Evaluation of *Lip balm* from Rambutan Fruit Extract', (November).
- Pujimulyani, D., Jannah, L., Setyowati, E., & Siregar, A. (2020) 'Cosmeceutical potentials of *Curcuma mangga* Val. extract in human BJ fibroblasts against MMP1, MMP3, and MMP13', *Heliyon*, 6(9), p. e04921. Available at: <https://doi.org/10.1016/j.heliyon.2020.e04921>.
- Pusmarani, J.P. (2023) 'Formulation and Antioxidant Activity of *Lip balm* Containing Banana Peel (*Musa paradisiaca* var. *Sapientum*) Methanol Extract', *Indonesian Journal of Pharmaceutical Science and Technology*, 1(1). Available at: <https://doi.org/10.24198/ijpst.v0i0.46009>.
- Rao, B. (2020) *Pharmaceutical Research Methodology and Bio-Statistics: Theory and Practice*.
- Rasyadi, Y., Agustin, D. and Aulia, G. (2022) 'Aktivitas Antioksidan *Lip balm* Ekstrak Etanol Bunga Kecombrang (*Eclipta alata* (Jack) R.M.S.m)', *Jurnal Insan Farmasi Indonesia*, 5(1), pp. 140–148. Available at: <https://doi.org/10.36387/jifi.v5i1.896>.
- Rostamailis (2005) *Perawatan Badan, Kulit dan Rambut*. Jakarta: Rineka Cipta.
- Sari, D.E.M. and Susilongingrum, D. (2022) 'Penentuan Nilai Spf Krim Tabir Surya Yang Mengandung Ekstrak Temu Mangga (*Curcuma mangga* Valetton & Zijp) Dan Titanium Dioksida', *Cendekia Journal of Pharmacy*, 6(1), pp. 102–111. Available at: <https://doi.org/10.31596/cjp.v6i1.183>.
- Sariwating, M. and Wass, E.S.R. (2020) 'Formulasi Sediaan *Lip balm* Kombinasi Perasan Buah Mentimun (*Cucumis sativus* L.) dan Buah Jeruk Nipis (*Citrus aurantiifolia*) Sebagai Pencerah Bibir', *Jurnal Jufdikis*, 2(1), pp. 21–26. Available at: <https://jurnal.stikeskesdam4dip.ac.id/index.php/JUFDIKES/article/view/154>.
- Septia Ningsih, D. et al. (2020) 'Skrining Fitokimia dan Penetapan Kandungan Total Fenolik Ekstrak Daun Tumbuhan Sapu-Sapu (*Bacopa frutescens* L.)', *Biotropika: Journal of Tropical Biology*, 8(3), pp. 178–185. Available at: <https://doi.org/10.21776/ub.biotropika.2020.08.03.06>.
- sheskey, Walter G, C. (2017) Paul J. Sheskey_ Walter G. Cook_ Colin G. Cable - *Handbook of Pharmaceutical Excipients* (2017).pdf.
- Sholehah, Y.Y., Malahayati, S. and Hakim, A.R. (2022) 'Formulasi dan Evaluasi Sediaan Lipbalm Ekstrak Umbi Bit Merah (*Beta vulgaris* L.) Sebagai Antioksidan', *Journal Pharmaceutical Care and Sciences*, 3(1), pp. 14–26. Available at: <https://doi.org/10.33859/jpcs.v3i1.205>.
- Simanullang, G. (2023) 'Formulasi dan Evaluasi Stabilitas Fisik Sediaan *Lip balm* Minyak Bekatul (Rice Bran Oil)', *Media Farmasi Indonesia*, 18(2). Available at: <https://doi.org/10.53359/mfi.v18i2.230>.
- Sudarwati, T.P.L. and Fernanda, M.A.H.F. (2019) *Aplikasi Pemanfaatan Daun Pepaya (Carica Papaya) Sebagai Biolarvasida Terhadap Larva Aedes aegypti*. Cetakan Pe. Edited by N.R. Hariyati. Gresik: Graniti.
- Sugiyono (2022) *Metode Penelitian Kuantitatif, Kualitatif dan R&D*. Ke-II. Bandung: Alfabeta.
- Suleman, A. W., Farina, R., Rahman, H. A. A., & Rahman, N. A. (2022) 'Formulasi Dan Evaluasi Stabilitas Sediaan *Lip balm* Ekstrak Kulit Buah Naga Merah (*Hylocereus polyrhizus*) Dengan Penambahan Minyak Zaitun Sebagai Emolien Serta Penentuan Nilai Spf (Sun Protection Factor)', *Medical Sains : Jurnal Ilmiah Kefarmasian*, 7(4), pp. 899–906. Available at: <https://doi.org/10.37874/ms.v7i4.428>.
- Susilongingrum, D. and Mugita Sari, D.E. (2021) 'Uji Aktivitas Antioksidan Dan Penetapan Kadar Flavonoid Total Ekstrak Temu Mangga (*Curcuma mangga* Valetton & Zijp) Dengan Variasi Konsentrasi Pelarut', *Cendekia Journal of Pharmacy*, 5(2), pp. 117–127. Available at: <https://doi.org/10.31596/cjp.v5i2.148>.
- Tampubolon, A. (2023) 'Formulasi *Lip balm* Ekstrak Lidah Buaya (*Aloe Vera*) Dan Buah Naga Merah (*Hylocereus Polyrhizus*) Sebagai *Lip balm* Formulation Of Aloe Vera Extract And Red Dragon Fruit (*Hylocereus Polyrhizus*) AS A Moisturizing Lips', 5(2).
- Wendersteyt, N.V., Wewengkang, D.S. And Abdullah, S.S. (2021) 'Uji Aktivitas Antimikroba Dari Ekstrak Dan Fraksi Ascidian *Herdmania Momus* Dari Perairan Pulau Bangka Likupang Terhadap Pertumbuhan MikrobA *Staphylococcus aureus*, *Salmonella typhimurium* DAN *Candida albicans*',

- Pharmacon, 10(1), p. 706. Available at: <https://doi.org/10.35799/pha.10.2021.32758>.
- Yuandani, Y. et al. (2021) 'Immunomodulatory Effects and Mechanisms of Curcuma Species and Their Bioactive Compounds: A Review', *Frontiers in Pharmacology*, 12. Available at: <https://doi.org/10.3389/fphar.2021.643119>.
- Yulianti, I. and Santoso, J. (2020) 'Identifikasi Tanin Dan Aktivitas Antioksidan Ekstrak Daun Benalu Mangga (*Dendrophthoe Petandra*) Menggunakan Metode Maserasi Dan Sokletasi', *Jurnal parapemikir PHB*, x(x), pp. 1–6.
- Zang, W. et al. (2024) 'Quantifying the dose-response relationship between exercise and health-related quality of life in patients undergoing haemodialysis: A meta-analysis', *Preventive Medicine Reports*, 42, p. 102737. Available at: <https://doi.org/https://doi.org/10.1016/j.pmedr.2024.102737>.